

September 3-10 2023

ISSPIC



International Symposium on Small Particles and Inorganic Clusters XXI

Book of Abstracts

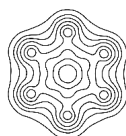


International Symposium on Small Particles and Inorganic Clusters

September 03 –08, 2023 in Berlin/Germany

<https://www.isspic21.de/>

We are thankful for financial support from



FCI
FONDS DER
CHEMISCHEN
INDUSTRIE



HUMBOLDT-UNIVERSITÄT
ZU BERLIN



TECHNISCHE
UNIVERSITÄT
BERLIN

HZB Helmholtz
Zentrum Berlin

FRITZ-HABER-INSTITUT
MAX-PLANCK-GESELLSCHAFT



Universität
Rostock



Traditio et Innovatio



universität
uulm

Local organizing committee:

Thorsten M. Bernhardt, University of Ulm (Chair)

Karl-Heinz Meiwes-Broer, Rostock University (Vice-Chair)

Thomas Möller, Technical University Berlin (Vice-Chair)

Sandra M. Lang, University of Ulm

Wolfgang Christen, Humboldt University of Berlin

Otto Dopfer, Technical University Berlin

Andre Fielicke, Fritz-Haber-Institute Berlin

Tobias Lau, Helmholtz-Institute Berlin and Freiburg University

Andrea Merli, Technical University Berlin

Jürgen P. Rabe, Humboldt University of Berlin

	Saturday 02.09.23	Sunday 03.09.23	Monday 04.09.23	Tuesday 05.09.23	Wednesday 06.09.23	Thursday 07.09.23	Friday 08.09.23		
09:00	Graduate Student Seminar	Graduate Student Seminar	Opening	Andrey Vilesov	Richard Palmer	Francesca Baletto	Bernd von Issendorff		
09:20			Scott Anderson					Lukas Bruder	Beatriz Roldán Cuenya
09:40			María López	Daniela Rupp	Christine Mottet	Joachim Sauer	Mihai Vaida		
10:00			Ewald Janssens					Olof Echt	Gunther Andersson
10:20			Stuart Mackenzie	Lunch break	Lunch break	Joost Bakker	Rajarshi Sinha Roy		
10:40			Lunch break					Lunch break	Lunch break
11:00			Lunch break	Registration Hotel Aquino	Simon Brown	Stefan Bromley	Excursions		
11:20									
11:40									
12:00									
13:00									
13:20									
13:40									
14:00									
14:20									
14:40									
15:00									
15:30									
15:50									
16:10									
16:30									
16:50									
17:10									
17:30									
18:00									
19:30									

- 09:00 Opening
- 09:20 **Scott Anderson** (INV 1)
Sub-nano electrocatalysts: Cluster size and support effects
- 10:00 **María J. López** (INV 2)
Activity of free and supported metal clusters for hydrogen applications
- 10:40 **Ewald Janssens** (HT 1)
Hydrogen adsorption on transition metal doped aluminum clusters
- 11:00 **Stuart Mackenzie** (HT 2)
Infrared investigations of molecular activation at metal centres
- 11:20 Lunch
- 13:00 **Simon Brown** (INV 3)
Percolating networks of nanoparticles and brain-like computation
- 13:40 **Lai-Sheng Wang** (INV 4)
Nanoclusters of Boron and metal borides
- 14:20 **Ori Cheshnovsky** (HT 3)
Absorption measurements of hexagonal grown silicon nanorods utilizing integrating sphere
- 14:40 **Peng Mao** (HT 4)
Nanocluster assembly of disordered plasmonic metasurfaces
- 15:00 Coffee break
- 15:30 **Tatsuya Tsukuda** (INV 5)
Electronic structures and optical properties of chemically-modified gold superatoms
- 16:10 **Ignacio Garzon** (HT 5)
Effect of the metal-ligand interface on the chiroptical activity of cysteine-protected metal nanoparticles
- 16:30 **Best talks from graduate student seminar**

Sub-nano electrocatalysts: Cluster size and support effects

Scott L. Anderson¹, Tugunosuke Masubuchi,¹ Zihan Wang¹, Michael O'Brien¹,
Anastassia N. Alexandrova², Zisheng Zhang,² Philippe Sautet,³ Simran Kumari³

¹ Chemistry Department, University of Utah, USA

² Dept of Chemistry and Biochem. UCLA, USA

³ Chemical Engineering Department, UCLA, USA

We use a combination of size-selected cluster deposition in UHV, *in situ* and *ex situ* electrochemistry, and density functional theory (DFT) to study the effects of catalytic cluster size and electrode support on electrocatalytic activity. These effects have been studied for the hydrogen evolution reaction (HER), the oxygen reduction reaction (ORR), and alcohol electro-oxidation. Small Pt_n soft-landed on indium tin oxide (ITO) and fluorine tin oxide (FTO) are found to have highly size dependent activity for HER in acid electrolyte. For the larger clusters, the activity per atom is roughly twice the activity for the atoms in the surface of bulk Pt, i.e., the activity can be quite high. DFT shows that the high activity is related to the fluxionality of the sub-nano clusters, which structurally evolve as the potential is scanned, such that at the HER threshold, they are able to bind substantially more H atoms *per* Pt atom, compared to bulk Pt or bulk-like Pt nano catalysts. On graphite (HOPG), the HER activity is even higher, soft-landed clusters sinter, but strong size effects are observed for cluster landed at high enough energies to become pinned. The effects of deposition energy will be discussed.

For ORR, the figure shows that activity for pinned Pt_n/HOPG are size dependent, and substantially higher than for the same cluster sizes soft-landed on FTO electrodes.

For alcohol oxidation, activity is also quite high for some cluster sizes, while some sizes are nearly inactive. In this case, the activity is correlated with the electronic properties of the clusters, as probed by X-ray photoelectron spectroscopy.

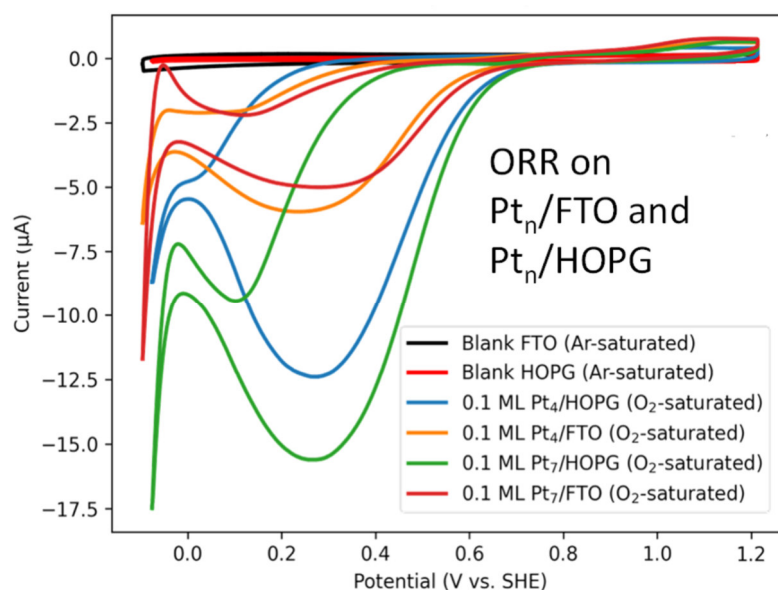


Figure 1: Comparing ORR activity for Pt₄ and Pt₇ deposited on FTO and HOPG

Activity of free and supported metal clusters for hydrogen applications

María J. López, E. Germán, J. Sandoval, J.A. Alonso

Departamento de Física Teórica, Atómica y Óptica, University of Valladolid, Spain

Hydrogen could play a key role in the decarbonization of the energy system facilitating the transition to clean and sustainable sources of energy. However, the use of hydrogen in transportation requires the safe and efficient storage of hydrogen on board. For this reason, there is a renewed interest in hydrogen-absorbing materials, with the goal of achieving high storage capacities suitable for practical applications. Transition metal (TM) nanoclusters have proved efficient catalytic activities for many reactions of interest and specifically towards hydrogen. Doping porous and layered carbon materials with some TM atoms and nanoclusters (palladium among others), enhances the hydrogen storage capacity of these materials. With this motivation we have performed electronic structure calculations within the Density Functional formalism to investigate the adsorption of hydrogen on TM nanoclusters, free and supported in several substrates to unravel the synergistic effect of the metal nanoparticles and of the carbonaceous support [1]. Graphdiyne, GDY, and boron-graphdiyne, BGDY, are two interesting novel carbon-based layered materials which consist on regular networks of triangular and hexagonal holes, respectively, whose edges are diacetylenic carbon chains. The hole structure provides a suitable framework to disperse the metal nanoparticles. Thus, Pd₆ fits well on the large holes of those porous layers. Hydrogen molecules adsorb and dissociate on the supported Pd₆ nanoclusters with small to medium dissociation barriers, 0.23-0.58 eV. These clusters are able to adsorb a large amount of hydrogen, five to six H₂ molecules per cluster, in dissociated and molecular form [2]. Hydrogen spilling from the metal nanoparticles to the substrate is hindered by large activation barriers, 1.37 eV on Pd₆GDY and 1.34 eV on Pd₆BGDY and therefore the storage of hydrogen occurs almost exclusively on the metal nanoparticles. These hydrogen-saturated nanoclusters can be viewed as nanohydrides. We then propose using BGDY and GDY layers as support platforms for metal nanohydrides. Nanohydrides of metals lighter than palladium with similar or higher affinity for hydrogen (such as cobalt) would substantially enhance the storage. A comparison of the activity towards hydrogen between pure TM nanoclusters and specific nanoalloys and between several carbon-based supports will be also provided.

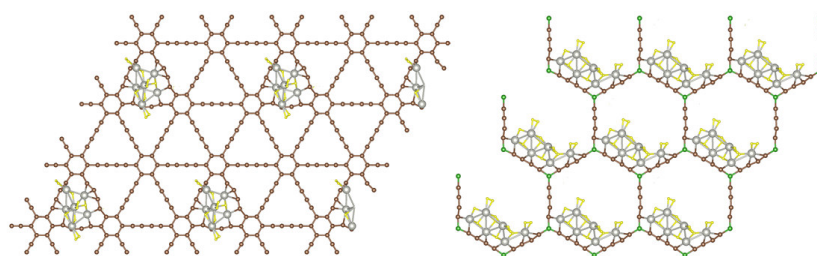


Figure 1: Nanohydride platforms formed by hydrogenated Pd₆ supported on GDY and BGDY layers.

[1] J.A. Alonso, M.J. López, *Phys. Chem. Chem. Phys.* **24** (2022) 2729-2751.

[2] E. German, J. Sandoval, A. Recio, A. Seif, J.A. Alonso, M.J. López, *Chemistry of Materials* **35** (2023) 1134.

Hydrogen adsorption on transition metal doped aluminum clusters

Ewald Janssens¹, Jan Vanbuel,¹ Meiye Jia¹, André Fielicke², Minh Nguyen³, Piero Ferrari^{1,4}

¹ Quantum Solid State Physics, Department of Physics and Astronomy, KU Leuven, Belgium

² Fritz-Haber-Institut der Max-Planck-Gesellschaft, Germany

³ Laboratory for Chemical Computation and Modeling, Van Lang University, Vietnam

⁴ Institute for Molecules and Materials, FELIX Laboratory, Radboud University, Netherlands

Hydrogen is expected to take as energy carrier a central role in the energy transition. The chemical storage of hydrogen in solid materials remains a critical point despite extensive research. Aluminum, one of lightest and most abundant metals on earth, is known to form metal hydrides with a high hydrogen weight percentage, but the hydrogenation of aluminum involves high activation barriers, which can be lowered by the presence of transition metals. To gain fundamental insight in the involved reaction kinetics and energetics, we studied the interaction of hydrogen gas with small Al_n^+ clusters as a function of the cluster size ($n=2-15$) and the presence of transition metal dopant atoms (V, Nb, Rh). Mass spectrometric studies demonstrated a remarkable cluster size and dopant dependent reactivity towards hydrogen gas. Comparing measured infrared multiple photon dissociation spectra of the hydrogenated clusters with density functional theory calculations of different structural isomers allowed for the identification of the hydrogen binding geometry. With rhodium as the dopant, hydrogen binds molecularly onto the dopant for the smallest clusters, but dissociates and spills over to an aluminum site for larger ones [1]. For the lighter transition metal vanadium, the dopant was only capable of dissociating a single hydrogen molecule, and the hydrogen remained bound at the vanadium site [2]. A strong enhancement of the adsorption capacity was found upon Nb doping of the Al clusters. Depending on the exact clusters size, different hydrogen adsorption sites were found, with as most remarkable geometry an octacoordinated Nb atom in the $NbAl_8H_8^+$ cluster [3].

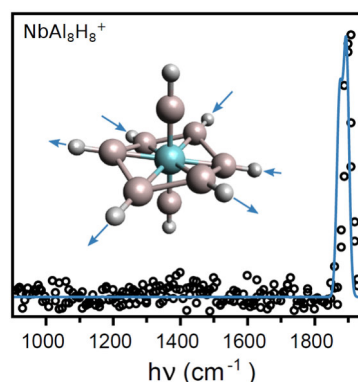


Figure 1: Infrared spectra of $NbAl_8H_8^+$ and its geometry with an octacoordinated central Nb atom, as identified by comparison of the measured and simulated infrared spectra [3].

- [1] M. Jia, J. Vanbuel, P. Ferrari, W. Schöllkopf, A. Fielicke, M.T. Nguyen, E. Janssens, J. Phys. Chem. C **124** (2020) 7624–7633
- [2] J. Vanbuel, E.M. Fernández, P. Ferrari, S. Gewinner, W. Schöllkopf, L.C. Balbás, A. Fielicke, E. Janssens, Chem. Eur. J. **23** (2017) 15638 – 15643
- [3] P. Ferrari, H.T. Pham, J. Vanbuel, M.T. Nguyen, A. Fielicke, E. Janssens, Chem. Commun. **57** (2021) 9518

Infrared Investigations of molecular activation at metal centres

Stuart R. Mackenzie¹

¹Physical and Theoretical Chemistry Laboratory, University of Oxford, UK

Infrared spectroscopy provides some of the most detailed and direct information on molecular activation. We have used different variants of this technique to explore small molecule binding at metal centres in ion-molecule complexes and on size-selected transition metal clusters.

In addition to CO₂ activation,^[1] we have recently focused on radical (NO)^[2] and/or non-symmetric ligands such as N₂O and OCS which offer multiple potential binding motifs and thus a richer isomeric distribution. I will present recent results on mixed-ligand systems such as M⁺(CO)_n(N₂O)_m in which we observe cooperative binding effects and intriguing non-statistical fragmentation dynamics.^[3]

I will also report on further examples in which infrared excitation of molecularly-bound adsorbates on transition metal clusters drives unexpected chemistry such as CO loss from Au_n⁺OCS and N₂ loss from M_n⁺(N₂O).^{[4],[5]} The studies involving Au_n⁺ clusters also revealed an extraordinary broadband infrared electronic absorption band arising from its 9-electron distorted tetrahedral structure.^[6]

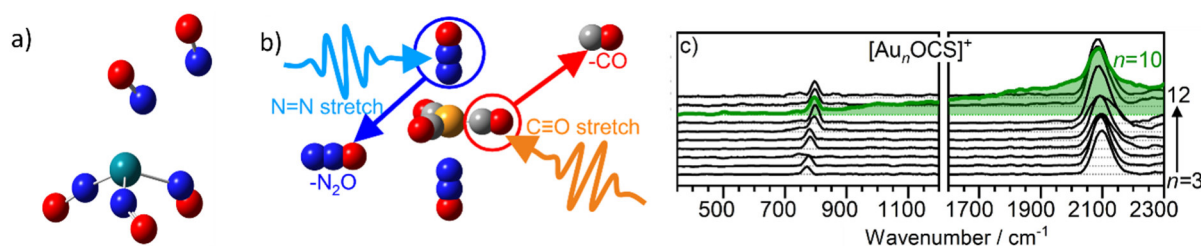


Figure 1: a) Rh⁺(NO)_n complexes,^[2] b) non statistical fragmentation in Au⁺(CO)_n(N₂O)_m mixed-ligand complexes^[3] and c) broadband infrared electronic excitation in Au₁₀⁺.^[6]

- [1] E. Brewer, A. Green, A. Gentleman,..., S.R. Mackenzie, Phys. Chem. Chem. Phys. A **24** (2022), 22716
- [2] G. Meizyte, P. Percy, P. Watson,..., S.R. Mackenzie, J. Phys. Chem. A **126** (2022) 9414
- [3] A. Green, R. Brown, G. Meizyte,..., S.R. Mackenzie, J. Phys. Chem. A **125** (2022), 7266
- [4] A. Green, S. Schaller,... A. Fielicke, S.R. Mackenzie, J. Phys. Chem. A **124** (2020), 5389
- [5] G. Meizyte, A. Green,... A. Fielicke, S.R. Mackenzie, Phys. Chem. Chem. Phys. A **22** (2020), 18606
- [6] A. Green, A. Gentleman,... A. Fielicke, S.R. Mackenzie, Phys. Rev. Lett. **127** (2021) 033002

Percolating Networks of Nanoparticles and Brain-like Computation

Simon A. Brown

The MacDiarmid Institute for Advanced Materials and Nanotechnology, School of Physical and Chemical Sciences, University of Canterbury, 8140, Christchurch, New Zealand.

Self-assembled networks of nanoparticles have recently emerged as important candidate systems for brain-like (or neuromorphic) information processing. The essence of the approach is to take advantage of the intrinsic dynamical properties of these networks to implement brain-inspired approaches to computation. Implementation of such approaches in hardware has the potential to overcome limitations in traditional integrated circuit technologies, while decreasing power consumption and improving performance.

Our percolating networks of nanoparticles (PNNs, Fig 1(a)) are self-assembled via simple deposition processes that are completely CMOS compatible, making them attractive for integration. The particles are deposited randomly on silicon substrates and the key to our approach is to terminate the deposition at the onset of conduction (the percolation threshold) when the properties of the network are dominated by tunnel gaps between groups of particles. The memristive tunnel gaps turn out to have neuron-like properties (Fig 1(b)), which means that PNNs can be viewed as networks of neurons.

I will give an overview of the brain-like properties of PNNs, highlighting both structural and dynamical properties. In particular, I will discuss critical avalanches of neuron-like spiking events. Criticality is a key feature of the biological brain that has been related to optimal information processing capability. More generally, electrical signals from the PNNs exhibit correlations and complexity that are similar to biological neural networks, further suggesting their utility for all-electronic implementations of various brain-like computational schemes. I will discuss demonstrations of time series prediction and classification tasks, and highlight key practical issues that make PNNs different to standard ‘reservoirs’ or artificial neural networks. As time allows, I will present new results demonstrating that the spiking behaviour of the ‘neurons’ can be exploited to perform other computational tasks, and discuss applications in the fields of secure data transmission and search and optimisation.

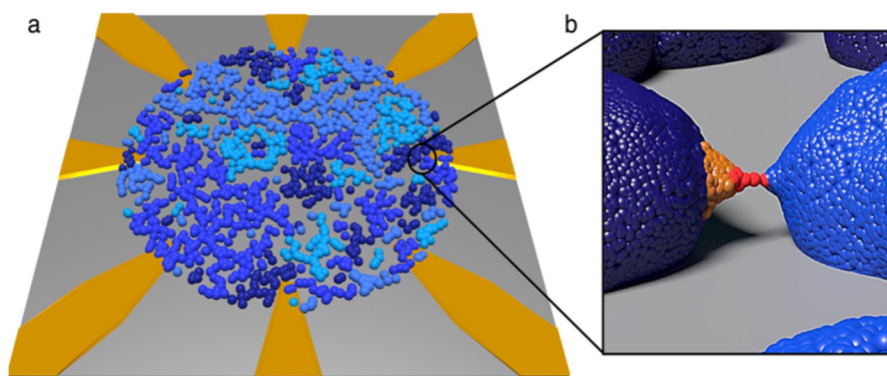


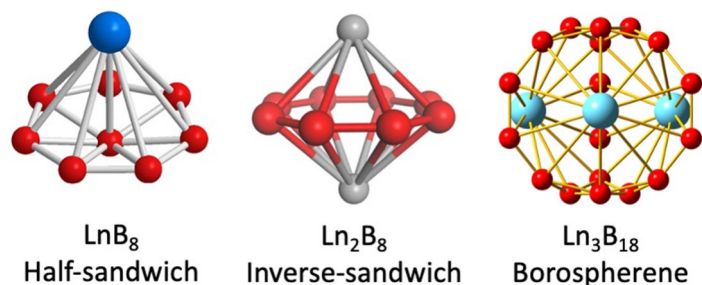
Figure 1. (a) A percolating network of nanoparticles in a multiple contact geometry. The different colours represent groups of particles that are in contact with one another. (b) The zoomed region shows a schematic of the growth of an atomic filament within a tunnel gap when a voltage is applied, leading to neuron-like spiking.

Nanoclusters of Boron and Metal Borides

Lai-Sheng Wang

Department of Chemistry, Brown University, Providence, RI 02912, USA

Photoelectron spectroscopy in combination with computational studies has shown that bare boron clusters possess planar structures [1], in contrast to that of bulk boron, which is dominated by three-dimensional polyhedral building blocks. The propensity for planarity has been found to be a result of both σ and π electron delocalization over the molecular plane [2]. The B_{36} cluster was found to have a highly stable planar structure with a central hexagonal vacancy, providing experimental evidence that single-atom boron-sheets with hexagonal vacancies (borophenes) are viable [3]. Borophenes have since been synthesized and characterized on inert substrates, forming a new class of synthetic 2D materials [4,5]. We have found that the B_{48}^- cluster possesses a bilayer structure [6], suggesting the feasibility of bilayer borophenes. Boron forms important bulk boride materials with most metals in the periodic table. Many transition-metal borides are superhard materials, while lanthanide borides are essential magnetic materials. Metal boride clusters are ideal systems to probe the metal-boron bonding in boride materials. We have observed that transition-metal atoms can be doped into the plane of boron clusters, indicating the possibility of metallo-borophenes [7]. However, lanthanide-doped boron clusters form half-sandwich complexes [8], inverse-sandwich complexes [9], as well as novel lanthanide boron cages [10].



- [1] L. S. Wang, *Int. Rev. Phys. Chem.* **35** (2016) 69-142.
- [2] A. P. Sergeeva, I. A. Popov, Z. A. Piazza, W. L. Li, C. Romanescu, L. S. Wang, A. I. Boldyrev, *Acc. Chem. Res.* **47** (2014) 1349-1358.
- [3] Z. A. Piazza, H. S. Hu, W. L. Li, Y. F. Zhao, J. Li, L. S. Wang, *Nature Commun.* **5** (2014) 3113.
- [4] A. J. Mannix, X. F. Zhou, B. Kiraly, J. D. Wood, D. Alducin, B. D. Myers, X. L. Liu, B. L. Fisher, U. Santiago, J. R. Guest, M. J. Yacaman, A. Ponce, A. R. Oganov, M. C. Hersam, N. P. Guisinger, *Science* **350** (2015) 1513
- [5] B. J. Feng, J. Zhang, Q. Zhong, W. B. Li, S. Li, H. Li, P. Cheng, S. Meng, L. Chen, K. H. Wu, *Nature Chem.* **8** (2016) 563-568.
- [6] W. J. Chen, Y. Y. Ma, T. T. Chen, M. Z. Ao, D. F. Yuan, Q. Chen, X. X. Tian, Y. W. Mu, S. D. Li, L. S. Wang, *Nanoscale* **13** (2021) 3868-3876.
- [7] W. L. Li, X. Chen, T. Jian, T. T. Chen, J. Li, L. S. Wang, *Nature Rev. Chem.* **1** (2017) 0071.
- [8] W. L. Li, T. T. Chen, W. J. Chen, J. Li, and L. S. Wang, *Nature Commun.* **12** (2021) 6467.
- [9] W. L. Li, T. T. Chen, D. H. Xing, X. Chen, J. Li, L. S. Wang, *Proc. Natl. Acad. Sci. (USA)* **115** (2018) E6972.
- [10] T. T. Chen, W. L. Li, W. J. Chen, X. H. Yu, X. R. Dong, J. Li, L. S. Wang, *Nature Commun.* **11** (2020) 2766.

Absorption measurements of hexagonal grown silicon nanorods utilizing Integrating sphere

Ori Cheshnovsky¹, Ranit Roy¹, Dushyant Kushavah¹, Guy Paiss¹, Yizhen Ren², Jos Haverkort², Alex Zunger³ and Erik P. A. M. Bakkers²

¹ School of Chemistry, Tel Aviv University, Israel

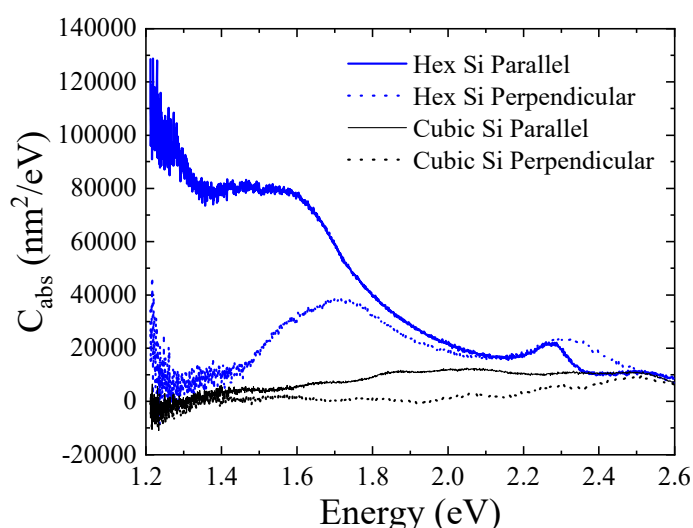
² Eindhoven University of Technology, The Netherlands

³ Renewable and Sustainable Energy Institute, University of Colorado, USA

Silicon is predicted to exhibit new and exciting properties when grown in a hexagonal crystal structure. The group of Bakkers recently met this challenge by transferring the hexagonal crystal structure from a template hexagonal gallium phosphide nanowire to an epitaxially grown silicon shell, such that hexagonal silicon is formed [1]. This paper presents a study on the distinct absorption features of hexagonal silicon nanowires (NWs) compared to cubic silicon NWs.

We present a methodology for measuring the absorption spectra of individual nano-objects based on focusing the wide bandwidth output of a supercontinuum laser on a sample situated in an integrating sphere. The collected scattering and reflectance are dispersed by an imaging spectrograph, allowing to extract the absorption over a wide photon energy range.

Fig. 1 depicts the absorption cross-section of an individual hex Si wire. The spectrum reveals distinct absorption peaks consistent with theoretical electronic structure calculations and absent from the weak absorption spectra of cubic Si nanowires. We will discuss further measurements and analysis needed to understand better the absorption properties of hexagonal silicon NWs and their potential applications in optoelectronics and energy conversion.



Absorption cross-section of hexagonal (Blue-160 diameter GaP core 14nm Hex Si shell) and cubic silicon NWs (Black - 60nm diameter wire) for two polarizations.

[1] H.I.T. Hauge, MA Verheijen, S Conesa-Boj et al. Nano letters **15** (2015), 5855-5860.

Nanocluster Assembly of Disordered Plasmonic Metasurfaces

Peng Mao¹, Changxu Liu², Yubiao Niu³, Richard E. Palmer³, Guanghou Wang¹, Stefan A. Maier⁴, Shuang Zhang⁵ and Min Han¹

¹ National Laboratory of Solid-State Microstructures and College of Engineering and Applied Sciences, Nanjing University, Nanjing 210023, China

² Electronic Engineering, University of Exeter, Exeter EX4 4QF, UK

³ Nanomaterials Lab, Faculty of Science and Engineering, Swansea University, Swansea SA1 8EN, UK

⁴ Department of Physics, Imperial College London, Prince Consort Road, London, SW7 2AZ, UK

⁵ Department of Physics, University of Hong Kong, Hong Kong 999077, China

Optical metasurfaces have opened an entirely new field in the quest to manipulate light. Gas-phase cluster beam technique provides a unique way to build nanocluster-based metasurfaces, especially in the field of disordered metasurfaces. Here, we demonstrate a series of disordered plasmonic metasurfaces fabricated with a controllable cluster beam deposition process [1-5]. Inspired by coupled mode theory and transformation optics, the designed metasurfaces shows tunable light absorption, and broadband field enhancement across the full visible wavelength. Not limited to its significance for the further understanding of the physics of disorder, our disordered plasmonic systems provide novel platforms for various practical applications such as structural colour patterning, surface-enhanced Raman Spectra (SERS), and solar energy conversion.

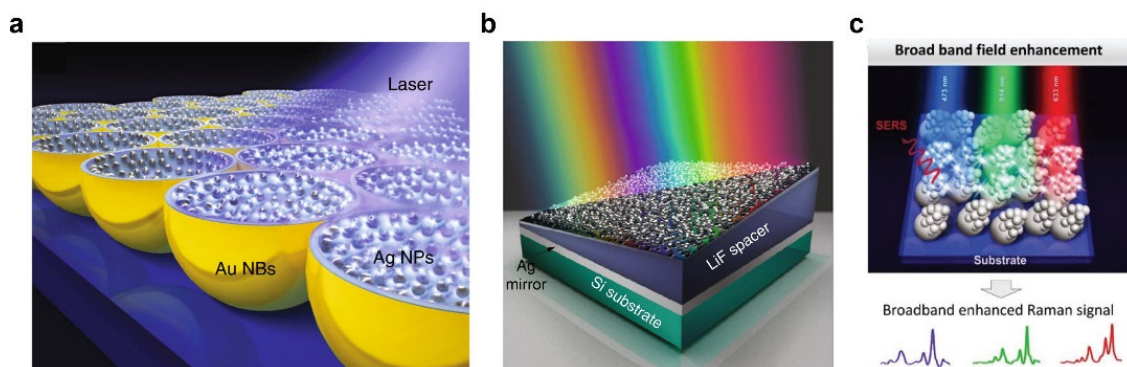


Figure 1: Nanocluster assembly of disordered plasmonic metasurfaces for field enhancement (a, c) and tunable light absorption (b).

- [1] P. Mao, C. Liu*, X. Li, M. Liu, Q. Chen, M. Han, S. A. Maier, E. H. Sargent* and S. Zhang*. **Light: Science & Applications**, 2021, 10(1), 1-9.
- [2] P. Mao, C. Liu, Y. Niu, Y. Qin, F. Song, M. Han, R. E. Palmer, S. A. Maier and S. Zhang*. **Advanced Materials**, 2021, 33 (23), 2007623.
- [3] P. Mao, C. Liu, F. Song, M. Han*, S. A. Maier* and S. Zhang*. **Nature Communications**, 2020, 11(1), 1-7.
- [4] P. Mao, C. Liu, G. Favraud, Q. Chen*, M. Han, A. Fratalocchi* and S. Zhang*. **Nature Communications**, 2018, 9, 5428.
- [5] P. Mao, C. Liu, Q. Chen, M. Han, S. A. Maier* and S. Zhang*. **Nanoscale**, 2020, 12, 93-102. (Front Cover)

Electronic Structures and Optical Properties of Chemically-modified Gold Superatoms

Tatsuya Tsukuda

Department of Chemistry, Graduate School of Science, The University of Tokyo

Gold clusters, consisting of a few to a hundred gold atoms, have attracted growing attention as building units of novel functional materials because they exhibit unique physicochemical properties due to their discrete electronic structures and non-fcc atomic packing structures. Recent progress in atomically precise synthesis, X-ray crystallography and theoretical calculations [1] has revealed that the ligand-protected Au clusters can be viewed as “chemically modified Au superatoms” owing to the atom-like electronic shell structures. For example, the magic stability of the icosahedral $M@Au_{12}$ core is associated with a closed electron configuration $(1S)^2(1P)^6$, similarly to that of noble gases. A unique feature of the superatoms compared to the conventional atoms is that their properties can be controlled by a variety of factors such as the number of constituent atoms, composition, shape, and surface modification [2, 3]. Our research goal is to develop the superatoms as nano-scale artificial elements. In this talk, I will introduce the following topics on chemically modified Au superatoms and their pseudo-molecules (superatomic molecules):

- (1) Atomically precise synthesis and structure determination [4–15]
- (2) Exploration of novel photophysical and photocatalytic properties [3–5,7,8,10]
- (3) Elucidation of electronic structures by gas-phase photoelectron spectroscopy [15–21]

References

- [1] T. Omoda, S. Takano, T. Tsukuda, *Small* **17** (2021) 2001439.
- [2] H. Hirai, S. Ito, S. Takano, K. Koyasu, T. Tsukuda, *Chem. Sci.* **11** (2020) 12233.
- [3] S. Takano, T. Tsukuda, *J. Am. Chem. Soc.* **143** (2021) 1683.
- [4] S. Takano, S. Hasegawa, M. Suyama, T. Tsukuda, *T. Acc. Chem. Res.* **51** (2018) 3074.
- [5] S. Takano, S. Ito, T. Tsukuda, *J. Am. Chem. Soc.* **141** (2019) 15994.
- [6] M. R. Narouz *et al.* *Nature Chem.* **11** (2019) 419.
- [7] M. R. Narouz *et al.* *J. Am. Chem. Soc.* **141** (2019) 14997.
- [8] S. Takano, H. Hirai, T. Nakashima, T. Iwasa, T. Taketsugu, T. Tsukuda, *J. Am. Chem. Soc.* **143** (2021) 10560.
- [9] E. Ito, S. Takano, T. Nakamura, T. Tsukuda, *Angew. Chem., Int. Ed.* **60** (2021) 645.
- [10] H. Hirai *et al.*, *Angew. Chem., Int. Ed.* **61** (2022) e202207290.
- [11] V. K. Kulkarni *et al.*, *J. Am. Chem. Soc.* **144** (2022) 9000.
- [12] P. A. Lummis *et al.*, *JACS Au* **2** (2022) 875.
- [13] R. W. Y. Man *et al.*, *J. Am. Chem. Soc.* **144** (2022) 2056.
- [14] T. Shigeta, S. Takano, T. Tsukuda, *Angew. Chem., Int. Ed.* **61** (2022) e202113275.
- [15] E. Ito, S. Ito, S. Takano, T. Nakamura, T. Tsukuda, *JACS Au* **2** (2022) 2627.
- [16] K. Hirata, R. Tomihara, K. Koyasu, T. Tsukuda, *Phys. Chem. Chem. Phys.* **21** (2019) 17463.
- [17] K. Kim *et al.*, *Angew. Chem., Int. Ed.* **58** (2019) 11637.
- [18] Y. Tasaka *et al.*, *J. Phys. Chem. Lett.* **11** (2020) 3069.
- [19] K. Koyasu, T. Tsukuda, *J. Chem. Phys.* **154** (2021) 140901.
- [20] S. Ito, Y. Tasaka, K. Nakamura, Y. Fujiwara, K. Hirata, K. Koyasu, T. Tsukuda, *J. Phys. Chem. Lett.* **13** (2022) 5049.
- [21] K. Nakamura, S. Ito, K. Koyasu, T. Tsukuda, *Phys. Chem. Chem. Phys.* **25** (2023).

Effect of the metal-ligand interface on the chiroptical activity of cysteine-protected metal nanoparticles

Ignacio L. Garzón

Instituto de Física, Universidad Nacional Autónoma de México, México

In this work, we describe recent experimental and theoretical studies on the adsorption of amino acids (cysteine) on metal nanoparticles. Specifically, cysteine interaction with gold, silver, and copper NPs is characterized by Raman spectroscopy and density functional theory calculations to elucidate the molecular conformation and adsorption sites for each metal. The experimental analysis of Raman spectra upon adsorption with respect to free cysteine indicates that while the C–S bond and carboxyl group are similarly affected by adsorption on the three metal NPs, the amino group is sterically influenced by the electronegativity of each metal, causing a greater modification in the case of gold NPs. A theoretical approach that takes into consideration intermolecular interactions using two cysteine molecules is proposed using a S–metal–S interface motif anchored to the metal surface. Similarities between the calculated Raman spectra and experimental data confirm the thiol and carboxyl as adsorption groups for gold, silver, and copper NPs and suggest the formation of monomeric “staple motifs.” [1,2]

Moreover, gold, silver, and copper small nanoparticles (NPs), with average size ≈ 2 nm, were synthesized and afterward protected with l- and d-cysteine, demonstrating emergence of chiroptical activity in the wavelength range of 250–400 nm for all three metals with respect to the bare nanoparticles and ligands alone. Silver-cysteine (Ag-Cys) NPs display the higher anisotropy factor, whereas gold-cysteine (Au-Cys) NPs show optical and chiroptical signatures slightly more displaced to the visible range. A larger number of circular dichroism (CD) bands with smaller intensity, as compared to gold and silver, is observed for the first time for copper cysteine (Cu-Cys) NPs. The manifestation of optical and chiroptical responses upon cysteine adsorption and the differences between the spectra corresponding to each metal are mainly dictated by the metal–ligand interface, as supported by a comparison with calculations of the oscillatory and rotatory strengths based on time-dependent density functional theory, using a metal–ligand interface motif model, which closely resembles the experimental absorption and CD spectra.

These results are useful to demonstrate the relevance of the interface between chiral ligands and the metal surfaces of Au, Ag, and Cu NPs, and provide evidence and further insights into the origin of the transfer mechanisms and induction of extrinsic chirality. [3]

1. Penélope Rodríguez-Zamora, Benjamin Salazar-Angeles, Fernando Buendía, Cédric A Cordero-Silis, Jorge Fabila, Lourdes Bazán-Díaz, Luz M. Fernández-Díaz, Lauro O. Paz-Borbón, Gabriela Díaz, Ignacio L. Garzón, *J. Raman Spectrosc.*, **51** (2020) 243
2. Penélope Rodríguez-Zamora, Cédric A. Cordero-Silis, Jorge Fabila, Jonathan C. Luque-Ceballos, Fernando Buendía, Alejandro Heredia-Barbero, Ignacio L. Garzón, *Langmuir* **38** (2022) 5418
3. Penélope Rodríguez-Zamora, Cédric A. Cordero-Silis, Georgina R. Garza-Ramos, Benjamin Salazar-Angeles, Jonathan C. Luque-Ceballos, Jorge C. Fabila, Fernando Buendía, Lauro Oliver Paz-Borbón, Gabriela Díaz, and Ignacio L. Garzón, *Small*, **17**, (2021) 2004288

- 09:00 **Andrey Vilesov** (INV 6)
Superfluid helium droplets
- 09:40 **Lukas Bruder** (INV 7)
Coherent multidimensional spectroscopy of doped clusters in the gas phase
- 10:20 **Daniela Rupp** (INV 8)
X-ray movies of melting and inflation in gas-phase plasmonic nanoparticle
- 11:00 **Olof Echt** (HT 6)
The smallest dicationic rare gas clusters
- 11:20 Lunch
- 13:00 **Stefan Bromley** (INV 9)
Silicate clusters and nanoparticles in the interstellar medium: Theory, experiment and observation
- 13:40 **Evan Bieske** (INV 10)
Exploring structures and properties of carbon clusters – chains, rings and fullerenes
- 14:20 **Piero Ferrari** (HT 7)
Laboratory infrared characterization of gas-phase sulfur clusters: solving the astronomic sulfur puzzle?
- 14:40 **Masashi Arakawa** (HT 8)
Reaction of size-selected iron-oxide cluster cations with methane: A model study of chemical processes in mars' atmosphere
- 15:00 Coffee break
- 15:30 **Junko Yano** (INV 11)
Water oxidation reaction in natural photosynthesis catalyzed by the Mn_4CaO_5 cluster
- 16:10 **Nouari Kebaili** (HT 9)
Reduction and biosorption of silver nanoparticles by bacteria
- 16:30 **Mauro Stener** (HT 10)
Chiral metal clusters: efficient and accurate computational approaches for plasmons, Circular Dichroism and ligand dynamics
- 16:50 **Jiaye Jin** (HT 11)
Ultrafast dynamics of mass-selected neutral silver clusters probed by femtosecond NeNePo spectroscopy
- 17:30 **Poster Session A**

Superfluid Helium Droplets

Andrey F. Vilesov

University of Southern California, Los Angeles, CA 90089, USA

This talk reviews studies of isolated sub-micrometer superfluid ^4He , normal fluid ^3He and mixed droplets via single-shot femtosecond X-ray coherent diffractive imaging at free electron laser facilities. [1,2] The droplets have sizable angular momentum, resulting in significant centrifugal distortion. [3,4] For visualization of vortices in superfluid ^4He droplets, Xe atoms were added to the droplets where they gather in cores forming thin filaments. [2,5] In comparison, Xe atoms in ^3He droplets gather in diffuse, ring-shaped structures along the equator. [6] The equilibrium figures of rotating superfluid droplets follow a series of oblate and prolate shapes that evolve along curves of stability as a function of reduced angular momentum and angular velocity. [5] In axisymmetric oblate droplets, all angular momentum is stored in triangular lattices of quantum vortices. In prolate droplets, however, capillary waves can contribute a substantial and, for large aspect ratios, even dominant amount of angular momentum. Further topics include quantum phase separation in mixed $^3\text{He}/^4\text{He}$ droplets and study of the arrangement of multiple charges on the surface of the droplets. [7]

*This work was supported by the NSF Grants No. DMR-1701077 and DMR-2205081.

- [1] L.F. Gomez *et al.*, *Science* **345**, 906 (2014).
- [2] R. M. P. Tanyag *et al.*, *Structural Dynamics* **2**, 051102 (2015).
- [3] C. Bernardo *et al.*, *Phys. Rev. B* **95**, 064510 (2017).
- [4] D. Verma *et al.*, *Phys. Rev. B* **102**, 014504 (2020).
- [5] S. M. O. O'Connell *et al.*, *Phys. Rev. Lett.* **124**, 215301 (2020).
- [6] A. J. Feinberg *et al.*, *Science Advances* **7**, abk2247 (2021).
- [7] A. J. Feinberg *et al.*, *Phys. Rev. Res.* **4**, L022063 (2022).

Coherent multidimensional spectroscopy of doped clusters in the gas phase

Lukas Bruder

¹ *Institute of Physics, University of Freiburg*

Understanding the role of environmental perturbations in molecular dynamics is an important challenge. In the condensed phase, strong line broadening and complex environments make a detailed analysis often difficult. We tackle this problem in the gas phase, where higher spectral resolution can be attained and environmental perturbations can be well controlled and tuned. To this end, we dope rare-gas clusters with different molecular species and study the molecule-cluster interaction in the confined and isolated nanosystems. In a unique approach, we combine this method with coherent multidimensional spectroscopy [1]. The latter technique applied in the gas phase provides very high spectral and temporal resolution, hence gives direct access to the ultrafast molecular dynamics, coupling and relaxation channels and allows us to lift ensemble inhomogeneities. We will report some recent applications. Our approach enabled resolving the ultrafast de-solvation of molecules in a quantum fluid (figure 1) [2]. We attained insight into binding configurations between single molecules and a cluster surface [3]. And recently, we started investigating specifically the coupling of molecular vibrations to the local cluster environment and the effect on the vibrational coherence lifetime.

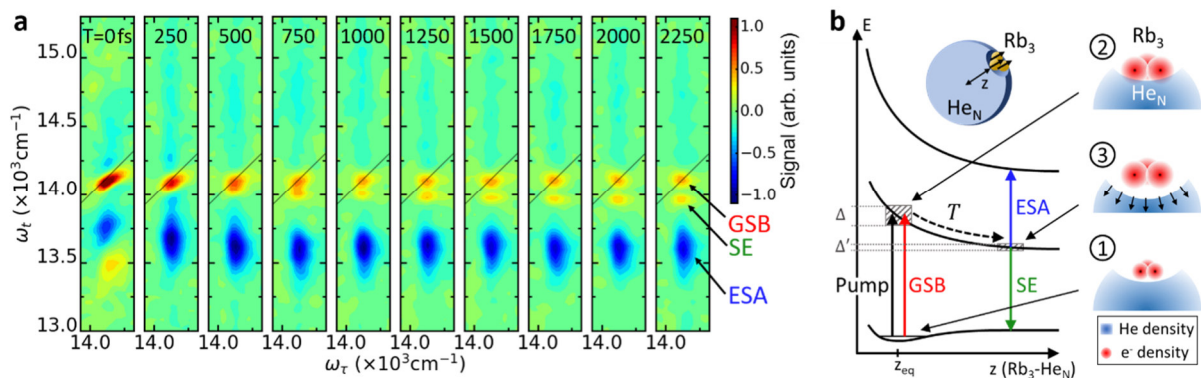


Figure 1: Ultrafast de-solvation of Rb_3 molecules attached to superfluid He nanodroplets, mapped with high temporal and spectral resolution in (a). The desolvation process is schematically sketched in (b). Adapted from [2].

- [1] L. Bruder et al., J. Phys. B: At. Mol. Opt. Phys. **52**, (2019) 183501
- [2] L. Bruder et al., *Nat Commun* **9**, (2018) 4823
- [3] U. Bangert, F. Stienkemeier, and L. Bruder, *Nat Commun* **13**, (2022) 3350

X-ray movies of melting and inflation in gas-phase plasmonic nanoparticles

D. Rupp¹, A. Colombo¹, S. Dold², A. Al Haddad³, J. Bielecki², F. Goy¹, C. Graf⁴, L. Hecht¹, G. Jakobs¹, M. Joschko⁴, G. Knopp³, K. Kolatzki¹, C. Peltz⁵, S. Rafie-Zinedine², T. Reichenbach^{6,7}, M. Sauppe¹, F. Schenk⁸, K. Schnorr³, Z. Sun³, P. Tümmler⁵, C.F. Ussling¹, M. Yarema⁸, N. Yazdani⁸, H. Zhang³, M. Moseler^{6,7}, C. Bostedt³, and B. von Issendorff⁶

¹Laboratory for Solid State Physics, ETH Zurich, Zurich, 8049, Switzerland;

²European XFEL GmbH, Schenefeld, 22869, Germany;

³Photon Science (PSD), Paul Scherrer Institut, Villigen, 5232, Switzerland;

⁴Department of Chemistry and Biotechnology, Darmstadt University of Applied Sciences, 64295 Darmstadt, Germany;

⁵Institute for Physics, University of Rostock, Rostock, 18059, Germany;

⁶Department of Physics, University of Freiburg, Freiburg, 79104, Germany;

⁷Fraunhofer Institute for Mechanics of Materials IWM, Freiburg, 79108, Germany;

⁸Institute for Electronics, ETH Zurich, Zurich, 8049, Switzerland

Via single-shot coherent diffractive imaging (CDI), the structure and dynamics of isolated nanosamples can be directly visualized: Intense and short pulses of X-ray free-electron lasers (XFELs) or intense high-harmonic generation (HHG) sources scatter off a free-flying nanostructure, forming an interference pattern that is captured with a large-area detector. With computer-based iterative phase-retrieval or forward-fitting methods a snapshot of the object's structure can be retrieved from the pattern. This has opened a door for studying intense laser-matter interaction with unprecedented detail.

We investigate the dynamics in laser-heated plasmonic nanoparticles via single-particle CDI. Silver nanocubes are brought into the gas phase and heated with laser pulses tuned to their surface plasmon resonance at a wavelength of 400 nm. This approach allows for a uniform heating of the nanoparticles at comparably low laser intensities, avoiding strong-field effects like tunneling and electron impact ionization. Depending on the heating laser's intensity, a wide range of processes is observed, from surface to full melting, internal boiling, cavitation, expansion and inflation, droplet vibrations, up to explosive boiling.

Molecular dynamics simulations show that the systems travel on rather similar trajectories through the phase diagram, differing only in whether and where the stability limit of the metastable superheated liquid is crossed.

These results exemplify the maturity of time-resolved single-particle coherent diffraction imaging for investigating ultrafast dynamics in matter, being now on a level where we can readily extract previously inaccessible physical quantities of matter under extreme conditions

The Smallest Dicationic Rare Gas Clusters

I. Stromberg, S. Bergmeister, E. Gruber, G. Schöpfer, M. Ončák, P. Scheier, O. Echt

Institut für Ionenphysik und Angewandte Physik, Universität Innsbruck, Austria

Small, highly charged droplets are unstable with respect to charge separation. Thus, for a specific charge state, there exists a minimum size below which the droplets will spontaneously undergo fission. Larger droplets feature a fission barrier but they may still go undetected depending on the amount and distribution of the excitation energy which, in turn, depends on how the ions are prepared. Still, the minimum appearance sizes n_a reported in the literature for various van der Waals- or hydrogen-bonded clusters are surprisingly robust [1]. For example, the modest decrease in the appearance size of doubly charged xenon clusters from $n_a = 53$ [2] to $n_a = 47$ [3] was mostly due to improved mass spectral resolution and ion yield.

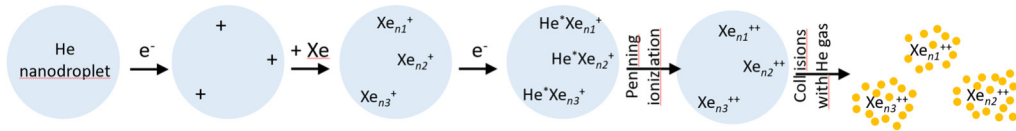


Figure 1: Synthesis of doubly charged xenon clusters

Here we report on a novel way to prepare doubly charged clusters which results in a two-fold reduction in n_a for Xe; for Kr and Ar the appearance size is reduced by about 30 %. The good agreement between various attempts to calculate the critical size at which the fission barrier vanishes, and experimental appearance sizes, is a thing of the past.

Fig. 1 illustrates the method. First, large helium nanodroplets are prepared by supersonic expansion of He and ionized by electrons, resulting in highly charged droplets [4]. These are doped with xenon atoms which will nucleate at the multiple charge centers. Subsequent bombardment of the droplets with electrons produces electronically excited He^* which convert the embedded Xe_n^+ to dications by Penning ionization [5]. The dications are then gently extracted by low-energy collisions of the droplets with helium gas, leading to bare Xe_n^{2+} .

Xe_{29}^{2+} and Xe_{31}^{2+} are clearly seen in the mass spectrum in Fig. 2; Xe_{25}^{2+} and Xe_{27}^{2+} are present as well. We have probed the dissociation channels of excited dications by colliding them with argon atoms. For Xe_{49}^{2+} and larger clusters we observe two channels: loss of one or more Xe atoms, and approximately symmetric fission into Xe_m^+ . Xe_{43}^{2+} , on the other hand, solely decays by fission.

Surprisingly, the mass spectrum also reveals doubly charged Xe and Kr dimers and trimers. We have studied Xe_2^{2+} using the coupled cluster theory at the CCSD/def2TZVP level and obtain a fission barrier of 0.51 eV (with inclusion of zero-point energy). Xe_3^{2+} features a fission barrier as well.

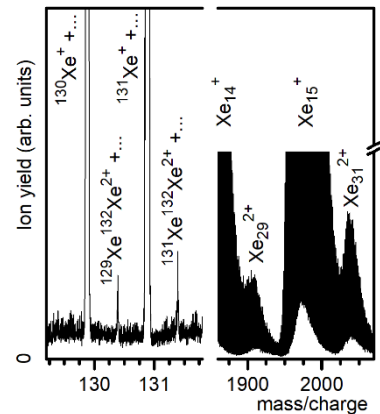


Fig. 2: Spectrum of Xe clusters

- [1] O. Echt, D. Kreisle, E. Recknagel, J.J. Saenz, R. Casero, and J.M. Soler, Phys. Rev. A **38** (1988) 3236.
- [2] K. Sattler, J. Mühlbach, O. Echt, P. Pfau, and E. Recknagel, Phys. Rev. Lett. **47** (1981) 160.
- [3] P. Scheier, G. Walder, A. Stamatovic, and T.D. Märk, J. Chem. Phys. **90**, (1989) 4091.
- [4] F. Laimer, L. Kranabetter, L. Tiefenthaler, S. Albertini et al., Phys. Rev. Lett. **123**, (2019) 165301.
- [5] H. Schöbel, P. Bartl, C. Leidlmair, M. Daxner, S. Zöttl et al., Phys. Rev. Lett. **105** (2010) 243402.

Silicate Clusters and Nanoparticles in the Interstellar Medium: Theory, Experiment and Observation

Stefan T. Bromley^{1,2}

¹ *1Departament de Ciència de Materials i Química Física & Institut de Química Teòrica i Computacional (IQTCUB), Universitat de Barcelona, Barcelona, Spain.*

² *Institució Catalana de Recerca i Estudis Avançats (ICREA), Barcelona, Spain.*

Silicates are ubiquitously found as small dust grains throughout the universe. These particles are frequently subject to high-energy processes in the diffuse interstellar medium (ISM), where they are broken up into many ultrasmall silicate fragments. The resulting species will likely range in size from the atomic scale (e.g. metal ions) to molecular and nanoscales (e.g. silicate nanoclusters with a few 10/100s of atoms). Due to their reduced size, even if such grains constitute a small mass percentage of the dust budget, they should form a highly numerous population with potential for seeding (re)growth of dust and influencing astrochemical processes. Here, we assess the structures, spectroscopic properties and astronomical relevance of such nanosilicates by employing accurate theoretical modelling [1] and cluster beam experiments [2]. By considering the distinct infrared (IR) spectra of nanosilicates with respect to that of larger silicate grains, we also predict that nanosilicate populations should be observable with the James Webb Space Telescope (JWST) [3]. These predictions will be compared with our latest JWST observations [4].

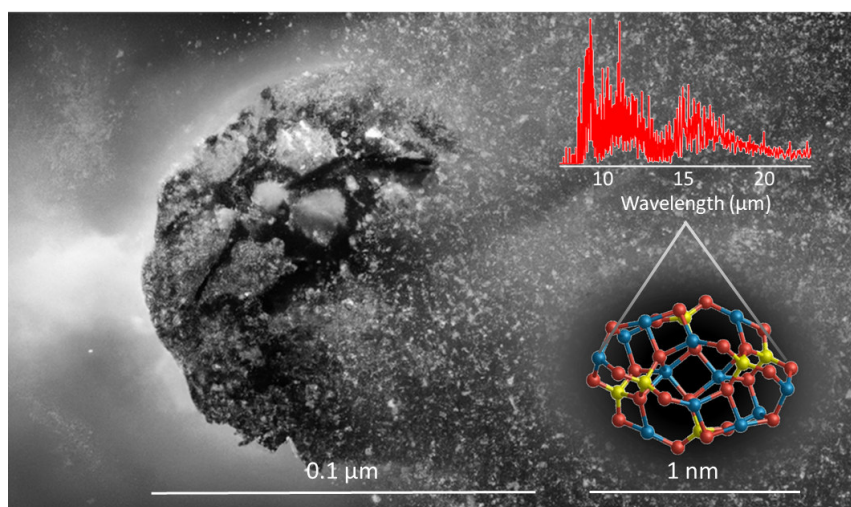


Figure 1: Energetic processing of a silicate dust grain into nanoclusters in the interstellar medium.

- [1] A. Macia Escatller, Tomas Lazaukas, S. M. Woodley, S. T. Bromley, Structure and Properties of Nanosilicates with Olivine (Mg_2SiO_4)_N and Pyroxene (MgSiO_3)_N Compositions ACS Earth and Space Chem. 2019, 3, 2390.
- [2] J. Mariño Guu, B-A. Ghejan, T. M. Bernhardt, J. M. Bakker, S. M. Lang, S T. Bromley, Cluster Beam Study of (MgSiO_3)⁺-Based Monomeric Silicate Species and Their Interaction with Oxygen: Implications for Interstellar Astrochemistry, ACS Earth Space Chem. 2022, 6, 10, 2465–2470,
- [3] S. T. Zeegers, J. Mariño Guu, F. Kemper, J. P. Marshall, S. T. Bromley, Predicting observable infrared signatures of nanosilicates in the diffuse interstellar medium, Faraday Discuss., 2023 - doi.org/10.1039/D3FD00055A.
- [4] Zeegers et al. Illuminating the dust properties in the diffuse ISM with JWST, 2021, JWST Proposal. Cycle 1, ID. #2183.

Exploring Structures and Properties of Carbon Clusters – Chains, Rings and Fullerenes

Evan Bieske, Sam Marlton, Chang Liu

School of Chemistry, University of Melbourne, Australia

Carbon possesses a remarkable ability to form molecules, clusters and solids with diverse and interesting architectures. Recently we have explored the structures and electronic properties of charged carbon clusters (C_n^+) and hydrogenated carbon clusters ($C_nH_m^+$) containing fewer than 60 carbon atoms through electronic spectroscopy [1,2]. Ion mobility studies show that with increasing size, carbon clusters progressively adopt structures as linear chains (for $n < 2-9$), rings ($n \geq 7$), bi-rings ($n \geq 22$) and fullerenes ($n \geq 30$), with some evidence for graphene structures for larger sizes. One of the challenges for spectroscopic studies is the coexistence of isomers for some sizes. For example, C_{36}^+ has ring, bi-ring and fullerene isomers. To address this challenge, we separate clusters according to size and shape before interrogating spectroscopically them in a cryogenically cooled ion trap. We will present and discuss electronic spectra of C_n^+ and $C_nH_m^+$ clusters, following the evolution of the clusters' properties with size, and consider the possible existence of the clusters in interstellar space.

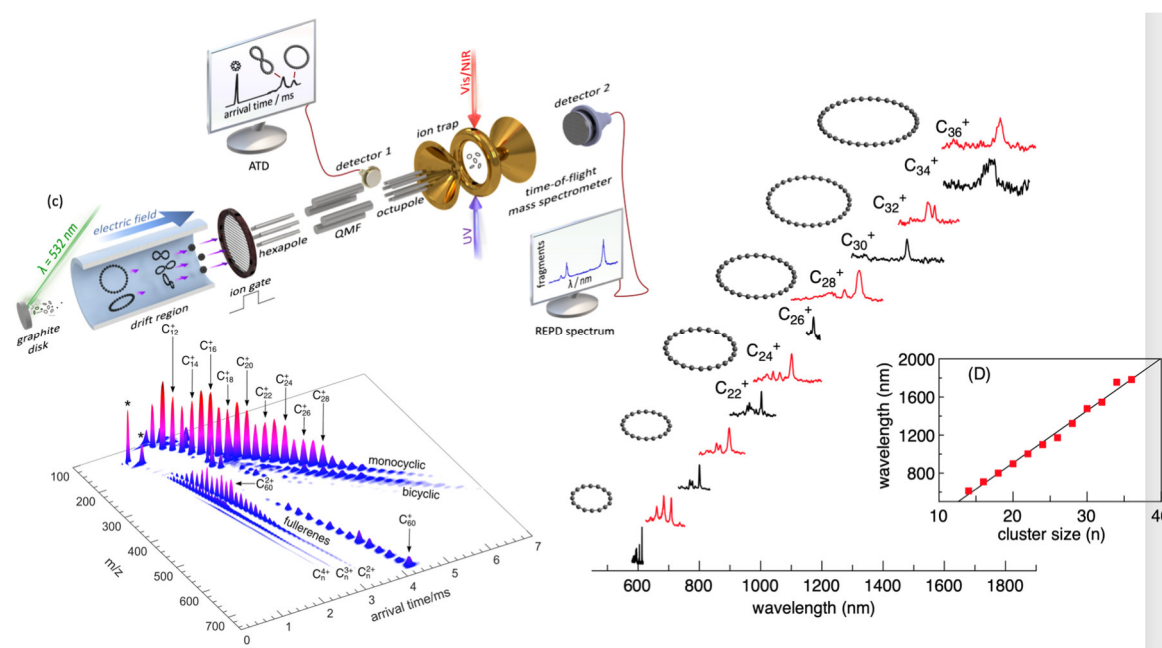


Figure 1: Apparatus for obtaining isomer-selected electronic spectra (top left), ion mobility mass spectrum (bottom left), and electronic spectra of C_n^+ rings in the visible and near IR (right).

- [1] S. J. P. Marlton, et al. Probing Colossal Carbon Rings J. Phys. Chem. **127** (2023) 1168–1178.
- [2] S. J. P. Marlton, et al. Disentangling Electronic Spectra of Linear and Cyclic Hydrogenated Carbon Cluster Cations, $C_{2n+1}H^+$ ($n = 3-10$). J. Phys. Chem. **126** (2022) 6678–6685.

Laboratory infrared characterization of gas-phase sulfur clusters: solving the astronomic sulfur puzzle?

Piero Ferrari,¹ Giel Berden,¹ Laurens B. F. M. Waters,^{1,2} Britta Redlich,¹ Joost M. Bakker¹

¹ HFML-FELIX, Radboud University, Nijmegen, Netherlands

² Department of Astrophysics, Radboud University, Nijmegen, Netherlands

Compared to diffuse interstellar environments and photon-dominated regions in space, the atomic sulfur concentration in dense molecular clouds and planet forming disks is depleted by a factor of 100 [1,2]. In contrast, abundant sulfur was recently detected in the atmosphere of an exoplanet [3], showing the efficient incorporation of sulfur into forming planets. In this respect, the chemical pathway of sulfur from diffuse interstellar regions, through clouds to planets, remains elusive and is often referred to as the *sulfur puzzle*. Hypotheses to account for the missing atomic sulfur include the formation of sulfur-bearing molecules, although the concentration of sulfur-based molecules currently observed in space is far from sufficient to account for all atomic S loss [4], or the embedding of sulfur in grain mantles at low temperatures and high densities [5]. A third alternative is the formation of sulfur clusters, but a fundamental step to elucidate on this possibility is relevant spectroscopic data. Here we show the first experimental far-IR spectra of neutral and charged (anionic and cationic) sulfur clusters, employing the light provided by the free electron laser FELIX (Nijmegen, The Netherlands). The experimental spectra of the investigated species show a remarkably good agreement with quantum chemical calculations, allowing us to predict abundance limits for detection with the recently commissioned James Webb Space Telescope (JWST). This could spur a targeted observational search of sulfur clusters, and the possibility of solving the sulfur mystery in dense molecular clouds and star-forming regions.

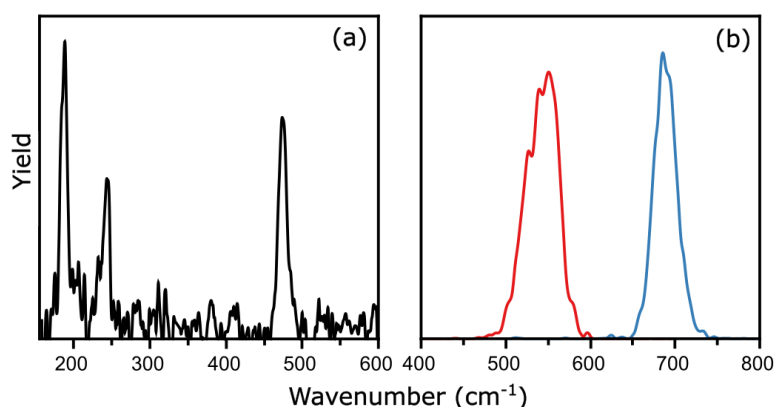


Figure 1: Infrared spectrum of S_8 (a), S_4^+ (b, blue) and S_4^- (b, red).

- [1] D. V. Mifsud, Z. Kaňuchová, P. Herczku, S. Ioppolo, Z. Juhász, S. T. S. Kovács, N. J. Mason, R. W. McCullough, B. Sulik, Space Sci. Rev. **217** (2021) 14.
- [2] Le Gal, R., et al. : 2021 ApJS 257, 12
- [3] S.-M. Tsai et al., Nature **617** (2023) 483.
- [4] J. R. Goicoechea, A. Aguado, S. Cuadrado, O. Roncero, J. Pety, E. Bron, A. Fuente, D. Riquelme, E. Chapillon, C. Herrera, C. A. Duran, A&A **647** (2021) A10.
- [5] Cazaux, S. et al.: 2022 A&A 657, A100

Reaction of Size-Selected Iron-Oxide Cluster Cations with Methane: A Model Study of Chemical Processes in Mars' Atmosphere

M. Arakawa,¹ S. Kono,¹ Y. Sekine,² A. Terasaki¹

¹ Department of Chemistry, Faculty of Science, Kyushu University, Japan

² Earth-Life Science Institute, Tokyo Institute of Technology, Japan

Small particles and clusters of minerals such as silicate (e.g., (Mg,Fe)SiO₃ and (Mg,Fe)₂SiO₄), and silica (SiO₂) are among the most abundant materials in space. It is prevalent hypothesis that, in the early stage of planetary formation, such materials contribute to chemical processes such as formation of organic molecules. Size-selected gas-phase clusters provide a good model for this chemistry, because it is possible to investigate reactions step by step with precise control in the number of atoms and molecules involved in the reaction. Furthermore, it has recently been suggested that silica and silicate clusters could be highly abundant in the interstellar medium [1,2]. In this context, we have reported reactions of gas-phase free silicate, MgSiO_m⁻, and silica, Si_nO_m⁻, cluster anions with CO and H₂O molecules [3,4]. In addition, coadsorption and subsequent reaction of CO and H₂ molecules on cobalt cluster cations, Co_n⁺, has been examined to discuss formation of organic molecules on the cluster [5].

Another chemical process attracting much attention recently is rapid methane loss in the atmosphere of Mars [6]. Observation by the Curiosity rover found temporary spikes of methane and its rapid loss, but the mechanism of the loss has not been clarified yet. Mars' soil is rich in iron oxide, and storms of iron-oxide particles (dust devils) occur very frequently. Because the iron-oxide cluster, Fe₂O₂, is known as an active center of enzyme, methane monooxygenase, we hypothesized that iron-oxide particles/clusters were responsible for the rapid loss. Numerous theoretical studies on the interaction of Fe₂O₂ with methane have been reported [7]. As for an experimental study, FeO⁺ was reported to mediate activation of methane [8]. In the present study, we report gas-phase reaction of size-selected iron-oxide cluster cations, Fe_nO_m⁺, with methane, CH₄, and deuterated methane, CD₄, molecules to verify our hypothesis, where methane activation was observed to produce Fe_nO_mCH₂⁺ and Fe_nO_mC⁺. The reactivity exhibited size dependence. For example, the rate coefficients of the methane activation for Fe₃O⁺ and Fe₄O⁺ were estimated to be 1×10^{-12} and 3×10^{-12} cm³ s⁻¹, respectively [9]. Based on these values, the presence of iron-oxide clusters/particles of 4×10^6 cm⁻³ (10^{-14} Pa) in Mars' atmosphere would explain the loss of methane.

[1] A. C. Reber, S. Paranthaman, P. A. Clayborne, S. N. Khanna, and A. W. Castleman, Jr., *ACS Nano* **2** (2008) 1729

[2] J. M. Guieu, B.-A. Ghejan, T. M. Bernhardt, J. M. Bakker, S. M. Lang, S. T. Bromley, *ACS Earth Space Chem.* **6** (2022) 2465

[3] M. Arakawa, R. Yamane, A. Terasaki, *J. Phys. Chem. A* **120** (2016) 139

[4] M. Arakawa, T. Omoda, A. Terasaki, *J. Phys. Chem. C* **121** (2017) 10790

[5] M. Arakawa, D. Okada, S. Kono, A. Terasaki, *J. Phys. Chem. A* **124** (2020) 9751

[6] C. R. Webster et al., *Science* **360** (2018) 1093

[7] K. Yoshizawa, T. Yumura, *Chem. Eur. J.* **9** (2003) 2347

[8] D. Schröder, H. Schwarz, *Angew. Chem. Int. Ed.* **29** (1990) 1433

[9] M. Arakawa, S. Kono, Y. Sekine, A. Terasaki, in preparation

Water oxidation reaction in natural photosynthesis catalyzed by the Mn_4CaO_5 cluster

Junko Yano

*Molecular Biophysics and Integrated Bioimaging Division,
Lawrence Berkeley National Laboratory, USA*

The water oxidation reaction in Photosystem II (PS II) produces most of the molecular oxygen in the atmosphere, which sustains life on Earth, and in this process releases four electrons and protons that drive the downstream process of CO_2 fixation in the photosynthetic apparatus. The catalytic center of PS II is an oxo-bridged Mn and Ca complex (Mn_4CaO_5) which is oxidized progressively upon the absorption of light by the reaction center chlorophylls of PS II, and the accumulation of four oxidative equivalents in the catalytic center. It results in the oxidation of two waters to dioxygen in the last step. X-ray free-electron lasers (XFEL) with intense femtosecond X-ray pulses has opened opportunities to visualize this reaction in PS II as it proceeds throughout the catalytic cycle. The method reveals notable structural changes during the catalytic cycle, including the insertion of O_x from a new water molecule, which disappears upon the completion of the reaction, implicating it in the O-O bond formation reaction [1-3]. We are also able to follow the structural dynamics of the ligand environment of the cluster and of channels within the protein important for substrate and product transport. It reveals well-orchestrated conformational changes in response to the electronic changes at the Mn_4Ca cluster.

We summarize our recent structural and spectroscopy studies of the catalytic reaction in PS II by following the structural changes along the reaction pathway under functional conditions.

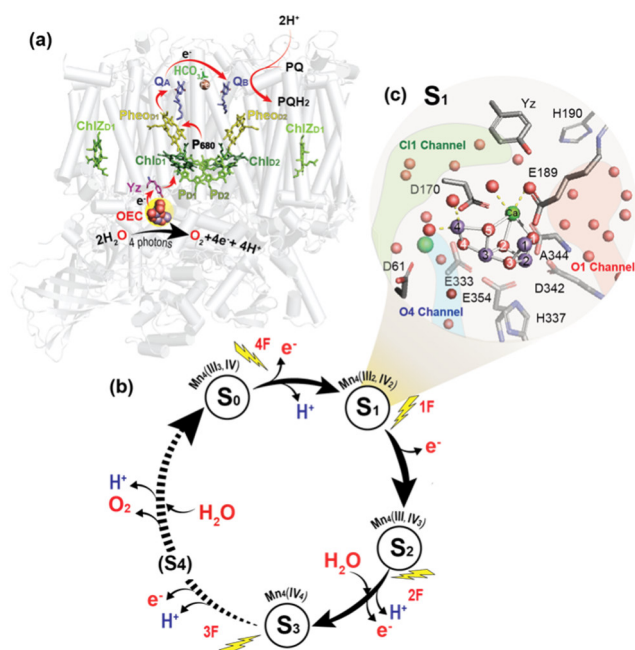


Figure 1: Water oxidation reaction in Photosystem II. (a) Electron transfer chain in PS II. (b) Kok cycle: S-state transition of the catalytic center during the reaction. (c) The structure of the Mn_4CaO_5 cluster in the S_1 state.

[1] M. Ibrahim et al., Proc. Natl. Acad. Sci. U.S.A. **117** (2020) 12624–12635.

[2] R. Hussein, et al. Nature Comm. **12** (2021) 6531. [3] A. Bhowmick, et al. Nature **617** (2023) 629–636.

Reduction and Biosorption of silver nanoparticles by bacteria

Nouari Kébaïli¹, Reem Tambosi¹, Soufian Ouchane²

¹ Laboratoire Aimé Cotton LAC, CNRS, Université Paris Saclay, France

² I2BC, CNRS, CEA, Université Paris Saclay, France

Successful use of bacteria in heavy metal remediation depends on their resistance to toxic metals and their ability to reduce and trap metal ions. The current study provides, using SEM, TEM and AFM, new insight into the ability of *R. gelatinosus* (and *E. coli*) cells to reduce silver (Ag^+) and trap silver nanoparticles (Ag-NPs) at their surface. According to EDX spectra analysis of whole cells, the Ag-NPs correspond mostly to silver chloride. Size distribution suggested several, may be competitive, stochastic nucleation processes. Together with the efflux system, this biosorption activity should function as part of the survival strategy allowing cells to withstand metal poisoning.

Like studies showing differential antibiotic susceptibility and the presence of subpopulations within planktonic or bacterial biofilms, we found that only a small subpopulation of cells had the ability of Ag^+ removal through the biosorption of Ag-NPs and act as scavengers and first defense line. We hypothesized that this striking phenotype was very likely related to metabolic heterogeneity introduced by variability in the physiological state of cells within the population. Future breakthroughs in bioremediation efforts will rely on the ability to separate subpopulations and the full characterization of the molecular components or factors involved in NPs biosorption.

Identifying those factors could be exploited to target metal nanomaterials to specific bacterial cells. On one hand, we disposed of probes for phenotypic heterogeneity, and on the other hand, hacking this defense mechanism can also allow nanoparticle bio-design using bacteria.

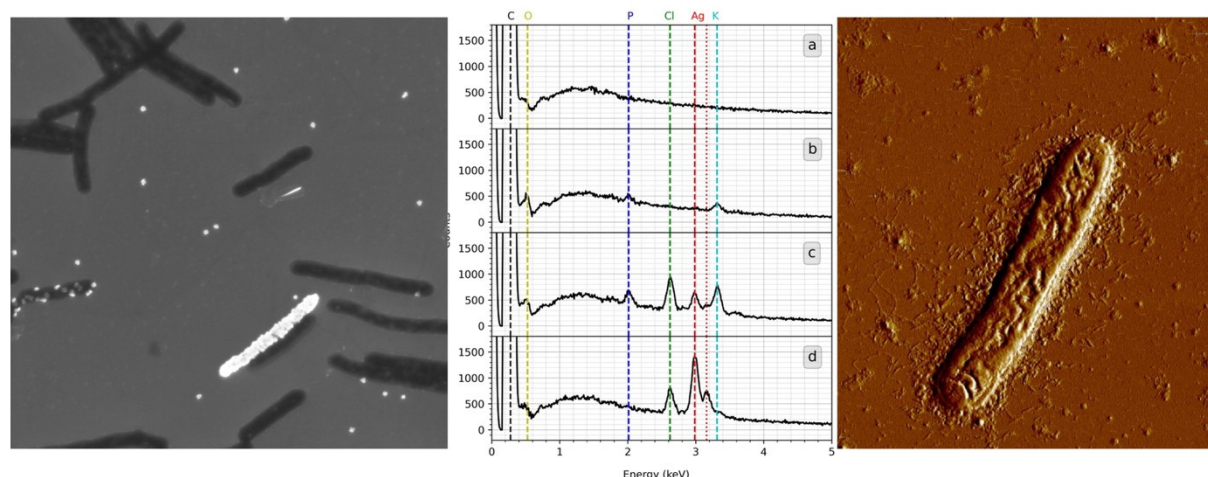


Figure 1: SEM, AFM images and EDS spectra of silver nanoparticles and bacteria interaction

Chiral metal clusters: efficient and accurate computational approaches for plasmons, Circular Dichroism and ligand dynamics

Mauro Stener¹, Alessandro Fortunelli²

¹*Dipartimento di Scienze Chimiche e Farmaceutiche, Trieste University, Via L. Giorgieri 1, 34127 Trieste, Italy, e-mail: stener@units.it*

²*CNR-ICCOM, Consiglio Nazionale delle Ricerche, via G. Moruzzi 1, 56124, Pisa, Italy.*

We have employed Time-Dependent Density Functional Theory (TDDFT) simulations using the polTDDFT implementation [1] within the AMS program, to assess various optical properties of chiral metal clusters. We start with a series of chiral gold nanowires to explore whether an enhancement of circular dichroism at the plasmon resonance is possible and identify its quantum mechanical origin [2]. We find that in linear chiral nanowires the dichroic response is suppressed by destructive interference of nearly degenerate components with opposite signs. This points to this phenomenon as a common and likely origin of the difficulty encountered so far in achieving a plasmonic CD response in experiment and suggesting nevertheless that these opposite components could be “decoupled” by using multiwall arrangements. In contrast, we predict a giant dichroic response for nanowires with three-dimensional helical coiling. Moreover, the effects of the conformational dynamics of 2-PET protective ligands on the electronic circular dichroism (ECD) of the chiral $\text{Au}_{38}(\text{SC}_2\text{H}_4\text{Ph})_{24}$ cluster are investigated [3]. We adopt a computational protocol in which ECD spectra are calculated at the TDDFT level on a series of conformations extracted from MD simulations by using the Essential Dynamics (ED) analysis, and then properly weighted to predict the final spectrum. This result unambiguously demonstrates the need to account for the conformational effects in the ECD modeling of chiral protected nanoclusters.

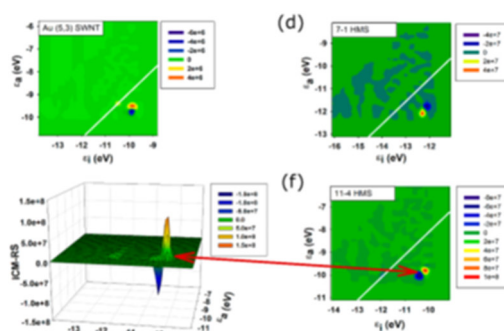


Figure 1: Analysis of the plasmonic CD signal in a gold nanowire.

- [1] O. Baseggio, G. Fronzoni and M. Stener, J. Chem. Phys. **143** (2015) 024106.
- [2] D. Toffoli, A. Russi, G. Fronzoni, E. Coccia, M. Stener, L. Sementa and A. Fortunelli, J. Phys. Chem. Lett. **12** (2021) 5829.
- [3] JM. Monti, G. Brancolini, E. Coccia, D. Toffoli, A. Fortunelli, S. Corni, M. Aschi, and M. Stener, J. Phys. Chem. Lett. **14** (2023) 1941.

Ultrafast Dynamics of Mass-selected Neutral Silver Clusters Probed by Femtosecond NeNePo Spectroscopy

Jiaye Jin¹, Max Grellmann,¹ Marcel Jorewitz,¹ Knut R. Asmis,¹

¹ *Wilhelm-Ostwald Institute für Physikalische und Theoretische Chemie, Universität Leipzig, Linnéstr. 2, 04103 Leipzig, Germany*

Silver clusters possess remarkable photoelectric and catalytic properties, making them a subject of current research. The studies on isolated clusters in the gas phase provides information on the inherent cluster properties in the absence of a perturbing environment. Here, we report our new setup and results on electronic-state-selected vibrational wave packet dynamics for mass-selected neutral silver clusters that allow us to obtain detailed information on molecular vibrations, including harmonic and anharmonic constants, in the femtosecond time domain as well as in the far-IR spectral range. For this purpose, we use a cryogenic ion-trap tandem mass spectrometer together with a femtosecond laser system [1] to perform femtosecond pump-probe spectroscopy involving with the negative-neutral-positive excitation scheme (fs-NeNePo).[2,3] The excitation scheme is shown in Figure 1.

We will present results on the vibrational wave packet dynamics of the ground electronic state $X^1\Sigma_g^+$ of the neutral silver dimer $^{107}\text{Ag}^{109}\text{Ag}$ and the ground state \tilde{X}^1A_g of the rhombic neutral silver tetramer Ag_4 . Frequency analysis of the fs-NeNePo spectra yields the harmonic frequency ($\omega_e = 192.3 \text{ cm}^{-1}$) as well as quadratic ($\omega_e x_e = 0.644 \text{ cm}^{-1}$) and cubic ($\omega_e y_e = 4 \cdot 10^{-4} \text{ cm}^{-1}$) anharmonic terms for the $X^1\Sigma_g^+$ state of silver dimer with high accuracy.[1] The frequency spectra of rhombic Ag_4 show dynamics mainly involving the four vibration modes ν_1 (189.1 cm^{-1}), ν_2 (112.4 cm^{-1}), ν_5 (81.2 cm^{-1}) and ν_6 (32.0 cm^{-1}). We also find a dependence of the transient spectra on the pump wavelength, trap temperature and the relative polarization of the two pulses. These valuable results reveal metal-metal bond vibrations on a specific potential energy surface governing the dynamics of mass-selected, neutral, and tag-free clusters at variable temperatures. Furthermore, fs-NeNePo spectroscopy promises new insights into the photoexcitation mechanics and the energy dissipation in a femtosecond time scale.

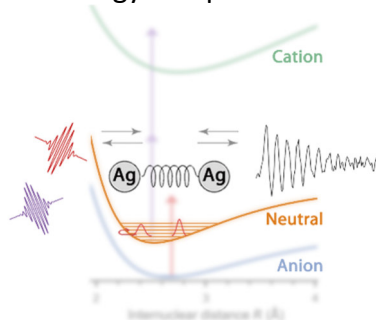


Figure 1: Experimental excitation scheme and concept of electronic-state-selected vibrational wave packet dynamics of mass-selected neutral metal clusters probed by fs-NeNePo spectroscopy.

- [1] J. Jin, M. Grellmann, K. R. Asmis, Phys. Chem. Chem. Phys. (2023), in peer review.
- [2] S. Wolf, G. Sommerer, S. Rutz, E. Schreiber, T. Leisner, L. Wöste, Phys. Rev Lett. **74** (1995), 4177.
- [3] L.D. Socaciu-Siebert, J. Hagen, J. Le Roux, D. Popolan, M. Vaida, S. Vajda, T.M. Bernhardt and L. Wöste, Phys. Chem. Chem. Phys., **7**,(2005), 2706.

- 09:00 **Richard Palmer** (INV 12)
Nanoclusters in the real world: Insights into deposited clusters from aberration-corrected electron microscopy
- 09:40 **Beatriz Roldán Cuenya** (INV 13)
From single atoms to clusters and nanoparticle catalysts in energy conversion
- 10:20 **Christine Mottet** (INV 14)
General tendencies of chemical ordering in Pt-based nanoalloys
- 11:00 **Gunther Andersson** (HT 12)
Atomic layer deposited overlayers on metal clusters
- 11:20 Lunch
- 13:20 Conference Excursion
- 19:30 Evening Event (Museum of Natural History Berlin)

Nanoclusters in the real world: Insights into deposited clusters from aberration-corrected electron microscopy

Richard E. Palmer

Nanomaterials Lab, Swansea University, Bay Campus, Swansea SA1 8EN

R.E.Palmer@swansea.ac.uk
swanseanano.uk

Compared with the notional case of an isolated cluster (nanoparticle) at $T=0$, as addressed in some foundation theoretical treatments, two key factors will shape the behaviour of clusters in the real world where we make experimental measurements. (i) The radiative environment (including the sample temperature and interaction with charged beams) and (ii) the material environment (including pressure/reactive gas and support). We will discuss four examples of the influence of these (coupled) factors; much of the work is unpublished.

- (1) Aberration-corrected electron microscopy at variable elevated temperature probes the melting and **isomeric energy differences** of arrays of size-selected gold clusters bound to point defects on a carbon surface (while subject to irradiation by 200keV electrons) [1,2]. This is pre-Covid work forms a brief basis for the talk.
- (2) **Video imaging of a single** deposited gold cluster on carbon at room temperature shows dynamic fluctuations between competing structures (isomers). Measurements at variable temperature enable equilibrium properties, branching ratios and relative barrier heights in the potential energy surface to be explored. The first such measurements will be reported.
- (3) A study of 1 nm silver clusters (on carbon) compares clusters stored in vacuum versus those **exposed to ambient** before TEM. The work shows dramatic differences in the isomer proportions (fcc dominant versus 1h dominant), probably due to the effect of sulphur contaminants on the structural energetics [3].
- (4) The role of the support is probed by studies of Au clusters assembled on carbon from sputtered gold atoms, where the transition from 2D to 3D morphology versus size appears to be delayed substantially compared with the free cluster. For Pt₁₃₀ clusters on cerium oxide, the 2D versus 3D competition depends on **which facet** of ceria supports the cluster.

If time allows, I will briefly report progress on the scale-up of cluster beam deposition towards the levels required for bespoke industrial manufacturing in vacuum. For example, implantation of lead clusters from the scaled-up MACS cluster beam into porous carbon creates an electrode architecture, illustrated by electrochemical generation of oxidising species for water treatment [4].

References

1. D.M. Foster, R. Ferrando, R.E. Palmer, Nature Comms. **9** 1323 (2018).
2. D.M. Foster, T. Pavloudis, J. Kioseoglou, R.E. Palmer, Nature Comms. **10** 2583 (2019).
3. J. Vernieres, N. Tarrat, S. Lethbridge, E. Watchorn-Rokutan, T. Slater, D. Loffreda, R.E. Palmer, Communications Chemistry **6** 19 (2023).
4. E. Kazimierska, Y. Niu, J. McCormack, C. Tizaoui, R.J. Cobley, R.E. Palmer, J. Nanoparticle Research **25** 1 (2023).

From Single Atoms to Clusters and Nanoparticle Catalysts in Energy Conversion

B. Roldan Cuenya

Department of Interface Science, Fritz Haber Institute, Berlin, Germany

Climate change concerns have spurred a growing interest in developing environmentally friendly technologies for energy generation. These include green H₂ production from water splitting and hydrocarbons and alcohols from the electrochemical reduction of CO₂ (CO₂RR). The latter offers an additional possibility to store renewable energy into chemical bonds.

Rational catalyst optimization requires however detailed knowledge on their structure and surface composition under reaction conditions, since even morphologically and chemically well-defined single atom, cluster and nanoparticle (NP) pre-catalysts will be susceptible to drastic modifications while at work.

This talk will provide insight into electronic, structural and chemical state transformations taking place during the oxygen evolution reaction (OER) over cobalt oxide clusters (Co₁-Co₂₀) and CoO_x(OH)_y NPs (1-9 nm) at alkaline pH and the CO₂RR over Metal-N-C (M= Cu, Co, Ni, Fe, Sn, Zn) single atom electrocatalysts. Here I will elaborate on the active state formation and the correlation between the evolving structure and composition of the electrocatalysts under working conditions and their electrocatalytic performance. Operando surface-sensitive X-ray photoelectron spectroscopy combined with X-ray absorption spectroscopy will be utilized to unveil reversible and irreversible changes in the geometric and electronic structure of our low dimensional catalysts during electrocatalysis, as well as their interaction with adsorbates and reaction intermediates. Our results are expected to open up new routes for the reutilization of CO₂ through its direct conversion into industrially valuable chemicals and fuels and the electrocatalytic generation of green H₂.

General tendencies of chemical ordering in Pt-based nanoalloys

Christine Mottet¹, Alexis Front²

¹CINaM – CNRS / Aix Marseille University, France

²Department of Chemistry and Materials Science, Aalto University, Finland

Pt-based nanoalloys are very promising as electrocatalysts for fuel cells [1] because the addition of a second metal reduces the costs for commercialization and in the same time improves the selectivity and durability, for example by suppressing CO poisoning. The catalytic activity depends on the shape, the atomic structure and the chemical arrangement of the two metals, this is what we model using numerical simulations and realistic interatomic potentials for Pt-(Pd, Co, Ag) nanoalloys.

Whereas Pt-Pd displays a Pd surface segregation and a Pt subsurface segregation keeping a mixed disordered core [2], the Co-Pt nanoparticles can present chemically ordered phases [3] which are proven to be more reactive than the disordered one [4].

We also considered Ag-Pt systems for which Ag surface segregation restrains the ordered phase to extend at large size [5]. We predict original chemical arrangements depending on the precise chemical composition inside the nanoparticles [6], that have not been observed so far experimentally... It consists in a structure with concentric shells, which should appear at concentration near the one corresponding to the L1₁ ordered phase in the core (see Figure 1).

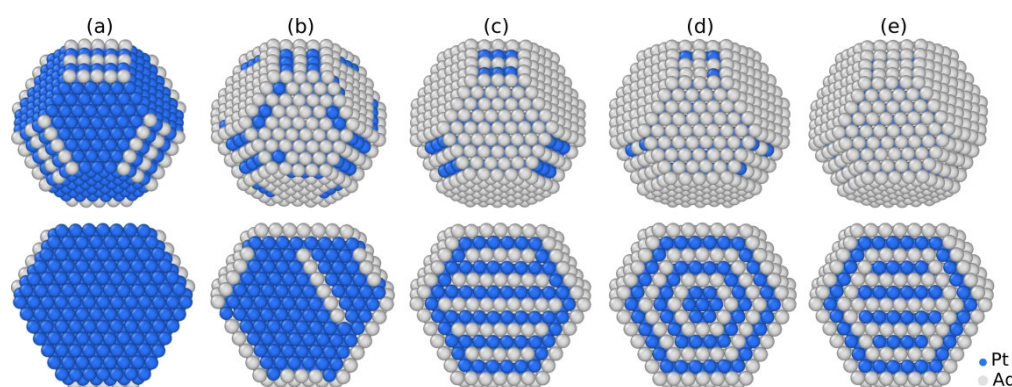


Figure 1: Snapshots of the TOh₁₂₈₉ at 200K with (a) 7 % of Ag, (b) 34 % of Ag, (c) 54 % of (d) 61 % of Ag and (e) 65 % of Ag. The top row represents the external surface, the bottom row displays a cutting view. Ag atoms are in grey and Pt atoms in blue

Multicomponent nanoalloys are also investigated as the ternary CoNiPt system.

- [1] X. Ren, Q. Li, L. Liu, B. Liu, Y. Wang, A. Liu, G. Wu, Sustainable Energy Fuels **4** (2020) 15.
- [2] A. De Clercq, S. Giorgio, C. Mottet, J. Phys.: Condens. Matter **28** (2016) 064006.
- [3] A. Front, C. Mottet, J. Phys. Chem. C **125** (2021) 16358.
- [4] M. Lebedeva, V. Pierron-Bohnes, C. Goyhenex, V. Papaefthimiou, et al., Electrochim. Acta **108** (2013) 605.
- [5] J. Pirart, A. Front, D. Rapetti, C. Andreazza-Vignolle, P. Andreazza, C. Mottet, R. Ferrando, Nature Communications **10** (2019) 1982.
- [6] A. Front, C. Mottet, Phys. Chem. Chem. Phys. **25** (2023) 8386.

Atomic Layer Deposited Overlayers on Metal Clusters

Mohammed Asiri^{1,2}, Arthaya Kai¹, G. F. Metha², G. G. Andersson¹

¹ *Flinders Centre for NanoScale Science and Technology, Flinders University, Australia*

² *Department of Chemistry, The University of Adelaide, Australia*

Metal clusters with a size of less than 100 atoms are suitable for modifying the electronic properties of semiconductor surfaces. [1, 2, 3] Metal clusters have been shown to be promising candidates as co-catalysts for photocatalytic water splitting due their discrete energy levels which depend on the number of atoms forming a cluster.[4] Size selected clusters with a specific number of atoms can be fabricated with a high degree purity either chemically or with gas phase cluster sources. However, using such clusters as co-catalysts requires implementing processes which suppress their agglomeration on catalyst surfaces. Atomic layer deposition (ALD) of thin coatings on top of surfaces covered with metal clusters has the potential to reduce the mobility of the clusters. The ALD layers must not be thicker than a few monolayers such that the discrete energy levels of the clusters make a contribution to the electronic structure of the surface. The key questions are a) what the minimum thickness of the coating is to reduce the mobility of the clusters and protect against agglomeration and b) whether the ALD coating grows on the substrate, the clusters or both.

In the present work we are investigating the deposition of Al₂O₃ coatings onto Au clusters which have been deposited onto TiO₂. Figure 1 shows concentration depth profiles measured with neutral impact collision ion scattering spectroscopy. The energy loss of the He projectiles increases with the layer thickness of the ALD layer and is around 2 Å for the 5 ALD layer deposited onto Au₁₀₁.

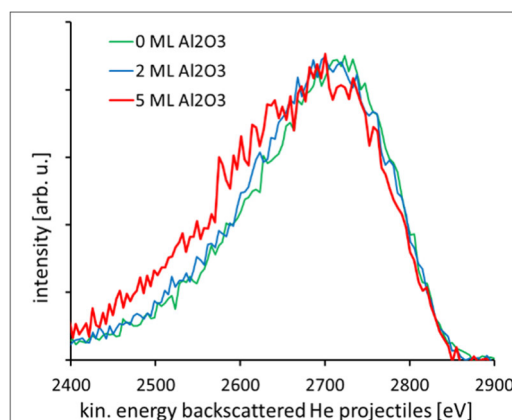


Figure 1: NCISS spectra for determining the layer thickness of the Al₂O₃ ALD layer on Au₁₀₁.

- [1] D. P. Anderson, J. F. Alvino, A. Gentleman, H. Al Qahtani, L. Thomsen, G. F. Metha, V. B. Golovko, and G. G. Andersson, PCCP 15, 3917 (2013).
- [2] G. G. Andersson, V. B. Golovko, J. F. Alvino, T. Bennett, O. Shipper, S. M. Mejia, H. Al Qahtani, R. Adnan, N. Gunby, D. P. Anderson, and G. F. Metha. J. Chem. Phys. 141, 014702 (2014).
- [3] G. Krishnan, H. S. Al Qahtani, J. Li, Y. Yin, N. Eom, V. B. Golovko, G. F. Metha, G. G. Andersson, J. Phys. Chem. C, 121, 28007 (2017).
- [4] W. Kurashige, R. Kumazawa, D. Ishii, R. Hayashi, Y. Niihori, S. Hossain, L. V. Nair, T. Takayama, A. Iwase, S. Yamazoe, T. Tsukuda, A. Kudo, Y. Negishi, J. Phys. Chem. C, 122, 13669 (2018).

- 09:00 **Francesca Baletto** (INV 15)
And yet it moves: dynamical processes at the nanoscale
- 09:40 **Yan Zhu** (INV 16)
Catalysis application in atomically precise metal clusters
- 10:20 **Joachim Sauer** (HT 13)
Effect of Fe and Co substitution on the structure and reactivity of $Al_8O_{12}^+$ cluster cations - a challenge for quantum chemistry
- 10:40 **Knut** HT 14)
Cryogenic ion trap vibrational spectroscopy of microhydrated $Fe_3O_4^+$: A gas phase model for iron oxide / water interactions
- 11:00 **Joost Bakker** (HT 15)
IR characterization of metal mediated methane coupling
- 11:20 Lunch
- 13:00 **Toshiharu Teranishi** (INV 17)
Transformations of inorganic nanocrystals by element substitution reactions
- 13:40 **Stefanie Dehnen** (INV 18)
Multinary clusters: Atomically-precise nanoobjects with uncommon properties
- 14:20 **Matthias Hillenkamp** (HT 16)
Are gold and silver miscible at the nanoscale?
- 14:40 **Akira Terasaki** (HT 17)
Probing orbital characters of silver and doped-silver cluster anions by photoelectron imaging spectroscopy
- 15:00 Coffee break
- 15:30 **Ruth Signorell** (INV 19)
Accelerated photochemistry within aerosol particles
- 16:10 **Denisia Popolan-Vaida** (HT 18)
Evolution of submicron organic aerosol particles produced in wildfires: Cloud condensation nuclei activity of fresh and aged vanillic acid aerosol particles
- 16:30 **Kit Bowen** (HT 19)
Electron-induced proton transfer (EIPT) and the nature of solvated electron-like clusters
- 16:50 **Olga Lushchikova** (HT 20)
Solvation of $Cu_n^{+/-}$ in He and H_2 at ultra-cold temperatures
- 17:30 **Poster Session B**

And yet it moves: dynamical processes at the nanoscale

Francesca Baletto

¹ Physics Dept., University of Milan Italy

We discuss a multiscale numerical approach, nanoCHE, to calculate in a fast and high-throughput fashion the current density and mass activity of individual isomers as well as to predict the activity of morphologically diverse but size-selected samples. From a structure-activity relationship based on a geometrical descriptor, which enables to distinguish and classify different isomers, Fig 1 depicts a 1-to-1 correspondence between isomers and activity. We apply nanoCHE to discuss the oxygen reduction activity of 1-3 nm Pt nanoparticles and nanosamples[1], both in the gas-phase and supported onto a MgO substrate[2] as the latter can induced significant structural rearrangements. We further discuss the extension of such multiscale approach to Cu nanoparticles and their ability in catalyzing CO₂ into methane [3]. In the latter, we discuss the effect of different formation processes likely to occur in various clusters sources.

1. K. Rossi et al., *ACS Cat.* **10** (2020) 3911
2. K. Rossi et al., *ChemPhysChem* **20** (2019) 3037
3. E. Gazzarini et al., *Nanoscale* **13** (2021) 5857

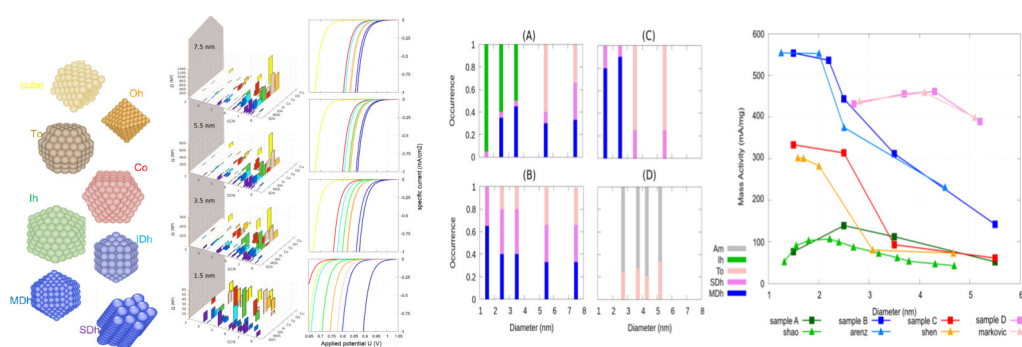


Figure 1: Characterisation of nanoparticle's shapes following the atop generalised coordination number and their corresponding activity, calculated using the nanoCHE model. ORR-mass activity of various Pt-nanosamples and their comparison with available experimental data. No adjustable parameters have been used only a different structural composition of the sample.

Catalysis Application in Atomically Precise Metal Clusters

Yan Zhu*

School of Chemistry and Chemical Engineering, Nanjing University, Nanjing 210093, China

*Email: zhuyan@nju.edu.cn

Atomically precise metal clusters with precise formulas and crystallographically determined structures, which can build a bridge between single atom and nanoparticles, become possible to unravel respective contributions of every atom in a cluster to its overall catalytic performances. This report is expected to provide a new scientific vision insight into catalytic conversion of CO₂ on atomically precise cluster catalysts, which is completely different from conversional nanoparticle or single-atom catalysts. The content will conclude recent advances of CO₂ electronic reduction catalyzed by Au clusters, chemical fixation of CO₂ into organic molecules, and CO₂ hydrogenation toward C₁ and C₂ products. It is anticipated that atomically precise metal cluster catalysts are promising alternatives to tackle the challenge of selectively converting CO₂ into high value products at an atomic-level.

Effect of Fe and Co substitution on the Structure and Reactivity of $\text{Al}_8\text{O}_{12}^+$ cluster cations - a challenge for quantum chemistry

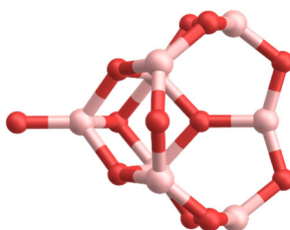
Stephen Leach,¹ Joachim Sauer,¹

Marcel Jorewitz,² Yake Li,² Sreekanta Debnath,² Arghya Chakraborty,² Knut R. Asmis²

¹ *Institut für Chemie, Humboldt-Universität, Unter den Linden 6, 10099 Berlin, Germany*

² *Wilhelm-Ostwald-Institut für Physikalische und Theoretische Chemie, Universität Leipzig, Linnéstrasse 2, 04103 Leipzig, Germany*

Transition metal substituted aluminium oxide clusters such as $\text{MAl}_7\text{O}_{12}^+$ ($\text{M}=\text{Fe}, \text{Co}$) are gas phase models for so-called “single atom catalysts” which have attracted increasing attention in recent years. Here, we deal with C–H bond activation by supported metal oxide catalysts and study the structure and reactivity of $\text{MAl}_7\text{O}_{12}^+$ clusters towards methane.



Comparison of calculated IR spectra (DFT, TPSSH functional) with the measured IR photo-dissociation spectra provides evidence that the substitution of Fe for Al in $\text{Al}_8\text{O}_{12}^+$ (Figure) is isomorphous, but accompanied by a change of the oxidation state on the transition metal, which converts the reactive terminal $\text{Al}-\text{O}^{\bullet-}$ bond into a non-reactive terminal $\text{M}=\text{O}$ double bond.

For $\text{M}=\text{Fe}$, the DFT predictions for the singlet and triplet states agree with experiments for both the IR spectrum and the reactivity towards methane, but these are not the lowest energy spin states. The lowest energy state is the quintet state for which the predicted IR spectrum does not agree with experiment. The results for $[\text{Al}_7\text{CoO}_{12}]^+$ are in line with those of $[\text{Al}_7\text{FeO}_{12}]^+$. This shows that Kohn-Sham density functional theory (DFT) is not predictive with regard to the relative stability of different spin states. Multi-reference wave-function calculations are required to correctly predict the lowest energy structure, but these cannot be converged for a system of this size. It is not sufficient to include into the active space the 3d states on M, and 2p states on the terminal O, the 2p states of the three other O atoms that are also bonded to the transition metal atom M cannot be ignored.

Cryogenic Ion Trap Vibrational Spectroscopy of Microhydrated Fe_3O_4^+ : A Gas Phase Model for Iron Oxide / Water Interactions

Fabian Müller,^{1,2,3} Florian A. Bischoff,¹ Joachim Sauer,¹ Matias R. Fagiani,^{2,3} Xiaowei Song,² Sreekanta Debnath,^{2,3} Sandy Gewinner,² Wieland Schöllkopf,² Knut R. Asmis³

¹ *Institut für Chemie, Humboldt-Universität zu Berlin, Germany*

² *Fritz-Haber-Institut der Max-Planck-Gesellschaft, Berlin, Germany*

³ *Wilhelm-Ostwald-Institut, Universität Leipzig, Germany*

Iron oxides, such as hematite ($\alpha\text{-Fe}_2\text{O}_3$) and magnetite (Fe_3O_4), are well known catalyst materials. Lately, there is also much interest in iron oxides as promising electrode materials for water splitting. In contrast to established noble metal catalysts, iron oxides are abundant, non-toxic, and adjustable in their redox properties. Their interaction with water is of great interest not only for the aforementioned applications but also for the understanding of dissolution and corrosion processes. However, investigating the reactivity of iron oxide surfaces towards water is a challenging task for both experiment and theory.

Here, we elucidate the structural changes upon microhydration of Fe_3O_4^+ , which serves as a computationally tractable gas phase model system, with up to four water molecules. To this end, we measure infrared photodissociation spectra and assign isomers based on the comparison with density functional theory simulations.[1,2] The initial oxygen-capped six-membered ring motif of bare Fe_3O_4^+ stays intact throughout the microhydration process. While the first three H_2O molecules dissociate upon adsorption, there is most likely molecular water attachment for the following one. The frequencies of the OH stretching vibrations associated with terminal and bridging hydroxyls are in excellent agreement with the results for surface OH species on hematite and magnetite. The calculated adsorption energies per H_2O molecule are much more exothermic than experimental reference value measured for iron oxide surfaces, which is attributed to the undercoordination of the cluster's iron sites comparable to oxygen defects in iron oxide surfaces.

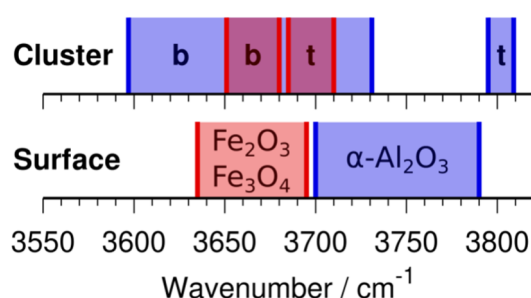


Figure 1: Spectral ranges of OH stretching vibrations (b: bridging, t: terminal) from cluster models (upper row) and surfaces (lower row). Red refers to iron oxide and blue to aluminum oxide systems.

- [1] M.R. Fagiani, X. Song, S. Debnath, S. Gewinner, W. Schöllkopf, K.R. Asmis, F.A. Bischoff, F. Müller, J. Sauer, J. Phys. Chem. Lett. **8** (2017), 1272.
- [2] F. Müller, J. B. Stückerath, F.A. Bischoff, L. Gagliardi, J. Sauer, S. Debnath, M. Jorewitz, K.R. Asmis, J. Am. Chem. Soc. **142** (2020) 18050.

IR characterization of metal mediated methane coupling

Joost M. Bakker¹, Frank J. Wensink¹, Peter B. Armentrout,²

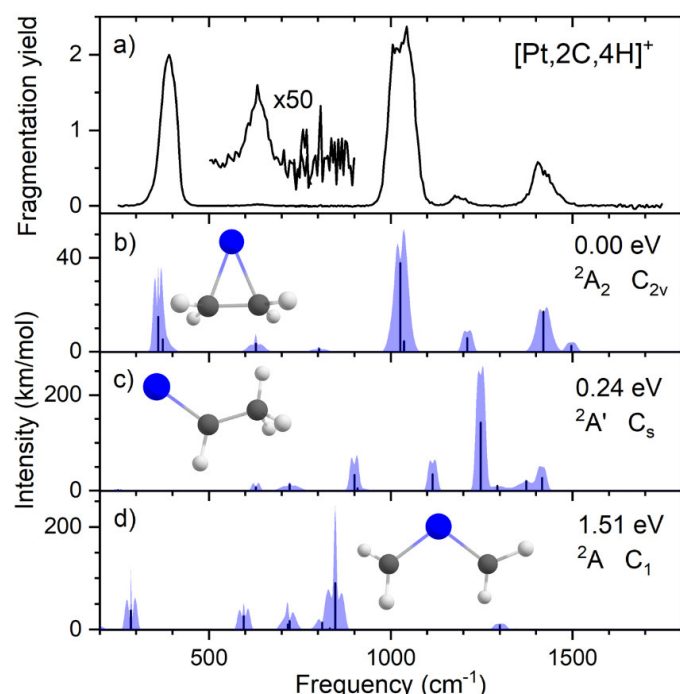
¹Radboud University, HFML-FELIX, Nijmegen, The Netherlands

²Department of Chemistry, University of Utah, Salt Lake City, United States

Large amounts of methane are present in natural gas, but its great stability hinders widespread utilization by the chemical industry. Conversion of methane requires a suitable, often transition metal-based catalyst. However, the reaction mechanism is often only poorly understood. To get insight in fundamental chemical interactions at the highest level of detail, we study the interaction between isolated metal ions and methane.

For this, we generate metal ions using laser vaporization and react them with methane in a radio-frequency ion trap. After the reaction we analyze the formed products via a combination of mass spectrometry and IR spectroscopy using the Free Electron Laser for IntraCavity Experiments FELICE. We elucidate product structures and reconstruct the reaction pathway by comparison with Density Functional Theory calculations.

In this contribution we focus on methane activation by Pt⁺ and Ru⁺ ions. Previously, it was shown that Pt⁺ ions can activate methane to form PtCH₂⁺.^[1] Here, we show how the subsequent reaction with more methane molecules leads to dehydrogenation and C–C coupling to form ethene on both Pt⁺ and Ru⁺ ions, and demonstrate the influence of pressure on the reaction outcome.^[2,3]



[1] V.J.F. Lapoutre, B. Redlich, A.F.G. van der Meer, J. Oomens, J.M. Bakker, A. Sweeney, A. Mookherjee, P.B. Armentrout, *J. Phys. Chem. A* **117** (2013), 4115

[2] O.W. Wheeler, M. Salem, A. Gao, J.M. Bakker, P.B. Armentrout, *J. Phys. Chem. A* **120** (2016) 6216

[3] F.J. Wensink, N. Roos, J.M. Bakker, P.B. Armentrout *Inorg. Chem.* **61** (2022), 11252

Transformations of Inorganic Nanocrystals by Element Substitution Reactions

Toshiharu Teranishi^{1,2}

¹ Institute for Chemical Research, Kyoto University, Japan

² Department of Chemistry, Graduate School of Science, Kyoto University, Japan

Elaborate chemical synthesis methods allow the production of various types of inorganic nanocrystals (NCs) with uniform shape and size distributions. Then, how can we synthesize NCs with thermodynamically metastable phases or very complex structures? The transformation of already-synthesized NCs via elemental substitutions, such as ion exchange reactions for ionic NCs [1-3] and galvanic replacement reactions for metal NCs [4], can overcome the difficulties facing conventional one-step syntheses. In particular, NC ion exchange reactions have been studied with numerous combinations of foreign ions and ionic NCs with various shapes. The functionality of the resulting ionic NCs, including semiconducting and plasmonic properties, can be easily tuned in a wide range, from the visible to near-infrared [5,6]. Here we focus on the full ion exchange reactions involving ionic NCs, highlighting important aspects such as the preservation of appearance and dimensions [7,8]. Finally, the formation of unprecedented Z3-type FePd₃ NCs by substituting a small amount of Pd with In is discussed on the basis of interelement miscibility among Fe, Pd, and In [9,10].

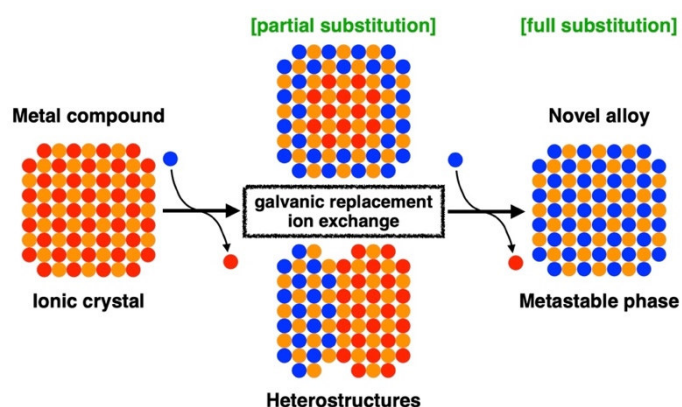


Figure 1: Formation of unprecedented NCs by using element substitution reactions.

- [1] M. Saruyama, R. Sato, T. Teranishi, *Acc. Chem. Res.* **54** (2021) 765–775.
- [2] M. Saruyama, T. Teranishi et al., *J. Am. Chem. Soc.* **133** (2011) 17598–17601.
- [3] S. Kim, M. Saruyama, T. Teranishi et al., *Chem. Sci.* **11** (2020) 1523–1530.
- [4] R. Sato, T. Teranishi et al., to be submitted.
- [5] Z. Lian, T. Teranishi et al., *J. Am. Chem. Soc.* **141** (2019) 2446–2450.
- [6] Z. Lian, T. Teranishi et al., *Nat. Commun.* **9** (2018) 2314.
- [7] H.-L. Wu, T. Teranishi et al., *Science* **351** (2016) 1306–1310.
- [8] Z. Li, M. Saruyama, T. Asaka, Y. Tatetsu, T. Teranishi, *Science* **373** (2021) 332–337.
- [9] K. Matsumoto, T. Teranishi et al., *Nat. Commun.* **13** (2022) 1047.
- [10] K. Matsumoto, R. Sato, T. Teranishi, *Trends Chem.* **5** (2023) 201–213.

Multinary Clusters: Atomically-Precise Nanoobjects with Uncommon Properties

Stefanie Dehnen¹

¹ Karlsruhe Institute of Technology, Institute of Nanotechnology, Herrmann-von-Helmholtz-Platz 1, 76344 Eggenstein-Leopoldshafen, Germany

The art of synthesis and numerous exciting properties have stimulated and inspired research in the field of cluster compounds worldwide. In particular, multinary clusters comprising main group metal atoms and one or two further components – further (semi)metal atoms or organic substituents – have attracted interest in recent times. The most obvious feature is the wide variety of different cluster compositions and architectures, but the resulting materials do also show unexpected functionalities that are promising in terms of practical applications.^[1-4]

While there are many different approaches to multinary clusters, our access makes use of binary precursor units of p-block elements in a coordination-chemical manner, with or without rearrangement of such units during cluster formation. Depending on the elemental composition, the products belong to the family of metallide clusters with metal atoms adopting negative charges,^[3] or form metalate architectures with metal atoms in positive oxidation states,^[4] which fundamentally affects the chemical and physical properties of the compounds. Multimetallic clusters like $[\text{An}@\text{Bi}_{12}]^{3-}$ ($\text{An} = \text{U}, \text{Th}$),^[5,6] $[\text{K}_2\text{Zn}_{20}\text{Bi}_{16}]^{6-}$,^[7] $[\text{Zn}_3(\text{Ge}_3\text{As})_4]^{6-}$,^[8] $[\{(\text{cod})\text{Ru}\}_4\text{Bi}_{18}]^{4-}$,^[9] or $[\{\text{CpRu}\}_3\text{Bi}_6]^-$,^[10] serve to study structural variations and help to gain new insights into cluster formation as well as uncommon electronic structures and bonding modes. In addition, they are promising candidates for cluster-based catalysis or precursors for new intermetallic nanostructures.

- [1] J. Zhang, X. Bu, P. Feng, T. Wu, *Acc. Chem. Res.* **53** (2020) 2261.
- [2] J.E. McGrady, F. Weigend, S. Dehnen, *Chem. Soc. Rev.* **51** (2022) 628.
- [3] R.J. Wilson, N. Lichtenberger, B. Weinert, S. Dehnen, *Chem. Rev.* **119** (2019) 8506.
- [4] N.W. Rosemann, J.P. Eußner, A. Beyer, S.W. Koch, K. Volz, S. Dehnen, S. Chatterjee, *Science* **352** (2016) 1301.
- [5] A.R. Eulenstein, Y.J. Franzke, N. Lichtenberger, R.J. Wilson, L. Deubner, F. Kraus, R. Clérac, F. Weigend, S. Dehnen, *Nat. Chem.* **13** (2021) 149.
- [6] N. Lichtenberger, R.J. Wilson, A.R. Eulenstein, W. Massa, R. Clérac, F. Weigend, S. Dehnen, *J. Am. Chem. Soc.* **138** (2016) 9033.
- [7] A.R. Eulenstein, Y.J. Franzke, P. Bügel, W. Massa, F. Weigend, S. Dehnen, *Nat. Commun.* **11** (2020) 5122.
- [8] S. Wei, B. Peerless, L. Guggolz, S. Mitzinger, S. Dehnen, *Angew. Chem. Int. Ed.* **62** (2023) e202303037.
- [9] F. Pan, S. Wei, L. Guggolz, A.R. Eulenstein, F. Tambornino, S. Dehnen, *J. Am. Chem. Soc.* **143** (2021) 7176.
- [10] B. Peerless, A. Schmidt, Y.J. Franzke, S. Dehnen, *Nat. Chem.* **15** (2023) 347.

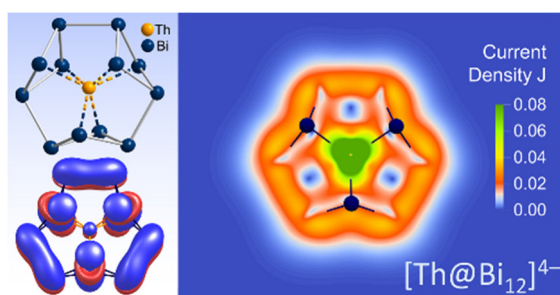


Figure 1: Th^{4+} -centered polybismuthide cluster with a strong diatropic ring current.

Are gold and silver miscible at the nanoscale?

M. Moreira^{1,2,3}, E. Cottancin¹, M. Pellarin¹, L. Roiban³, K. Masenelli-Varlot³, V. Rodrigues³, D. Ugarte³, Matthias Hillenkamp^{1,2}

¹ Institute of Light and Matter, University of Lyon 1 – CNRS UMR5306, France

² Instituto de Física Gleb Wataghin, UNICAMP, CP 6165, 13083-970 Campinas, SP, Brazil

³ University of Lyon, INSA-Lyon, UCBL, MATEIS, CNRS UMR 5510, Villeurbanne, France.
matthias.hillenkamp@univ-lyon1.fr

Bimetallic nanoparticles (BNPs) play an important role in today's research and applications due to the great tunability of their physico-chemical properties through their composition, size, shape, environment and chemical order. The last point, i.e. the spatial distribution of elements inside the BNP is very difficult to quantify despite its importance as e.g. the catalytic activity and selectivity differs strongly between homogeneously alloyed and segregated structures such as core/shell or Janus.

One of the most widely studied BNP systems is AgAu. While perfectly miscible in the bulk, many contradictory studies on its chemical structure at the nanoscale exist in the literature, both alloyed and segregated structures are reported experimentally and theoretically. From the experimental point of view these contradictions can be related to interface effects (notably for passivated BNPs) and metastable, kinetically trapped structures. The fundamental question, whether or not Ag and Au are *intrinsically* miscible at the nanoscale, is thus still open.

Here we present results obtained by Energy-dispersive X-ray spectroscopy performed in a Scanning Transmission Electron Microscope (STEM-EDX) combined with two complementary machine learning techniques for data treatment (Principal Component Analysis PCA and Non-negative Matrix Factorization NMF). We are able not only to quantify the overall chemical composition on the single particle level, but also to establish for the first time quantitative radial profiles for sub-10nm BNPs. Fig. 1 shows such a chemical gradient of the relative Ag atomic fraction in a 7 nm Ag₅₀Au₅₀ BNP. Here a clear silver enrichment at the surface is evidenced. We attribute this segregation to the higher chemical reactivity of silver with oxygen that generates a chemical driving force inducing Ag diffusion towards the NP surface. For oxidation-protected and annealed (relaxed) AgAu BNPs in the range between 4 and 8 nm we find almost complete miscibility, with nevertheless a slight Ag enrichment at the surface. The question of AgAu miscibility or segregation is governed by a competition between surface and volume effects.

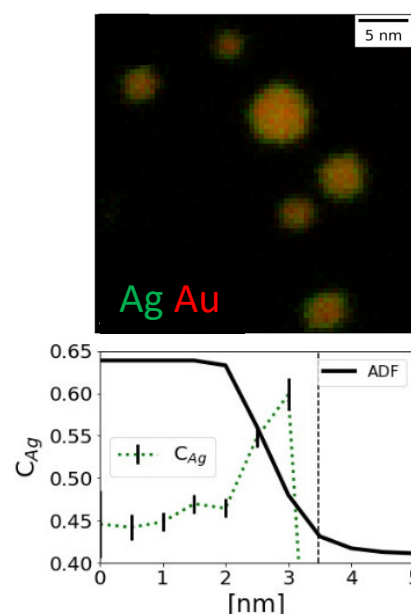


Fig.1 top: EDX maps of oxidized AgAu BNP with Ag and Au counts in green and red. Bottom: radial distribution of the Ag atomic fraction with 0.5 nm spatial resolution for biggest BNP. The thick line is the Annular Dark Field intensity and shows the size of the BNP.

Probing orbital characters of silver and doped-silver cluster anions by photoelectron imaging spectroscopy

Takuya Horio, Masashi Arakawa, Akira Terasaki

Department of Chemistry, Kyushu University, Japan

Photoelectron imaging is a powerful technique to visualize orbital characters of clusters as first demonstrated by Bartels et al. for sodium cluster anions [1]. Here we improve its acquisition rate up to 100 kHz for enabling highly efficient measurements [2], which is applied to silver cluster anions and their variants doped with a transition-metal atom [3].

Electronic structures of alkali- and coinage-metal clusters are known to be well-described by a three-dimensional quantum well based on the jellium model, where its quantum levels (electronic shells of 1S, 1P, 1D, 2S, ...) are occupied by free electrons originating from the valence of constituent atoms. To probe orbital characters of these quantum levels, we first performed photoelectron-imaging experiment on size-selected Ag_N^- up to $N = 20$. Notably, the fastest photoelectrons from Ag_{18}^- ($1S^2 1P^6 1D^{10} 2S^1$) were emitted along the polarization of the incident light as shown in Fig. 1a, indicating indeed the S-type character of the outermost orbital [3]. The experiment was further performed on doped species, Ag_NSc^- , where anisotropy similar to Ag_{18}^- was observed in the image of $\text{Ag}_{15}\text{Sc}^-$ as shown in Fig. 1b, suggesting $1S^2 1P^6 1D^{10} 2S^1$ configuration with Sc 3d and 4s electrons participating in the shell filling [3]. It was also observed that $\text{Ag}_{14}\text{Sc}^-$, with one-less Ag atom, shows a high vertical detachment energy as manifested in Fig. 1c indicating slow photoelectrons, which suggests shell-closure up to 1D orbital with 18 valence electrons. The experiment is now extending to other dopant elements, Ag_NM^- ($M = \text{Sc-Ni}$), across the periodic table, being motivated by our findings of magic sizes in their size-dependent reactivity [4].

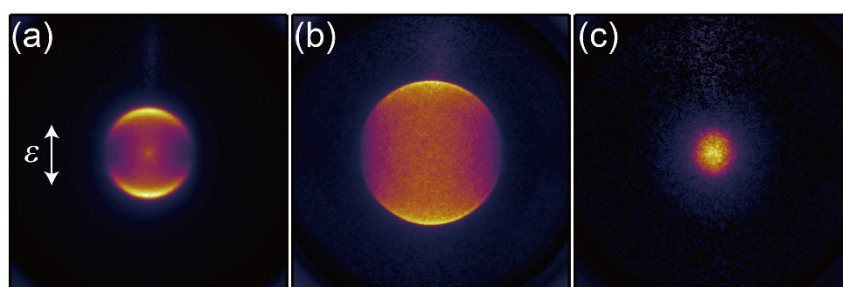


Figure 1: Photoelectron images of (a) Ag_{18}^- , (b) $\text{Ag}_{15}\text{Sc}^-$, and (c) $\text{Ag}_{14}\text{Sc}^-$ obtained by a detachment laser at 404 nm with linear polarization indicated by the double arrow.

- [1] C. Bartels, C. Hock, J. Huwer, R. Kuhn, J. Schwöbel, B. von Issendorff, *Science* **323** (2009) 1323.
- [2] T. Horio, K. Minamikawa, T. Nishizato, H. Hashimoto, K. Matsumoto, M. Arakawa, A. Terasaki, *Rev. Sci. Instrum.* **93** (2022) 083302.
- [3] K. Minamikawa, T. Nishizato, H. Hashimoto, K. Matsumoto, M. Arakawa, T. Horio, A. Terasaki, *J. Phys. Chem. Lett.* **14** (2023) 4011.
- [4] K. Minamikawa, S. Sarugaku, M. Arakawa, A. Terasaki, *Phys. Chem. Chem. Phys.* **24** (2022) 1447.

Accelerated photochemistry within aerosol particles

Ruth Signorell

Department of Chemistry and Applied Biosciences, ETH Zurich, CH-8093 Zurich,
Switzerland
rsignorell@ethz.ch

We report two special photoamplification phenomena in small particles that can accelerate photochemical reactions and affect electron reduction reactions.

Photochemical processes have been identified as the main causes of degradation and oxidation of matter in atmospheric aerosol particles. When light interacts with an aerosol particle, the light intensity can be greatly amplified inside the particle as the latter acts as a light-amplifying cavity. These optical confinement effects result in an acceleration of photochemical reactions in aerosol particles compared with reactions in extended condensed matter. We have studied and quantified the acceleration of in-particle photochemistry using photoacoustic spectroscopy [1] and X-ray spectro-microscopic imaging of single aerosol particles [2].

Electrons solvated in liquid ammonia or water are powerful reducing agents. Here, we report a new way to generate low-energy electrons in situ that might even enhance such reduction reactions [3]. Using double-imaging photoelectron-photoion coincidence spectroscopy, we demonstrate for sodium-doped ammonia nanoclusters how ultraviolet photoexcitation generates spin-paired solvated dielectrons, which subsequently relax through electron-transfer-mediated decay. When the dielectrons decay, an electron is formed that recombines with the solvent molecules together with a second low-energy electron that is ejected. The latter is available for reduction reactions.

1. J.W. Cremer, K.M. Thaler, C. Haisch, R. Signorell, „Photoacoustics of single laser-trapped nanodroplets for the direct observation of nanofocusing in aerosol photokinetics”, *Nat. Commun.*, 7, 10941 (2016)
2. P.C. Arroyo, G. David, P.A. Alpert, E.A. Parmentier, M. Ammann and R. Signorell, „Amplification of light within aerosol particles accelerates in-particle photochemistry”, *Science*, 376, 293-296 (2022).
3. S. Hartweg, J. Barnes, B.L. Yoder, G.A. Garcia, L. Nahon, E. Miliordos and R. Signorell, „Solvated dielectrons from optical excitation: An effective source of low-energy electrons”, *Science*, accepted, 10.1126/science.adh0184, (2023)

Evolution of submicron organic aerosol particles produced in wildfires: Cloud condensation nuclei activity of fresh and aged vanillic acid aerosol particles

Chloe Ayala, Arden M. Floyd, Elaina Berger, Denisia M. Popolan-Vaida

Department of Chemistry, University of Central Florida, United States

In recent years, the incidence of wildfires has considerably increased globally, with fire seasons starting earlier and ending later than usual due to changes in snowpack, precipitation, and temperature, which are attributed in part to climate change.[1-2] Wildfires are responsible for the emission of a variety of gases and organic particles in the atmosphere with profound impacts on air quality, visibility, and human health.[3-4] The aerosol particles produced by wildfires can contribute to the climate change by scattering or absorbing solar radiation, affecting the radiative balance of the planet through cooling or warming effects, or by acting as cloud condensation nuclei (CCN).

Phenolic acids aerosol particles are abundant products of biomass burning and have been often used as tracers for the type of biomass burned. Among them, vanillic acid aerosol particles are known to be produced as a result of high temperature ignition of lignin. Despite their abundance, little is known about their reactivity and CCN activity. Here we report the CCN activity behaviour of fresh and aged vanillic acid aerosol particles to assess their impact on the mechanism of cloud formation.

The reactivity of vanillic acid aerosol particles with ozone and their CCN activity before and after the reaction with ozone is investigated in a flow tube reactor in conjunction with a high-resolution Orbitrap mass spectrometer, a scanning mobility particle sizer, and a CCN counter. An atomizer and an electrostatic classifier are used to produce monodisperse vanillic acid aerosol particles from an aqueous solution of vanillic acid. The monodisperse particles are subsequently injected into the flow tube reactor and exposed to controlled amounts of ozone at a well-defined residence time.

Even though vanillic acid aerosol particles are found to slowly react with ozone, with a reactive uptake coefficient in the order of 10^{-7} , the oxidation of vanillic acid aerosol particles leads to a dramatic increase of their CCN activity. This study emphasizes the importance of investigating the rate of change in CCN activity of phenolic acids under the combined effects of several atmospheric parameters such as oxidants and relative humidity to accurately describe their role in cloud formation.

- [1] W.M. Jolly, M.A. Cochrane, P.H. Freeborn, Z.A. Holden, T.J. Brown, G.J. Williamson, D.M.J.S. Bowman, *Nat. Commun.* **6** (2015) 7537.
- [2] J.T. Abatzoglou, A. P. Williams, *PNAS* **113** (2016) 11770.
- [3] R. Aguilera, T. Corringham, A. Gershunov, T. Benmarhnia, *Nat. Commun.* **12** (2021) 1493.
- [4] J.C. Liu, A. Wilson, L.J. Mickley, F. Dominici, K. Ebisu, Y. Wang, M.P. Sulprizio, R.D. Peng, X. Yue, J.-Y. Son, G.B. Anderson, M.L. Bell, *Epidemiology* **28** (2017) 77.

Electron-Induced Proton Transfer (EIPT) and the Nature of Solvated Electron-Like Clusters

Kit Bowen, Gaoxiang Liu, Xinxing Zhang, Moritz Blankenhorn, and Tatsuya Chiba

Department of Chemistry, Johns Hopkins University, USA

The study of solvated electron-like clusters is a classic topic in chemical physics. It is widely accepted that while small cluster anions of, for example $(\text{H}_2\text{O})_n^-$, can be described as surface electron states, larger versions including bulk solvated electrons themselves are best described by the cavity model. An alternative view, for which we have substantial experimental evidence, is that solvated electron-like clusters, such as $(\text{NH}_3)_n^-$ and $(\text{H}_2\text{O})_n^-$, are formed by electron-induced proton transfer. In particular, $(\text{NH}_3)_n^-$ would be described as $e^- \text{NH}_4^+ \dots (\text{NH}_3)_{n-2} \dots \text{NH}_2^-$, where the e^- in the pseudo-Rydberg NH_4 molecule, $e^- \text{NH}_4^+$, is a roving (delocalized) electron, and where the NH_2^- moiety is a sub-anion. Likewise, $(\text{H}_2\text{O})_n^-$ would be described as $e^- \text{H}_3\text{O}^+ \dots (\text{H}_2\text{O})_{n-2} \dots \text{OH}^-$, where the e^- in the pseudo-Rydberg H_3O molecule, $e^- \text{H}_3\text{O}^+$, is a roving (delocalized) electron, and where the OH^- moiety is a sub-anion. Through a staircase of related experiments, we have built a case for this point of view. To some extent, echoes of other models for solvated electron-like clusters can be discerned within the EIPT description of these species. Electron-induced proton transfer reflects the extraordinary power of an excess electron to make the unexpected a reality.

Solvation of $\text{Cu}_n^{+/-}$ in He and H_2 at ultra-cold temperatures

Olga V. Lushchikova¹, J. Reichegger¹, S. Kollotzek¹, F. Zappa¹, M. Gatchell², M. Bartolomei³, J. Campos-Martínez³, T. González-Lezana³, F. Pirani³, P. Scheier¹

¹ Institut für Ionenphysik und Angewandte Physik, Universität Innsbruck, Austria

² Department of Physics, Stockholm University, Sweden

³ Instituto de Física Fundamental, IFF-CSIC, Spain

Given copper's versatility and wide-ranging uses, understanding how it interacts with hydrogen and helium at the atomic level can contribute to the development of innovative materials for energy storage, catalysis, and other applications. However, the solvation of Cu in H_2 and He poses experimental and theoretical challenges.

In the present study, we demonstrate the solvation of cationic and anionic Cu clusters in He and H_2 . The binding of a large number of He and H_2 to Cu clusters can be achieved utilizing multiple charged superfluid He nanodroplets, with an internal temperature of 0.4 K. With this method, solvation of both cations and anions becomes possible, due to charging of the He droplets before doping.[1] By studying different charge states and cluster sizes we can get insights into the effect of the electronic and geometric structure of the cluster on the solid-solvent interaction.

Helium and hydrogen atoms can attach themselves to metal clusters, thereby stabilizing specific structures known as "magic" structures. By determining the number of solvent atoms required to form such magic structures, we can draw conclusions about the properties of the cluster itself.

For example, the structure $\text{Cu}_n^{+/-}$ can be revealed by calculating the most stable structures with the experimentally determined number of He atoms forming the first magic ion.[2] The results found are in good agreement with previous experimental and theoretical studies, except for Cu_5^+ , which has been a subject of controversy in the past.[3]

When Cu clusters are solvated in H_2 , it is found that cations can also form a Cu-H core, resulting in an additional solvation series. The first shell of H_2 is bound very strongly, but the binding energy substantially decreases for the following ones. Similarly, to He, H_2 binds very weakly onto anionic clusters, and no formation of Cu-H core is observed.

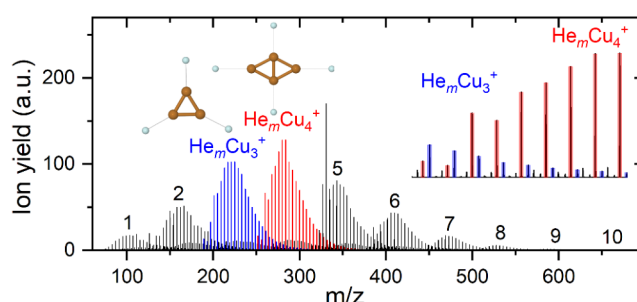


Figure 1: Mass spectrum of Cu_n^+ solvated in He accompanied by the assigned structures of $\text{Cu}_{3,4}^+$.

- [1] L. Tiefenthaler, *et al.*, Review of Scientific Instruments, **91** (2020), 11.
- [2] O. V. Lushchikova, *et al.*, The Journal of Physical Chemistry Letters, **10** (2019), 2151-2155.
- [3] O. V. Lushchikova, *et al.*, Physical Chemistry Chemical Physics, **25** (2023), 8463-8471.

- 09:00 **Bernd von Issendorff** (INV 20)
A closer look at the electronic structure of simple metal clusters
- 09:40 **Gereon Niedner-Schatteburg** (HT 21)
Cryo studies of spontaneous N₂ activation and cleavage
- 10:00 **Mihai Vaida** (INV 21)
Tracking the ultrafast reaction dynamics of methyl halide molecules adsorbed on metal clusters and embedded in molecular clusters at surfaces using femtosecond laser pulses
- 10:40 **Lutz Schweikhard** (HT 22)
Delayed photodissociation of (poly)anionic tin clusters investigated at ClusterTrap
- 11:00 **Rajarshi Sinha Roy** (HT 23)
Orbital magnetism in atomically precise metal clusters from ab-initio real-time TDDFT
- 11:20 **Kevin Oldenburg** (HT 24)
Silver cluster plasmons revisited
- 11:40 **Uzi Landman**
Concluding remarks and perspectives

A closer look at the electronic structure of simple metal clusters

Bernd v. Issendorff

¹ *Physikalisches Institut, Universität Freiburg*

Simple metal clusters are close to ideal few to many particle quantum systems; they can be seen as a well-defined number of electrons trapped in the harmonic potential produced by the almost homogeneously charged spherical ion background.

This leads to the well known electron shell structure discovered almost 50 years ago [1], a highly discretized density of states consisting of angular momentum eigenstates. But it also has direct consequences for dynamics like photoemission; as we could recently demonstrate, the angular distribution of photoelectrons exhibits a universal behavior in accordance with a very simple model [2].

Nevertheless, the almost free electrons in simple metal clusters do interact with the structured ion background, which perturbs and mixes the electronic states. Characterizing this perturbation by measuring the electronic density of states via photoelectron spectroscopy can therefore yield information about the cluster geometric structure. In fact, this has been one of the main tools in cluster physics for cluster geometry determination; it, however, only works if measured spectra are sufficiently well resolved to distinguish between different isomers and if good calculations of the electronic density of states are available.

On both the experimental and the theoretical part a significant progress has been made over recent years, permitting a much more detailed insight into the electronic structure of metal clusters and its interplay with the geometric structure. I will discuss examples of simple metal cluster systems of increasing complexity, from sodium over copper and silver to gold. Here a number of unexpected geometric structures can be identified, as well as exotic electronic states.

[1] W. D. Knight, K. Clemenger, W. A. de Heer, W. A. Saunders, M. Y. Chou, and M. L. Cohen, Electronic Shell Structure and Abundances of Sodium Clusters, *Phys. Rev. Lett.* **52**, 2141 (1984)

[2] A. Piechaczek, C. Bartels, C. Hock, J.-M. Rost, and B. von Issendorff, Decoherence-Induced Universality in Simple Metal Cluster Photoelectron Angular Distributions, *Phys. Rev. Lett.* **126**, 233201 (2021)

Cryo studies of spontaneous N₂ activation and cleavage

Daniela V. Fries, Christopher Wiehn, Max Luczak, Gereon Niedner-Schatteburg

Rheinland-Pfälzische Technische Universität (RPTU), 67663 Kaiserslautern

We utilize N₂ adsorption to atomically precise transition metal (TM) clusters to investigate their surface morphologies at the fundamental level, and as a treasure quest for N₂ activation [1,2]. Isothermal uptake kinetics reveal evidence for rough and smooth surfaces [3-7], and IR photon dissociation (IRPD) spectra of cluster adsorbate complexes unravel N₂ coordination motifs [8-13]. Concomitant DFT modelling helps to elucidate our experimental findings. In some cases the DFT modelling revealed pathways of N₂ activation and of spontaneous N₂ cleavage [11]. The co-adsorption of N₂ and H₂ reveals an anti-cooperative effect [12].

This presentation summarizes the current understanding of charge state and spin state dependencies of the TM cluster N₂ interactions, and it exemplifies recent results on Cobalt and Ruthenium clusters. It shall, moreover, discuss self promotion and poisoning, and it concludes with an outlook onto future prospects.

[1] GNS. in *Structure and Bonding* Vol. 174 1-40 (Springer, 2017). [2] Dillinger, S. & GNS. in *Fundamentals and Applications of Fourier Transform Mass Spectrometry* (Elsevier, 2019). [3] Mohrbach, J., Dillinger, S., and GNS. *Cryo Kinetics and Spectroscopy of cationic nickel clusters: Rough and smooth surfaces*. J. Phys. Chem. C **121**, 10907 (2017) [4] Mohrbach, J., Dillinger, S. & GNS. *Probing cluster surface morphology by cryo kinetics of N₂ on cationic nickel clusters*. J. Chem. Phys. **147**, 184304 (2017). [5] Ehrhard, A. A., Klein, M. P., Mohrbach, J., Dillinger, S. & GNS. *Cryokinetics and spin quenching in the N₂ adsorption onto rhodium cluster cations*. Mol. Phys. **119**, 1953172 (2021). [6] Straßner, A., Klein, M. P., Fries, D. V., Wiehn, C., Huber, M. E., Mohrbach, J., Dillinger, S., Spelsberg, D., Armentrout, P. B. & GNS. *Kinetics of stepwise nitrogen adsorption by size-selected iron cluster cations: Evidence for size-dependent nitrogen phobia*. J. Chem. Phys. **155**, 244306 (2021). [7] Ehrhard, A. A., Klein, M. P., Mohrbach, J., Dillinger, S. & GNS. *Cryo kinetics of N₂ adsorption onto bimetallic rhodium-iron clusters in isolation*. J. Chem. Phys. **156**, 054308 (2022). [8] Klein, M. P., Ehrhard, A. A., Mohrbach, J., Dillinger, S. & GNS. *Infrared Spectroscopic Investigation of Structures and N₂ Adsorption Induced Relaxations of Isolated Rhodium Clusters*. Topics in Catalysis **61**, 106 (2018). [9] Dillinger, S., Mohrbach, J. & GNS. *Probing cluster surface morphology by cryo spectroscopy of N₂ on cationic nickel clusters*. J. Chem. Phys. **147**, 184305 (2017). [10] Dillinger, S., Klein, M. P., Steiner, A., McDonald, D. C., Duncan, M. A., Kappes, M. M. & GNS. *Cryo IR Spectroscopy of N₂ and H₂ on Ru₈⁺: The Effect of N₂ on the H-Migration*. J. Phys. Chem. Lett. **9**, 914 (2018). [11] Fries, D. V., Klein, M. P., Steiner, A., Prosenc, M. H. & GNS. *Observation and mechanism of cryo N₂ cleavage by a tantalum cluster*. Phys. Chem. Chem. Phys. **23**, 11345 (2021). [12] Straßner, A., Wiehn, C., Klein, M. P., Fries, D. V., Dillinger, S., Mohrbach, J., Prosenc, M. H., Armentrout, P. B. & GNS. *Cryo spectroscopy of N₂ on cationic iron clusters*. J. Chem. Phys. **155**, 244305 (2021). [13] Klein, M. P., Ehrhard, A. A., Huber, M. E., Straßner, A., Fries, D. V., Dillinger, S., Mohrbach, J. & GNS. *Cryo infrared spectroscopy of N₂ adsorption onto bimetallic rhodium-iron clusters in isolation*. J. Chem. Phys. **156**, 014302 (2022).

Tracking the ultrafast reaction dynamics of methyl halide molecules adsorbed on metal clusters and embedded in molecular clusters at surfaces using femtosecond laser pulses

Mihai E. Vaida

*Department of Physics and Renewable Energy and Chemical Transformations Cluster,
University of Central Florida, Orlando, FL, United States*

The detection of intermediate species during surface photoinduced reactions and the correlation of their dynamics with the properties of the surface is crucial to fully understand and control heterogeneous reactions. In this study, a technique that combines time-of-flight mass spectrometry with laser spectroscopy and fast surface preparation with molecules is employed to investigate the mechanism of photoinduced reactions through the direct detection of intermediate species and final products.

In the first part of the talk an example is presented in which the ultrafast photodissociation dynamics of CH_3Br molecules adsorbed on variable-size Au clusters on MgO thin films is investigated by monitoring the CH_3^+ transient evolution as a function of Au cluster size. In addition, extreme-UV photoemission spectroscopy in combination with theoretical calculations is employed to study the electronic structure of the Au clusters on MgO thin films. Changes in the ultrafast dynamics of the CH_3^+ fragment are correlated with the electronic structure of Au as it evolves from monomers to small nonmetallic clusters to larger nanoparticles with a metallic character.

In the second part of the talk, another example is presented in which the photoinduced reaction dynamics in CH_3I clusters formed on oxide surfaces is investigated. The focus will be on understanding the bimolecular formation dynamics of I_2 and reformation dynamics of the parent molecule after the photoinduced dissociation of CH_3I inside the cluster.

Delayed photodissociation of (poly)anionic tin clusters investigated at ClusterTrap

Alexander Jankowski¹, Paul Fischer¹, Grunwald-Delitz¹, Klavs Hansen², Lutz Schweikhard¹

¹ *Institute of Physics, University of Greifswald, 17487 Greifswald, Germany*

² *Center for Joint Quantum Studies and Dep. of Phys., School of Sci., Tianjin 300072, China Center for Theor. Phys., Key Laboratory of Theor. Phys., Lanzhou, Gansu 730000, China*

At ClusterTrap [1], time-resolved measurements of the delayed photodissociation of metal clusters [2] have recently been extended to negative species. Here, we report about investigations on anionic tin clusters.

In contrast to previous experiments, where the decay of the precursors and the appearance of the charged product clusters could be well described by single exponential functions [2], the decay data of Sn_{22}^- show significant deviations from this simple behavior. An adequate description requires decay-rate distributions of the precursors that point to corresponding excitation-energy distributions of the cluster ensembles.

In another set of experiments, photodissociation has been applied to doubly-negative clusters. Similar to the case of dianionic lead clusters [3], the dianionic tin clusters (of a certain size range) decay by fission into singly-charged fragment particles. However, several of those fragments are observed [4] – in contrast to just two complementary ones as in the case of lead.

To disentangle the decay pathways, time-resolved photodissociation measurements of Sn_{34}^{2-} have been performed. We report about the decay behavior as a function of photon energy. In particular, the data analysis shows the changing probabilities of electron emission vs. fragmentation as well as the excitation-energy dependence of the decay rates. It also reveals two distinct laser-wavelength regions of delayed decay by single-photon and by two-photon absorption.

Higher anionic charge states of tin clusters have been observed, opening the possibility for studies involving decays of a different magnitude of complexity.

[1] L. Schweikhard *et al.*, Eur. Phys. J. D **9** (1999) 15, F. Martinez *et al.*, Eur. Phys. J. D **63** (2011) 255,

F. Martinez *et al.*, Int. J. Mass Spectrom. **365-366** (2014) 266

[2] U. Hild *et al.*, Phys. Phys. A **57** (1998) 2786, M. Vogel *et al.*, Phys. Rev. Lett. **87** (2001) 013401

[3] S. König *et al.*, Phys. Rev. Lett. **120** (2018) 163001

[4] M. Wolfram *et al.*, Eur. Phys. J. D **74** (2020) 135

Orbital Magnetism in Atomically Precise Metal Clusters from Ab-Initio Real-Time TDDFT

Deru Lian¹, Yanji Yang¹, Giovanni Manfredi², Paul-Antoine Hervieux², Rajarshi Sinha-Roy^{1,3}

¹ *Université de Lyon, Université Claude Bernard Lyon 1, CNRS, Institut Lumière Matière, F-69622, VILLEURBANNE, France.*

² *Université de Strasbourg, Institut de Physique et Chimie des Matériaux de Strasbourg, F-67000 Strasbourg, France*

³ *European Theoretical Spectroscopy Facility (ETSF), Web: <http://www.etsf.eu>*

Transfer of angular momentum from helicity-controlled laser fields to a nonmagnetic electronic system can lead to the creation of magnetization. Recently optically induced magnetization has been also quantified in plasmonic gold nanoparticles [1] and also reported for graphene disks [2]. The underlying mechanism, the inverse Faraday effect, in metallic nanoparticles has been studied using different theoretical approaches, e.g., using hydrodynamic modeling of electrons [3]. In comparison, theoretical investigations into the magnetism induced by rotating plasmonic fields in smaller nanoparticles, namely clusters, have only been accomplished recently from a quantum-mechanical many-body perspective using jellium description and time-dependent density-functional theory (TDDFT) [4]. It has been shown that an elliptically polarized laser field gives rise to a magnetic moment, which is maximum at the localized surface plasmon resonance (LSPR) frequency. The primary contribution to the magnetic moment comes from surface currents, although a size-dependent bulk contributions due to the quantum-mechanical nature of the system (Friedel oscillations) still persist. In this work, the investigation is further extended to study the generation of orbital angular in clusters of simple and noble metals having precise structure. In particular the influences of geometry and chemical composition on the LSPR-induced magnetic moment is studied in clusters having a few atoms to a few tens of atoms.

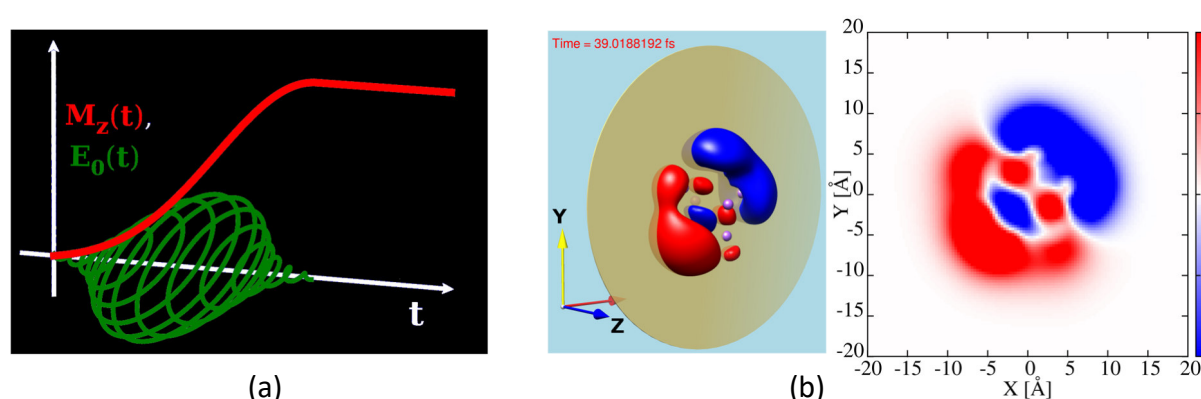


Figure : (a) Driving field (green) and induced magnetization (red). (b) Corresponding induced density.

- [1] O. H.-C. Cheng, D. H. Son, M. Sheldon, *Nature Photonics* **14**, 365 (2020)
- [2] J. W. Han, P. Sai, D. But, E. Uykur, S. Winnerl, G. Kumar, M. L. Chin, R. L. Myers-Ward, M. T. Dejarld, K M. Daniels, T. E. Murphy, W Knap, M Mittendorff, URL <https://arxiv.org/abs/2307.04512> (2023)
- [3] J. Hurst, P. M. Oppeneer, G. Manfredi, P.-A. Hervieux, *Phys. Rev. B* **98**, 134439 (2018)
- [4] R. Sinha-Roy, J. Hurst, G. Manfredi, P.-A. Hervieux, *ACS Photonics* **7**, 2429 (2020)

Silver cluster plasmons revisited

Kevin Oldenburg^{1,2}, Ingo Barke², Karl-Heinz Meiwes-Broer^{1,2}

¹ELMI-MV, University of Rostock, 18059 Rostock, Germany

²Department „Life, Light & Matter“, and Institute of Physics, University of Rostock, Germany

Whereas the subject of collective electron excitations in metal clusters has been and still is subject in each of the twenty ISSPIC conferences, it still bears interesting facets to be studied. Since early work [1-3], numerous publications dealt with the question in how far a dielectric embedding or a supporting environment influences or even determines the measured plasmon energy, and its width [4]. Compiling literature data (e.g. [5]), it appears that convincing studies of the size dependence for clean clusters in the range of few nm are lacking. Observed size trends for such particles in contact to material may be affected by secondary effects. Indeed, chemical reactivity is known to be connected to the cluster size, which in turn might govern the properties of the respective dielectric environment. Furthermore, due to the interactions with a surface, strong field inhomogeneities can occur leading to the excitation of higher order modes [6]. Thus, a clear size effect of the dipole plasmon resonance might be hidden.

This odd situation makes it worthwhile to direct a new view onto plasmon excitations. Prerequisite is an as clean as possible preparation of the systems without ligands or contamination, on the best known or least interacting substrates. For analysis electron energy loss spectroscopy (EELS) has proven to come with several advantages like the possibility to choose the excitation volume with high precision, an important feature to get a more general view on plasmon excitations.

In our contribution we investigate the locally excited plasmonic response of individual silver clusters in the size range of a few nm. The gas-phase produced clusters were size-selected and soft landed on holey carbon substrates and 2D materials. Figure 1 exemplarily shows a high angle annular dark-field (HAADF) STEM image of a 11 nm silver nanoparticle at the edge of a carbon film. Clearly visible is its plasmon resonance in the electron energy loss spectrum. The results are discussed with respect to the role of local excitation position, making it possible to distinguish different plasmon modes, and the dielectric surrounding, i.e. the substrate and possible surface adsorbates.

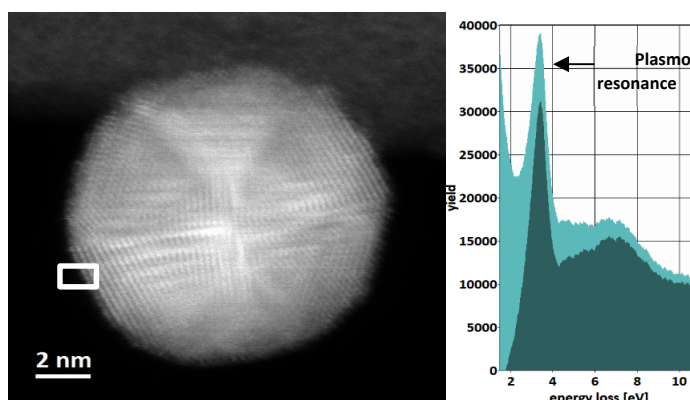


Figure 1 HAADF STEM image of a silver cluster at the edge of a carbon substrate (left) together with the unprocessed (green) and background corrected (dark green) EEL spectra taken at the marked position (right).

[1] H. Abe, K.P. Charlé, B. Tesche, W. Schulze, Chem. Phys. **68** (1982) 137; [2] U. Kreibig, M. Vollmer. Optical properties of metal clusters. Springer Ser. Mat. Sci 25 (1995); [3] S. Fedrigo, W. Harbich, J. Buttet, Phys. Rev. **47** (1993) 10706; [4] A. Campos et al., Nature Physics **15** (2019) 275; [5] H. Haberland, Nature **494** (2013), E1-E2; [6] S. Kadkhodazadeh et al., ACS Photonics **4** (2017) 2, 251–261

Abstracts Poster Session A (Tuesday)

3d metal doping of cobalt clusters to tune the activity toward CO₂

Deepak Pradeep,¹ Barbara Zamora Yusti,^{2,3} Rutger Zijlstra,¹ Mate Szalay,^{2,3} Tibor Höltzl,^{2,3} László Nyulászki,³ Joost M. Bakker¹

¹ *Radboud University, HFML-FELIX Laboratory, Nijmegen, Netherlands*

² *Department of Inorganic and Analytical Chemistry, Budapest University of Technology and Economics, Hungary*

³ *Furukawa Electric Institute of Technology, Budapest, Hungary*

The increasing atmospheric CO₂ concentration leads to global warming and climate destabilization. One potential way to mitigate CO₂ emissions is by converting CO₂ into useful chemicals. In industry, for example, methanol is produced by direct hydrogenation of CO₂ over a Cu-ZnO-Al₂O₃ catalyst.^[1] A detailed understanding of the reaction mechanisms is required for a rational design of more active and selective catalysts.

Gas-phase metal clusters can form an idealized model system for the active sites of the complex catalysts.^[2] We aim to investigate on a molecular level how the doping of clusters with foreign elements affects their reactivity.^[3] To test this experimentally, we aim to study the interaction of first-row transition metal-doped clusters with CO₂ and H₂ using IR photo fragmentation spectroscopy complemented by DFT calculations. For this, we present a newly commissioned dual-laser, dual-target cluster source and show how the doping of cationic cobalt clusters by single vanadium or iron atoms affects the adsorption mode of CO₂.

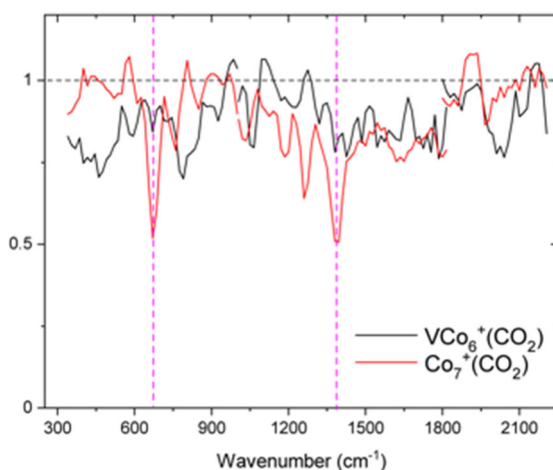


Figure 1: IR depletion spectra for cationic V-doped Co cluster and pure Co cluster with CO₂. The band near 2100 cm⁻¹ (C-O stretch vibration) for the doped cluster indicates dissociation of CO₂.

[1] Waugh, K. C. Methanol Synthesis. *Catal. Today*, **15** (1) (1992), 51–75.

[2] Lang, S. M.; Bernhardt, T. M. *Phys. Chem. Chem. Phys.*, **14** (2012), 9255–9269.

[3] Szalay, M.; Buzsáki, D.; Barabás, J.; Faragó, E.; Janssens, E.; Nyulászki, L.; Höltzl, T. *Phys. Chem. Chem. Phys.*, **23** (38) (2021), 21738–21747.

Infrared Photodissociation Studies of Nitric Oxide on Metal and Metal Oxide Centres

Philip A. J. Pearcy¹, Gabriele Meizyte¹, Edward I. Brewer¹, Alice E. Green¹, Matthew Doll¹, Olga Duda¹, Peter D. Watson¹, Stuart R. Mackenzie¹.

¹ Department of Chemistry, University of Oxford, United Kingdom.

Nitrogen oxides, commonly known as NO_x, are known to cause detrimental effects on the environment as well as on air quality [1]. This in turn can have a harmful effect on human health. Current mitigation strategies to deal with NO_x includes using catalytic converters that harness the surface catalytic chemistry of transition metal atoms and clusters dispersed across a support [2]. Understanding the fundamental metal–ligand interactions that are important in catalytic chemistry between transition metal centres and nitric oxide (NO) molecules is therefore very useful. The isolated metal–ligand complexes can be studied using gas-phase infrared photodissociation (IRPD) spectroscopy in conjunction with quantum calculations. In my presentation, I will discuss our recent experimental and computational findings on the formation of NO dimers within Group 9 metal nitrosyl complexes (M(NO)_n⁺, M=Co,Rh,Ir) [3], as well as our preliminary work on the differences between Pt and PtO nitrosyl clusters (Pt/PtO(NO)_n⁺).

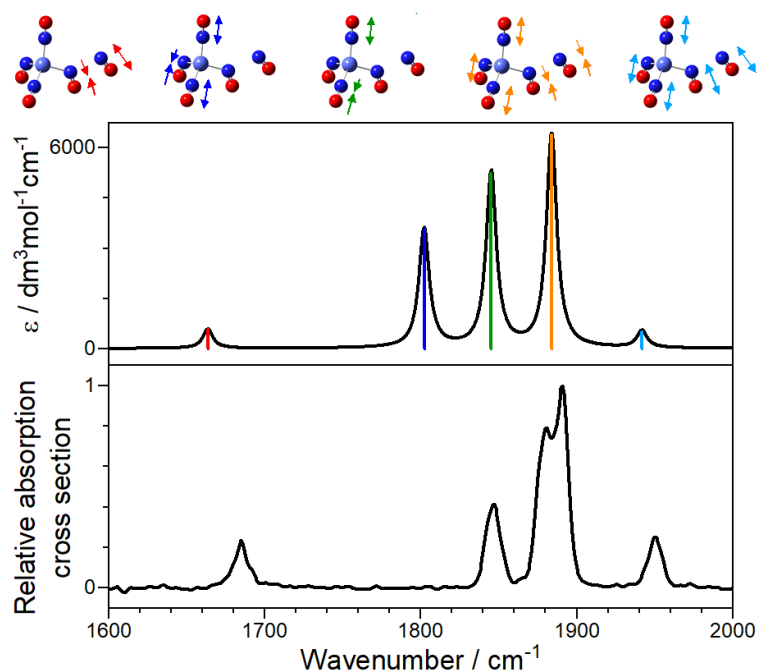


Figure 1: Top: Simulated spectrum of Co(NO)₅⁺, with colour-coded mode vectors relating to the vibrations shown on the simulated species. Bottom: Experimental Co(NO)₅⁺ IRPD spectrum.

- [1] T. Boningari, P. G. Smirniotis, *Current Opinion in Chemical Engineering* **13** (2016) 133–141
- [2] M. Shelef, *Catalysis Reviews* **11** (1975) 1–40
- [3] G. Meizyte, *et al.*, *Journal of Physical Chemistry A* **126** (2022) 9414–9422

The X-ray fingerprint of reactive transition metal-oxygen species

Mayara da Silva Santos^{1,2}, Robert Medel³, Simon Kruse^{1,4}, Max Flach^{1,2}, Olesya S. Ablyasova^{1,2}, Martin Timm¹, Bernd von Issendorff², Konstantin Hirsch¹, Vicente Zamudio-Bayer¹, Tony Stüker³, Sebastian Riedel³, J. Tobias Lau^{1,2}

¹ Abteilung für Hochempfindliche Röntgenspektroskopie, Helmholtz-Zentrum Berlin für Materialien und Energie, Germany

² Physikalisches Institut, Universität Freiburg, Germany

³ Institut für Chemie und Biochemie—Anorganische Chemie, Freie Universität Berlin, Germany

⁴ Institut für Physik, Humboldt Universität zu Berlin, Germany

Discovering compounds that present transition metals with unusual oxidation states or reactive oxygen species (superoxide, peroxide and oxygen-centered radical) is of great scientific and technological interests, as they have key applications as oxidizing agents, catalysts, or reaction intermediates, and can improve the performance of materials for energy conversion and storage.[1,2]

Here, we use X-ray absorption spectroscopy (XAS) at the oxygen K and metal L₃, M₃ or N₃ edges of gas-phase [MO_n]⁺ systems (M = transition metal, *n* = integer) to identify the spectroscopic signatures of oxygen ligands and assign the oxidation state of the metal.[3] The cationic species are mass selected and accumulated in the cryogenic ion trap. X-ray absorption spectra are then recorded in partial ion yield mode.[4] Our ion trap is installed at the undulator beamline UE52-PGM at the Berlin synchrotron radiation facility BESSY II operated by the Helmholtz-Zentrum Berlin.

Reactive species, such as oxygen-centered radicals and species containing high-valent transition metals, are analyzed in stable conditions in the ground state inside the cryogenic ion trap. This method is here demonstrated to be an important tool to identify the character of oxygen ligands, offering direct access to element specific electronic structures.

[1] Y. X. Zhao, et al., Phys. Chem. Chem. Phys. **13** (2011) 1925–1938

[2] S. Riedel and M. Kaupp, Coord. Chem. Rev. **253** (2009) 606–624

[3] M. da S. Santos, et al., Angew. Chem. Int. Ed. (2022) e202207688

[4] K. Hirsch, et al., J. Phys. B: At., Mol. Opt. Phys. **42** (2009) 154029

Activation of CO₂ by free metal oxide clusters

Pavol Mikolaj, Sandra M. Lang, Thorsten M. Bernhardt

Institute of Surface Chemistry and Catalysis, Ulm University, Ulm, Germany

Motivated by the performance of the industrially employed Cu/ZnO catalyst for direct CO₂ hydrogenation [1], the European training network CATCHY [2] seeks to develop new and high-performance cluster-based catalysts. As part of this project, we utilize transition metal oxide clusters in the gas phase as model systems to study the fundamental driving forces that determine the reactive and catalytic properties of such catalysts.

So far, we have investigated the interaction of CO₂ with small copper oxide, cobalt oxide and yttrium oxide clusters via infrared multiple-photon dissociation (IR-MPD) spectroscopy (collaboration with J. Bakker, FELIX laboratory). Clusters were produced by laser ablation of a metal target in the presence of He carrier gas seeded with O₂. Independent of the metal, cluster formation appears to be strongly charge dependent, with cations preferably forming oxygen-rich clusters, while anions tend to form stoichiometric and oxygen-deficient clusters. To study the cluster-CO₂ interaction, a CO₂/He mixture was subsequently introduced in an adjacent flow tube reactor and the resulting reaction products were investigated via infrared spectroscopy.

In the case of cationic copper and cobalt oxide complexes, the characteristic Fermi dyad of CO₂ is observed, indicating the presence of physisorbed, unactivated linear CO₂. In contrast, all anionic cluster complexes show bands which are characteristic for an activated bent CO₂ molecule (cf. Figure 1). Most interestingly, the IR-MPD spectra of yttrium oxide-CO₂ complexes appear to be more complex than the spectra of the copper and cobalt oxide complexes, potentially indicating different CO₂ binding motifs.

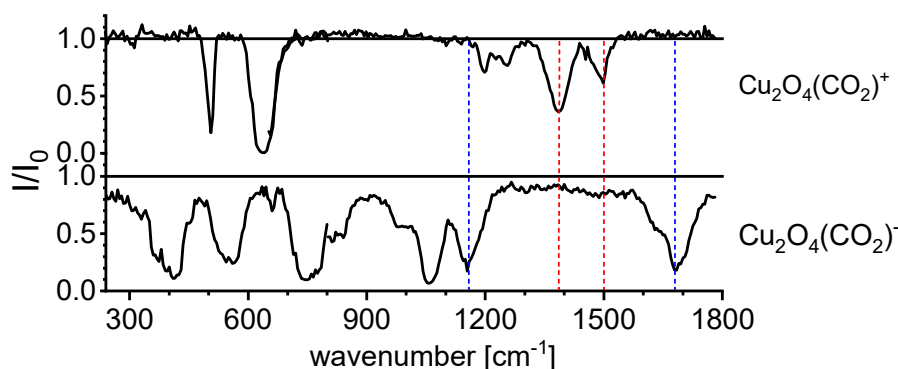


Figure 1: Comparison of IR-MPD spectra of a cationic and anionic Cu₂O₄(CO₂) cluster complex. The red lines indicate the Fermi dyad, the blue lines indicate characteristic modes of an activated CO₂ molecule.

- [1] J. Artz, T.E. Müller, K. Thenert, J. Kleinekorte, R. Meys, A. Sternberg, A. Bardow & W. Leitner, Chem. Rev. **118**(2) (2018) 434-504.
- [2] <https://www.catchy-etn.eu/>

Co-adsorption of H₂ and CO₂ on Cu_n⁺ clusters: model for the CO₂ reduction catalyst?

Joost M. Bakker¹, Olga V. Lushchikova^{1,2}, Hossein Tahmasbi,³ Ludo Juurlink,³ Jörg Meyer,³ Máté Szalay,⁴ Tibor Höltzl^{4,5}

¹Radboud University, HFML-FELIX, Nijmegen, The Netherlands

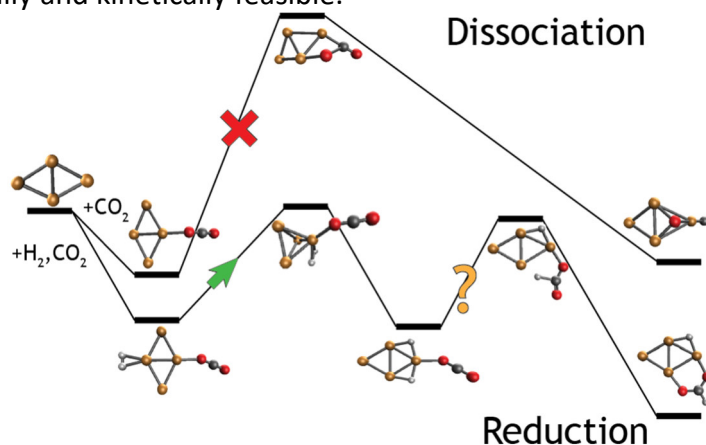
²Institut für Ionenphysik und Angewandte Physik, Universität Innsbruck, Austria

³Leiden Institute of Chemistry, Leiden University, The Netherlands

⁴Department of Inorganic and Analytical Chemistry, Budapest University of Technology and Economics, Hungary

⁵Furukawa Electric Institute of Technology, Budapest, Hungary

To understand elementary reaction steps in the hydrogenation of CO₂ over copper-based catalysts, we experimentally study the adsorption of CO₂ and H₂ onto cationic Cu_n⁺ clusters, both individually and in co-adsorption. For this, we react Cu_n⁺ clusters formed by laser ablation with H₂, CO₂, or both, in a flow tube-type reaction channel and characterize the products formed by IR multiple-photon dissociation spectroscopy employing the IR free-electron laser FELICE. We analyze the spectra by comparing them to spectra of the individual adsorption products and with Density Functional Theory calculations. We find that cationic clusters cannot activate CO₂, which is rationalized by the existence of a large activation barrier, whereas H₂ adsorbs both dissociatively and molecularly. In the co-adsorption experiment, no evidence is found for CO₂ reduction to formate, even though DFT suggests it is both thermodynamically and kinetically feasible.



- [1] O.V. Lushchikova, D.M.M.M. Huitema, P. López-Tarifa, L. Visscher Z. Jamshidi, J.M. Bakker, J. Phys. Chem. Lett. **10** (2019) 2151
- [2] O.V. Lushchikova, H. Tahmasbi, S. Reijmer, R. Platte, J. Meyer, J.M. Bakker, J. Phys. Chem. A **125** (2021) 2836.
- [3] O.V. Lushchikova, M. Szalay, H. Tahmasbi, L.B.F. Juurlink, J. Meyer, T. Höltzl, J.M. Bakker, Phys. Chem. Chem. Phys. **23** (2021) 26661
- [4] O.V. Lushchikova, M. Szalay, T. Höltzl, J.M. Bakker, Faraday Discuss. **242** (2023) 252

Elucidating the Structure and Reactivity of First Row Transition Metal Oxide Clusters by Combining Experiment and Theory

W. Schwedland¹, F. Müller¹, S. Leach¹, H. Windeck¹, Y. Li², A. Chakraborty², F. Berger¹, K. Asmis², J. Sauer¹

¹ Institut für Chemie, Humboldt-Universität zu Berlin, Germany

² Wilhelm-Ostwald-Institut, University of Leipzig, Germany

Methane, as the most stable alkane with overall low reactivity compared to other hydrocarbons, poses a special challenge for the conversion into more valuable compounds. Recently, Zi-Yu Li *et al.* proposed a new methane activation mechanism for a gold containing metal oxide gas phase cluster, which promotes heterolytic C-H bond cleavage via an adjacent Lewis acid-base pair.^[1] Here, we propose a similar reactivity for gas phase first row transition metal oxide clusters $M_2AlO_4^+$ ($M = Fe, Co$).

The unusual key-like structure of $M_2AlO_4^+$ has been identified by employing a genetic algorithm with subsequent local optimization using DFT. It has been further verified by comparison of DFT-predicted IR spectra with IRPD measurements.

The structure and reactivity of $M_2AlO_4^+$ differs from that of the mono-substituted analogues $MA_2O_4^+$, which possess radical character, as well as from that of $Al_3O_4^+$.^[2] Our results show that, while the structure is the same for both the cobalt and iron cluster, only the cobalt cluster exhibits reactivity towards methane and enables subsequent formaldehyde formation as shown by mass spectrometry measurements.

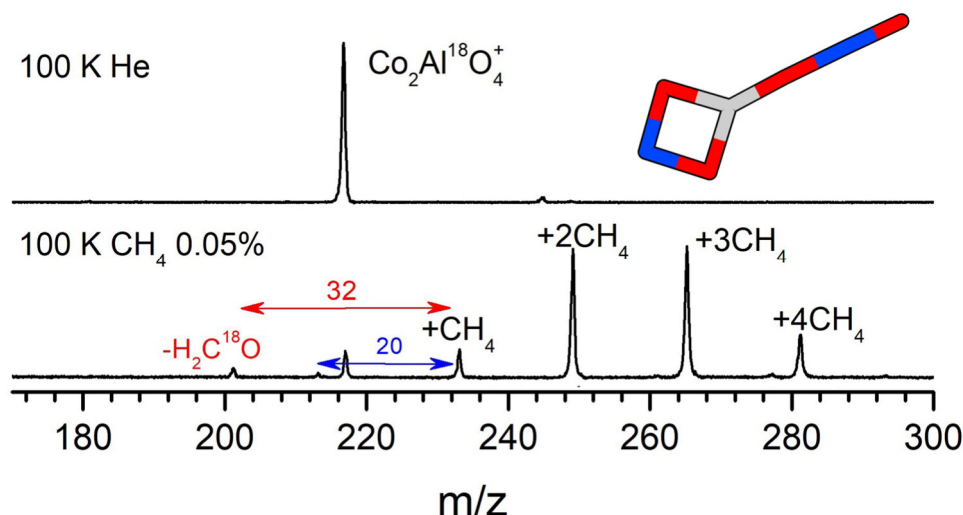


Figure 1: Mass spectrometry measurement on the reactivity of $Co_2AlO_4^+$ with methane.

[1] Z. Li *et al.*, J. Am. Chem. Soc. **138** (2016) 9537–9443.

[2] F. Müller *et al.*, J. Am. Chem. Soc. **142** (2020) 18050–18059.

CO₂ and H₂ activation on zinc-doped copper clusters

Bárbara Zamora¹, László Nyulászi^{1,2} and Tibor Höltzl^{1,2,3*}

¹Department of Inorganic and Analytical Chemistry, Budapest University of Technology and Economics, H-1111-Budapest, Műegyetem rkp 3 Hungary

²ELKH-BME Computation Driven Chemistry research group H-1111-Budapest, Műegyetem rkp. 3 Hungary

³Furukawa Electric Institute of Technology, Nanomaterials Science Group, H-1158 Budapest Késmárk utca 28/A, Hungary

Copper-based catalysts are commonly used to facilitate the CO₂ hydrogenation into useful chemicals. Here we systematically investigate the CO₂ and H₂ activation and dissociation on small Cu_nZn^{0/+} (n=3-6) clusters using Density Functional Theory. Our findings reveal that Cu₆Zn acts as a superatom, exhibiting an enlarged HOMO-LUMO gap and displaying inertness towards the activation or dissociation of CO₂ or H₂. While other neutral clusters exhibit weak CO₂ activation, with the exception of the otherwise unstable Cu₄Zn, the cationic clusters tend to preferentially bind CO₂ in a monodentate, non-activated manner. Generally, CO₂ activation is not favored. Conversely, H₂ dissociation is favored on all investigated clusters, except for Cu₆Zn.

We interpreted the bidentate CO₂ binding on the clusters based on the atomic charges and the energy decomposition analysis, which showed that the cluster donates electrons to the antibonding orbital of CO₂, thereby leading to its activation. In contrast to extended surfaces, the frontier orbitals of the clusters contribute mainly to the charge transfer. As the frontier orbital occupations and the orbital energies strongly depend on the number of itinerant electrons, CO₂ binding is also cluster-size dependent.

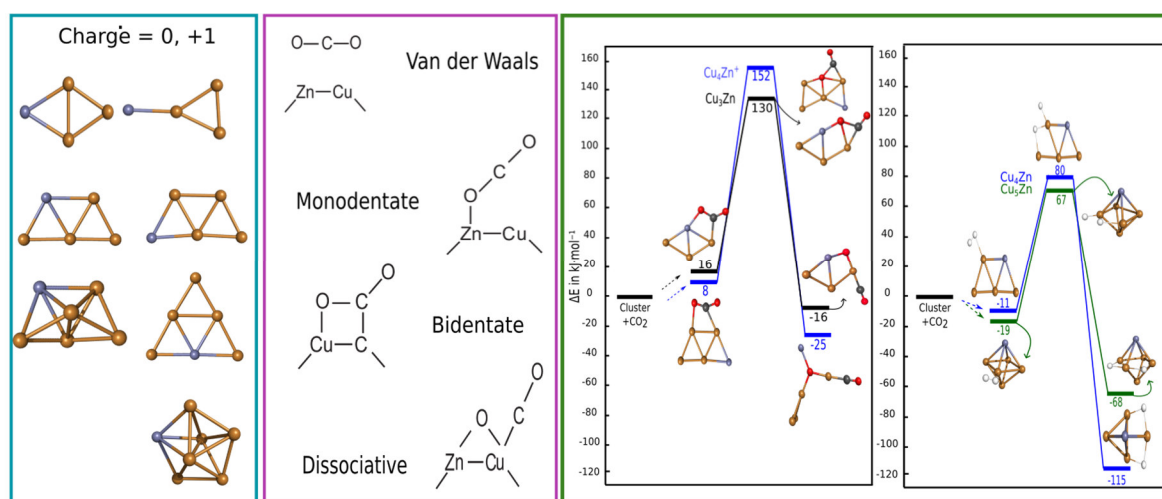


Figure 1: From left to right: Structural search of Cu_nZn (n=3-6) clusters, CO₂ and H₂ binding modes, and the CO₂ and H₂ dissociation reactions mechanisms.

[1] Zamora, B. Nyulászi, L. Höltzl, T. CO₂ and H₂ activation on zinc-doped copper clusters. [Manuscript submitted for publication].

Metal Oxidation: A common mechanism from clusters to bulk phase

Shaun Ard,¹ Al Viggiano,¹ Nicholas Shuman¹

¹ Air Force Research Laboratory, Space Vehicles Directorate, Kirtland Air Force Base, New Mexico 87117, USA

The Plasma Chemistry group at the Air Force Research Laboratory utilizes temperature dependent kinetics to derive mechanistic details of ion-molecule reactions. This capability has been expanded to study metal cluster systems in recent years. A broad commonality in the mechanism for oxidation of metals by molecular oxygen has been identified in both the gas-phase and on surfaces, extending across main-group, transition, and lanthanide metals and for anionic, cationic, and neutral systems. The lack of a dipole moment and small polarizability of molecular oxygen result in very weakly attractive ground-state potentials. Reactivity is only possible where an electronic transition, such as electron transfer to O₂ forming a superoxide, occurs at sufficiently long range to access a more deeply bound complex. Often, these surfaces cross where the entrance potential is repulsive, leading to a small activation barrier, early in the reaction coordinate. This barrier is generally rate limiting for these reactions with height correlated to the energetic cost of the electronic transition. Examples to be discussed include several metal anion cluster systems and their analogous surfaces, as well as lanthanide neutral and cation reactions.

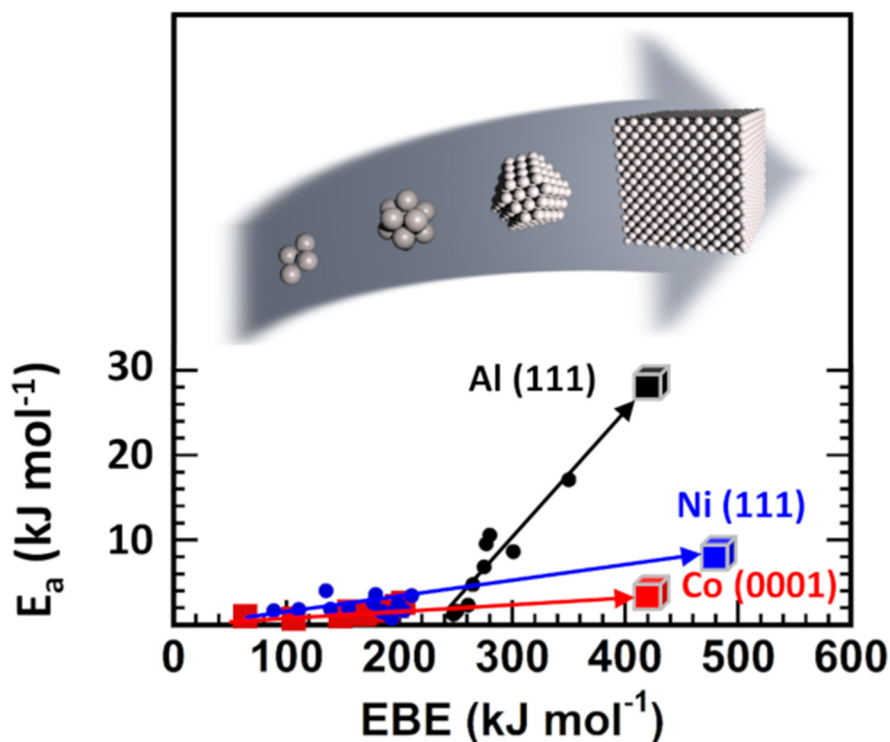


Figure 1: Observed barriers for the reactions of M_n^- (Al-black, Ni-blue, and Co-red with $1 < n < 20$) with O_2 as a function of electron binding energy.

Gas-phase Pd and PdZn clusters deposited on ZnO and SiO₂ as model catalyst for CO₂ hydrogenation to methanol

Imran Abbas¹, Sumant Phadke^{2,3}, Joao Coroa^{1,4}, Jinlong Yin⁴, Olga Safonova², Christophe Coperet³, Didier Grandjean¹, Ewald Janssens¹

¹Quantum Solid-State Physics, KU Leuven, Celestijnenlaan 200D, 3001 Leuven, Belgium

²Paul Scherrer Institute, Villigen PSI, 5232, Switzerland

³Department of Chemistry and Applied Biosciences, ETH Zürich, CH-8093 Zurich, Switzerland

⁴Teer Coatings Ltd., West Stone House, West Stone, Berry Hill Industrial Estate, Droitwich, WR9 9AS, UK

imran.abbas@kuleuven.be

Supported Pd nanoparticles have demonstrated promising catalytic activity for the hydrogenation of CO₂ into methanol, but the nature of the metal-support interface and its role in the reaction mechanism remains a topic of ongoing research [1-3]. In this study, we produced model catalysts by directly depositing well-defined Pd and PdZn clusters onto ZnO and SiO₂ powders using the Cluster Beam Deposition (CBD) technology. The clusters were deposited in high vacuum onto one gram of each pre-dried oxide powder placed in a vibrating cup to ensure the uniform deposition of size-controlled clusters containing 500 to 700 atoms. The cluster sizes were determined through in-situ time-of-flight mass spectrometry, and the loading of 0.1 wt% Pd clusters on the oxide powders was confirmed using ICP-OES. For the activity testing, the samples were in situ activated in pure hydrogen at 120°C for 30 minutes before conducting the catalytic tests. The catalytic activity tests for CO₂ hydrogenation were performed at 200-250°C and 40 bar, using 0.4g of each sample loaded in a plug flow reactor with a 5 mL/min feed gas mixture of 3H₂:1CO₂.

A very low concentration of Pd clusters (0.1 wt%) on ZnO was found to promote the hydrogenation of CO₂ to methanol and CO, while only minimal activity was observed for Pd/SiO₂. Fig. 1 illustrates a four-fold increase in the CO₂ hydrogenation rate compared to the sum of blank ZnO and Pd/SiO₂, confirming the excellent Pd-ZnO synergy in these model catalysts. To further investigate the Pd-ZnO synergy and uncover the structure-activity relationship, in-situ X-ray absorption spectroscopy was performed under CO₂ hydrogenation conditions. The use of well-defined Pd and PdZn catalysts enables a detailed investigation of the Pd-Zn and Pd-ZnO interfaces to unravel their structure-activity relationship.

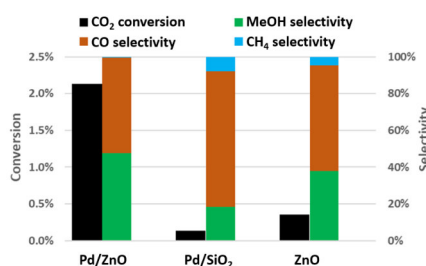


Fig: CO₂ conversion and product selectivity measured at 210°C and 40 bar of 3H₂:1CO₂ flowing at 5 mL/min.

- [1] M. Zabilskiy, et al. *Angew. Chem. Int. Ed.* **2021**, 202, 17053–17059.
- [2] S.R. Docherty et. al. *JACS Au* **2021**, 1, 450–458.
- [3] H. Bahruji et al. *J. Catal.* **2016**, 133–146.

Multiple NO adsorption on Au_{10}^- and Au_9Zn^- planar clusters. A comparative DFT study

Eva M. Fernández¹, L. Carlos Balbás²

¹ Dpto. de Física Fundamental, Universidad Nacional de Educación a Distancia, Spain

² Dpto. de Física Teórica Atómica y Óptica, Universidad de Valladolid, Valladolid, Spain
emfernandez@fisfun.uned.es

The doping of atomic clusters with transition metal atoms modifies to a lesser or greater extent the catalytic properties of pure specimens. In this work we study, by means of DFT calculations, the sequential adsorption of up to six NO molecules on Au_{10}^- and Au_9Zn^- clusters to learn how precise modifications of the atomic and electronic environment, namely one atom and a valence electron, affect the bonding of multiple NO molecules to anionic gold clusters. Our calculations confirm that these clusters have D_{3h} planar symmetry as previously determined through photoelectron spectroscopy experiments [1]. We verify also that pure $\text{Au}_{10}(\text{NO})_n^-$ compounds with $n \leq 6$ do not form adsorbed $(\text{NO})_2$ dimers, in agreement with reported experiments [2,3]. Instead, we obtain that the ground state of the doped $\text{Au}_9\text{Zn}(\text{NO})_6^-$ compound contains a $(\text{NO})_2$ cis dimer bridging two non-corner Au atoms of the $\text{Au}_9\text{Zn}(\text{NO})_4^-$ compound. The discussion of calculated adsorption energies, spin multiplicities, bond lengths, charge trends, strength frequencies of adsorbed NOs, and projected density of states (PDOS), brings additional testable differences between $\text{Au}_{10}(\text{NO})_n^-$ and $\text{Au}_9\text{Zn}(\text{NO})_n^-$ compounds with $n \leq 6$. In particular, the spin magnetic moment of these pure and doped compounds increases as the number of adsorbed NOs increases up to $n=4$ molecules, and then suddenly decreases for $n=5$ compounds, in a drastic manner specially for the Zn-doped ones.

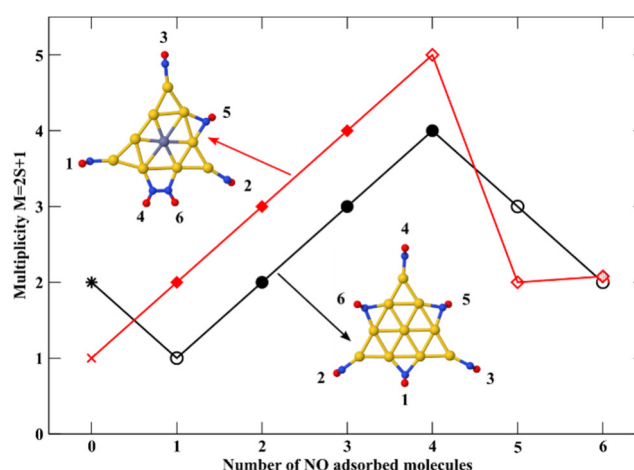


Figure 1: Sequential adsorption of n NO molecules at Au_{10}^- and Au_9Zn^- triangular clusters lead to planar compounds with increasing spin multiplicity up to $n=5$, and forms a $(\text{NO})_2$ dimer on the Zn doped cluster when the sixth NO molecule is absorbed.

- [1] M. Kulichenko, W.-J. Chen, Y.-Y. Zhang, C.-Q. Xu, J. Li and L.-S. Wang, J. Phys. Chem. A, 2021, 125, 4606.
- [2] J. Ma, X. Cao, M. Chen, B. Yin, X. Xing and X. Wang, J. Phys. Chem. A, 2016, 120, 9131.
- [3] J. Ma, T. Wang, J. Yang, J. Hu and X. Xing, Phys. Chem. Chem. Phys., 2020, 22, 25227.

Tuning of chemical affinity and reactivity in cobalt- and porphyrin-based 2D MOFs probed by ambient pressure spectroscopies

Francesco Armillotta^{1,2}, Davide Bidoggia², Stefania Baronio², Alessandro Sala³, Mattia Scardamaglia⁴, Suyun Zhu⁴, Maria Peressi², Erik Vesselli^{2,3}

¹*Institute of Condensed Matter Physics, École Polytechnique Fédérale de Lausanne, Switzerland*

²*Physics Department, University of Trieste, Italy*

³*TASC Laboratory, CNR-IOM Trieste, Italy*

⁴*Lund MAX IV Laboratory, Sweden*

2D MOF are optimal model systems to study single atom catalysis, thanks to their well-defined chemical environment and stability. Tetra-pyridyl porphyrins have already shown to be interesting tectons for the self-assembly of bi-metallic 2D structures with surprising electrochemistry activity in ORR and OER [1]. In this work, we show, by means of IR-Vis Sum Frequency Generation and Ambient Pressure XPS, that the Co species present in CoTPyP and CoTPyPCo layers (Fig. 1A,B) have different chemical activities. In particular, we demonstrate that Co^{II} TPyP is responsible for the formation of the hydroperoxyl (OOH) (reaction intermediate in oxygen reduction reaction), in the co-presence of 0.1 mbar H_2O and 10^{-3} mbar O_2 (Fig. 1C) [2]. On the other hand, the presence of the additional Co in Co^{III} TPyPCo^I deactivates the layer towards the same reaction, but increases its affinity towards CO on Co^{III} TPyPCo^I. We also demonstrate anti-cooperativity in the CO adsorption curve, which suggests the presence of long-range electronic interactions within the MOF, together with the evolution of the anharmonic constant of the C-O potential energy, the latter being intimately related to the CO cleaving energy (Fig. 1D) [3].

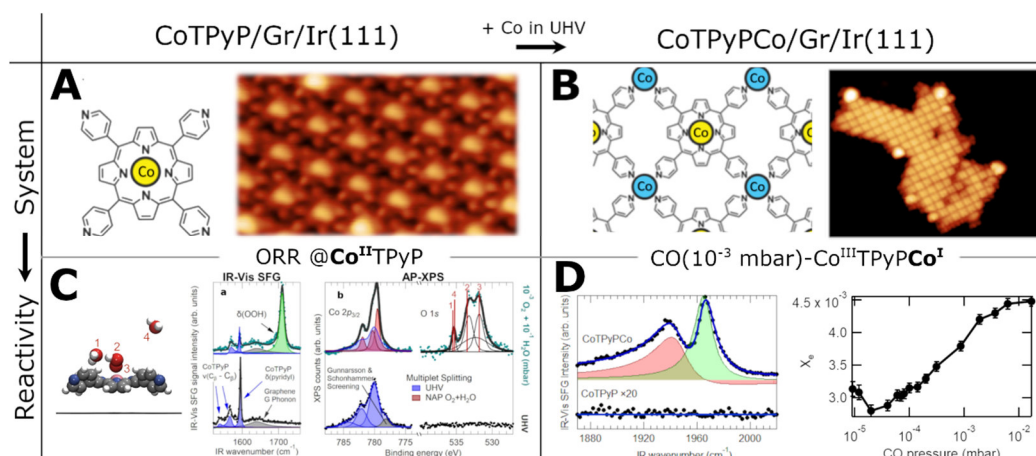


Figure 1: A) CoTPyP molecular structure and STM (10x5 nm); B) CoTPyPCo molecular structure and STM 30x30 nm; C) Evidence of OOH formation on Co^{II} TPyP in 0.1 mbar H_2O and 10^{-3} mbar O_2 [2]; D) CO ligation on Co^{III} TPyPCo^I and evolution of C-O anharmonic coefficient as function of CO pressure.

- [1] B. Wurster, D. Grumelli, D. Hötger, R. Gutzler, K. Kern, JACS **138** (2016) 3623-3626
- [2] F. Armillotta, D. Bidoggia, et al., M. Peressi, E. Vesselli, ACS Catalysis **12** (2022) 7950-7959
- [3] F. Armillotta, D. Bidoggia, et al., M. Peressi, E. Vesselli, *in preparation*

Water Oxidation on Free Calcium-Manganese-Oxide Clusters: Gas Phase Model Systems for the Catalytically Active Center of Photosystem II

Sandra M. Lang¹, Thorsten M. Bernhardt¹

¹ *Institute of Surface Chemistry and Catalysis, Ulm University, Germany*

Artificial photosynthesis, i.e. the conversion of solar energy into storable fuels via oxidation of water, represents one of the hot topics of today's catalysis research. In nature, this reaction takes place at an inorganic CaMn_4O_5 cluster embedded in the organic environment of photosystem II. Inspired by this natural catalyst, we aim to elucidate fundamental properties of calcium-manganese oxide clusters of different nuclearity, Mn/O ratio, and Ca content in order to aid the future design of new artificial water oxidation catalysts.

In a first step, we studied the reactivity of isolated cationic manganese oxide clusters of different size and composition with D_2^{16}O and H_2^{18}O . Employing a unique combination of gas-phase ion trap reactivity studies, infrared multiple-photon dissociation (IR-MPD) spectroscopy, and first-principles calculations we revealed the facile water deprotonation¹ and the exchange of the oxygen atoms of the cluster with water oxygen atoms² as well as the potential of di-manganese oxide clusters as water oxidation catalysts (to H_2O_2).³ In a further step we investigated binary calcium manganese oxide clusters ($\text{Ca}_{4-x}\text{Mn}_x\text{O}_4^+$ and $\text{Ca}_{5-x}\text{Mn}_x\text{O}_5^+$) and identified cluster compositions which are able to mediate the water oxidation reaction.^{3b,4} A detailed theoretical investigation (by U. Landman and coworkers, GaTech Atlanta, USA) of these clusters identified multiple roles of Ca and Mn and the necessity of a fine interplay between these two elements in order to enable the water oxidation reaction.⁵

- [1] Lang, S. M.; Bernhardt, T. M.; Kiawi, D. M.; Bakker, J. M.; Barnett, R. N.; Landman, U., *Angew. Chem. Int. Ed.* **2015**, *127*, 15328
- [2] Lang, S. M.; Fleischer, I.; Bernhardt, T. M.; Barnett, R. N., *J. Phys. Chem. C* **2015**, *119*, 10881.
- [3] (a) Lang, S. M.; Fleischer, I.; Bernhardt, T. M.; Barnett, R. N.; Landman, U., *Nano Lett.* **2013**, *13*, 5549; (b) Lang, S. M.; Zimmermann, N.; Bernhardt, T. M.; Barnett, R. N.; Yoon, B.; Landman, U., *J. Phys. Chem. Lett.* **2021**, *12*, 5248; (c) Lang, S. M.; Bernhardt, T. M.; Bakker, J. M.; Yoon, B.; Landman, U., *Mol. Phys.* **2023**, e2192306.
- [4] Mauthe, S.; Fleischer, I.; Bernhardt, T. M.; Lang, S. M.; Barnett, R. N.; Landman, U., *Angew. Chem. Int. Ed.* **2019**, *131*, 8592
- [5] Lang, S. M.; Helzel, I.; Bernhardt, T. M.; Barnett, R. N.; Landman, U., *J. Am. Chem. Soc.* **2022**, *144*, 15339.

Activation of CO₂ on size-selected copper clusters

Reider A. M.¹, Lushchikova O.¹, Kappe M.¹, Schmidt M.¹, Scheier P.¹

¹ *Institute for ion physics and applied physics, University of Innsbruck, Technikerstraße 25, 6020 Innsbruck, Austria*

Global urbanisation and industrialisation undoubtedly led to the crucial problem of global warming due to the accumulation of various greenhouse gases. Among these, the atmospheric concentration of CO₂ has increased drastically, with still rising levels, as its anthropogenic origin is stemming mainly from fossil fuel combustion. Consequently, research has been conducted to recycle CO₂ into valuable chemicals, where, as a first step, the reactions typically rely on the activation of CO₂ through a catalyst. The industrial conversion of CO₂ to methanol is commonly achieved at elevated temperatures and pressures through a Cu/ZnO/Al₂O₃ catalyst [1]. Besides this, several other catalysts for the hydrogenation of CO₂ to methanol have been investigated, where overall, copper based catalysts prove to be the most efficient ones. As this efficiency is influenced by the structural and electronic properties of the catalyst, studies suggest that the doping of the catalytic substrates with size-selected Cu clusters can enhance the catalytic activity [2]. Hence, detailed insight into the fundamental reaction steps of hydrogenation of CO₂ over Cu clusters on a molecular level is necessary to optimise any industrial processes.

In this sense, IR spectra offer the possibility to investigate the structures resulting from adsorption of CO₂ on cationic or anionic Cu_n clusters. Previous studies suggest that CO₂ is physisorbed on cationic copper clusters (Cu_n⁺, with n = 4-7) and show no signs of activation or reduction [3]. However, several studies on anionic metal clusters, such as experimental IR spectra of carbon doped Cu clusters

(C_mCu_n⁻, with m = 1-2, n = 3-10) [4] suggest a strong size dependent activation and dissociation of CO₂.

In this work, we want to investigate the reactions and structural properties of CO₂ on pure anionic Cu_n clusters via IR spectroscopy. To do so, we utilise superfluid helium nanodroplets as an ultra-cold and inert reaction matrix for the formation of Cu_n⁻ clusters and adsorption of CO₂, where additional He attachment serves as a non-perturbing messenger for high-resolution IRMPD spectra.

This work is supported by the Lise-Meitner grant M3229 and the Austrian Science Fund, FWF via projects number P34563 and W1259.

- [1] M. Behrens et al., Science 759, 2012
- [2] B. Yang et al., J. Phys. Chem. C 121, 19, 2017
- [3] Lushchikova, O. et al., Phys. Chem. Chem. Phys. 47, 23, 2021
- [4] Lushchikova, O. et al., Faraday Discussions 242, 2022

Modelling Metal Nanoparticle Structure and Dynamics in Reactive Environments

Beien Zhu¹, Yi Gao¹

¹ *Phonon Science Research Center for Carbon Dioxide, Shanghai Advanced Research Institute, Chinese Academy of Sciences, Shanghai 201210, China.*

Structure of metal nanoparticles is the key factor influencing their properties. In the recent 20 years, in situ experimental observations show that the structure of nano metals/alloys will evolve with the changing reaction conditions dramatically and in real time. Studying the structure and dynamics of nanoparticle in reactive environments are important for identifying, designing or tuning the active sites of nanocatalysts. Compared to the development of in situ experimental techniques, the development of dynamic simulation models is slow. Until recently, the quantitative prediction of structure of metal nanoparticle became possible. In this talk, we will introduce the progress of theoretical modeling in this field of our group. The main contents include: 1) the multiscale structure reconstruction (MSR) model for precious description of morphology of metal nanoparticle under reaction conditions [1]; 2) the dynamic activity-structure relation studied by combining the MSR model and reaction kinetic simulation methods [2, 3]; 3) the development of modeling the kinetic process of nanomaterial structure transformation induced by reactive gas adsorptions [4]; 4) cutting-edge works accomplished by using dynamic theoretical modeling and advanced in situ experimental characterization [5, 6].

References:

- [1] B. Zhu, J. Meng, W. Yuan, X. Zhang, H. Yang, Y. Wang, Y. Gao, *Angew. Chem. Int. Ed.* **59** (2020) 2171.
- [2] X.-Y. Li, B. Zhu, Y. Gao, *J. Phys. Chem. C* **125** (2021) 19756.
- [3] X. Duan, X.-Y. Li, B. Zhu, Y. Gao, *Nanoscale* **14** (2022) 17754
- [4] Y. Han, X.-Y. Li, B. Zhu, Y. Gao, *J. Phys. Chem. A* **126** (2022) 6538.
- [5] W. Yuan, B. Zhu, X.-Y. Li, T. W. Hansen, Y. Ou, K. Fang, H. Yang, Z. Zhang, J. Wagner, Y. Gao, Y. Wang, *Science* **367** (2020) 428.
- [6] W. Yuan, B. Zhu, K. Fang, X.-Y. Li, T. W. Hansen, Y. Ou, H. Yang, J. Wagner, Y. Gao, Y. Wang, Z. Zhang, *Science* **371** (2021) 517.

Molecular Activation of OCS and CO₂ in Cationic Holmium Complexes

Peter D. Watson¹, Edward I. Brewer,¹ Jonathan Mason,¹ Philip, A. J. Pearcy,¹ Stuart R. Mackenzie¹

¹ Department of Chemistry, University of Oxford, United Kingdom

Capture of pollutant gases and their transformation into useful chemical feedstocks are attractive for both reducing emissions and the generation of valuable material. We present an infrared photodissociation spectroscopy study of cationic holmium complexes with CO₂[1] and OCS. Due to relatively few studies on its catalytic activity in these cases, holmium is chosen for its ability to adopt +3 charge states in solution and by extension donate electron density, thereby activating bound molecules. In both systems, reactivity within the laser ablation source results in the formation of corresponding oxide and sulfide complexes which exhibit significant molecular activation of the solvating gas molecules ($\sim 100\text{ cm}^{-1}$ red-shift). Comparison with computational infrared spectra of the CO₂ and OCS complexes suggest the formation of carbonate ($\{\text{CO}_3\}^{\bullet\delta-}$) and thiocarbonate ($\{\text{COS}_2\}^{\bullet\delta-}/\{\text{CO}_2\text{S}\}^{\bullet\delta-}$) moieties respectively.

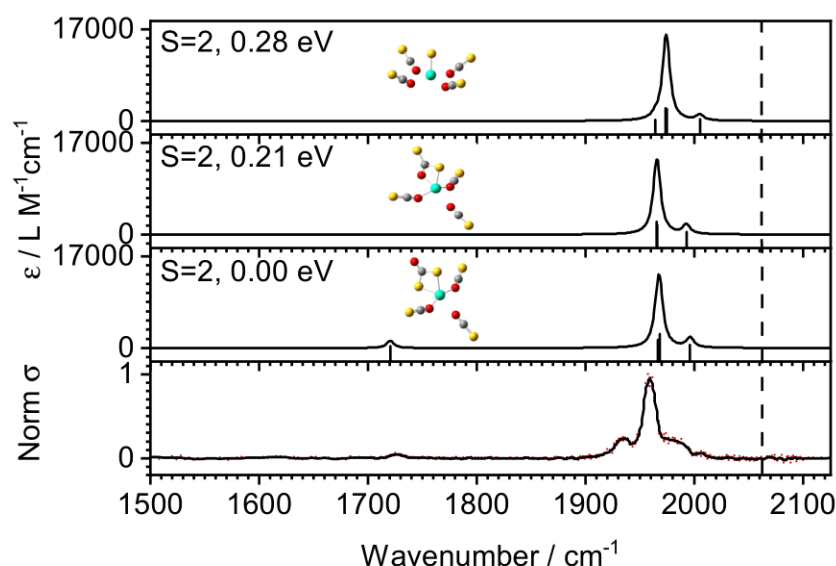


Figure 1: Comparison between experimental IRPD spectrum and predicted IRPD spectra for $[\text{HoS}(\text{OCS})_4]^+$. The dashed line represents the 'free' OCS stretch (2062 cm^{-1}).

[1] E.I. Brewer, A.E. Green, et al., PCCP **24** (2022) 22716.

Gas-Phase CuPd Bimetallic Cluster-Modified Electrodes as Model Electrocatalysts for CO₂ Conversion

Dimitra Papamichail^{1*}, Deema Balalta², Imran Abbas¹, Jason Song³, Thomas Altantzis⁴, Sara Bals², Deepak Pant³, Ewald Janssens¹, Didier Grandjean¹, Peter Lievens¹

¹ *1Quantum Solid State Physics, KU Leuven, Celestijnenlaan 200D, 3001 Leuven, Belgium*

² *Electron Microscopy of Materials Research (EMAT), University of Antwerp, Groenenborgerlaan 171, 2020 Antwerp, Belgium*

³ *Separation and Conversion Technology, Flemish Institute for Technological Research (VITO), Boeretang 200, 2400 Mol, Belgium*

⁴ *Applied Electrochemistry and Catalysis Group (ELCAT), University of Antwerp, Universiteitsplein 1, 2610 Wilrijk, Belgium*

Copper-based electrocatalysts possess the unique ability to convert CO₂ to multicarbon products such as ethylene – a precursor in many industrial processes. However, their stability and product selectivity remain insufficient. A promising approach to overcome these shortcomings and design better CO₂RR electrocatalysts is to tune Cu selectivity by forming bimetallic Cu-M systems [1] while establishing their detailed structure-selectivity relationship. To achieve this, we used laser ablation Cluster Beam Deposition (CBD) [2] to produce well-defined bimetallic cluster-modified electrodes [2]. More specifically, CuPd clusters with an original average size of 2.5 nm and mass loadings of 1-2 μg cm⁻² were deposited onto a carbon support. To produce a model catalyst which allows the independent investigation of the electronic and geometric structural effects induced to Cu by the second element, a Cu_{0.9}Pd_{0.1} composition was selected [3]. CuPd cluster-decorated electrodes were tested for CO₂ electrolysis and methane (C₁), and ethylene (C₂) were found among the products. As it is shown from the electrocatalytic activity trends, the evolution of C₂ products is correlated with the cluster mass loading. In addition, the cluster coverage influences the onset of the competitive H₂ production (HER). High resolution (Scanning) Transmission Electron Microscopy ((S)TEM) coupled with Energy-dispersive X-ray spectroscopy (EDX), and X-ray Photoelectron Spectroscopy (XPS) analyses of the as-prepared cluster-modified electrodes, show that the clusters feature some degree of CuPd alloying in the ambient. CuPd cluster-based systems will then be investigated in-situ using X-ray absorption spectroscopy to unravel their structure-catalytic performance relationship.

[1] X. Zhang et al., *Materials Today Advances*, 7 (2020) 100074

[2] V. C. Chinnabathini, et al., *Nanoscale*, 15 (2023) 6696-6708

[3] L. Zaza et al., *ACS Energy Letters* 7 (2022,), 4, 1284–1291 N

What Contributes to the Chiral Optical Response of the Glutathione-Protected Au₂₅ Nanocluster?

M. Monti¹, M. F. Matus,² S. Malola², A. Fortunelli³, M. Aschi⁴, M. Stener¹, H. Häkkinen^{2,5}

¹ Department of Chemical and Pharmaceutical Sciences, University of Trieste, Italy.

² Department of Physics, Nanoscience Centre, University of Jyväskylä, Finland.

³ CNR-ICCOM, National Research Council of Italy, Italy.

⁴ Department of Physical and Chemical Sciences, University of L'Aquila, Italy.

⁵ Department of Chemistry, Nanoscience Centre, University of Jyväskylä, Finland.

Chirality in thiolate-protected gold nanoclusters (RS-AuNCs) was first detected by Whetten *et al.* [1] who worked on AuNCs passivated by the L-glutathione (GSH). Since then, significant progresses have been made in the synthesis, characterization, and investigation of the optical properties of RS-AuNCs. [2-3] The interest in studying such systems is due to their potential applications, *e.g.*, as catalysts, [4] sensors, [5] and optical devices. [6]

In this work, we focus on the chiral [Au₂₅(GSH)₁₈]⁻¹, particularly interesting for the selective binding of target molecules such as the glutathione-S-transferase. [7] Combining classical molecular dynamics (MD) simulations, essential dynamics (ED) analysis and time-dependent density functional theory calculations, we were able to analyze its UV-visible CD spectrum (see Fig. 1). Both conformational and solvent effects revealed to play a fundamental role on the CD response of [Au₂₅(GSH)₁₈]⁻¹, with the water particularly influencing the UV energy range. Our results show that the CD peaks in this region can have up to 50% of the intensity originating from transitions involving electronic states of the solvation shell. Furthermore, the water shell itself assumes a chiral arrangement due to the interactions (*e.g.*, H-bonds) with the organic GSH ligands, showing a non-null CD response. Therefore, this work demonstrates the importance of including environmental factors in theoretical studies of RS-AuNCs to get a comprehensive understanding of their chiroptical response.

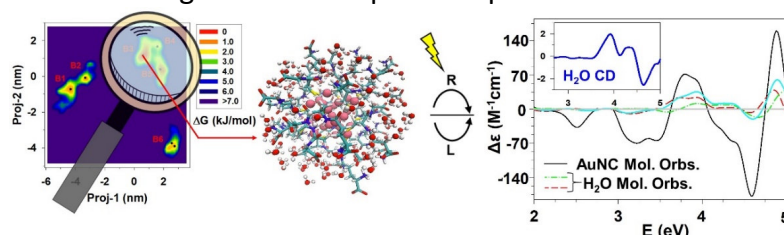


Figure 1: The MD trajectory is investigated by mean of the ED analysis obtaining a 2D conformational landscape (left panel) from which we can extract the most probable conformers (middle panel). On such structures we calculate the UV-CD spectra, also splitting the contribution to the transitions of the AuNC and water shell molecular orbitals (right panel).

- [1] T. G. Schaff, R. L. Whetten, *J. Phys. Chem. B.* **104** (2000) 2630.
- [2] C. Gautier, T. Bürgi, *Chem. Phys. Chem.* **10** (2009) 483.
- [3] F. Hidalgo, C. Noguez, *Nanoscale* **8** (2016) 14457.
- [4] M. M. Maye, J. Luo, L. Han, N. N. Kariuki, C. Zhong, *J. Gold Bull.* **36** (2003) 75.
- [5] H. Wohltjen, A. W. Snow, *Anal. Chem.* **70** (1998) 2856.
- [6] R. C. Price, R. L. Whetten, *J. Phys. Chem. B.* **110** (2006) 22166.
- [7] M. Zheng, X. Huang, *J. Am. Chem. Soc.* **126** (2004) 12047.
- [8] M. Monti, M. Stener, M. Aschi, *J. Comput. Chem.* **43** (2022) 2023.

Diphosphine-Protected M@Au₁₂ Superatoms (M = Au, Pd, Pt, Rh, Ir, Ru): Doping for Efficient Photoluminescence and Photocatalysis

Haru Hirai,¹ Shinjiro Takano,¹ Takuya Nakashima,² Takeshi Iwasa,^{3,4} Tetsuya Taketsugu,^{3,4}
Tatsuya Tsukuda¹

¹ Department of Chemistry, Graduate School of Science, The University of Tokyo, Japan

² Department of Chemistry, Graduate School of Science, Osaka Metropolitan University, Japan

³ Department of Chemistry, Faculty of Science, Hokkaido University, Japan

⁴ Institute for Chemical Reaction Design and Discovery (WPI-ICReDD), Hokkaido University, Japan

Ligand-protected gold superatoms are attracting nanomaterials because of their unique physicochemical properties arising from their geometrical and electronic structures. Doping of heterometal atoms is a promising approach to tune their physicochemical properties because the potential landscape for confining the valence electrons can be altered by the element, number, and location of the dopants.^[1] Although various heterometal-doped gold superatoms have been reported, the general understanding for the doping effects has not yet been established. To address this issue, we systematically synthesized and investigated photoluminescence (PL) properties of icosahedral M@Au₁₂ superatoms (M = Au, Pd, Pt, Rh, Ir, Ru) protected by two kinds of diphosphine ligands.

The dpmm-protected M@Au₁₂ superatoms (M = Rh, Ir, Ru; dpmm = bis(diphenylphosphino)methane; Figure 1a) exhibited intense PL. For example, Ru@Au₁₂ showed phosphorescence with a quantum yield (QY) of ~37% at room temperature, while the nature of PL switched to fluorescence at <130 K.^[2] This temperature-dependent behavior was rationalized by the small energy gap between S₁ and T₁ minima found by the theoretical prediction which can facilitates faster intersystem crossing. The PL QY of these superatoms increased by doping M element located at the lower left of the periodic table, which was attributed to the expansion of the HOMO–LUMO gap.

Similar trend was observed in the PL QY of the dppe-protected M@Au₁₂ (M = Au, Pd, Pt, Rh, Ir; dppe = 1,2-bis(diphenylphosphino)ethane; Figure 1b).^[3] The dppe-protected M@Au₁₂ superatoms (M = Pt, Ir) promoted photocatalytic cycloaddition reaction of bisenone, with much higher efficiency than the undoped Au₁₃.^[3] These studies provide a rational design principle for improving the photophysical properties and photocatalytic activities of Au superatoms via doping of heterometal elements.

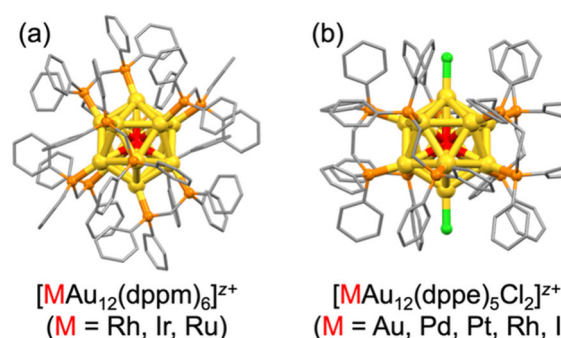


Figure 1: Structures of M@Au₁₂ superatoms protected by (a) dpmm and (b) dppe and Cl ligands.

[1] Omoda, T. *et al. Small* **2020**, 17, 2001439.

[2] Takano, S. *et al. J. Am. Chem. Soc.* **2021**, 143, 10560.

[3] Hirai, H. *et al. Angew. Chem., Int. Ed.* **2022**, 61, e202207290

Gas phase synthesis and spectroscopy of silver cluster-porphyrin hybrids

Frederic Ußling², Tobias Bischoff¹, Andre Knecht¹, Thomas Möller¹, Andrea Merli¹

¹ *Institut für Optik und Atomare Physik, Technische Universität Berlin, Germany*

² *Laboratory for Solid State Physics, ETH Zurich, Switzerland*

Small gas-phase silver clusters on porphyrin templates are promising devices towards the development of materials with tailored optical properties [1]. In this study, we report first synthesis of hybrid systems consisting of cationic silver clusters and free base octaethylporphine (OEP) or silver doped octaethylporphine (AgOEP). The hybrids were prepared in a collision cell. A size dependence of the hybrid cluster was observed in the mass spectra due to the influence of the metallic core in the vaporized porphyrin. Using the frequency-doubled signal of a nanosecond OPO laser system, we investigate the optical properties of $\text{Ag}_3[\text{Ag}(\text{OEP})]^+$ by photodissociation spectroscopy. Comparing the spectra of the hybrid system with the spectra of Ag_3^+ and $\text{Ag}(\text{OEP})^+$, we conclude that the electronic structure of the cationic silver trimer may be partially preserved. With these results, we can speculate about the bond type between metallic cluster and the porphyrin and the role of the metallic core for the hybrid system's geometric structure.

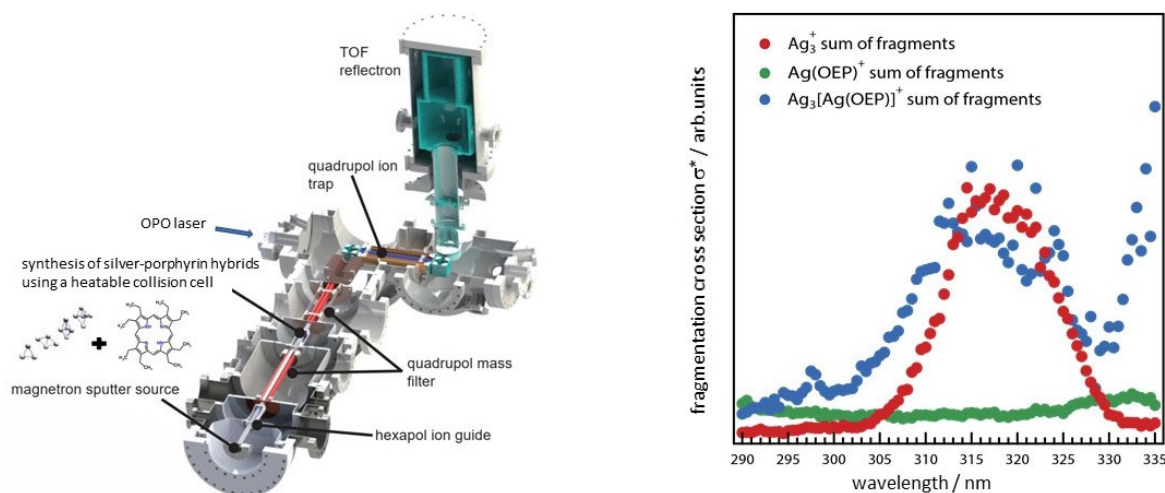


Figure 1: Experimental setup used for the synthesis and investigation of silver cluster porphyrin hybrids. Photodissociation spectra of $\text{Ag}_3[\text{Ag}(\text{OEP})]^+$ as well as the fragments Ag_3^+ and $\text{Ag}(\text{OEP})^+$

[1] M. I. S. Röhr, P. G. Lisinetskaya, R. Mitric, J. Phys. Chem. A, **120** (2016), 4465-4472

Comparison of experimental high-resolution UV-Vis absorption spectra for a series of ligand protected nanoalloys with boosted hybrid kernel TDDFT simulations

P. D'Antoni¹, A. Fortunelli², L. Sementa³, F. Maran^{4,5}, S. Bonacchi⁴ and M. Stener¹

¹ *Dipartimento di Scienze Chimiche e Farmaceutiche, Università degli Studi di Trieste, Italy*

² *CNR-ICCOM, Consiglio Nazionale delle Ricerche, Italy*

³ *CNR-IPCF, Consiglio Nazionale delle Ricerche, Italy*

⁴ *Dipartimento di Scienze Chimiche, Università di Padova, Italy*

⁵ *Department of Chemistry, University of Connecticut, United States*

Nowadays, the tuning of electronic and optical properties of thiolate protected noble metal clusters by doping with transition metals has gained much interest [1,2]. By simulating their optical response, we can better rationalize the experiments and provide important insights into the design of such systems. Of course, that assumes the availability of fast and robust computational schemes and experimental data rich in detailed information. Here we present such a virtuous combination applied to the study of $[\text{Ag}_{25}(\text{SR})_{18}]^-$ nanocluster, its Pt doped analogous $[\text{Ag}_{24}\text{Pt}(\text{SR})_{18}]^{2-}$ and the golden version $\text{Au}_{24}\text{Pt}(\text{SR})_{18}$.

For these clusters the UV-Vis photoabsorption spectra, up to 5 eV, were obtained at low temperature (77 K). This enables to compare the resulting fine structure with simulations carried out using a new, approximated yet fast and reliable, approach to TDDFT [3].

The principal spectral features of each system are analyzed in terms of molecular orbitals contributions and Independent Component Map of Oscillator Strength.

This work brings together an accurate and affordable computational approach and detailed experimental data proving the reciprocal influence and importance.

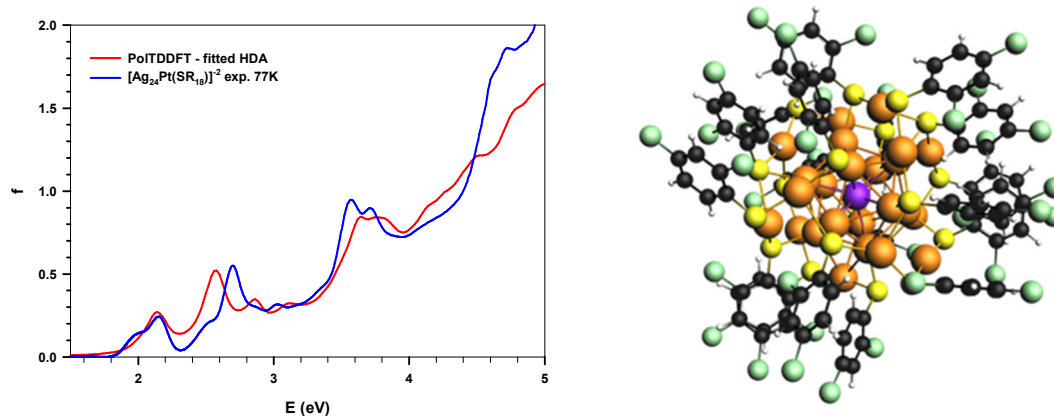


Figure 1: comparison between experiment and simulated spectrum for bimetallic nanocluster $[\text{Ag}_{24}\text{Pt}(\text{SR})_{18}]^{2-}$ (left panel), the geometry of it (right panel).

- [1] W. Fei, S. Antonello, T. Dainese, A. Dolmella, M. Lahtinen, K. Rissanen, A. Venzo, F. Maran, J. Am. Chem. Soc. **141** (2019) 16033
- [2] J. Yan, H. Su, H. Yang, S. Malola, S. Lin, H. Häkkinen, N. Zheng, J. Am. Chem. Soc. **137** (2015) 11880
- [3] M. Medves, L. Sementa, D. Toffoli, G. Fronzoni, A. Fortunelli, M. Stener, J. of Chem. Phys. **152** (2020) 184104

Evaluation of Superatomic Electronic Structures of Ligand-Protected Gold/Silver Supratoms by Gas-Phase Photoelectron Spectroscopy

Shun Ito¹, Kiichirou Koyasu,¹ Tatsuya Tsukuda¹

¹ Department of Chemistry, Graduate School of Science, The University of Tokyo, Japan

Ligand-protected gold/silver clusters have gathered much interest as new functional nanomaterials [1]. High stability of a benchmark system $[\text{Au}_{25}(\text{PET})_{18}]^-$ (PET = 2-PhC₂H₄S) with an icosahedral Au₁₃ core has been explained by the electronic shell closure of superatomic orbitals with $(1\text{S})^2(1\text{P})^6$ configuration [2]. Such a superatom concept has been applied to rationalize the doping effect on the electronic structure of $[\text{MAu}_{24}(\text{PET})_{18}]^-$ and the bonding scheme in a bi-icosahedral Au₂₃ core of Au₃₈(PET)₂₄ [3]. We have elucidated superatomic electronic structures of ligand-protected Au/Ag superatoms by gas-phase anion photoelectron spectroscopy (PES) (Figure 1a [4]).

Free anions of ligand-protected superatoms were produced by an electrospray ionization source, mass-selected by a time-of-flight mass spectrometer, and irradiated with a UV pulsed laser in a magnetic-bottle type photoelectron spectrometer for PES. PE spectra of $[\text{M}_{25}(\text{SR})_{18}]^-$ (M = Au, Ag) (Figure 1b [5]) demonstrated that the corresponding neutrals have large electron affinities comparable to those of halogen atoms and thus they can be categorized as superhalogens [6]. PES on $[\text{M}\text{Ag}_{24}(\text{SR})_{18}]^-$ (M = Ag, Au, Pd⁺, Pt⁺) (Figure 1b [5]) revealed that the doping of Pd/Pt at the central position upshifted the energy levels of 1P superatomic orbitals, which can be explained by the two-step jellium model [8]. The PE spectra of $[\text{MAu}_{37}(\text{PET})_{24}]^-$ (M = Pd, Pt) (Figure 1c [7]) with bi-icosahedral MAu₂₂ cores exhibit two distinct peaks at the spectral onset, which are assigned to molecular orbitals constructed by bonding and antibonding interaction between the 1P superatomic orbitals of Au₁₃ and MAu₁₂ [3].

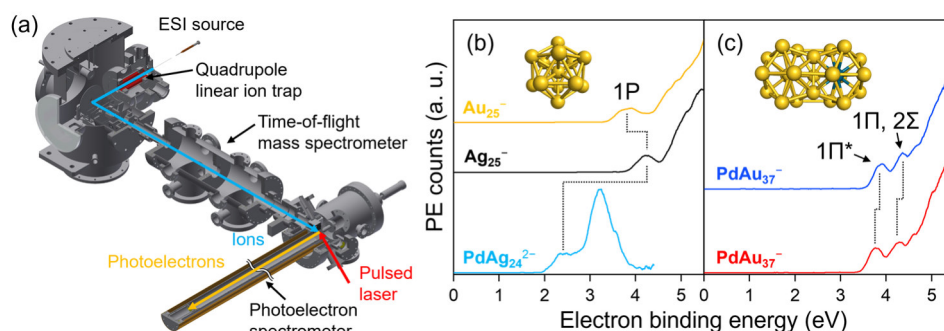


Figure 1: (a) Schematic view of the apparatus. PE spectra of (b) $[\text{Au}_{25}(\text{PET})_{18}]^-$, $[\text{Ag}_{25}(\text{DMBT})_{18}]^-$, and $[\text{PtAg}_{24}(\text{DMBT})_{18}]^{2-}$ and (c) $[\text{MAu}_{37}(\text{PET})_{24}]^-$ (M = Pd, Pt). The inset shows the structures of the cores.

- [1] S. Takano, T. Tsukuda, *J. Am. Chem. Soc.* **143** (2021) 1683.
- [2] M. Walter, J. Akola, O. Lopez-Acevedo, P. D. Jadzinsky, G. Calero, C. J. Ackerson, R. L. Whetten, H. Grönbeck, H. Häkkinen, *Proc. Natl. Acad. Sci.* **105** (2008) 9157.
- [3] L. Cheng, C. Ren, X. Zhang, J. Yang, *Nanoscale* **5** (2013) 1475.
- [4] S. Ito, K. Koyasu, S. Takano, T. Tsukuda, *J. Phys. Chem. Lett.* **12** (2021) 10417.
- [5] S. Ito, Y. Tasaka, K. Nakamura, Y. Fujiwara, K. Hirata, K. Koyasu, T. Tsukuda, *J. Phys. Chem. Lett.* **13** (2022) 5049.
- [6] D. E. Bergeron, A. W. Castleman, T. Morisato, S. N. Khanna, *Science* **304** (2004) 84.
- [7] E. Ito, S. Ito, S. Takano, T. Nakamura, T. Tsukuda, *JACS Au* **2** (2022) 2627.
- [8] E. Janssens, S. Neukermans, P. Lievens, *Curr. Opin. Solid State Mater. Sci.* **8** (2004) 185.

Atomically-Precise, Highly Luminescent NHC-Au₁₃ Clusters as Robust Bioimaging Agents

Dennis A. Buschmann¹, Shinjiro Takano¹, Yoshikatsu Sato², Masakazu Nambo², Cathleen M. Crudden^{2,3}, Tatsuya Tsukuda¹

¹ Graduate School of Science, The University of Tokyo, Japan, Japan

² Institute of Transformative Bio-Molecules, Nagoya University, Japan

³ Department of Chemistry, Queen's University, Kingston, ON, Canada

The continuous demand for new cancer therapeutics has spurred research on nanotechnology-based cancer immunotherapy [1]. Especially gold nanoparticles and clusters have emerged as versatile bioimaging and therapy agents due to their easily tunable photophysical properties and high biostability [2,3]. Here we wish to report on the synthesis and characterization of icosahedral Au₁₃ clusters protected by N-heterocyclic carbene (NHC) ligands [4], bearing ester and carboxy functional groups to promote stability in cellular environment. Furthermore, their applicability as bioimaging agents was screened.

Mono- and bidentate NHC-gold complexes were synthesized according to standard procedures, using a novel ethylbenzoate NHC ligand, (Me₂S)AuCl and K₂CO₃. Subsequent reduction with NaBH₄ afforded atomically-precise, NHC-protected Au₁₃ clusters, and their molecular structure was determined by single-crystal X-ray diffraction analysis (Figure 1, left). Saponification in basic aqueous media gave water-soluble, carboxybenzyl-NHC-Au₁₃ clusters. The photoluminescence behavior of the clusters was scrutinized (Figure 1, right), revealing high photoluminescence quantum yields up to 27%. Biostability studies were performed, showing very little cytotoxicity toward HeLa cells for all clusters. Fluorescence imaging studies were conducted, again with HeLa cells. The Au₁₃ clusters displayed high cell uptake and accumulation in the cells, as well as bright emission in fluorescence imaging, making them promising bioimaging agents for future medicinal chemistry applications.

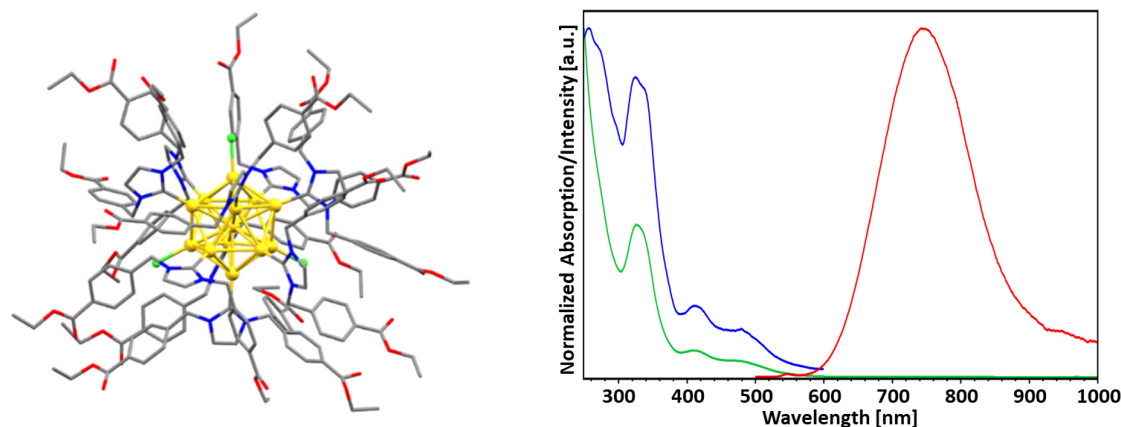


Figure 1: Single-crystal structure (left) and absorption (green), excitation (blue), and emission (red) spectra (right) of benzoate-NHC-Au₁₃ cluster [Au₁₃(NHC^{COOEt})₉Cl₃].

- [1] J. Lou, L. Zhang, G. Zheng, *Adv. Therap.* **2** (2019), 1800128.
- [2] C. J. Murphy *et al.*, *Acc. Chem. Res.* **41** (2008), 1721.
- [3] S. Palmal, N. R. Jana, *WIREs Nanomed. Nanobiotechnol.* **6** (2014), 102.
- [4] M. R. Narouz, H. Häkkinen, T. Tsukuda, C. M. Crudden *et al.*, *Nat. Chem.* **11** (2019), 419.

Correlating the Impact of Heteroatoms Core-Tailoring of Atomically Precise $\text{Ag}_{25}(\text{SR})_{18}$ Nanoclusters on the Photocatalytic Activities

Ye Liu¹, Nicola Pinna¹ and Yu Wang¹

¹ Department of Chemistry, IRIS Adlershof & The Center for the Science of Materials Berlin, Humboldt-Universität zu Berlin

Research on the anisotropic structures of nanomaterials has expanded the fundamental understanding of their structure-property relationships, whereby a wide range of applications have been developed. Herein, we go deeper into this relationship by studying the electronic properties and photocatalytic activities of the atomically precise $\text{Ag}_{25}(\text{SR})_{18}$ nanoclusters. The central metal atom in an atomically precise Ag_{25} nanocluster (NC) is replaced with a single Pd, Pt, and Au atom, respectively, and employed as a model system to study the structure–property–activity relationship at the atomic level. While the geometric structures are well-preserved after doping, the electronic structures of Ag_{25} NCs are significantly altered. Results show that heteroatoms doping has a negative impact on performance, particularly in the cases of Pd and Au doping. Ultraviolet photoelectron spectroscopy measurements and density functional theory calculations suggest that the lower activities are due to an energy mismatch between the levels of doped NCs and TiO_2 .^{1, 2} These findings not only reveal the impact of heteroatoms doping on the electronic properties and photocatalytic activities of NCs, but can also guide the design of heterometallic NCs for photocatalytic applications.

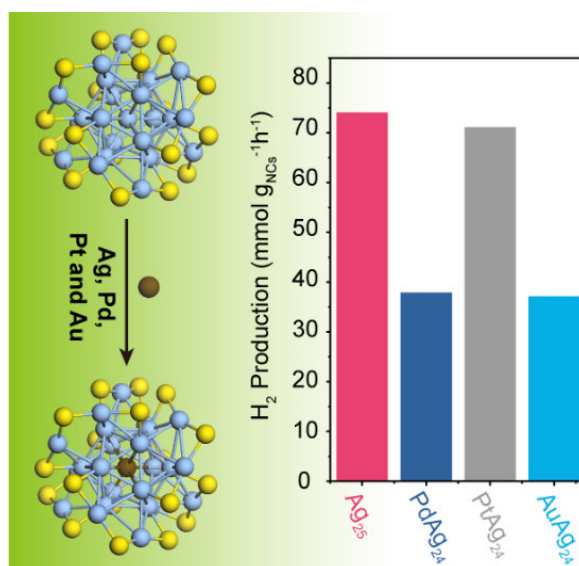


Figure 1: Schematic illustration of the photocatalytic activities of $\text{MAg}_{24}(\text{SR})_{18}$ nanoclusters

1. Liu Y, Long D, Springer A, Wang R, Koch N, Schwalbe M, et al. Correlating Heteroatoms Doping, Electronic Structures, and Photocatalytic Activities of Single-Atom-Doped $\text{Ag}_{25}(\text{SR})_{18}$ Nanoclusters. *Solar RRL*. 2023;7(6):2201057.
2. Wang Y, Liu XH, Wang Q, Quick M, Kovalenko SA, Chen QY, et al. Insights into Charge Transfer at an Atomically Precise Nanocluster/Semiconductor Interface. *Angew Chem Int Ed Engl*. 2020;59(20):7748-54.

Surface Modulation on $\text{Au}_{25}(\text{SR})_{18}$ NCs *via* the Ligand Exchange Induced Size/Structure Transformation

Saniya Gratiuous¹, Adarsh Kv,² and Sukhendu Mandal¹

¹ Indian Institute of Science Education and Research, Thiruvananthapuram, India

² Indian Institute of Science Education and Research, Bhopal, India

Fundamental understanding of the structure-property correlations and the rational design of nanoclusters (NCs) has been a long-held aspiration in the field of nanoscience. To a great extent, transformation chemistry can be utilized in this regard to understand the structural growth patterns and corresponding property evolutions in atomically precise metal NCs.^[1,2] Therefore, understanding the transformation mechanism is of paramount importance to functionalize and tailor the surface properties and achieve rational synthesis and design of NCs. Ligand exchange induced size/structure transformation (LEIST) is a common transformation methodology where a precursor NC is thermally activated in presence of an excess amount of exogenous thiol to undergo size/structure transformation.^[3] The LEIST methodology can thus be employed to impart specific properties to the NCs by modifying the surface ligands. Herein, we have carried out a comparative study on LEIST of $[\text{Au}_{23}(\text{S}-\text{C}_6\text{H}_{11})_{16}]^-$ NCs using the $p\text{-XC}_6\text{H}_4\text{SH}$, $\text{X} = \text{F}, \text{Cl}, \text{Br}, \text{and H}$ under thermal conditions. We have tuned the electronegativity at the para position of the incoming benzenethiols and tried to understand the changes in the transformation products as well as mechanism with this slightest change in the incoming thiol structure. Time-dependent UV-vis spectroscopy and MALDI-MS spectrometry were employed to monitor the transformation process and both revealed the formation of $[\text{Au}_{25}(p\text{-XC}_6\text{H}_4\text{S})_{18}]^-$ NCs, $\text{X} = \text{F}, \text{Cl}, \text{Br}, \text{H}$. Single crystals of the as-obtained NCs revealed the structural similarity of the $[\text{Au}_{25}(p\text{-XC}_6\text{H}_4\text{S})_{18}]^-$ NCs to the previously reported Au_{25} NCs.^[4] However, the $[\text{Au}_{25}(p\text{-BrC}_6\text{H}_4\text{S})_{18}]^-$ NCs showed an inconsistency in the transformation mechanism and the photophysical properties compared to the $[\text{Au}_{25}(p\text{-XC}_6\text{H}_4\text{S})_{18}]^-$ NCs, $\text{X} = \text{F}, \text{Cl}, \text{H}$. Further the ultrafast transient absorption spectroscopy was employed for in-depth understanding of the varying electronic effect of incoming thiols on the transformation mechanism as well as product formation.

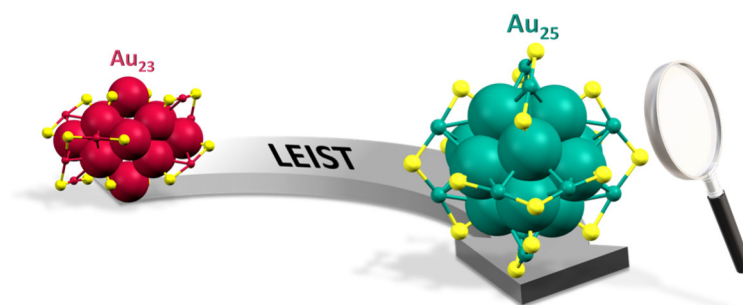


Figure 1: Detailed investigation into the LEIST of $\text{Au}_{23}(\text{SR})_{16}$ NCs to $\text{Au}_{25}(\text{SR}')_{18}$ NCs

- [1] X. Kang, M. Zhu, *Chem. Mater.* **2019**, 31, 9939–9969.
- [2] C. Zeng, Y. Chen, A. Das, R. Jin, *J. Phys. Chem. Lett.* **2015**, 6, 2976–2986.
- [3] R. Jin, C. Zeng, M. Zhou, Y. Chen, *Chem. Rev.* **2016**, 116, 10346–10413.
- [4] X. Kang, H. Chong, M. Zhu, *Nanoscale* **2018**, 10, 10758–10834.

Influence of the magnetic field configuration of a magnetron on the cluster growth mechanism in a sputtering gas aggregation source

João Coroa^{1,2}, Giuseppe Sanzone¹, Hailin Sun¹, Ewald Janssens², Jinlong Yin¹

¹ Teer Coatings Ltd, West Stone, Droitwich, Worcestershire, WR9 9AS, UK

² Department of Physics and Astronomy, KU Leuven, B-3001 Leuven, Belgium

Cluster production using physical methods provides several advantages compared with chemical routes, such as better control of the size distribution and the minimised impact on the environment. On the other hand, their slow deposition rate has inhibited the physical approaches from being used more widely. To address this issue, we have systematically studied the influence of aerodynamics on the efficiency of cluster transportation in a cluster source [1]. Another important factor that needs to be considered is the influence of magnetic field configuration on the magnetron sputtering device.

In the 1980s, it was found that by tuning the unbalance degree of the magnetic field configuration, one can significantly increase the number of electrons escaping from the plasma sputtering region, increase the ion flux and the associated high ion bombardment on the substrate and thus produce very dense thin films [2]. Subsequently, simulations have been carried out to better understand how the unbalanced magnetic field influences the sputtering parameters [3].

Although significant progress has been made in the understanding of how the magnetic field influences the magnetron sputtering process, there are very few reports about its influence on cluster formation. An exception is a recent work by Vaidulych et al [4], where it is argued that a decrease in the magnetic field assisted with an increase in the flow of the carrier gas greatly improves the deposition rate of the nanoparticles. However, in this approach, the sputtering rates across experiments were not strictly maintained, which might influence the results in an unexpected way. Furthermore, a concrete explanation of how this magnetic field affects cluster growth is still missing.

In this work, preliminary simulation results on the influence of different magnetic field configurations are shown. The electromagnetic modelling software package OPERA was used to optimise the magnetic field configuration, and the configurations of the magnetic field on a magnetron were physically varied to validate the simulation results. Plasma density was measured at different magnetic configurations in an attempt to investigate its influence on the density of charged particles surrounding the target. A hypothesis will be proposed to explain cluster growth mechanisms under the influence of different plasma spatial distributions.

[1] G. Sanzone, P. Lievens, Review of Scientific Instruments **vol. 92** (2021) p. 033901

[2] B. Window, N. Savvides, Vacuum Science and Technology A Vacuum, Surfaces and Films **vol. 4** (1986) pp. 196 – 202

[3] I. Svadkovski, S. Zavatskiy, Vacuum **vol. 68** (2002) pp. 283–290

[4] M. Vaidulych, H. Biederman, Plasma Processes and Polymers **vol. 16** (2019) p. 08

Prospects and experimental challenges for matter-wave interferometry with massive metal clusters

Bruno E. Ramírez-Galindo, Sebastian Pedalino, Tomás de Sousa, Stefan Gerlich, Philipp Geyer, and Markus Arndt

*University of Vienna, Faculty of Physics & Vienna Doctoral School in Physics,
Boltzmannngasse 5, 1090 Vienna, Austria*

Almost a hundred years after the publication of Louis de Broglie's hypothesis, matter-wave interference experiments have shown the validity of the wave-particle duality for increasingly massive and complex systems. Recent experiments at the Long-Baseline Universal Matter-Wave Interferometer (LUMI) have shown interference of functionalized oligoporphyrins with masses above 25 *kDa* [1]. However, experiments with more massive objects are required to provide advanced tests of macroscopicity and wavefunction collapse models [2]. With this in mind, we turn to metal clusters to seek quantum interference of nanoparticles with masses up to 10^6 *Da*.

Here we present suitable source and detection schemes for interferometry experiments with yttrium and hafnium metal clusters [3]. A magnetron sputtering source is found suitable for the generation of a continuous metal cluster beam with a wide range of masses (80 - 800 *kDa*) and a small velocity distribution ($v = 100$ m/s, $\Delta v/v < 10\%$). Yttrium and hafnium nanoclusters, whose ionization energies below 4.6 eV and photoionization cross-sections within the range of 10^{-14} to 10^{-15} cm^2 , are found to be compatible with the use of photoionization gratings and detection with 1 W of 266 nm UV laser light focused to 40×500 μm^2 .

We present some of the open technical challenges. Special emphasis is made on the alignment criteria for angular and translational degrees of freedom of all light gratings [4], the vacuum requirements, and vibrational isolation mechanisms. We discuss how each of these challenges is being addressed in the laboratory to push the limits of quantum interference.

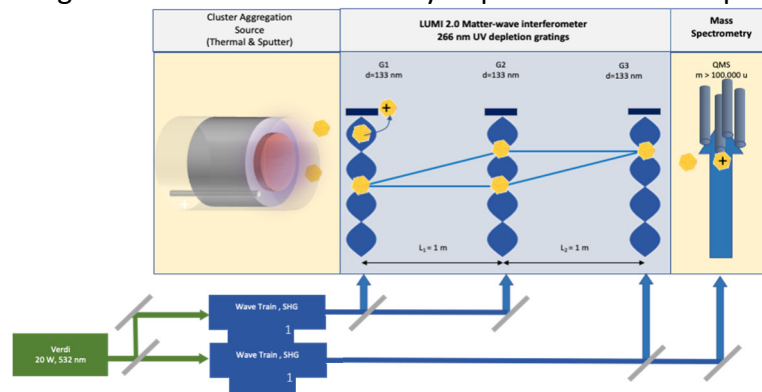


Figure 1: Current setup of the LUMI 2.0 matter-wave interferometer. Left to right: magnetron sputtering source, 266 nm standing light wave gratings, and mass filtered photoionization detector.

- [1] Fein, Y. Y., Geyer, P., Zwick, P., Kiałka, F., Pedalino, S., Mayor, M., Gerlich, S., & Arndt, M. (2019). *Nature Physics*, 15(12).
- [2] Kiałka, F., Fein, Y. Y., Pedalino, S., Gerlich, S., & Arndt, M. (2022). *AVS Quantum Science*, 4(2), 020502.
- [3] Pedalino, S., de Sousa, T., Fein, Y. Y., Gerlich, S., & Arndt, M. (2022). *Physical Review A*, 106(2), 023312.
- [4] Pedalino, S., Ramírez Galindo, B., de Sousa, T., Fein, Y. Y., Geyer, P., Gerlich, S., & Arndt, M. (2023). *Quantum Sensing, Imaging, and Precision Metrology*, 12447, 100–109.

Revealing dynamic trapping of nanoparticles in a gas phase aggregation source by in-situ diagnostics

J. Drewes¹, O. Polonskyi¹, S. Rehders¹, T. Strunskus^{1,3}, H. Kersten^{2,3}, F. Faupel^{1,3}, A. Vahl^{1,3}

¹ *Institute for Materials Science – Chair for Multicomponent Materials, Faculty of Engineering, Kiel University, Kaiserstraße 2, D-24143 Kiel, Germany*

² *Chair for Plasma Technology, Institute of Experimental and Applied Physics, Kiel University, Leibnizstr.19, D-24098 Kiel, Germany*

³ *Kiel Nano Surface and Interface Science KiNSIS, Kiel University, Christian-Albrechts-Platz 4, D-24118 Kiel, Germany*

Gas phase synthesis of nanoparticles (NPs) and NP beam deposition methods such as via a Haberland-type gas aggregation source (GAS) attract substantial research interest due to their capability of depositing surfactant-free, highly pure NPs and being compatible with both, a range of other vapor phase deposition methods and a large variety of different substrates. The concept of a magnetron-based GAS was already introduced in the early 1990s [1] and a broad theoretical framework on the condensation of NPs from supersaturated vapors in GAS has evolved [2]. However, the observation of trapping of NPs within the aggregation zone close to the target indicated the importance of the interplay between NP growth, transport properties and their dynamics, which is still under active research.

In this contribution it is demonstrated to which extent photon-based *in-situ* diagnostics can be applied to understand dynamic trapping processes inside a GAS. Ag-based NPs are chosen as a reference material due to their high deposition rate and plasmon absorption peak of them in the UV-Vis range. UV-Vis spectroscopy is applied to locate the AgNPs inside the GAS, and by recording spectra continuously a time resolution in the range of 100ms is achieved. A shift of aggregation length and relative position of the UV-Vis light beam is induced by moving the magnetron in and out of the GAS chamber. Via UV-Vis spectroscopy it was found that gas flow and pressure strongly impact the trapping location of NPs [3]. To further extend the lateral resolution and increase the information on trapping locations towards 2D, laser light scattering of a green laser (532nm, outside of plasmonic absorption peak of Ag NPs) was applied. With this method it was possible to obtain spatially and temporally resolved information on NP trapping, indicating the inherent dynamics in the trapping processes [4].

Acknowledgements

Funded by the Deutsche Forschungsgemeinschaft (DFG, German Research Foundation) – Project-ID 434434223 – SFB 1461 and Grant/Award Number: PO2299/1-1.

[1] H. Haberland, M. Karrais, M. Mall, Y. Thurner, J. Vac. Sci. Technol. A (1992) 10, 3266

[2] Y. Huttel, Gas-Phase Synthesis of Nanoparticles, Wiley-VCH Verlag GmbH & Co. KGaA, Weinheim, Germany (2017)

[3] J. Drewes, S. Ali-Ogly, T. Strunskus, O. Polonskyi, H. Biederman, F. Faupel, A. Vahl, Plasma Processes and Polymers (2021) e2100125

[4] J. Drewes, S. Rehders, T. Strunskus, H. Kersten, F. Faupel, A. Vahl, Particle and Particle Systems Characterization (2022) 2200112

A novel electrochemical cell for the *in situ* X-ray absorption spectroscopic investigation of cluster-based CO₂-electroreduction catalysts

Maximilian Winzely¹, Juan Herranz¹, Justus S. Diercks¹, Olga Safonova¹, Peter Rüttimann¹, Adam H. Clark¹, Paul Leidinger¹, Sumant Phadke¹, Thomas J. Schmidt^{1,2}

¹ Paul Scherrer Institut, CH-5232 Villigen, Switzerland

² Laboratory of Physical Chemistry, ETH Zurich, CH-8093 Zürich, Switzerland

The electrochemical conversion of CO₂ into valuable products (e.g., CO or HCOOH) is a promising prospect to slow down global warming. While catalysts with a promising selectivity towards such C₁-products have been identified (e.g. Pd) [1], further improvements in their activity, selectivity and stability are needed. The required design of such improved catalysts can be greatly aided by recent advancements in the synthesis of mass-selected, (sub-) nanometric metal clusters by the so called cluster beam deposition (CBD) method and their subsequent characterization by *in situ* x-ray absorption spectroscopy (XAS).[2] However, constraints intrinsic to the CBD method limit the attainable catalyst loadings to ultra-low values $\leq 10 \mu\text{g}_{\text{metal}}/\text{cm}_{\text{geom}}^2$. This would in turn translate into unpractically long spectral acquisition times when performing *in situ* XAS measurements in a standard configuration (i.e., with an X-ray beam incidence of 45 or 90° with regards to the electrode plane). To tackle this problem we have developed a new spectroelectrochemical XAS flow cell that enables spectral acquisition in fluorescence mode using an X-ray beam incidence angle of $\leq 0.1^\circ$ with regards to the working electrode's substrate plane, i.e., in a so called grazing incidence (GI) configuration (see Figure 1). In this acquisition configuration we successfully recorded an *in situ* spectrum of palladium in the metallic and full hydride state with a time resolution of 5 minute per spectrum while using a Pd-loading as low as $10 \mu\text{g}_{\text{Pd}}/\text{cm}^2$.

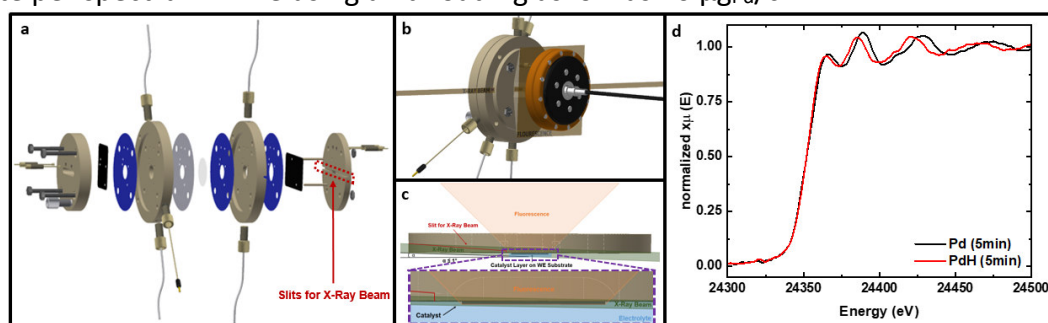


Figure 1: a) Technical drawing of the GIXAS cell assembly b) Experimental setup at the beamline including the GIXAS cell and fluorescence detector (represented as an orange disk) c) Detailed sketch of the outer working electrode part to visualize the grazing incidence of the X-Ray beam on the electrocatalyst. d) *in situ* XA-spectra of the Pd/C working electrode with a loading of $10 \mu\text{g}_{\text{Pd}}/\text{cm}^2$ polarized to the metallic and full hydride states (Pd vs. PdH, respectively) which were recorded within 5 minutes

[1] J.S. Diercks, B. Pribyl-Kranewitter, J. Herranz, P. Chauhan, A. Faisnel, T.J. Schmidt, Journal of The Electrochemical Society 168 (2021) 064504.

[2] A. Yadav, Y. Li, T.W. Liao, K.J. Hu, J.E. Scheerder, O.V. Safonova, T. Holtzl, E. Janssens, D. Grandjean, P. Lievens, Small 17 (2021) e2004541

High-Pressure Grazing Incidence Cell for *In Situ* XAS Characterization of Nanoparticles on Planar Substrates under CO₂ Hydrogenation Conditions

S. Phadke^{1,2*}, J. Coroa^{3,4}, I. Abbas⁴, J. Yin³, D. Grandjean⁴, E. Janssens³, C. Copéret², O. V. Safonova¹

¹ Paul Scherrer Institut, CH-5232 Villigen, Switzerland, *sumant.phadke@psi.ch

² ETH Zürich, Vladimir Prelog Weg 1–5, CH-8093 Zürich, Switzerland

³ Teer Coatings Ltd, Droitwich, Worcestershire, WR9 9AS, UK

⁴ KU Leuven, B-3001 Leuven, Belgium

Well-defined model catalysts studied under realistic CO₂-to-methanol hydrogenation conditions offer structure-activity insights, which enables a more profound understanding and a better design of methanol synthesis catalysts. In contrast to conventionally prepared catalysts, physical synthesis methods such as cluster beam deposition (CBD) can produce model nanoparticles of precise atomic structure and composition [1]. Depositing such nanoparticles on various planar substrates at very low metal loadings (0.1 – 10 µg/cm²) provides an opportunity to understand particle size's effects and the catalyst's support on the reactivity. However, such model catalysts also present a challenge for *in situ* structural characterization using bulk-sensitive methods, such as X-ray absorption spectroscopy (XAS), since they are optimized for studying catalysts with about three to four orders of magnitude higher metal loading [2]. To address this, we have developed a grazing incidence (GI) *in situ* XAS cell that enables the study of the structure of these model catalysts under CO₂-to-methanol hydrogenation conditions at relevant temperatures and pressures.

We have successfully measured *in situ* XAS data for nanoparticles deposited on flat substrates using fluorescence detection. In particular, we obtained high-quality Pd K- and Au L₃-edge XAS data in 30–60 min for Pd and Ag_{0.7} Au_{0.3} nanoparticles with ca. 2.5 – 10 µg/cm² loading at 230°C temperature and 20 bar pressure of reactive gases (CO₂:3H₂:Ar). With this proof-of-concept, we now intend to investigate innovative bimetallic systems produced by gas-phase cluster deposition and contribute to a rational design of CO₂ hydrogenation catalysts.

[1] G. Sanzone, J. Yin, and H. Sun, *Front. Chem. Sci. Eng.* vol. 15 (2021), pp. 1360

[2] P. J. Chupas, K. W. Chapman, C. Kurtz, J. C. Hanson, P. L. Lee, and C. P. Grey, *J. Appl. Crystallogr.* vol. 41 (2008), pp. 822

Phase and contrast tunable Interferometric Scattering (iSCAT) Microscope

Ranit Roy¹, Gyanendra Singh¹ and Ori Cheshnovsky¹

¹*School of Chemistry, Tel Aviv University, Israel*

Fluorescence microscopy is a non-invasive imaging technique widely used in life sciences. It utilizes fluorophores and tagging to identify sub-cell organelles down to nanometric size. Despite its dominance in single molecule-optical imaging, its use is limited by hurdles, such as photobleaching, the need to label and altered properties due to labelling.

Interferometric Scattering Microscopy (iSCAT) has been developed as a high-speed, label-free sensitive tool, which can be beneficial in addressing the limitations of fluorescence microscopy. By capturing the interferometric signal, originating from the interference of the light scattered by a nanostructure and the reference reflection of the proximate substrate, an iSCAT image is formed. iSCAT has been successfully advanced to detect proteins and to crudely resolve their mass down to a mass of 60kDa [1,2], equivalent to a ~2nm gold nanoparticle.

We will present a method to enhance the signal-to-noise and contrast of the iSCAT image, increase its sensitivity, and allow the detection of smaller particles. Our methodology is based on the tunability of the phase and the relative amplitude of the reflected and scattered signal. For instance, the ratiometric contrast of a 10nm gold nanoparticle bound to a coverslip is 0.15 in our method, compared to 0.03 in previous publication [3].

[1] M. Piliarik, & V. Sandoghdar, Nature communications **5** (2014), 4495.

[2] G. Young, N. Hundt, D. Cole, A. Fineberg, J. Andrecka, A. Tyler, et al., Science **360** (2018), 423-427.

[3] L. Melo, A. Hui, M. Kowal, E. Boateng, Z. Poursorkh, E. Rocheron, J. Wong, A. Christy, and E. Grant, The Journal of Physical Chemistry B **125** (2021), 12466-12475

DEMIST “Dual-Events Momentum Imaging Spectroscopy Tool”

S. Sasikumar¹, T.Mazza¹, M. Devetta², M. Coreno³, S. Riboldi⁴, Paolo Piseri⁴

² *The European XFEL GmbH, Hamburg, Germany*

² *IFN CNR, Milano, Italy*

³ *ISM CNR at Elettra, Trieste, Italy*

⁴ *Dipartimento di Fisica “Aldo Pontremoli” & CIMaNa, Università degli Studi di Milano, Italy*

We present a novel project funded by Italian Ministry of University and Research devoted to the building of an instrument which design is dedicated to gas-phases studies on systems ranging from simple molecules to complex cluster agglomerates. The original design has been developed based on the experience matured over several years of development of free clusters core-level spectroscopy experiments and related equipment. The apparatus features electrons and ions multiple-coincidence analysis in a momentum imaging spectrometer employing a single position-sensitive 3D detector with high efficiency for both electrons and ions. After proof of principle demonstration at GasPhase@ELETTRA and the implementation with a table top optical source, the proposal for a dedicated apparatus to be made available to Users has received approval through the Italian PRIN (Projects of Relevant National Interest) funding measure (Project DEMIST “Dual-Events Momentum Imaging Spectroscopy Tool”). The apparatus is meant to expand the portfolio of techniques available to the Scientific Community via Open Access at the GasPhase beamline of ELETTRA Synchrotron Radiation Facility.

Studying clusters with a multi-reflection time-of-flight mass spectrometer

Paul Fischer¹, Paul F. Giesel¹, Lutz Schweikhard¹

¹ Institute of Physics, University of Greifswald, 17487 Greifswald, Germany

Multi-reflection time-of-flight (MR-ToF) mass spectrometers store ion bunches between two opposing electrostatic mirrors at kinetic energies of a few kiloelectronvolts. The continuous reflection of the bunches combined with their temporal re-focusing by the reflectron-like mirrors enables high mass resolving powers. This makes MR-ToF devices powerful tools for fast, high-resolution isobar separation [1] and precision mass measurements [2] in nuclear physics. They also offer easy access for cross- or merged-beam experiments due to an open geometry and, being entirely electrostatic, have no intrinsic mass limits.

At the University of Greifswald, an MR-ToF mass spectrometer is in operation for the study of atomic clusters produced by laser ablation or magnetron sputtering (Fig. 1). Cases of interest include the photodissociation of lead-doped bismuth clusters, the selection and analysis of which requires high mass resolving powers [3], or the time-resolved decay of hot indium clusters [4]. The ability to investigate stored clusters with variable resolution also enables studies with ions distributed across broad mass ranges such as carbon fullerenes produced by laser ablation of glassy carbon [5].

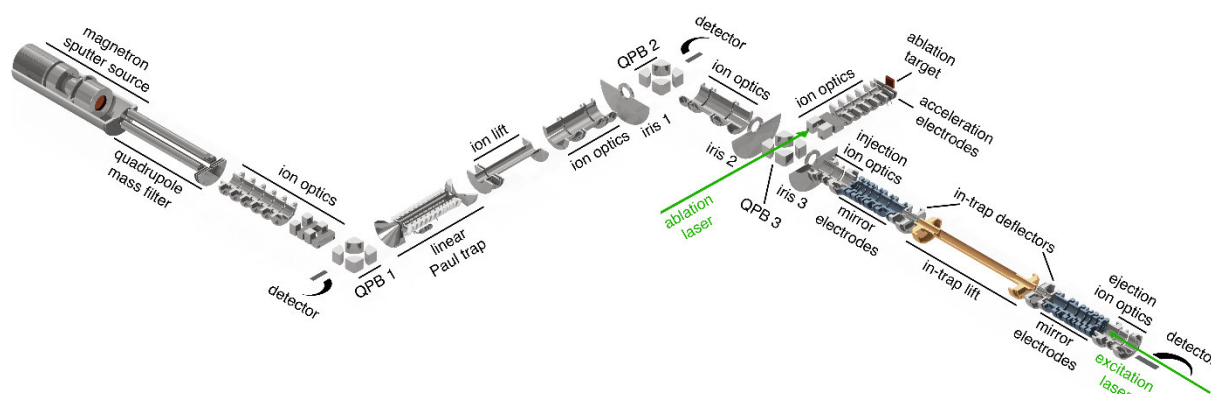


Figure 1: Setup for the study of atomic clusters at the University of Greifswald. Clusters are produced by laser ablation or magnetron sputtering. A linear Paul trap accumulates and bunches ions produced from either source. The MR-ToF analyzer consists of two stacks of mirror electrodes and an in-trap lift.

- [1] R. N. Wolf et al., Phys. Rev. Lett. **110** (2013) 041101
- [2] F. Wienholtz et al., Nature **498** (2013) 346
- [3] P. Fischer et al., Phys. Rev. Res. **1** (2019) 033050
- [4] P. Fischer et al., Phys. Rev. Res. **2** (2020) 043177
- [5] P. Fischer et al., Phys. Rev. Res. **4** (2022) 043187

Characterization of the parameters for gas phase CaMn_4O_5 cluster. Sample preparation by mass spectrometry

A. Hreben^{1,2}, O.S. Ablyasova^{1,3}, M. Timm¹, M. Flach^{1,3}, M. da Silva Santos^{1,3},
B. von Issendorff³, K. Hirsch¹, V. Zamudio-Bayer¹, J.T. Lau^{1,3}

¹ *Abteilung für Hochempfindliche Röntgenspektroskopie, Helmholtz-Zentrum Berlin für
Materialien und Energie, Albert-Einstein-Straße 15, 12489 Berlin, Germany;*

² *Institut für Chemie, Humboldt-Universität zu Berlin, Brook-Taylor-Straße 2, 12489 Berlin,
Germany*

³ *Physikalisches Institut, Universität Freiburg, Hermann-Herder-Straße 3, 79104 Freiburg,
Germany;*

Photosynthesis is the basic process of life as we know it. Despite numerous studies, the details of the natural process are still not elucidated. One of the central problems remains the investigation of the CaMn_4O_5 cluster, which is a main active part of enzyme Photosystem II (PS II) due to its oxygen-evolving functions [1]. A consistent understanding of the electronic and geometric state of this complex is necessary due to the increasing importance of artificial catalytical complexes. However, the sample production of this cluster from the chloroplast of cyanobacteria and plants is complicated [2], so the selection of the ideal sample plays a crucial role. Thus, we are going to look into the other way of the sample preparation and prepare the CaMn_4O_5 cluster in a gas phase.

We perform the sample production of the CaMn_4O_5 cluster in the Ion trap end station [3], located in the BESSY II synchrotron facility at HZB. On this experimental set-up, we are able to produce different types of warm and cold gas-phase clusters using a magnetic sputtering source [4] and detect them with a Time-of-Flight mass spectrometer. We are using a sandwich of calcium and manganese metal targets, with the latter functioning as perforated sputtering mask. The experiment was performed with different hole sizes for the selection of the optimal parameters of CaMn_4O_5 production. We conduct this research as the basis for upcoming x-ray absorption spectroscopy (XAS) experiments with the complex.

[1] W. Lubitz et al. Water oxidation in photosystem II, *Photosynthesis Research*, **2019**, 142, 105–125

[2] M. Kubin et al. Soft x-ray absorption spectroscopy of metalloproteins and high-valent metal-complexes at room temperature using free-electron lasers, *Structural Dynamics*, **2017**, 4, 054307

[3] K. Hirsch et al. X-ray spectroscopy on size-selected clusters in an ion trap: from the molecular limit to bulk properties, *J. Phys. B: At. Mol. Opt. Phys.*, **2009**, 42, 154029

[4] Haberland et al. Thin films from energetic cluster impact: A feasibility study, *J. Vac. Sci. Technol.*, **1992**, A 10, 3266

Signatures of intermolecular decay processes in alkali-halide molecules embedded in He nanodroplets

S. De¹, S. Mondal², L. B. Ltaief³, R. Gopal⁴, V. Sharma⁵, M. Coreno⁶, R. Richter⁶, M. Mudrich³, S. R. Krishnan^{*1}

¹ Quantum Center of Excellence for Diamond and Emergent Materials, and Department of Physics, Indian Institute of Technology Madras, India

² Department of Physics, Indian Institute of Science Education and Research, Pune, India

³ Department of Physics and Astronomy, Aarhus University, Denmark

⁴ Department of Physics, Tata Institute of Fundamental Research, Hyderabad, India

⁵ Department of Physics, Indian Institute of Technology Hyderabad, India

⁶ Elettra-Sincrotrone Trieste, Basovizza, Trieste, Italy

Superfluid He nanodroplets doped with foreign atoms or molecules can be served as a model system to study interatomic/intermolecular decay processes due to their very simple electronic structure and high excitation and ionization potential [1,2]. When local electronic decay is energetically forbidden, ICD allows the energy or charge exchange between the neighbouring atoms or molecules, leading to the ionization of neighbours, typically in a femtosecond timescale [3,4]. Here, we will present the interatomic/intermolecular decay mechanism of RbI doped in He nanodroplets by resonant photoexcitation at 21.6 eV. Electron spectra contain low energetic electrons having energy in the range of 0 - 5 eV, and the ion spectra contain high energetic ions peaked around 0.5 eV and 1.2 eV, respectively, for I⁺ and Rb⁺ ions. The measured ion-ion coincidence map, which is capable of revealing multiple ionization, does not show any signatures of the double ionization process. Hence, the high kinetic energy ions (Rb⁺ and I⁺) come from the dissociation of singly ionized parent RbI cluster ions. Our result is surprising because similar high kinetic energy ions were detected only in the case of double ICD or ETMD processes [5,6].

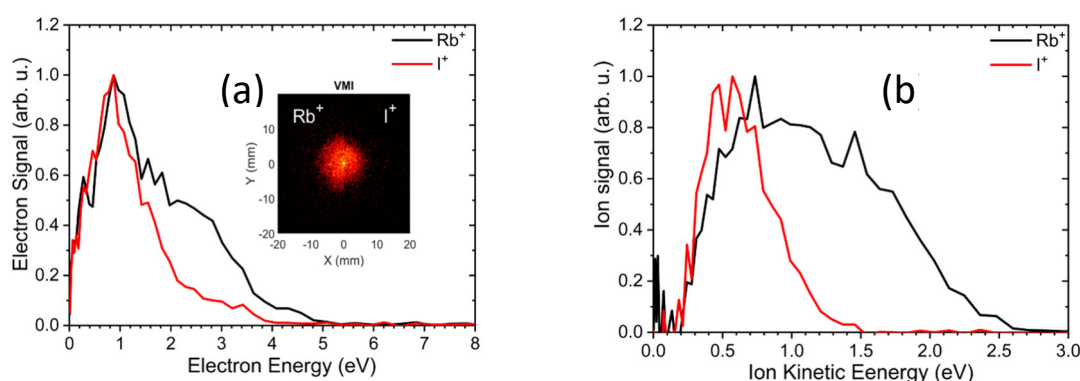


Figure 1: a) Electron kinetic energy distributions in coincidence with Rb⁺ (black line), and I⁺ (red line), respectively. Inset shows the corresponding VMI images, and b) Ion kinetic energy distributions of Rb⁺ (black line) and I⁺ (red line), respectively. The photon energy is 21.6 eV, and He stagnation conditions are backing pressure, $P_b = 50$ bars, and nozzle temperature, $T_n = 14$ K.

- [1] Stienkemeier F, Lehmann KK. *J. Phys. B-At Mol Opt.* 2006; **39**(8):R127.
- [2] Mudrich M, Stienkemeier F. *Int. Rev. Phys. Chem.* 2014; **33**(3):301-39.
- [3] Cederbaum LS, Zobeley J, Tarantelli F. *Phys. Rev. Lett.* 1997; **79**(24):4778.
- [4] Zobeley J, Santra R, Cederbaum LS. *J. Chem. Phys.* 2001; **115**(11):5076-88.
- [5] LaForge AC, et al. *Nat. Phys.* 2019; **15**(3):247-50.
- [6] Ltaief LB, Phys. Chem. Chem. Phys. 2020;22(16):8557-64.

Generation of Large Vortex-Free Superfluid Helium Nanodroplets and imaging with X-rays

Anatoli Ulmer,^{1,2} Andrea Heilrath,^{1,3} Björn Senfftleben,^{3,4} Sean M. O. O'Connell-Lopez,⁵ Björn Kruse,⁶ Lennart Seiffert,⁶ Katharina Kolatzki,^{3,7} Bruno Langbehn,¹ Andreas Hoffmann,³ Thomas M. Baumann,⁴ Rebecca Boll,⁴ Adam S. Chatterley,⁸ Alberto De Fanis,⁴ Benjamin Erk,⁹ Swetha Erukala,⁵ Alexandra J. Feinberg,⁵ Thomas Fennel,⁶ Patrik Grychtol,⁴ Robert Hartmann,¹⁰ Markus Ilchen,^{4,9} Manuel Izquierdo,⁴ Bennet Krebs,⁶ Markus Kuster,⁴ Tommaso Mazza,⁴ Jacobo Montano,⁴ Georg Noffz,¹ Daniel E. Rivas,⁴ Dieter Schlosser,¹⁰ Fabian Seel,¹ Henrik Stapelfeldt,⁸ Lothar Strüder,¹⁰ Josef Tiggesbäumker,^{6,11} Hazem Yousef,⁴ Michael Zabel,⁶ Pawel Ziolkowski,⁴ Michael Meyer,⁴ Yevheniy Ovcharenko,⁴ Andrey F. Vilesov,^{5,12} Thomas Möller,¹ Daniela Rupp,^{3,7} and Rico Mayro P. Tanyag^{1,8}

¹ Institute of Optics and Atomic Physics, Technische Universität Berlin, Hardenbergstraße 36, 10623 Berlin, Germany

² Department of Physics, Universität Hamburg, Luruper Chaussee 149, 22761 Hamburg, Germany

³ Max-Born-Institute for Nonlinear Optics and Short Pulse Spectroscopy, Max-Born-Straße 2A, 12489 Berlin, Germany

⁴ European XFEL, Holzkoppel 4, 22869 Schenefeld, Germany

⁵ Department of Chemistry, University of Southern California, 920 Bloom Walk, Los Angeles, California 90089, USA

⁶ Institute for Physics, Universität Rostock, Albert-Einstein-Straße 23, 18059 Rostock, Germany

⁷ Laboratory for Solid State Physics, Swiss Federal Institute of Technology in Zurich, John-von-Neumann-Weg 9, 8093 Zurich, Switzerland

⁸ Department of Chemistry, Aarhus University, Langelandsgade 140, 8000 Aarhus C, Denmark

⁹ Deutsches Elektronen-Synchrotron DESY, Notkestr. 85, 22607 Hamburg, Germany

¹⁰ PNSensor GmbH, Otto-Hahn-Ring 6, 81739 Munich, Germany

¹¹ Department "Life, Light and Matter," Universität Rostock, Albert-Einstein-Straße 23, 18059 Rostock, Germany

¹² Department of Physics and Astronomy, University of Southern California, 920 Bloom Walk, Los Angeles, California 90089, USA

Superfluid helium nanodroplets are an ideal environment for the formation of metastable, self-organized dopant nanostructures. However, the presence of vortices often hinders their formation. Here, we demonstrate the generation of vortex-free helium nanodroplets and explore the size range in which they can be produced. From x-ray diffraction images of xenon-doped droplets, we identify that single compact structures, assigned to vortex-free aggregation, prevail up to 10^8 atoms per droplet. These findings build the basis for exploring the assembly of far-from-equilibrium nanostructures at low temperatures.

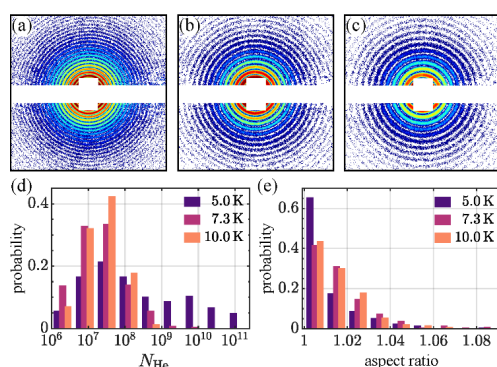


Figure 1: Selected diffraction images of p droplets obtained at a nozzle temperature of (a) 5.0 K, (b) 7.3 K, and (c) 10.0 K. The size distributions given in panel (d), and their aspect ratio distribution in panel (e). The numbers of diffraction images used for the size (aspect ratio) distributions are 291 (2) for 5.0 K, 766 (488) for 7.3 K, and 272 (214) for 10.0 K.

[1] A. Ulmer et al. Phys. Rev. Lett. 2023 in press

Optical Properties of Helium Nanodroplets around the 1s2p Resonance Probed with Coherent Diffraction Imaging

L. Hecht¹, C. Callegari², A. Colombo¹, M. di Fraia², T. Fennel³, K. Kolatzki¹, B. Kruse³, B. Langbehn⁴, T. Möller⁴, C. Peltz³, P. Piseri⁵, O. Plekan², K. Prince², M. Sauppe¹, M.L. Schubert¹, B. Senfftleben⁶, P. Tümmeler³, D. Rupp¹

¹ETH Zurich, ²FERMI Trieste, ³Uni Rostock, ⁴TU Berlin, ⁵Uni Milano, ⁶XFEL Hamburg

Due to their simple electronic structure, helium nanodroplets are a perfect model system for studying intense laser-matter interaction. With the availability of intense short-wavelength pulses from free electron lasers and high-harmonic sources, novel opportunities have emerged which enable coherent diffraction imaging of individual droplets. We utilize single-shot, single-particle diffraction images to derive information about the sample's shape, density, and optical properties. With the advent of intense attosecond short wavelength pulses, we focus on studying electron dynamics.

We recorded diffraction images of helium nanodroplets ($\langle R \rangle = 350$ nm) at different photon energies from 19.5 eV to 24 eV, i.e. around the 1s2p resonance, as a baseline for time-resolved studies. We fitted diffraction patterns from round droplets with Mie theory, an analytical solution of Maxwell's equation. Mie theory allows for describing the entire scattering interaction for a homogeneous and static spherical particle in a non-absorbing medium. When comparing our fitted results with literature values of liquid helium's optical properties [1, 2], we observe two characteristics that divert from expectation.

First, close to resonance, Mie fitting becomes less reliable. Here, absorption becomes much higher, presumably leading to ionization and plasma formation. Subsequently, the assumption of a homogenous sample does not hold, and the diffraction images encode an evident change in the electronic structure of the nanodroplet during the interaction with the femtosecond pulse.

Second, our results indicate that the absorption values in the literature might be overestimated for sub-resonant photon energies. Below the first resonance of helium, Mie fitting with helium ground state optical properties should work perfectly fine. Thus, no light-induced changes are foreseen, confirmed by simultaneously measured ion spectra. Surprisingly, however, the recorded average scattering intensities rise below 20 eV to much higher values than expected. Here, we use CDI as a novel method to study the absorption in the mentioned spectral range.

[1] C. M. Surko et al., Phys. Rev. Lett. 23 (1969) pp. 842-846

[2] A. A. Lucas et al., Phys. Rev. B 28 (1983) pp. 2485-2496

Efficient and accurate simulation of wide-angle single-shot scattering

Paul Tuemmler¹, Björn Kruse¹, Christian Peltz¹, Thomas Fennel¹

¹ *Institute for Physics, University of Rostock, Germany*

In recent years coherent diffractive imaging has been established as a powerful method for the structural investigation of unsupported nanoparticles. A large number of studies have been successfully performed in the small angle regime, where the recorded scattering image is directly connected to the target's density projection along the optical axis [1]. An established technique to invert the scattering image is the well-known phase retrieval algorithm. Single-shot 3d information only becomes available when scattering signal can be recorded at wide scattering angles, which typically requires wavelengths of several object diameters [2]. However, in this scattering regime a direct inversion via phase retrieval is no longer possible and iterative forward fitting schemes have to be applied. These schemes require many iterations and therefore heavily rely on an efficient method to calculate scattering images. Unfortunately, optical parameters in the long wavelength regime are typically quite far from vacuum parameters, such that absorption and multiple scattering effects become important [3]. So far, available methods either lack the necessary accuracy (e.g. MSFT methods [4]) or the numerical efficiency (e.g. FDTD).

Here we present a rigorous split step method that retains the efficiency of multislice methods, while yielding accuracy comparable to Mie and FDTD methods.

- [1] L. Gomez et al., *Science* **345**(6199):906-909 (2014).
- [2] I. Barke et al., *Nat. Commun.* **6**, 6187 (2015).
- [3] D. Rupp et al., *Nat. Commun.* **8**, 493 (2017).
- [4] A. Colombo et al., *J. Appl. Cryst.* **55**, 1232-1246 (2022).

Coherent diffractive imaging of ultrafast plasma dynamics in isolated nanoparticles

C Peltz¹, J A Powell², P Rupp³, A Summers², T Gorkhover⁴, F. Gerke⁵, M Gallei⁵, I Halfpap⁵, E Antonsson⁵, B Langer⁵, C Trallero-Herrero², C Graf⁶, D Ray⁷, Q Liu³, T Osipov⁷, M Bucher⁷, K Ferguson⁷, S Möller⁷, S Zharebtsov³, D Rolles², E Rühl⁵, G Coslovich⁷, R N Coffee⁷, C Bostedt⁸, A Rudenko², M F Kling⁷, T Fennel¹

¹ *Institute for Physics, University of Rostock, Germany*

² *Department of Physics, Kansas State University, USA*

³ *Department of Physics, Ludwig-Maximilians-Universität Munich, Germany*

⁴ *Institute for Experimental Physics, University of Hamburg, Germany*

⁵ *Physical Chemistry, Freie Universität Berlin, Germany*

⁴ *Applied Physics Department, Stanford University, USA*

⁵ *Polymer Chemistry, Saarland University, Germany*

⁶ *Department of Chemistry and Biotechnology, Darmstadt University of Applied Sciences, Germany*

⁷ *Linac Coherent Light Source, USA*

⁸ *Paul-Scherrer Institute, Switzerland*

In recent years coherent diffractive imaging (CDI) at X-ray free-electron lasers (FELs) has been established as an excellent method for structural investigations of unsupported nanoparticles. Applications range from the visualization of quantum vortices in superfluid Helium nanodroplets to the observation of highly symmetric metastable morphologies in free metal clusters. However, beyond these somewhat static applications, the method can be readily extended to time-dependent investigations utilizing pump-probe excitation-visualization schemes in order to track initiated electronic and or ionic dynamics.

A particularly interesting scientific question associated with ionic dynamics is the sudden free expansion of solid-density plasmas into free space¹. A fundamental process of significance in a wide range of research fields from astrophysics to high-harmonic generation. In respective x-ray scattering experiments at LCLS, we studied the ultrafast expansion of laser-driven silica nanoparticles with time resolved coherent diffractive imaging. We were able to characterize the early expansion phase (<150fs) with few-femtosecond temporal and nanometer spatial resolution, exposing the so far inaccessible shell-wise expansion dynamics including the associated startup delay and rarefaction front velocity². In recent follow-up experiments at XFEL in Hamburg we returned to the SiO₂ nanoparticles as a target but operated in a regime of much weaker excitation. A first analysis shows that the early expansion phase proceeds very similar, however, on the longer picosecond timescale we observe features that indicate the recovery of a sharp density profile at the nanoparticle surface.

[1] C. Peltz, C. Varin, T. Brabec, T. Fennel, Phys Rev Lett **113** (2014) 133401

[2] C. Peltz et al., New Journal of Physics **25** (2022) 043024

Dancing in the blue light: an ultrafast movie on superheated silver nanocubes

Alessandro Colombo¹, Simon Dold², Andre Al Haddad³, Johan Bielecki², Fanny Goy¹, Christina Graf⁴, Linos Hecht¹, Georg Jakobs¹, Maximilian Joschko⁴, Gregor Knopp³, Katharina Kolatzki¹, Christian Peltz⁵, Safi Rafie-Zinedine², Thomas Reichenbach^{6,7}, Mario Sauppe¹, Florian Schenk⁸, Kirsten Schnorr³, Zhibin Sun³, Paul Tümmeler⁵, Carl Frederic Ussling¹, Maksym Yarema⁸, Nuri Yazdani⁸, Hankai Zhang³, Michael Moseler^{6,7}, Christoph Bostedt³, Daniela Rupp¹ and Bernd von Issendorff⁶

¹Laboratory for Solid State Physics, ETH Zurich, 8049 Zurich, Switzerland

²European XFEL GmbH, 22869 Schenefeld, Germany

³Photon Science (PSD), Paul Scherrer Institut, 5232 Villigen, Switzerland

⁴Department of Chemistry and Biotechnology, Darmstadt University of Applied Sciences, 64295 Darmstadt, Germany

⁵Institute for Physics, University of Rostock, 18059 Rostock, Germany

⁶Department of Physics, University of Freiburg, 79104 Freiburg, Germany

⁷Fraunhofer Institute for Mechanics of Materials IWM, 79108 Freiburg, Germany

⁸Institute for Electronics, ETH Zurich, 8049 Zurich, Switzerland

X-ray Free Electron Lasers allow to get snapshots of isolated nanomatter resolved in both space and time through the Coherent Diffraction Imaging (CDI) technique [1]. Short-living structures surviving only fractions of a picosecond, triggered by the interaction of the sample with intense radiation, can be accessed with nanoscale spatial resolution. Here we present an investigation on the dynamics of superheated silver clusters [2]. Silver cubes of around 100 nm in size are efficiently heated via a 400 nm laser, resonant with their Mie plasmon frequency [3]. Their electronic density is then probed through X-ray CDI at different time delays, building a full-fledged movie of the dynamical processes happening in the superheated silver nanocubes. Experimental results reveal, for low laser intensities, a gentle melting process taking place in hundreds of picoseconds, reshaping the silver cubes towards spherical droplets. More complex and intriguing dynamics are instead observed for higher laser intensities, which span from inflation of the sample due to cavitation effects to violent explosions in few tens of picoseconds. These imaging results, aided by molecular dynamics simulations, enable the investigation of thermodynamic properties of silver in regions of its phase diagram hardly accessible so far. Furthermore, they potentially provide new insights into the interaction of the hot electron gas with the nuclei, for example by unveiling the contribution of its increased pressure to the excitation of the particle's breathing mode vibrations.

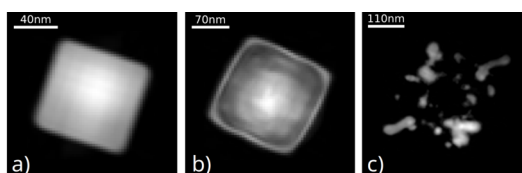


Figure 1: Examples of imaging results. A pristine nanocube is shown in a). Dynamics at different time delays are reported in b) and c).

[1] J. Miao, R. L. Sandberg, and C. Song, IEEE J Sel Top Quantum Electron **18** (2011) 399-410

[2] A. Colombo, S. Dold, P. Kolb et al., Sci Adv **9** (2023) eade5839

[3] S. Dold, T. Reichenbach, A. Colombo et al., "Melting, bubble-like expansion and explosion of superheated plasmonic nanoparticles", in preparation

Full Quantum Dynamic Simulation of the fs-NeNePo Spectra of the Ce_2 Cluster

Nikita Kavka¹, Jiaye Jin², Max Grellmann², Knut R. Asmis², Roland Mitrić¹

¹ *Institut für Physikalische und Theoretische Chemie, Universität Würzburg, Germany*

² *Wilhelm-Ostwald-Institut für Physikalische und Theoretische Chemie, Universität Leipzig, Germany*

In this study, the wavepacket dynamics of Ce_2 is investigated using femtosecond pump-probe spectroscopy employing the negative-neutral-positive excitation scheme (fs-NeNePo) [1] [2]. The transient fs-NeNePo spectra obtained at various pump wavelengths (centered at 1450 nm, 1640 nm, 1740 nm and 1860 nm) and a fixed probe pulse at 400 nm exhibit oscillatory signals of Ce_2^+ in the positive delay times, as depicted in Figure 1. To gain a comprehensive understanding of the experimental observations, high-level quantum-chemical calculations at the CASSCF(8,15) level, incorporating spin-orbit coupling, are performed. The calculations yield valuable insights into the complex potential energy surfaces (PESs) of Ce_2 , Ce_2^+ and Ce_2^- , shedding light on the fundamental properties of these species. Quantum dynamical calculations are employed to reproduce the observed oscillations in the fs-NeNePo spectra and to gain insights into the entangled dynamics of vibrational wave packets on the electronic potential energy surfaces of neutral Ce_2 . These findings highlight the critical role of employing multireference and relativistic methodologies in accurately describing the electronic structure of Ce_2 .

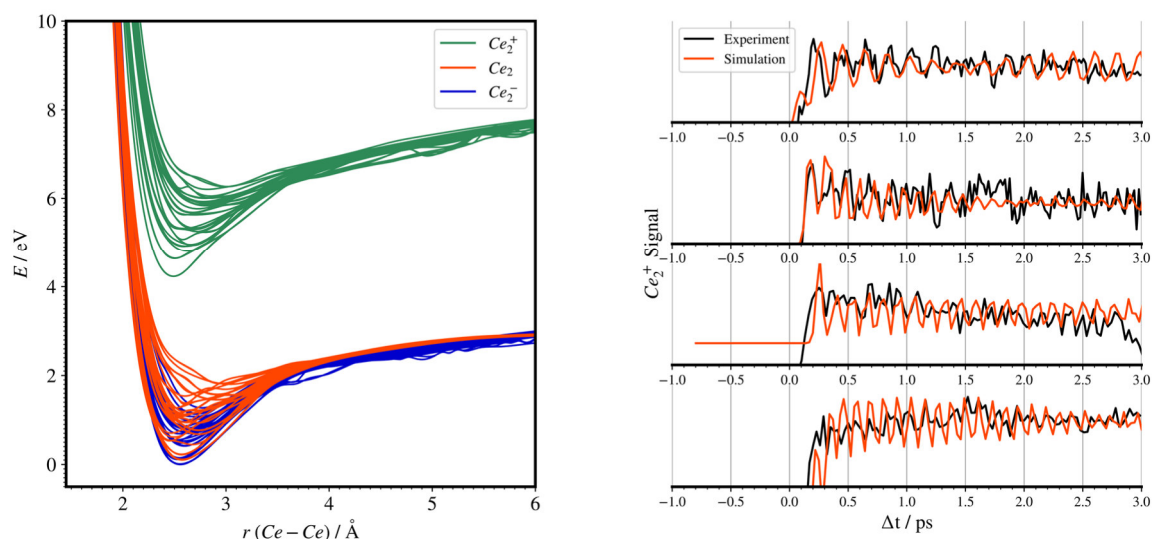


Figure 1: Left: Potential energy surfaces of Ce_2 , Ce_2^+ and Ce_2^- calculated at the CASSCF(8,15) level of theory. Right: Comparison of the experimental NeNePo signals of Ce_2 with the corresponding simulation.

[1] J. Jin, M. Grellmann, K. R. Asmis, submitted (2023)

[2] S. Wolf, G. Sommerer, S. Rutz, E. Schreiber, T. Leisner, L. Wöste, Phys. Rev Lett. **74** (1995), 4177.

Femtochemistry on nano-structured surfaces: Non-metal to metal transition determines ultrafast photodissociation dynamics on supported gold clusters

Mihai E. Vaida,^{1,2} Thorsten M. Bernhardt³

¹*Department of Physics, University of Central Florida, Orlando, Florida 32816, United States*

²*Renewable Energy and Chemical Transformations Cluster, University of Central Florida, Orlando, Florida 32816, United States*

³*Institute of Surface Chemistry and Catalysis, University of Ulm, 89069 Ulm, Germany
thorsten.bernhardt@uni-ulm.de*

The detection of intermediate species and the correlation of their ultrafast dynamics with the morphology and electronic structure of a surface is crucial to fully understand and control heterogeneous photoinduced and photocatalytic reactions. In this work, the ultrafast photodissociation dynamics of CH₃Br molecules adsorbed on variable size Au clusters on MgO/Mo(100) is investigated by monitoring the CH₃⁺ transient evolution using a pump-probe technique in conjunction with surface mass spectrometry.

Furthermore, extreme-ultraviolet photoemission spectroscopy in combination with theoretical calculations are employed to study the electronic structure of the Au cluster on MgO/Mo(100). Changes in the ultrafast dynamics of CH₃⁺ fragment are correlated with the electronic structure of Au as it evolves from monomers to small nonmetallic clusters to larger nanoparticles with a metallic character. This work provides a new avenue to a detailed understanding of how surface photoinduced chemical reactions are influenced by the composition and electronic structure of the surface.

- [1] M. E. Vaida; T. M. Bernhardt, Surface-aligned femtochemistry: Real-time dynamics of photoinduced I₂ formation from CD₃I on MgO(100), *ChemPhysChem* **11** (2010) 804.
- [2] M. E. Vaida; T. M. Bernhardt, Tuning the ultrafast photodissociation dynamics of CH₃Br on ultrathin MgO films by reducing the layer thickness to the 2D limit. *Chem. Phys. Lett.* **688** (2017) 106.
- [3] M. E. Vaida, T. Rawall, T. M. Bernhardt, B. M. Marsh, T. S. Rahman, S. R. Leone, Non-metal to metal transition of magnesia supported Au clusters affects the ultrafast dissociation dynamics of adsorbed CH₃Br molecules, *J. Phys. Chem. Lett.* **13** (2022) 4747.

Stable Surface Plasmon Resonances in Small Alumina-Embedded Silver Clusters

M. Moreira^{1,2}, E. Cottancin¹, M. Pellarin¹, O. Boisron¹, V. Rodrigues², J. Lermé¹, Matthias Hillenkamp^{1,2}

¹ *Institute of Light and Matter, University of Lyon 1 – CNRS UMR5306, France*

² *Instituto de Física Gleb Wataghin, UNICAMP, CP 6165, 13083-970 Campinas, SP, Brazil*

matthias.hillenkamp@univ-lyon1.fr

Localized Surface Plasmon Resonances are ubiquitous for the characterization and in applications of noble metal nanoparticles. Their dependence on chemical composition, size, shape and environment is widely studied since decades but still many aspects are subject of controversy. Here we experimentally investigate surfactant-free and mass-selected silver nanoparticles embedded in alumina matrices in the size range between several atoms and more than 4 nm diameter, spanning the whole range from large nanoparticles, accurately described by classical Mie theory, down into the range of quantum size effects. Strong and stable resonances are observed for all sizes down to less than 50 atoms, i.e. ~ 1 nm diameter, without significant line shift or broadening as a function of size. With the help of semi-quantal simulations, we identify all signals as surface plasmon resonances. The absence of peak shifts is rationalized as due to the dielectric oxide environment and the constant width of the resonances as a convolution of inhomogeneities in the local environment and inherent broadening due to Landau damping. We discuss our results in comparison to ligand-stabilized nanoclusters and rationalize the different contributions to the Hamiltonian describing the systems.

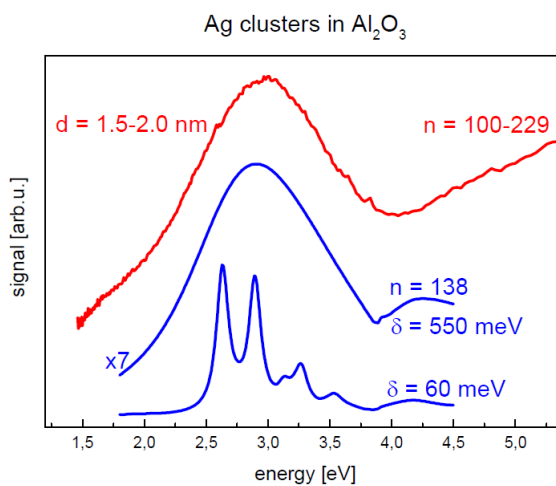


Figure 1: Top (red): experimental optical absorption spectrum for mass-selected Ag clusters embedded in alumina. The minimal and maximal numbers of atoms per particle transmitted through the mass spectrometer (n) and the corresponding diameters (d) are indicated. The blue curves are simulated spectra with the parameter describing line broadening fixed to $\delta = 60$ meV and 550 meV, respectively.

Broadband and Spectrally Selective Photothermal Conversion through Nanocluster Assembly of Disordered Plasmonic Metasurfaces

Ji-an Chen¹, Peng Mao¹ and Min Han¹

¹ National Laboratory of Solid-State Microstructures and Collaborative Innovation Centre of Advanced Microstructures, Nanjing University, Nanjing 210093, China

Engineering plasmonic photothermal conversion is of notable importance in a range of applications. Through judicious design, plasmonic metal metasurfaces have been realized for efficient light absorption, thereby leading to photothermal conversion through non-radiative decay of plasmonic modes. However, current plasmonic metasurfaces suffer from inaccessible spectral ranges, costly and time-consuming nano-lithographic top-down techniques for fabrication, and difficulty of scale-up. Here, we demonstrate a new type of disordered metasurface created by densely packing plasmonic nanoclusters of ultra-small size (~ 12 nm) on a planar optical cavity. The system either operates as a broadband absorber or offers a reconfigurable absorption band right across the visible region[1-2], resulting in continuously wavelength-tunable photothermal conversion. We further present a method to measure the local temperature of plasmonic metasurfaces via surface-enhanced Raman spectroscopy (SERS), by incorporating single-walled carbon nanotubes (SWCNTs)[3] as a SERS probe within the metasurfaces. Our disordered plasmonic system, generated by a bottom-up process, offers excellent performance and compatibility with efficient photothermal conversion[4]. Moreover, it also provides a novel platform for various hot-electron, photodetection, photocatalysis, and solar energy harvesting functionalities.

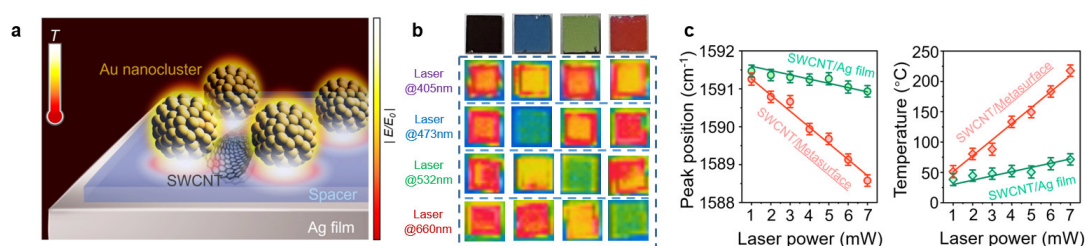


Figure 1: (a) Schematic diagram of the geometric structure and material composition of the designed three-layer metasurface. (b) Thermal image of the four metasurfaces under illumination by 405 nm, 473 nm, 532 nm and 633 nm laser. (c) Raman shift of the G⁺ peak and measured temperature as a function of laser power.

- [1] Mao, P., et al. Nat Commun, 2020. 11(1): p. 1538.
- [2] Mao, P., et al. Adv Mater, 2021. 33(23): p. 2007623.
- [3] Zhang, X., et al. Nanoscale, 2014. 6(8): p. 3949.
- [4] Chen, J., et al. Nano letter, 2023. Accepted.

The role of symmetry in confined bulk plasmons excited by electron beams in metal clusters

E. Ogando¹, M. Urbieto,² A. Rivacoba³, J. Aizpurua³, N. Zabala^{3, 4}

¹ Department of Physics, Faculty of Pharmacy, UPV/EHU, Spain.

² Department of Applied Physics, Faculty of Engineering of Gipuzkoa, UPV/EHU, Spain.

³ Materials Physics Center (CSIC - UPV/EHU); Donostia International Physics Center; Spain.

⁴ Department of Electricity and Electronics, FCT-ZTF, UPV/EHU, Spain.

The recent progress in electron energy loss spectroscopy (EELS) has allowed to get new insights into the properties and dynamics of plasmons in metal clusters with unprecedented precision and resolution [1,2]. Nevertheless, the interpretation of the spectra relies on a comprehensive understanding of the underlying electron response at the nanoscale, which goes beyond the widespread classical dielectric theory.

In this study, we combine both atomistic time-dependent density functional theory [3] and a linear hydrodynamic model to investigate EELS in sodium nanoclusters. We examine the EEL probability as a function of the cluster size, beam energy, and impact parameter, with a particular focus on the confined bulk plasmons (CPBs), which have received less attention than localized surface plasmons (LSPs) in the literature, although CBPs are efficiently excited for penetrating trajectories.

Our findings demonstrate that the position and intensity of the CBP peaks are highly responsive to variations in the impact parameter and kinetic energy of the electron beam. Additionally, we identify a clear interplay between the symmetry of these plasmonic modes and the phase of the field generated by the electron beam as the underlying mechanism governing the complex bulk EELS spectrum of the CPBs. These findings contribute to the understanding of the intricate plasmonic response in nanoclusters.

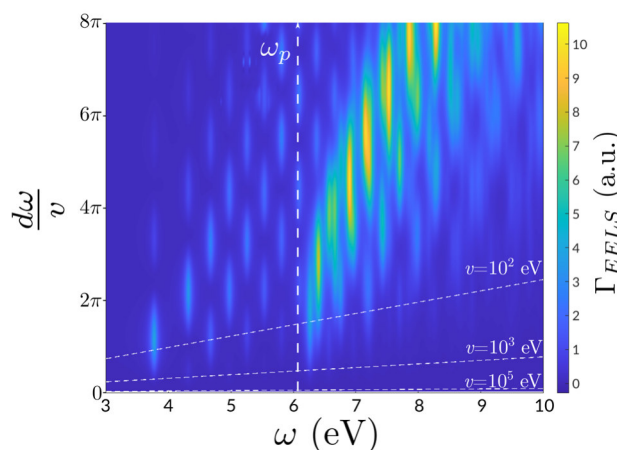


Figure 1: EELS probability as a function of energy and phase $d\omega/v$ of the electron beam, for the nanoparticle diameter $d=3$ nm and azimuthal beam trajectory. The CPBs (above ω_p) show a complex excitation pattern, contrary to the pattern of LSPs.

[1] P. E. Batson, N. Dellby, and O. L. Krivanek, *Nature* **418**, (2022) 617.

[2] T. Christensen, W. Yan, S. Raza, A.-P. Jauho, N.A. Mortensen, and M. Wubs, *ACS Nano* **8**, (2014) 1745.

[3] P. Koval, M. Barbry and D. Sanchez-Portal, *Computer Physics Communications* **236** (2019) 188.

Plasmon resonances in anionic silver clusters Ag_N^{z-}

N. Iwe¹, K. Raspe¹, F. Martinez¹, M. Hillenkamp², J. Lermé²,
L. Schweikhard³, K.-H. Meiwes-Broer^{1,4}, J. Tiggesbäumker^{1,4}

¹*Institute of Physics, University of Rostock, Germany*

²*Institut Lumière Matière, Claude Bernard University Lyon 1, France*

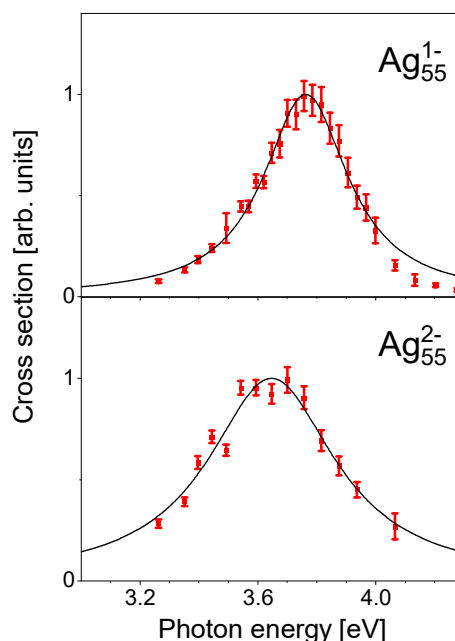
³*Institute of Physics, University of Greifswald, Germany*

⁴*Department of Life, Light and Matter, University of Rostock, Germany*

Numerous applications ranging from efficient solar cells [1] to cancer treatment [2] profit from the interaction between nanoparticles and light. In the case of metal clusters, one often takes advantage of collective resonances of the valence electrons, which lead to a strong increase of the cross section at a certain wavelength. Previous studies already showed, that the resonance energy can be tuned via size and charge state of the nanoparticles [3,4]. However, systematic measurements to explore the development of the plasmonic resonance in metal clusters concentrate on small sizes. In the case of free silver particles only few experimental results are available for systems larger than $N = 20$ atoms [5,6]. Furthermore, collective excitations have not been shown yet for multiply charged species.

We conduct photoelectron spectroscopy on anionic silver clusters Ag_N^{z-} in a size range $N = 7 - 800$ and with up to $z = 7$ excess electrons. By extracting photodetachment cross sections (Fig. 1), we gain insights into the collective resonances, which are compared to density functional theory calculations. At $N = 55$, we observe a transition from a blueshift to a redshift of the plasmon energies with decreasing cluster size. On top, distinct quantum-size effects show up. Additionally, with increasing number of excess electrons, the plasmon shifts to lower energies, whereby the effect is more pronounced in smaller sizes.

Figure 1: Photodetachment cross sections of silver clusters Ag_{55}^{z-} with $z = 1, 2$ excess electrons (red) and fitted Lorentz curves (black).



- [1] H. A. Atwater, A. Polman, *Nature Mat.* **9** (2010) 205
- [2] L. R. Hirsch et al., *Proc. Nat. Acad. Sci.* **100** (2003) 13549
- [3] J. Tiggesbäumker et al., *Phys. Rev. A* **48** (1993) R1749
- [4] J. Tiggesbäumker et al., *Chem. Phys. Lett.* **260** (1996) 428
- [5] N. Iwe et al., *Phys. Chem. Chem. Phys.* **25** (2023) 1677
- [6] H. Hövel et al., *Phys. Rev. B* **48** (1993) 18178–18188

Plasmonic resonance of mass-selected Bismuth clusters

Siqi Lu^{1,2}, Kuo-juei Hu^{1,2}, Fengqi Song^{1,2}

¹ National Laboratory of Solid State Microstructures, Collaborative Innovation Center of Advanced Microstructures, and School of Physics, Nanjing University, Nanjing 210093, China

² Atom Manufacturing Institute (AMI), Nanjing 211805, China

As a typical half-metal, Bulk bismuth presents unique properties based on its low-overlapped valence and conduction band, highly anisotropic Fermi surface as well as long mean free path of electrons[1]. It is worth noting that the properties of bulk Bi are radically altered by strong quantum size effects due to the low carrier density and small electron effective mass. For decades, Bismuth nanoparticles with limited size have been widely investigated. However, controversies remain up to now on the start point of quantum size effect and the influence on the plasmonic response of Bi nanoclusters[2-4].

Here we report a study on the plasmonic evolution of Bi clusters from 50 nm nanoparticles to 309 atoms mass-selected ones. Bi clusters are produced using a magnetron sputtering gas phase condensation cluster beam source. A time-of-flight mass filter is used to select clusters of specific atom numbers, offering a mass resolution of $M/\Delta M \approx 50$. Under the protection of tableted transparent KBr powder, Bi clusters are non-oxidized. The plasmonic resonance of Bi clusters is investigated by UV-vis and EELS spectra. In brief, surface plasmonic absorption peaks show a monotonous blue shift from ~ 290 to ~ 236 nm with decreased atom numbers, while the volume ones show a reversed redshift from 17 to 15 eV. In-depth researches are carried out on this unusual behavior.

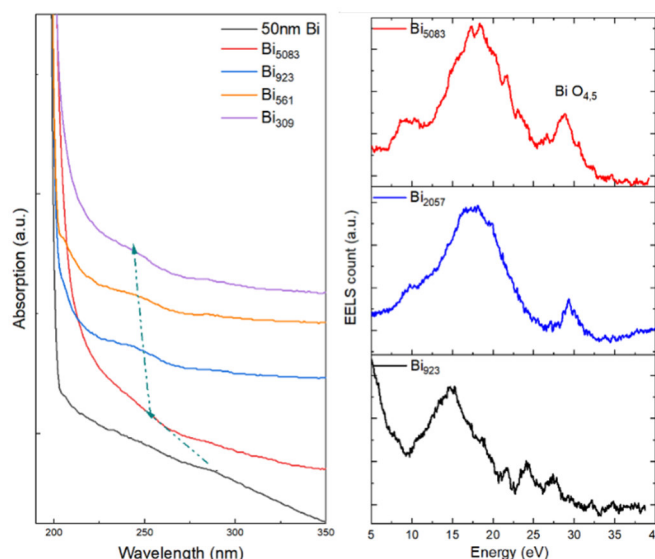


Figure 1: UV-vis and EEL spectra of mass-selected Bismuth clusters on their plasmonic response.

[1] Ph. Hofmann. Progress in Surface Science **81** (2006), 191–245

[2] Donaji Velasco-Arias, Inti Zumeta-Dubé, David Díaz, Patricia Santiago-Jacinto, Víctor-Fabián Ruiz-Ruiz, Silvia-Elena Castillo-Blum, and Luis Rendón. The Journal of Physical Chemistry C **116** (2012), 14717-14727

[3] Johann Toudert, Rosalia Serna, Iván Camps, Jacek Wojcik, Peter Mascher, Esther Rebollar, and Tiberio A. Ezquerro. The Journal of Physical Chemistry C **121** (2017), 3511-3521

[4] Siqi Lu, Lin Xie, Kang Lai, Runkun Chen, Lu Cao, Kuo-juei Hu, Xuefeng Wang, Jinsen Han, Xiangang Wan, Jianguo Wan, Qing Dai, Fengqi Song, Jiaqing He, Jiayu Dai, Jianing Chen, Zhenlin Wang, Guanghou Wang. National Science Review **8** (2021), nwaa282

Magnetic deflection of sodium doped solvent clusters

D. P. Borgeaud dit Avocat, J. V. Barnes, H. Yang, E. Simmen, B. L. Yoder, R. Signorell

ETH Zürich, Department of Chemistry and Applied Biosciences, Zürich 8093, Switzerland

Since the discovery of concentration-dependent colors of alkali metal-ammonia solutions in the early 19th century [1], excess electrons in alkali metal solutions have been found to be important in many areas. They are ubiquitous in liquid-phase chemistry [2] and play an essential role in chemical reactions [3] and biology [4]. Extensive experimental and theoretical work has been performed on solvated electrons in alkali metal solutions [2] (and references therein). However, the underlying correlation effects of solvated electrons are still not well understood. While magnetic measurements have probed such effects on alkali metal solutions [5, 6], diamagnetic and paramagnetic species have not yet been identified in such bulk phase experiments [2].

We present a study of the magnetic properties of sodium-doped solvent ammonia, water, dimethyl ether, and methanol clusters ($\text{Na}(\text{Solv})_n$, $n=1-4$) [7, 8]. Using a pulsed Stern-Gerlach deflector, we measure the magnetic deflection of a neutral cluster beam using both Velocity Map and Spatial Map Imaging detection. The experimental deflection is compared with molecular dynamics simulations based on the Zeeman interaction of a free spin $\frac{1}{2}$ system. The comparison reveals unperturbed magnetic properties of a spin $\frac{1}{2}$ system for both NaNH_3 and NaH_2O . All other studied clusters $\text{Na}(\text{NH}_3)_n$ ($n=2-4$), $\text{Na}(\text{H}_2\text{O})_n$ ($n=2-4$), $\text{Na}(\text{DME})_n$ ($n=1-3$) and $\text{Na}(\text{MeOH})_n$ ($n=1-4$), by contrast, show reduced deflection compared with that of a spin $\frac{1}{2}$ system. These deviations from a spin $\frac{1}{2}$ behavior are attributed to intra-cluster spin-relaxation effects occurring on time scales similar to or faster than the experiment. Determining spin relaxation times for these systems allows us to identify experimental trends in their magnetic behavior. These trends are discussed in terms of spin-vibrational coupling of thermally accessible rovibrational eigenstates.

- [1] W. Weyl, *Ann. Phys.*, **1864**, 199, 355.
- [2] E. Zurek, P. P. Edwards and R. Hoffmann, *Angew. Chem., Int. Ed.*, **2009**, 48, 8198.
- [3] B. C. Garrett, et al., *Chem. Rev.*, **2005**, 105, 355.
- [4] E. Alizadeh, T. M. Orlando, and L. Sanche, *Annu. Rev. Phys. Chem.*, **2015**, 66, 379.
- [5] N. W. Taylor and G. N. Lewis, *PNAS*, **1925**, 11, 456.
- [6] S. Freed and N. Sugarman, et al., *J. Chem. Phys.*, **1943**, 11, 354.
- [7] J. V. Barnes, et al., *Phys. Chem. Chem. Phys.*, **2021**, 23, 846.
- [8] J. V. Barnes, et al., submitted, 2023.

Magnetism of single-doped paramagnetic tetrel clusters studied by Stern-Gerlach experiments: Impact of the diamagnetic ligand field and paramagnetic dopant

Filip Rivic, Andreas Lehr, Rolf Schäfer

Eduard-Zintl-Institute, Technical University Darmstadt, Germany

The magnetic behavior of clusters results from a complex interplay of geometric and electronic structure and is therefore closely linked to the chemical bonding between the atoms involved. In order to gain a better understanding of magnetism and thus chemical bonding, diamagnetic tetrel clusters were alloyed with a paramagnetic dopant. In this way, on the one hand, the influence of the diamagnetic tetrel ligands on the magnetism can be studied in detail and, on the other hand, it can be followed how the paramagnetic defect influences the chemical bonding in nanoclusters.

For this purpose, Stern-Gerlach experiments were carried out on clusters of the type MSn_N ($M = \text{Mn, Fe}$; $N = 11, 12, 14, 17$). By varying the nozzle temperature of the laser vaporization cluster source, the thermal excitation, in particular of the vibrational degrees of freedom, can be changed in a controlled manner. At low temperatures, i.e. when a large part of the clusters is in the vibrational ground state, often super-atomic behavior can be observed. [1] In contrast, at high nozzle temperatures, i.e. when the vibrations of the clusters are thermally excited, spin relaxation takes place in the magnetic field and an exclusively one-sided deflection of the cluster beam is observed. [2] This deflection results from the average magnetic dipole moment $\bar{\mu}_z$ of the cluster ensemble with respect to the external magnetic field B_z . It turns out that the value of $\bar{\mu}_z$ can vary by more than an order of magnitude if only the number of diamagnetic tetrel atoms is changed. For example, the MnSn_{17} cluster is more than 15 times more magnetic than the MnSn_{14} cluster.

The analysis of the temperature dependence of $\bar{\mu}_z$ can be used to determine $g^2S(S+1)$ so that possible combinations of the electronic g -factor and the spin multiplicity S are obtained. Since the g -factor can be unambiguously determined from the occurrence of the super-atomic behavior at low temperatures, a consistent picture of the magnetic behavior of the clusters appears. Deviations of the g -factor from the free electron value are due to additional orbital contributions to the magnetic moment. [3] Based on relativistic quantum chemical calculations, the g -factors can be related to the geometric and electronic structure of the clusters. This makes it possible to understand in detail the experimentally observed magnetic behavior when the number of tetrel atoms is varied or when the paramagnetic dopants are exchanged.

[1] U. Rohrmann and R. Schäfer, Phys. Rev. Lett. **111** (2013) 133401.

[2] T. M. Fuchs and R. Schäfer, Phys. Rev. A **100** (2019), 012512.

[3] F. Rivic, A. Lehr, T. M. Fuchs and R. Schäfer, Faraday Discuss., **242** (2023) 231-251.

Magnetism of cobalt and chromium oxide clusters

Peter Lievens, Kobe De Knijf, Johan van der Tol, Piero Ferrari and Ewald Janssens
*Quantum Solid-State Physics, Department of Physics and Astronomy, Faculty of Science,
KU Leuven, Celestijnenlaan 200d - box 2414, 3001 Leuven, Belgium.*

The unique characteristics of small transition metal clusters, as well as their oxides, continue to raise interest in the scientific community, while their unique functional properties are directing them toward novel applications. From a fundamental point of view metal and metal oxide clusters of just a few atoms constitute ideal model systems, which allow to gain fundamental insight in the interplay between geometry and electronic structure that shapes their properties. This also is the case for the evolution of magnetic order in transition metals with size, from the atom to the bulk, where complex competitions between ferromagnetism, anti-ferromagnetism and paramagnetism have been observed.

In this contribution we will present investigations of the evolution with size and composition of the magnetism of small cobalt oxide and chromium oxide clusters. We used Stern-Gerlach magnetic deflection experiments to investigate the magnetism of $\text{Co}_{3-16}\text{O}_m$ ($m \leq 20$) and $\text{Cr}_{3-14}\text{O}_m$ ($m \leq 5$). The clusters were produced in a cryogenically cooled laser ablation source and their temperatures in flight were determined by velocity distribution measurements [1]. The energetic competition between $4s$ and $3d$ atomic states was found to determine the magnetism of small cobalt and chromium clusters, and it can be anticipated that this is strongly influenced by (partial) oxidation. Both pure cobalt and cobalt oxide clusters are found to be ferromagnetic, with magnetism being fairly robust for suboxides and somewhat reduced towards highly oxidized clusters. Computations of spin magnetism for selected clusters attribute the effect of oxidation on the magnetic response to electron transfer from the cobalt $3d$ and $4s$ valence orbitals to oxygen [2]. In the case of chromium suboxides, magnetism is strongly size and composition dependent, with anti-ferromagnetic and ferromagnetic interactions competing. The magnetization is in general lower as compared to their cobalt counterparts. Also in this case magnetism is determined by electron transfer from chromium to oxygen, with an important role for dimer-based cluster geometries for small sizes, as well as super-exchange interactions between the Cr atoms [3].

This research is supported by the Research Foundation Flanders (project G0A0519N) and by the KU Leuven Research Council (C14/18/073 and C14/22/103). P.F. acknowledges the FWO for a Senior postdoctoral grant.

- [1] J. van der Tol and E. Janssens, *Size-dependent velocity distributions and temperatures of metal clusters in a helium carrier gas*, Phys. Rev. A. 102, 022806 (2020), doi.org/10.1103/PhysRevA.102.022806
- [2] K. De Knijf, J. van der Tol, P. Ferrari, S. Scholiers, G.-L. Hou, P. Lievens, and E. Janssens, *Influence of oxidation on the magnetism of small Co oxide clusters probed by Stern–Gerlach deflection*, Phys. Chem. Chem. Phys. 25, 171 (2023), doi.org/10.1039/d2cp05202d
- [3] K. De Knijf et al., to be published.

Fabrication and Characterization of Hard Magnetic Janus Nanoplatelets using template of silica particles

Ali Tufani¹, Darja Lisjak¹

¹ *Department for Materials Synthesis, Jožef Stefan Institute, Slovenia*

Janus particles contain at least two different chemical or physical functional faces and show different properties in a single particle, such as polar and non-polar. Janus nanoparticles have been extensively used in catalysts, nanosensors, and cancer therapy [1]. One of the interesting Janus nanoparticles is magnetic Janus nanoparticles that combine surface anisotropy with anisotropic magnetic properties and shape [2]. Research on hard magnetic Janus nanoparticles is rare. Most studies are focused on Janus nanoparticles synthesized from spherical, superparamagnetic core nanoparticles. Here, we propose producing Janus hard magnetic nanoplatelets based on barium hexaferrite (BHF NPLs) using silica particles as the template. We expect an increase in the batch scale as opposed to classic templates from solid substrates.

The BHF NPLs were synthesized using a hydrothermal method [3]. Commercial micron-sized silica particles were dispersed in a solution of the positively charged poly(allylamine hydrochloride) (PAH) ensuring an electrostatic attachment of PAH on negatively charged silica particles. Then, the silica-PAH particles were dispersed in a solution of oppositely charged poly(sodium 4-styrene sulfonate) (PSS) to coat PSS on the particles. This coating process was repeated for three times forming three bilayers of PAH-PSS with the negatively charged PSS as the outer layer. BHF NPLs suspended in water with a positive charge at pH 4 were attached to the silica particles masking one surface of NPLs with silica particles. Then, phosphonate-based and silane-based ligands were attached to the free surface of the BHF NPLs. Finally, the functionalized NPLs were de-attached from silica particles using pH 10 DI water and Janus NPLs were collected magnetically. The Janus NPLs were characterized with different methods and their properties were compared with isotropic (i.e., the NPLs functionalized on both sides) and core BHF NPLs. The immobilization of NPLs on the silica templates was analyzed using scanning electron microscopy (SEM). The surface properties of NPLs were investigated using zeta potential. The attachment of ligands was analyzed by Fourier transform infrared (FTIR) spectroscopy. The NPLs morphology, structure, and chemical composition were studied using a transmission electron microscope (TEM) and energy-dispersive X-ray spectroscopy (EDS). Magnetic properties were measured by a vibrating sample magnetometer (VSM).

[1] X.Li, L.Chen, D.Cui, W.Jiang, L.Han, N.Niu, *Coord. Chem. Rev.* **454** (2022) 214318

[2] A.Spinosa, J.Reguera, A.Curcio, Á.Muñoz-Noval, C. Kuttner, A. Van de Walle, L.M. Liz-Marzán, C. Wilhelm *Small*. **16** (2020) 1904960

Theoretical investigation of copper oxide clusters in the pure form and using vanadium substitution

Nour El Houda Bensiradi^{1,2}, Meriem Nassar¹, Nafila Zouaghi³

¹*Laboratoire de Chimie Théorique Computationnelle et Photonique, Faculté de chimie, USTHB BP32, 16111 El Alia, Algiers, Algeria ;* ²*Ecole Normale Supérieure Bachir El-Ibrahimi, Kouba, Algeria, Kouba .*

³*Laboratoire d'Etude et de Développement des Techniques de Traitement et d'Épuration des Eaux et de Gestion Environnementale, Ecole Normale Supérieure Bachir El-Ibrahimi, Kouba, Algeria*

Copper oxide (CuO) has a wide range of applications such as photocatalysis for degradation of dyes, gas sensors, switches optics, and solar cells. It is used as a raw material in production of pigments in the field of ceramics, glass and materials plastics. It is also used in the electrolytic copper plating of baths; thus in the field of pyrotechnics to produce blue lights [1,2]. CuO also has antibacterial properties by preventing the aggregation of nanoparticles of metals from the same copper family and improving their capacity antimicrobial against pathogens [3].

Copper oxides have recently gained wide interest because of their promising applications in optoelectronic devices, as well as the medical field (hemoglobin) and the preparation of dyes.

In the present work, we are interested on the theoretical study and the characterization of the structural and energetic properties of a series of (CuO)_n cluster where n = 2,4,6, as well as the determination of their activity and their UV-Visible absorption spectra. The studied clusters are presented in the pure form and using substitutions of copper with vanadium atoms. Through this study we expect to investigate the effects of vanadium substitution on proposed clusters.

Calculations are performed using the density functional theory (DFT) included in the Gaussian program.

[1] A. K. Sundramoorthy et al, Scientific Reports, **Vol 5**(2015). 10716

[2] K. Bongchul et al, J. Phys. Chem. C, Vol **115** (48) (2011) pp 23664–23670.

[3] J. Adhikary, B. Das, S. Chatterjee, S. Kumar Dash, S. Chattopadhyay, S. Roy, J.W Chen, T. Chattopadhyay, J. Mol. Struct. **Vol 1113** (2016) 9-17

Structures, properties, and reactivity of doped semiconductor and transition metal and clusters

Jonathan T. Lyon,¹ Madison Winkeler,¹ Ciara N. Richardson,¹ Ryan Carlin,¹ Joey Quilliam¹

¹*Department of Chemistry, Murray State University, Murray, KY, USA*

Strongly bound atomic clusters are often used as models for the active sites in heterogeneous catalysis and materials chemistry. In this size region, cluster structures and properties can drastically change with the addition of a single atom, or by doping with different elements [1]. The small clusters presented here contain between 2 and 20 atoms. Theoretically, our primarily undergraduate research group at Murray State University utilize global optimization techniques to search for low energy candidate geometric isomers, and perform high level calculations (e.g., double hybrid DFT) to explore the unique properties of silicon and transition metal clusters doped with multiple atoms of different elements. Natural Bond Orbital and Adaptive Density Partitioning Analysis allows for a detailed understanding of the internal cluster bonding. Of particular interest presented here are the transition between exohedral and endohedral doped clusters, particularly silicon clusters doped with multiple transition metal atoms. We also make note of the differences between dopant atom types and concentrations, cluster growth patterns, and the unique structures found for these strongly bound doped clusters. Ongoing experimental spectroscopic endeavors will also be briefly presented.

[1] J. T. Lyon "Building Blocks: Investigating the Structures, Properties, and Reactivity of Strongly Bound Atomic Clusters at a PUI" in *Physical Chemistry Research at Undergraduate Institutions*, vol. 2, Hopkins, T. and Parish, C. A., Eds. ACS Books (2022) 165-179.

IRPD and XAS of the mixed metal oxide clusters $[\text{FeAl}_2\text{O}_4]^+$ and $[\text{FeAl}_7\text{O}_{12}]^+$

Tatiana Penna^{1,2}, Francine Horn^{1,2}, Knut R. Asmis^{*,1}, Stephen Leach³, Joachim Sauer^{*,3}, Martin Timm^{4,5}, Mayara da Silva Santos^{4,5}, Konstantin Hirsch⁵, Vicente Zamudio-Bayer⁵, Tobias Lau^{*,4,5}

¹ *Wilhelm-Ostwald-Institut für Physikalische und Theoretische Chemie, Universität Leipzig, Germany*

² *Fritz-Haber-Institut der Max-Planck-Gesellschaft, Berlin, Germany*

³ *Institut für Chemie, Humboldt-Universität zu Berlin, Germany*

⁴ *Physikalisches Institut, Albert-Ludwigs-Universität Freiburg, Germany*

⁵ *Abteilung für Hochempfindliche Röntgenspektroskopie, Helmholtz-Zentrum Berlin für Materialien und Energie, Germany*

Studies on metal oxide clusters in the gas phase are aimed at gaining a better atomistic understanding of single-site catalysts. Here, we study the structure and reactivity of cationic model systems using a combination of mass spectrometry infrared photodissociation (IRPD) spectroscopy, x-ray absorption spectroscopy (XAS) and electronic structure calculations ranging from density functional theory to multi-reference electron correlation methods.

The reactivity of the aluminium oxide cations $[\text{Al}_3\text{O}_4]^+$ and $[\text{Al}_8\text{O}_{12}]^+$ is fundamentally different and can be controlled by Fe substitution. The electronically closed-shell $[\text{Al}_3\text{O}_4]^+$ has a cone like structure and is unreactive towards methane activation, while $[\text{FeAl}_2\text{O}_4]^+$ shows a planar bicyclic structure with a terminal oxygen radical ($\text{Al}-\text{O}^{\bullet}$) that can abstract H from CH_4 [1,2]. In contrast, $[\text{Al}_8\text{O}_{12}]^+$, which contains an $\text{Al}-\text{O}^{\bullet}$ group and activates methane[3,4], becomes unreactive towards methane upon Fe substitution. We find that Fe-substitution proceeds isomorphously forming $[\text{FeAl}_7\text{O}_{12}]^+$ containing a terminal Fe(IV) oxo group. Additional information is obtained by XAS, either by probing at the K-edge of oxygen in order to gain further information on the presence of a radical oxygen species, or at the L-edge of iron to determine the oxidation state of the Fe-atom.

[1] F. Müller, J.B. Stückrath, F.A. Bischoff, L. Gagliardi, J. Sauer, S. Debnath, M. Jorewitz, K.R. Asmis, J. Am. Chem. Soc., **42** (2020) 18050–59.

[2] G. Santambrogio, E. Janssens, S. Li, T. Siebert, G. Meijer, K. R. Asmis, J. Döbler, M. Sierka, J. Sauer, J. Am. Chem. Soc., **130** (2008) 15143.

[3] M. Sierka, J. Döbler, J. Sauer, G. Santambrogio, M. Brümmer, L. Wöste, E. Janssens, G. Meijer, K. R. Asmis, Angew. Chem., Int. Ed. **46** (2007), 3372–3375.

[4] S. Feyel, J. Döbler, R. Hökendorf, M. K. Beyer, J. Sauer, H. Schwarz, Angew. Chem., Int. Ed., **47** (2008), 1946–1950.

Effect of the surface on the physicochemical properties of subnanometer supported bimetallic clusters: A DFT study

Andrés Álvarez-García, Jonathan Casildo Luque-Ceballos, Lauro Oliver Paz-Borbón, Ignacio L. Garzón

*Instituto de Física
Universidad Nacional Autónoma de México
Apartado Postal 20-364, Ciudad de México 01000, México*

Bimetallic clusters are of interest because they exhibit novel properties compared to their pure monoatomic analogs. In addition, the substrate can play a significant role in the structure, stability, and reactivity of subnanometer clusters [1]. In this work, we report a theoretical study of Pt-Re and Au-Pd clusters supported on MgO(100) and TiO₂(110) surfaces, respectively. The MgO(100) surface is flat and non-reducible, while the TiO₂(110) surface has channels (protruding oxygen atoms, O_{2c}) and is reducible. The structural and vibrational changes of the clusters on this reducible surface are more drastic than those obtained on the non-reducible surface. These structural changes occur to adapt the cluster to the surface. The charge transfer is different for these systems; Au-Pd clusters supported on TiO₂(110) have a positive charge, while Pt-Re clusters deposited on MgO(100) have a negative charge [2,3]. The cohesion energy of Au-Pd clusters on TiO₂(110) depends on the metal-metal and metal-support interactions [4]. In contrast, metal clusters on MgO(100) show that the cluster-support interaction is not dominant [5]. Thus, this study provides insight into tuning the cluster-substrate interactions that can influence the catalytic behavior of supported metal clusters.

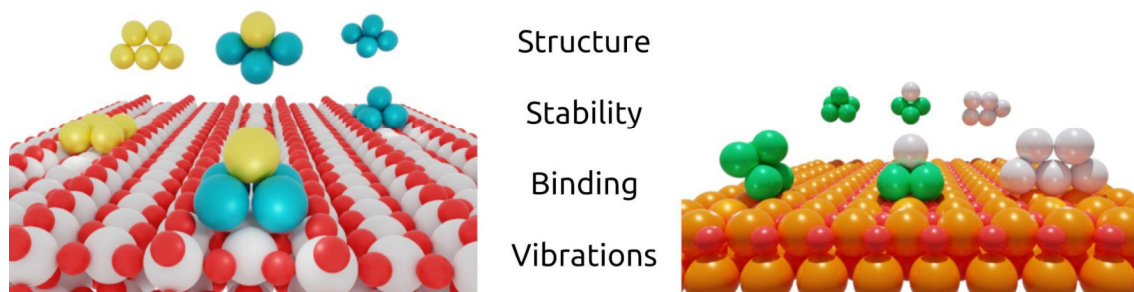


Figure 1: Effect of the surface on physicochemical properties of subnanometer bimetallic clusters.

- [1] Stefan Vajda and Michael G. W, ACS Catalysis **5** (2015) 7152–7176
- [2] Andrés Álvarez-García, Jonathan Casildo Luque-Ceballos, Lauro Oliver Paz-Borbón, and Ignacio L. Garzón, Computational Materials Science **214** (2022) 111697.
- [3] Steeve Chrétien and Horia Metiu, The Journal of Chemical Physics **127** (2007) 084704
- [4] Andrés Álvarez-García, Jonathan Casildo Luque-Ceballos, Lauro Oliver Paz-Borbón, and Ignacio L. Garzón, Surface Science **733** (2023) 122287.
- [5] Igor A. Pašti, Miloš R. Baljžović, Laura P. Granda-Marulanda and Natalia V. Skorodumova. Physical Chemistry Chemical Physics **17** (2015) 9666-9679

Optical properties of alloy AgAu clusters: revisiting chemical configuration and the influence of the d band

Hans-Christian Weissker¹, Florent Calvo²

¹ *Department, Centre Interdisciplinaire de Nanoscience de Marseille, CNRS & Aix-Marseille University, Marseille, France*

² *Laboratoire Interdisciplinaire de Physique, CNRS & Université Grenoble Alpes, France*

Gold and silver are, for all their chemical similarities, optically very different. In particular, small Ag clusters show a localized surface-plasmon resonance (LSPR), whereas in Au clusters smaller than about 300 atoms the resonance is absent due to coupling with the interband transitions from the d electrons. This opens the possibility to tune cluster properties depending on composition and chemical configuration [1].

Past work on AgAu alloy clusters has shown that the outermost shell of atoms is crucial for the overall optical properties [2]. This is intuitively natural because the size effects on the plasmon energy are due to the intricate equilibrium between the electron spill-out, the reduced screening from the d electrons, and the interfaces with the matrix [3], all taking place at the surface. However, the translation between these effective concepts and the results of atomistic calculations is not straightforward.

In this work, we revisit these questions using a realistic multi-step rearrangement pathway [4] in which the Ag and Au atoms dynamically change interior and surface positions in a 55-atom AgAu nanoalloy. In addition, we consider larger core-shell clusters of 561 atoms where the plasmon is already present in gold and where the numbers of surface and interior atoms are comparable.

Calculations using Time-dependent Density-Functional Theory are, in particular, analyzed in view of the nature of transitions so as to elucidate the contributions of surface and interior atoms for the interband transitions, thus providing a clearer picture of the nature of the nanoalloys' optical properties.

[1] Chinnabathini et al., *Nanoscale*, 15, 6696 (2023).

[2] López-Lozano, *J. Phys. Chem. C*, 117, 3062 (2013).

[3] Campos et al., *Nature Physics*, 15, 275 (2019).

[4] Calvo et al., *J. Chem. Phys.* 139, 111102 (2013).

Towards Stable Nanoalloys Mixing Au or Ag With Al or In with Localized Surface Plasmon Resonances in the UV Range

Emmanuel Cottancin,¹ Élise Camus,¹ Murilo Moreira,¹ Michel Pellarin,¹ Nicholas Blanchard,¹ Olivier Boisson,¹ Jean Lermé,¹ Lucian Roiban,² Pascal Andreazza,³ and Matthias Hillenkamp¹

¹ Univ. Lyon 1, CNRS, iLM, UMR 5306, F- 69622 Villeurbanne, France

² Univ Lyon, INSA Lyon, UCBL, CNRS, MATEIS, UMR5510, F-69621 Villeurbanne, France

³ Université d'Orléans, CNRS, ICMN, UMR7374, F-45071 Orléans, France

Bimetallic nanoparticles (BNPs) are promising for fundamental research and applications, as their physicochemical properties can be tuned or enhanced with respect to the monometallic particles. In this context, the atomic and chemical structure and the optical response of A_xB_{1-x} BNPs combining gold or silver (A) with aluminium or indium (B) were investigated for various stoichiometries in order to examine if stable alloyed phases could exist and promote localized surface plasmon resonances (LSPR) in the UV range. [1,2]

The structure and morphology of matrix embedded-BNPs of a few nanometers, produced by laser vaporization, were analysed by transmission electron microscopy (TEM) and optical absorption measurements compared with Mie calculations in the dipolar approximation. The BNPs' internal structure was further investigated by *in situ* x-ray photoelectron spectroscopy and synchrotron-based x-ray scattering techniques giving complementary information about the chemical state of the constituent elements and structural heterogeneities in the BNPs. Finally, the restructuring of the partially oxidized BNPs annealed in a reducing atmosphere was also probed by environmental TEM. [3] The complementary techniques of characterization show that silica-embedded silver-based Ag-In and Ag-Al BNPs form metallic silver-rich alloyed cores surrounded by an indium or aluminium oxide shell. The initial LSPRs are in the UV range for both systems, but the difference in the kinetics of oxidation between indium and aluminium involves less blue-shifted LSPRs for Ag-Al BNPs. In the case of gold-based BNPs embedded in silica, we show evidence of ordered nanoalloys just after air exposure and the appearance of gold and indium (or aluminium) demixing during oxidation. The initial LSPR of Au-In BNPs is the one furthest in the UV range among the four systems with an LSPR peak centered at 254 nm, which is a sign of the formation of the $AuIn_2$ alloy. Furthermore, recent experiments show very promising complete alloying and stability in air for alumina-protected $AuIn_2$ BNPs (see the LSPR in the UV range stable over time in figure 1).

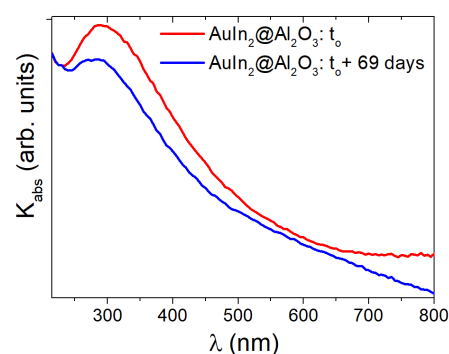


Figure 1: absorption spectra of alumina-embedded $AuIn_2$ BNPs

[1] É. Camus, J. Ramade, M. Pellarin, N. Blanchard, M. Hillenkamp, C. Langlois, L. Roiban and E. Cottancin, *Eur. Phys. J. Appl. Phys.*, 2022, **97**, 59.

[2] É. Camus, M. Pellarin, N. Blanchard, O. Boisson, M. Hillenkamp, L. Roiban, P. Andreazza and E. Cottancin, *Faraday Discussions*, 2023, **242**, 478-498.

[3] J. Ramade, C. Langlois, M. Pellarin, L. Piccolo, M. A. Lebeault, T. Epicier, M. Aouine and E. Cottancin, *Nanoscale*, 2017, **9**, 13563-13574.

Alloying bulk immiscible W-Cu systems into clusters

Yongxin Zhang^{1,2}, Fengqi Song^{1,2}

¹ National Laboratory of Solid State Microstructures, Collaborative Innovation Center of Advanced Microstructures, and School of Physics, Nanjing University, Nanjing 210093, China

² Atom Manufacturing Institute (AMI), Nanjing 211805, China

Bimetallics typically exhibit properties that are completely different from elementary substance [1]. However, due to its thermodynamic immiscibility and easy oxidation, alloying bimetallic nanoparticles still remains extremely challenging [2]. The alloying of the bulk immiscible system ($\Delta H_{\text{mix}} > 0$) in thermodynamic equilibrium are prevented by Gibbs free energy of mixing ($\Delta G_{\text{mix}} = \Delta H_{\text{mix}} - T\Delta S_{\text{mix}}$, with mixing Entropy ΔS_{mix} at temperature T). It is worth noting that W-Cu is a typical immiscible binary system with very high ΔH_{mix} ($> +30$ KJ/mol), making it difficult to alloy under ordinary methods [3].

Here, we report the strategy of reducing the mixing enthalpy of bimetallic systems based on size effect to achieve nanoscale alloying, especially for the bulk immiscible system. Mass-selected W-Cu nanoclusters were produced by magnetron sputtering gas phase condensation cluster beam source equipped with time-of-flight (TOF) mass selector, with a mass resolution of $M/\Delta M \approx 50$. Detailed structure and composition properties of these clusters are characterized by STEM, XPS, EDS, etc. The element proportion and structure of alloy clusters is adjusted by changing the synthesis parameters of cluster beam source. From the EDS result, signs of miscibility are shown and from the STEM results, no core-shell structures are found. The present work provides a method for alloying bulk immiscible systems into nanoparticles, expanding the range of alloying system.

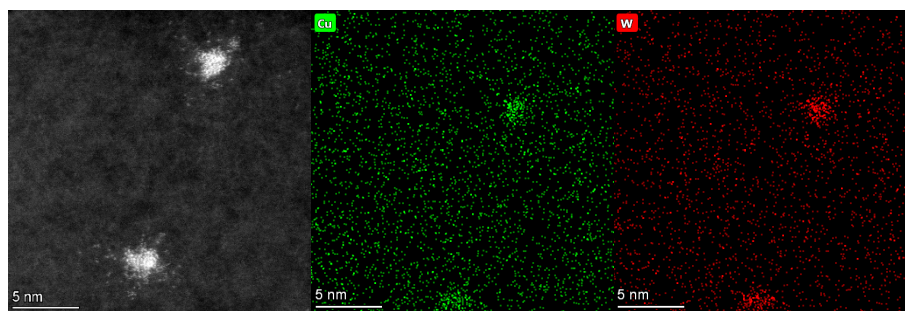


Figure 1: The STEM and EDS mapping of mass-selected W-Cu cluster

- [1] C. P. Yang, B. H. Ko, S. Hwang, Z. Y. Liu, Y. G. Yao, W. Luc, M. J. Cui, A. S. Malkani, T. Y. Li, X. Z. Wang, J. Q. Dai, B. J. Xu, G. F. Wang, D. Su, F. Jiao, L. B. Hu. *Science Advances* **6** (2020) eaaz6844
- [2] Y. Yao, Z. Huang, L. A. Hughes, J. Gao, T. Li, D. Morris, S. E. Zeltmann, B. H. Savitzky, C. Ophus, Y. Z. Finck, Q. Dong, M. Jiao, Y. Mao, M. Chi, P. Zhang, J. Li, A. M. Minor, R. Shahbazian-Yassar, L. Hu. *Matter* **4** (2021), 2340-2353.
- [3] J. Feng, D. Chen, P. V. Pikhitsa, Y. H. Jung, J. Yang, M. Choi, *Matter* **3** (2020) 1646-1663.

Chemical Reactivity of Boron Substituted Aluminum Superatoms on Organic Substrates

Tomoya Inoue¹ and Atsushi Nakajima¹

¹ Department of Chemistry, Faculty of Science and Technology, Keio University, Japan

Nanoclusters are promising building blocks for functional nanomaterials due to their high designability which could control the material properties by tuning constituent elements and number of constituent atoms. Among them, there is a specific class of nanoclusters so called “superatoms” exhibiting high chemical stability in gas phase, which satisfy both an electron shell closure of superatomic orbitals and a geometrically packed structure. Aluminum 13-mer anion ($\text{Al}@ \text{Al}_{12}^-$) is one of the most representative superatoms which shows high chemical stability in gas phase based on 40 electron shell closure of 2P superatomic orbitals and icosahedral (I_h) structure. When the central Al atom is replaced by a smaller and homologous boron (B) atom, the $\text{B}@ \text{Al}_{12}^-$ superatom exhibits higher stability because of relaxing the strains of Al_{12} cage while maintaining 40 electron shell closure [1]. The substitution with homologous elements enables us to design geometric structures and electron density distributions, while keeping total number of valence electrons.

To utilize such superatoms as functional nanomaterials, it is required to achieve surface decoration with the superatoms optimized physically and chemically, and to evaluate the stability in condensed phase. Recently, it has been revealed that Al_n^- ($n=7-24$) and Al_{12}B^- could be stabilized on a surface pre-decorated by a *p*-type organic molecule of hexa-*tert*-butyl-hexa-*peri*-hexabenzocoronene (HB-HBC; $\text{C}_{66}\text{H}_{66}$) [2]. In this study, Al_nB^- ($n=6-14$) was deposited on a HB-HBC decorated substrate, in which the reactivity of Al_nB was evaluated by combining x-ray photoelectron spectroscopy (XPS) and oxygen molecule exposure defined by Langmuir ($1 \text{ L} = 1.33 \times 10^{-3} \text{ Pa} \times 1 \text{ s}$).

XPS (Mg K α : $h\nu = 1253.6 \text{ eV}$) spectra were measured around Al 2*p* and O 1*s* core levels for Al_n ($n=7-15$) and Al_nB ($n=6-14$) immediately after deposited on the HB-HBC substrates at 0.6 ML equivalent. For pure Al_n ($n=7-15$) deposited on the HB-HBC substrate, a sharp Al 2*p* peak was observed at a binding energy of 73 eV in all sizes, where the energy position for metal Al (Al^0), while O 1*s* signal was hardly observed. On the other hand, for Al_nB on the HB-HBC substrates, the Al 2*p* XPS shows a size-dependent change from a sharp Al^0 peak to a broad peak observed at 75-76 eV, where almost the same energy with Al oxide (Al^{3+}). In fact, O 1*s* signal was increased with the decrease of size from $n=12$. For Al_6B , the Al 2*p* peak appeared as almost one oxidized component of Al^{3+} despite immediately after deposition. Therefore, small Al_nB nanoclusters are highly activated by B atom substitution even with the deposition on HB-HBC substrate. To quantitatively estimate a reactivity, the relative reactivity of Al_{n+1} and Al_nB based on that of Al_{12}B was evaluated from the decrement of Al^0 component in Al 2*p* with oxygen molecule exposures. For size of n less than 11, the relative reactivity of Al_nB was 3 to 20 times higher than that of Al_{n+1} which is the same number of constituent atoms. On the other hand, for n larger than 12, the relative reactivity of Al_nB was equal to or less than that of Al_{n+1} , indicating nanoclusters were chemically stabilized by forming icosahedral Al_{12} cage, overcoming the activation effect of B atom.

[1] A. Nakajima, T. Kishi, T. Sugioka, K. Kaya, *Chem. Phys. Lett.* **187** (1991) 239-244.

[2] M. Shibuta, T. Inoue, T. Kamoshida, T. Eguchi, A. Nakajima, *Nat. Commun.* **13** (2022) 1336.

Abstracts Poster Session B (Thursday)

Gas phase deposition of well-defined bimetallic gold-silver clusters for photocatalytic applications

Vana Chinnappa Chinnabathini^{1,2,3}, Fons Dingenen^{2,3}, Rituraj Borah^{2,3}, Imran Abbas¹, Johan van der Tol¹, Zviadi Zarkua¹, Francesco D'Acapito⁴, Thi Hong Trang Nguyen¹, Peter Lievens¹, Didier Grandjean¹, Sammy W. Verbruggen^{2,3}, Ewald Janssens¹

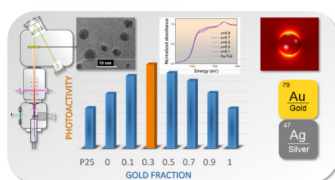
1.QSP, Department of Physics and Astronomy, KU Leuven, Belgium.

2.Sustainable Energy, Air & Water Technology (DuEL), University of Antwerp, Belgium.

3. NANOlaboratory Center of Excellence, University of Antwerpen, Groenenborgerlaan 171, 2020, Antwerpen, Belgium.

4. CNR-IOM-OGG c/o ESRF LISA CRG - The European Synchrotron, Grenoble, France.

Cluster beam deposition is employed for fabricating well-defined bimetallic plasmonic photocatalysts to enhance their activity while facilitating a more fundamental understanding of their properties. $\text{Au}_x\text{Ag}_{1-x}$ clusters with compositions ($x = 0, 0.1, 0.3, 0.5, 0.7, 0.9$ and 1) spanning the metals miscibility range were produced in the gas-phase and soft-landed on TiO_2 P25-coated silicon wafers with an optimal coverage of 4 atomic monolayer equivalents. Electron microscopy images show that at this coverage most clusters remain well dispersed whereas EXAFS data are in agreement with the finding that the deposited clusters have an average size of *ca.* 5 nm and feature the same composition as the ablated alloy target. A composition-dependant electron transfer from Au to Ag that is likely to impart chemical stability to the bimetallic clusters and protect Ag atoms against oxidation is additionally evidenced by XPS and XANES. Under simulated solar light, $\text{Au}_x\text{Ag}_{1-x}$ clusters show a remarkable composition-dependent volcano-type enhancement of their photocatalytic activity towards degradation of stearic acid, a model compound for organic fouling on surfaces. The Formal Quantum Efficiency (FQE) is peaking at the $\text{Au}_{0.3}\text{Ag}_{0.7}$ composition with a value that is twice as high as that of the pristine TiO_2 P25 under solar simulator. Under UV the FQE of all compositions remains similar to that of pristine TiO_2 . A classical electromagnetic simulation study confirms that among all compositions $\text{Au}_{0.3}\text{Ag}_{0.7}$ features the largest near-field enhancement in the wavelength range of maximal solar light intensity, as well as sufficient individual photon energy resulting in a better photocatalytic self-cleaning activity. This allows ascribing the mechanism for photocatalysis mostly to the plasmonic effect of the bimetallic clusters through direct electron injection and near-field enhancement from the resonant cluster towards the conduction band of TiO_2 . These results not only demonstrate the added value of using well-defined bimetallic nanocatalysts to enhance their photocatalytic activity but also highlights the potential of the cluster beam deposition to design tailored noble metal modified photocatalytic surfaces with controlled compositions and sizes without involving potentially hazardous chemical agents.



- [1] T.W. Liao, S.W. Verbruggen, N. Claes, A. Yadav, D. Grandjean, S. Bals, P. Lievens, *Nanomaterials* **8** (2018) 30.
- [2] S.W. Verbruggen, M. Keulemans, B. Goris, N. Blommaerts, S. Bals, J.A. Martens, S. Lenaerts, *Applied Catalysis B: Environmental* **188** (2016) 147-153.
- [3] T.W. Liao, A. Yadav, K. Hu, J. van der Tol, S. Cosentino, F. D'Acapito, R.E. Palmer, C. Lenardi, R. Ferrando, D. Grandjean, P. Lievens, *Nanoscale* **10** (2018) 6684-6694.
- [4] A. Mills, J.S. Wang, *J. Photochem. Photobiol. A*, **182** (2006) 181-186.

Photocatalysis and photosensitization using atomically precise metal nanoclusters for solar energy harvesting and conversion

Yu Wang,¹ Ye Liu,¹ Nicola Pinna¹

¹ Department of Chemistry, Humboldt-Universität zu Berlin, Germany

Metal nanoclusters (NCs) with atomic precision are a unique family of metal nanomaterials that are readily crystalized into single crystals, representing ideal models to unravel structure-property relationship at atomic level. By tuning the number of metal atoms in the core, the composition and the protecting ligand of metal NCs, their physicochemical properties can be precisely controlled. The strong, broad light absorption ability and the long-lived excited states make metal NCs promising candidates as photosensitizer, and might replace traditional dyes. Their discrete energy levels allow them to prevent charge recombination at the semiconductor by efficiently separating the photoinduced charge carriers. Moreover, these metal NCs themselves can act as active catalysts. In the first part of the talk, we demonstrate the differences of working principle between metal NCs and their particle counterparts in photocatalytic system. The metal NC modified TiO_2 catalyst is found to exhibit a five times higher performance than TiO_2 modified with metal nanoparticles in the photocatalytic H_2 production reaction.^[1] In the second part, we present the strategy to tune the charge transfer pathways of metal NCs sensitized semiconductors in photoelectrochemical system. While metal NCs serve as catalyst for oxidation reactions when loaded on n-type semiconductor, they serve as catalyst for reduction reactions when loaded on p-type semiconductor.^[2] In the last part, we will use Au_{25} NC as an example to demonstrate how the protecting ligand and the composition of the metal NC influence the overall performance of a NC/semiconductor system in photocatalytic H_2 production.^[3,4]

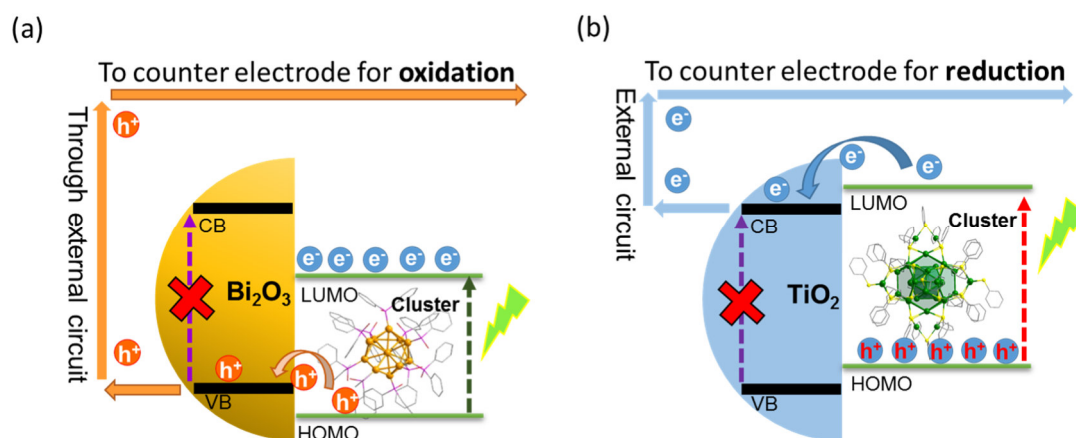


Figure 1: Different charge transfer pathways when NCs are loaded on different type of semiconductors.

[1] Wang, Y.; Liu, X.-H.; Wang, Q.; Quick, M.; Kovalenko, A. S.; Chen, Q.-Y.; Koch, N.; Pinna, N. *Angew. Chem. Int. Ed.* **2020**, *59*, 7748-7754.

[2] Wang, Y.; Liu, X.-H.; Wang, R.; Cula, B.; Chen, Z.-N.; Chen, Q.-Y.; Koch, N.; Pinna, N. *J. Am. Chem. Soc.* **2021**, *143*, 9595-9600.

[3] Liu, Y.; Wierzbicka, E.; Springer A.; Pinna N.; Wang, Y. *J. Phys. Chem. C* **2022**, *126*, 1778-1784.

[4] Liu, Y.; Long, D.; Springer A.; Wang, R.; Koch, N.; Schwalbe, M.; Pinna N.; Wang, Y. *Solar RRL* **2023**, *7*, 2201057.

Hydride-containing superatomic alloys as efficient HER catalysts

Rhone P. Brocha Silalahi,¹ Tzu-Hao Chiu,¹ Chen-Wei Liu¹

¹ Department of Chemistry, National Dong Hwa University, Hualien, Taiwan 97401

In our systematic studies of coinage metal hydrides stabilized by dichalcophosphate ligands ($E_2P(OR)_2^-$; E = S, dtp; Se, dsep) [1], we have demonstrated that interstitial hydrides in nanoclusters can reduce M(I) to M(0) and form stable superatoms [2]. Importantly, hydride-containing eight-electron alloy clusters, $PtHAg_{19}(dtp/dsep)_{12}$, which hydride position was unequivocally confirmed by single crystal neutron diffraction, were rationalized by DFT calculations that the incorporated hydrogen atom provides its electron to the superatomic system, allowing it to reach the nearest *magic* closed-shell electron count [3]. In this presentation, first hydride-containing 2-electron palladium/copper alloys, $[PdHCu_{11}\{S_2P(O^iPr)_2\}_6(C\equiv CPh)_4]$ (**PdHCu₁₁**) as highly HER-active, and $[PdHCu_{12}\{S_2P(O^iPr)_2\}_5\{S_2PO(O^iPr)\}(C\equiv CPh)_4]$ (**PdHCu₁₂**), are synthesized via the treatment of $[PdH_2Cu_{14}\{S_2P(O^iPr)_2\}_6(C\equiv CPh)_6]$ (**PdH₂Cu₁₄**) [4] with trifluoroacetic acid (TFA). X-ray diffraction reveals that the **PdHCu₁₁** kernel consists of a central PdH unit encapsulated within a vertex-missing Cu₁₁ cuboctahedron. On the other hand, the **PdHCu₁₂** can be viewed as a complete PdH-centered Cu₁₂ cuboctahedron. Both the hydride in **PdHCu₁₁** and **PdHCu₁₂** are located within a PdCu₃ tetrahedron. While in **PdHCu₁₂**, one of the six dithiophosphates is di-anionic arisen from acid-induced de-esterification. Due to the unique open structural feature, the **PdHCu₁₁** shows excellent HER activity, much better than **PdHCu₁₂** and **PdH₂Cu₁₄**, with the onset potential of -0.05 V (at 10 mA cm^{-2}) and the Tafel slope of 40 mV dec^{-1} . The Faradaic efficiency for H₂ production reaches 96% at -0.05 V and can be further increased to over 99% at -0.10 V. Our study strongly suggests that the central Pd site, which is not completely shielded, is the key for high HER activity and may provide guidelines for correlating catalyst structures and HER activity [5].

- [1] R. S. Dhayal, W. E. van Zyl, C. W. Liu, *Acc. Chem. Res.* **49** (2016), 86-95.
- [2] W. E. van Zyl, C. W. Liu, *Chem. Eur. J.* **28** (2022), e202104241.
- [3] T.-H. Chiu, J.-H. Liao, F. Gam, Y.-Y. Wu, X. Wang, S. Kahlal, J.-Y. Saillard, C. W. Liu, *J. Am. Chem. Soc.* **144** (2022), 10599-10607.
- [4] K. K. Chakrahari, R. P. B. Silalahi, T.-H. Chiu, X. Wang, N. Azrou, S. Kahlal, Y.-C. Liu, M.-H. Chiang, J.-Y. Saillard, C. W. Liu, *Angew. Chem. Int. Ed.* **58** (2019), 4943-4947.
- [5] R. P. B. Silalahi, Y. Jo, J.-H. Liao, T.-H. Chiu, E. Park, W. Choi, H. Liang, S. Kahlal, J.-Y. Saillard, D. Lee, C. W. Liu, *Angew. Chem. Int. Ed.* **62** (2023), e202301272.

Ru/TiO₂ Catalysts in the CO₂ Methanation Investigated by Operando X-ray Absorption Spectroscopy

Joachim Bansmann¹, Ali Abdel-Mageed^{1,2}, Shilong Chen^{1,3}, and R. Jürgen Behm^{1,4}

¹ Institute of Surface Chemistry and Catalysis, Ulm University, 89081 Ulm, Germany

² Leibniz-Institut für Katalyse e.V. (LIKAT Rostock), 18059 Rostock, Germany Institute of

³ Inorganic Chemistry, Kiel University, 24118 Kiel, Germany

⁴ Institute of Theoretical Chemistry, Ulm University, 89081 Ulm, Germany

The CO₂ methanation (known as Sabatier reaction) is an important catalytic reaction for the conversion of CO₂ to methane in H₂ rich gas mixtures over Ni and Ru catalysts and has recently gained increasing interest due to its application in the power-to-gas technology.

Here, we concentrate on physical and chemical properties of Ru nanoparticles on Ru/TiO₂ catalysts in the CO₂ methanation using TiO₂ (P90) supports. The catalysts were mainly investigated at the European Synchrotron radiation Facility ESRF (Grenoble, France), ID 24, using time resolved Operando X-ray absorption spectroscopy (XAS) at the Ru K edge in a CO₂ reformat gas mixture at atmospheric pressure (15.5% CO₂, balance H₂) at 190°C. Additionally, we applied a stepwise increase in the temperature up to 350°C in the reaction gas mixture in order to activate the catalysts followed by measurements at 190°C. X-ray Absorption spectroscopy (XANES) data showed a very high content of metallic Ru species during the activation period, cf. Figure 1. The effect of the activation step on the activity of the catalyst will be discussed based on simultaneously recorded IR data. Additional XANES data were recorded at the Ti K edge of the support material of the catalyst at ELETTRA (Trieste, Italy). The results will be compared to results from the CO methanation over Ru/TiO₂ from our group.

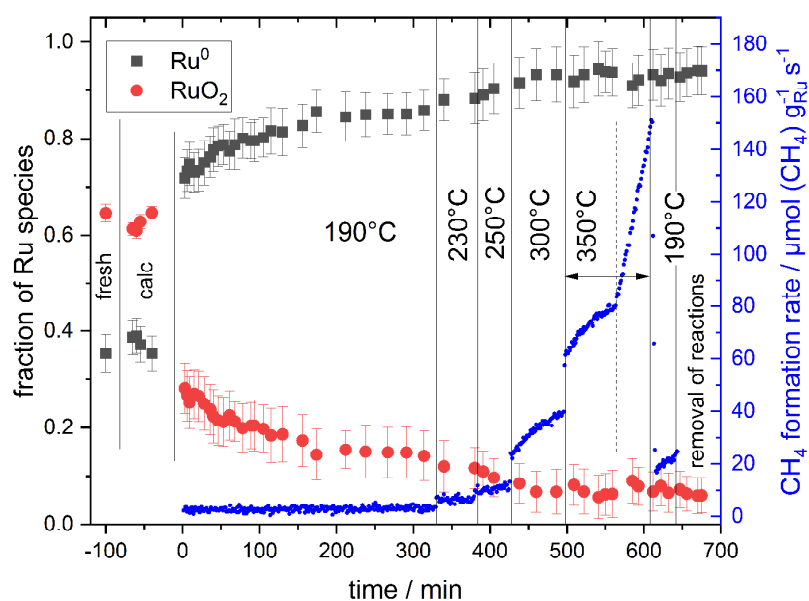


Figure 1: Operando X-ray absorption spectroscopy: correlation of the fraction of metallic and oxidic Ru species during reaction with the CH₄ formation rate

Construction and Application of Atomically Dispersed Catalysts

Daojian Cheng

State Key Laboratory of Organic-Inorganic Composites, Beijing University of Chemical
Technology, Beijing 100029, People's Republic of China
e-mail of presenting author: chengdj@mail.buct.edu.cn
WEB page: <http://www.nanoalloy.com.cn/>

Atomically dispersed catalysts (ADCs) have attracted much attention in catalysis region due to its nearly 100% atomic utilization rate. However, developing universal construction method and precise regulation of the coordination environment are the main difficulties to the development of ADCs^[1]. To solve these problems, we put forward some facile approaches for the accurate and universal preparation of ADCs. Notably, for carbon-based carriers, Ru, Pt, Rh, Ir, Au, Mo, etc. ADCs could be fabricated by a facile room temperature impregnation method^[2, 3]. More importantly, a volcano-type relation between oxidation states and hydrogen evolution activity could be observed by controlling the local coordination environments of metal atoms, further suggesting the importance of local coordination regulation^[4]. In addition, for metal oxide/hydroxide carriers, 22 kinds of ADCs could also be synthesized by a one-step electroreduction method^[5]. A library of atomically dispersed catalysts is constructed and the coordination reconstruction mechanism for ADCs is emphasized. The developed atomically dispersed catalysts in our works could display excellent activity in many reaction systems, mainly including water splitting, electroreduction of carbon dioxide, hydrogenation, hydroformylation reaction and so on. We believe the developed construction methods and the understanding of structure-activity relationship contribute to guide the development of highly active and low cost catalysts in the future.

1. Xu, H.; **Cheng, D.***; Cao, D.*; & Zeng, X.* Nat. Catal., 2018, 1, 339-348.
2. Yang, L.;(##), **Cheng, D (# Co-first author)**.; Xu, H.; Zeng, X.; Wan, X.; Shui, J.; Xiang, Z. & Cao, D*. PNAS, 2018, 115, 6626-6631.
3. Cao, D.; Wang, J.; Xu, H.; **Cheng, D.***. Small, 2021, 2101163.
4. Cao, D.; Xu, H.; Li, H.; Feng, C.; Zeng, J.*; **Cheng, D.***. Nat. Commun., 2022, 13, 5843.
5. Cao, D.; Zhang, Z.; Cui, Y.; Zhang, R.; Zhang, L.; Zeng, J.*; **Cheng, D.***. Angew. Chem. Int. Ed. 2023, 62, e202214259.

Chemical ordering of Au-Ni nanoparticles and their activities in oxygen reduction reaction

Arravind Subramanian¹, Sergey M. Kozlov^{1*}

¹ *Department of Chemical and Biomolecular Engineering, National University of Singapore, Engineering Drive 4, Singapore 117585, Singapore*

Bimetallic catalysts play a significant role in conquering the activity volcano as a specific composition of metals tends to increase the yield and selectivity of the catalyst. Modelling bimetallic catalysts presents a challenge in determining the most-stable chemical ordering, which refers to the arrangement of atoms in the nanoparticle or surface. Precisely matching the surface structure and properties of experimentally synthesized materials in computational models is crucial and it requires complex task of identifying the most-stable chemical ordering from a multitude of possible arrangements. Here we present an improved Monte-Carlo-based method to determine the most-stable chemical ordering using a set of energetic descriptors obtained from an initial set of up to 30 different structures with typical chemical orderings. Initially, Au-Ni (431) kinked surfaces with 20:80, 40:60, 60:40, 80:20 Au:Ni ratios were simulated using this method. The most-stable structures were predicted to exhibit a core-shell arrangement (Ni-core, Au-shell). Subsequently, the effect of 1/4th monolayer of oxygen and hydroxide on the corner, edge, and terrace descriptors was studied on the Au-Ni (431) kinked surface, revealing the migration of Ni atoms from the core to the shell under reaction conditions. The developed method was then applied to nanoparticles with four different compositions, once again predicting a core-shell arrangement, as depicted in Figure 1. Finally, to determine the chemical ordering and composition which shows high activity towards oxygen reduction reaction (ORR), we built (431) kinked surfaces and nanoparticles of various compositions using the obtained bare and OH-based energetic descriptors by performing Monte-Carlo at 300 K representing the reaction conditions. Based on the overall activity, one can choose a specific composition which better represent the surface arrangement of atoms for ORR at reaction conditions.

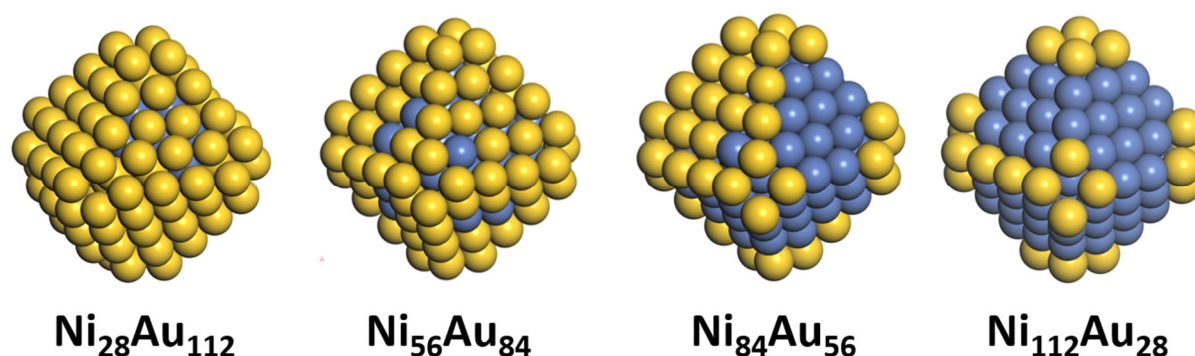


Figure 1: Most-stable chemical ordering of Au-Ni nanoparticles of different compositions

Size-studies of Au and Cu nanoparticles for CO₂ electroreduction: every parameter counts

Esperanza Sedano Varo¹, Rikke Egeberg Tankard¹, Julius Lucas Needham¹, Alexander Juul Nilsen¹, Joakim Kryger-Baggesen², Christian Danvad Damsgaard², Jakob Kibsgaard¹

¹ Department of Physics, Technical University of Denmark, Denmark

² Department of Physics, VISION – Center for Visualizing Catalytic Processes, Denmark

Nanoparticles are extensively utilized in various industrial processes due to their enhanced catalytic performance resulting from a high surface-to-bulk ratio. Modulating the size of these nanoparticles allows for manipulation of their activity and selectivity^{1,2}, which is particularly intriguing in the context of CO₂ electroreduction, a process yielding 16 different products where enhancing selectivity is of significant interest³. However, investigating these minute catalysts in electrochemistry poses considerable challenges, given the multitude of parameters that influence apparent selectivity.

In this study, we thoroughly examine the intrinsic selectivity of size-selected nanoparticles by meticulously controlling all relevant parameters, including size, loading, impurities, and shape. Our methodology aims to meticulously manage these variables to establish experimental structure-activity relationships and generate reliable, transferable knowledge applicable to other catalytic studies, both fundamental and experimental. Here, we present several parameters with significant impacts on the selectivity and activity of the nanocatalysts, along with the results demonstrating the influence of these controlled parameters on the accuracy of size-based performance studies of the nanoparticles.

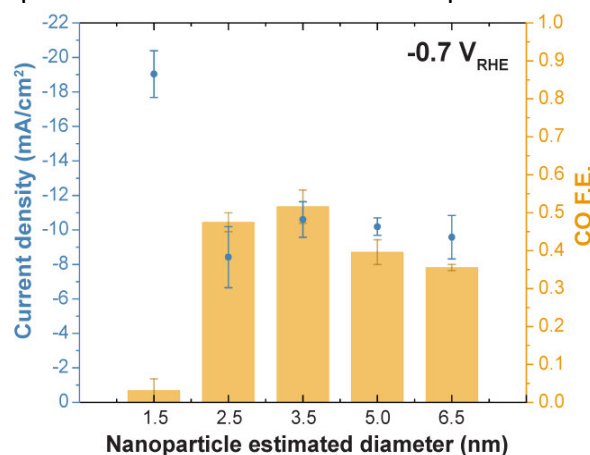


Figure 3. Size study on the CO faradaic efficiency of Au nanoparticles

1. Mistry, H. *et al.* Exceptional size-dependent activity enhancement in the electroreduction of CO₂ over Au nanoparticles. *J Am Chem Soc* **136**, 16473–16476 (2014).
2. Zhu, W. *et al.* Monodisperse Au Nanoparticles for Selective Electrocatalytic Reduction of CO₂ to CO. *J. Am. Chem. Soc* **14**, 35 (2013).
3. Nitopi, S. *et al.* Progress and Perspectives of Electrochemical CO₂ Reduction on Copper in Aqueous Electrolyte. *Chemical Reviews* vol. 119 7610–7672 Preprint at <https://doi.org/10.1021/acs.chemrev.8b00705> (2019).

Stable mass-selected AuTi nanoparticles for CO oxidation

Filippo Romeggio^{1,†}, Rikke E. Tankard^{1,†}, Stefan K. Akazawa^{1,2}, Alexander Krabbe¹, Olivia F. Sloth¹, Niklas M. Secher¹, Sofie Colding-Fagerholt^{1,2}, Stig Helveg^{1,2}, Richard E. Palmer³, Christian D. Damsgaard^{1,2}, Jakob Kibsgaard^{1,2}, Ib Chorkendorff¹

¹*Department of Physics, Technical University of Denmark, Kongens Lyngby, Denmark*

²*Center for Visualizing Catalytic Processes (VISION), Department of Physics, Technical University of Denmark, 2800 Kongens Lyngby, Denmark*

³*College of Engineering, Swansea University, Bay Campus, Swansea, UK*

Addressing stability in reactive conditions is a big challenge when working with clusters and nanoparticles¹. The stability of < 5 nm gold nanoparticles has been a central focus since their catalytic properties were discovered. To enhance their stability during CO oxidation at high temperatures, one common approach involves modifying their interactions with the supporting material, while another approach involves incorporating another metal into the nanoparticles themselves, forming an alloy with gold. Previous studies have suggested that AuTi alloy nanoparticles could offer improved stability^{2,3}. This research presents direct observations that demonstrate the enhanced stability of AuTi alloy nanoparticles compared to pure Au nanoparticles during CO oxidation. The alloyed nanoparticles exhibited activity comparable to that of the pure Au nanoparticles, but they displayed significantly higher stability at elevated temperatures. Detailed investigations employing Low Energy Ion Scattering, X-ray Photon Spectroscopy, and Environmental Transmission Electron Microscopy unveiled the structure of the AuTi nanoparticles. These characterizations revealed an Au core surrounded by an alloy shell consisting of AuTi. Remarkably, this structure remained stable even under reactive conditions at 320°C, and an incremental increase in activity was observed over a duration of more than 140 hours. This work reaffirms the potential of nanoparticle alloying as a mean to tune both catalytic activity and stability, emphasizing the importance of employing complementary and in-situ characterization techniques to advance the optimization of nanoparticle catalyst design.

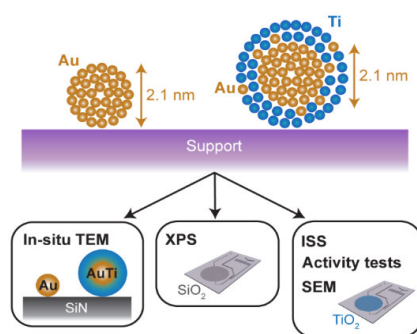


Figure 4: Overview of methods and substrates for catalyst characterization⁴.

- [1] Seh, Z. W.; Kibsgaard, J.; Dickens, C. F.; Chorkendorff, I.; Nørskov, J. K.; Jaramillo, T. F., *Science* 355 (2017).
- [2] Liu, S.; Xu, W.; Niu, Y.; Zhang, B.; Zheng, L.; Liu, W.; Li, L.; Wang, J, *Nat Commun* 10 (2019).
- [3] Niu, Y.; Schlexer, P.; Sebok, B.; Chorkendorff, I.; Pacchioni, G.; Palmer, R. E., *Nanoscale* 10 (2018).
- [4] Tankard R. E., Romeggio F., Akazawa S. k., Krabbe A., Sloth O. F., Secher N. M., Colding-Fagerholt S., Helveg S., Palmer R. E., Damsgaard C. D., Kibsgaard J., Chorkendorff I., *ACS Catalysis* (2023, *in preparation*).

***In situ* (S)TEM Characterization of a Pd/ZnO Catalyst for CO₂ Hydrogenation and Selective Methanol Synthesis**

Deema Balalta¹, Imran Abbas², Dimitra Papamichail², Didier Grandjean², Ewald Janssens², Peter Lievens², Thomas Altantzis³, Sara Bals¹

¹*Electron Microscopy for Materials Research (EMAT), University of Antwerp, Belgium*

²*Quantum Solid-State Physics, Department of Physics and Astronomy, KU Leuven, Belgium*

³*Applied Electrochemistry and Catalysis Group (ELCAT), University of Antwerp, Belgium*

Pd/ZnO has been recognized as an effective catalyst for the conversion of CO₂ into methanol. While the Pd-Zn alloy phase has traditionally been seen as the key active component, methanol formation does not occur in the presence of an inert oxide support (such as Al₂O₃ or SiO₂), indicating that the presence of both zinc oxide and palladium or palladium-zinc phases is necessary to achieve high activity and selectivity for methanol under industrial conditions.

To optimize the Pd/ZnO catalytic performance we need a thorough understanding of the reaction mechanism and active site structure, as well as the nature of active sites during reaction conditions. *In-situ* Scanning Transmission Electron Microscopy (S)TEM can provide a deeper understanding of the changes occurring at the nanometer and atomic scale when catalytic clusters are exposed to aggressive reaction environments, which in turn have a major impact on their catalytic behavior¹. In our study, Pd clusters are prepared using a magnetron sputtering cluster source and are deposited on ZnO powders. The catalyst was drop-casted on the bottom chip of a MEMS nanoreactor to monitor the reduction process.

In situ reduction in the TEM was carried out at 350 °C, using a reactant gas mixture of 5:95 ratio of H₂:He with a flow of 0.1 ml/min, and by maintaining the pressure at 500 mbar for 1 hour. High resolution (S)TEM imaging allowed us to track the structural changes of the Pd clusters on the ZnO support. The measured interatomic distances agree with the PdZn alloy tetragonal structure, confirming the formation of an alloy during the reduction step.

Currently, the deposition of clusters on powders is limited to very low loadings. In our lab, we recently designed a chip holder to mount the *in situ* bottom chip inside the cluster source, an approach that can allow for higher cluster loadings to be achieved. The chip windows will accommodate the drop-casted support material and the clusters will be deposited directly on the support's surface. Moreover, the holder can house a shadow mask for a more critical deposition to certain regions of interest. With this improvement, we can study more particles and perform complementary (S)TEM spectroscopic techniques. This will not only allow for better statistics on more particles, but also clarify the role of the palladium-zinc alloy phase in facilitating this reaction.

1. Matteo Monai et al. ,Restructuring of titanium oxide overlayers over nickel nanoparticles during catalysis.Science380,644-651(2023).

Ultrafast wettability alteration: The decisive moments of adsorption on supported particles

Christian Weigelt¹, Mihai E. Vaida², Thorsten M. Bernhardt¹

¹ *Institute of Surface Chemistry and Catalysis, Albert-Einstein-Allee 47, 89081 Ulm, Germany*

² *UCF Department of Physics, 4111 Libra Drive, Orlando, FL 32816-2385, USA*

The detection of intermediate species during photoinduced surface chemical reactions and the ability to correlate their ultrafast dynamics with the morphology and electronic structure of the surface is crucial to fully understand and control photoinduced or photocatalytic reactions.

In this investigation, the ultrafast photodissociation dynamics of CH₃Br molecules on variable size Au clusters grown on MgO/Mo(100) has been investigated using the pump-probe femtosecond-laser mass spectroscopy technique [1]. Collaborative photoemission investigations in conjunction with femtosecond extreme ultraviolet laser pulses are employed to sensitively detect the changes in the electronic structure of the Au clusters as they are grown on MgO/Mo(100) [2].

Further prospective research directions aim at the investigation of catalytic water splitting facilitated by supported manganese oxide clusters. In this respect, previous comparative gas phase catalytic model systems provide an extremely promising perspective [3].

[1] M. E. Vaida, T. M. Bernhardt: Tuning the ultrafast photodissociation dynamics of CH₃Br on ultrathin MgO films by reducing the layer thickness to the 2D limit, *Chem. Phys. Lett.* 688, 106 (2017).

[2] M. E. Vaida, T. M. Bernhardt, T. Rawal, D. Le, B. M. Marsh, T. S. Rahman, S. R. Leone: Ultrafast photodissociation dynamics of CH₃Br on MgO films decorated with variable size Au nanoparticles, to be submitted.

[3] S. Mauthe, I. Fleischer, T. M. Bernhardt, S. M. Lang, R. N. Barnett, U. Landman: A gas phase Ca_nMn_{4-n}O₄⁺ cluster model for the oxygen evolving complex of photosystem II, *Angew. Chem. Int. Ed.* 58, 8504 (2019). S. M. Lang, N. T. Zimmermann, T. M. Bernhardt, R. N. Barnett, B. Yoon, U. Landman: Size, stoichiometry, dimensionality, and Ca-doping of manganese oxide based water-oxidation cluster catalysts: An oxyl/hydroxy mechanism for oxygen-oxygen coupling, *J. Phys. Chem. Lett.* 12, 5248 (2021).

Size dependence of catalytic activity of well-defined Pt nanosystem supported on CeO₂ for CO oxidation reaction

Nicola Da Roit¹, Joachim Czechowsky,² Marco Neumaier,³ Carina Maliakkal,³ Di Wang,³ Manfred Kappes,^{2,3} Maria Casapu,² Silke Behrens¹

¹ *Institute of Catalysis Research and Technology, ³Institute of Nanotechnology, Karlsruhe Institute of Technology, Hermann-von Helmholtz-Platz 1, 76344 Eggenstein-Leopoldshafen, Deutschland;* ² *Institute of Chemical Technology and Polymer Chemistry, Karlsruhe Institute of Technology, Engesserstraße 20, 76131 Karlsruhe, Germany*

Supported metal catalysts are complex systems whose performance depends on various materials parameters and synergistic effects. Through the use of ligands, advanced techniques in cluster / small nanoparticle (NP) synthesis allow precise control over the particle size and even the number of active metal atoms in clusters, and thus the development of well-defined powder model catalysts [1,2]. Polyol reduction is a flexible method that enables the synthesis of both well-defined NPs and atomically precise clusters starting from various precursor compounds dissolved in high-boiling polyols [3].

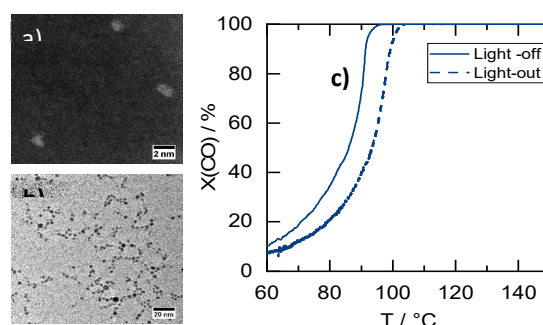


Figure 1. a) STEM-HAADF image of Pt₁₇(PPh₃)₈(CO)₁₂²⁺ cluster [4]; b) TEM image of Pt NPs with average size of 3.5nm; c) Light-off/Light-out curves for CO oxidation catalysis of Pt NPs anchored on CeO₂

We show the synthesis of platinum clusters and NPs within a size range from 1 to 5 nm *via* a polyol process using different types of ligands and reaction conditions. The clusters and NPs were analyzed by electron microscopy with energy-dispersive X-ray analysis (TEM, STEM-HAADF, EDS), infrared spectroscopy (FT-IR, ATR), dynamic light scattering (DLS), mass spectroscopy (MS) and optical emission spectroscopy with inductively coupled plasma (ICP-OES). We anchor the clusters and NPs on a metal oxide support to prepare model catalysts for emission control catalysis. The influence of cluster / NP size on the catalytic performance was investigated for CO oxidation.

- (1) Casapu, M.; Fischer, A.; Gänzler, A. M.; Popescu, R.; Crone, M.; Gerthsen, D.; Türk, M.; Grunwaldt, J.-D. *ACS Catal.* **7** (1), 2017, 343–355.
- (2) Sharapa, D. I.; Doronkin, D. E.; Studt, F.; Grunwaldt, J.; Behrens, S. *Adv. Mater.* **31** (26), 2019, 1807381.
- (3) Dong, H.; Chen, Y.-C.; Feldmann, C. *Green Chem.* **17** (8), 2015, 4107–4132.
- (4) Nair, L. V.; Hossain, S.; Wakayama, S.; Takagi, S.; Yoshioka, M.; Maekawa, J.; Harasawa, A.; Kumar, B.; Niihori, Y.; Kurashige, W.; Negishi, Y. *J. Phys. Chem. C* **121** (20), 2017, 11002–11009.

Structure-selectivity of Cu_{2-x}Se towards CO_2 electroreduction

Wenjian Hu^{1,2}, Deema Balalta³, Jason Song², Imran Abbas¹, Zhiyuan Chen², Thomas Altantzis⁴, Jan Vaes², Didier Grandjean¹, Sara Bals³, Ewald Janssens¹, Deepak Pant²

¹ Quantum Solid-State Physics (QSP), Department of Physics & Astronomy, KU Leuven, Belgium

² Separation and Conversion Technology, Flemish Institute for Technological Research (VITO), Belgium

³ Electron Microscopy for Materials Science (EMAT), University of Antwerp, Belgium

⁴ Applied Electrochemistry and Catalysis Group (ELCAT), University of Antwerp, Belgium

Copper selenides, forming both non-stoichiometric and stoichiometric phases, are an important family of transition metal chalcogenides (TMCs) [1]. Despite their promising electrocatalytic performance, active site identification in Cu_{2-x}Se nanostructures remains a challenge. The varying product selectivity among similar nanostructures, yielding products like formic acid [2], CO [3], and methanol [4], highlights the need to understand structure-performance relationships for improved Cu_{2-x}Se electrocatalyst design. This work highlights the structure-selectivity relationship in Cu_{2-x}Se under CO_2 electroreduction at $-1.4 \text{ V}_{\text{RHE}}$ yielding 23% of methanol in its pristine form and 82.1% CO at partial current density of 27.7 mA cm^{-2} after chemical- (H_2O_2 etching) and electro-activation. Low and high magnification STEM images reveal that the pristine Cu_{2-x}Se catalyst is comprised of $\text{Cu}_{1.71}\text{Se}$ wires with a cubic structure while the chemically activated one $[\text{Cu}_{2-x}\text{Se}]\text{O}_y$ displays wire-like characteristics enveloped by thin, folded oxide layers. In situ Raman under electro activation of $[\text{Cu}_{2-x}\text{Se}]\text{O}_y$ at -1.6 V shows a drastic reduction of the Cu-Se bond signal with time suggesting a degradation of the CuSe while a Cu_2O signal appearing and constantly growing once the potential is returned to OCP suggests that metallic Cu segregated under electro-activation is then oxidized into Cu^{1+} after activation. Ex situ EXAFS of $[\text{Cu}_{2-x}\text{Se}]\text{O}_y$ confirms the progressive transformation of the Cu_{2-x}Se into Cu_{1-z}Se phase through segregation of Cu that forms a mixture of Cu^{1+} and Cu^{2+} after reaction. A more moderate Cu segregation also occurs in pristine Cu_{2-x}Se as no Cu_{1-z}Se phase transformation is detected. In good agreement with EXAFS, post-activated catalysts reveal the presence of agglomerates of Cu_2O cubes (cubic, Pn-3m) with 50 to 90 nm edges amidst smaller Cu_{2-x}Se particulates. The copper selenide system's changing selectivity, which depends on activation, could be explained by the combined impact of copper segregation and the interactive effects between metallic Cu and the residual structures of Cu_{2-x}Se or Cu_{1-z}Se .

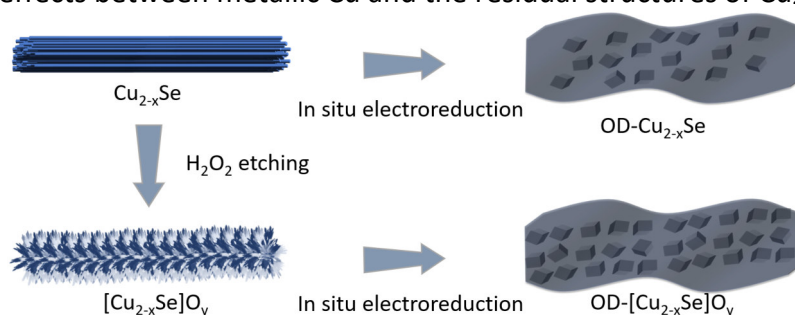


Figure 1: In situ structural evolution of Cu_{2-x}Se -coated Cu_2O nanocubes

- [1] Shaohua Zhang, Zhen Li., et al., *Advanced Materials* **28** (2016) 8927
- [2] Junyuan Duan, Tiaoyou Zhai., et al., *Nature Communications* **13** (2022) 2039
- [3] Jiajun Wang, Wenbin Hu., et al., *Advanced Materials* **34** (2022) 2106354
- [4] Dexin Yang, Buxing Han., et al., *Nature Communications* **10** (2019) 677

Embedded Metallic Cu Centers Extend Conversion of CO₂ on 2D Plasmonic CuSe Photothermal Catalysts

Janobiddinkhuja Bahodurov¹, Fan Lu Meng², Ji Shi Wei², Minmin Gao², Tian Xi Zhang¹, Sergey M. Kozlov¹ and Ghim Wei Ho³

¹ Department of Chemical and Biomolecular Engineering, National University of Singapore, Singapore

² Department of Electrical and Computer Engineering, National University of Singapore, Singapore

³ Department of Material Science and Engineering, National University of Singapore, Singapore

We present a novel approach for efficient CO₂ photoreduction through the utilization of a photochemical-photothermal synergistic catalyst composed of embedded Cu/CuSe structures. Our study demonstrates the enhanced performance achieved by incorporating Se vacancies and in-plane metallic Cu clusters within CuSe nanosheets, which extend the photothermal conversion beyond the intrinsic plasmonic wavelength of CuSe and provide robust catalytic active sites. By employing density functional theory (DFT) calculations and experimental characterization, we have elucidated the crucial role of in-plane metallic Cu in promoting CO₂ and reducing the activation energy of the rate-determining step in the subsequent conversion process. Furthermore, our findings highlight the influence of Se vacancies in inducing new gap states for infrared (IR)-light broadening. As a result, the production rate of CO has shown a significant threefold improvement. This pioneering work introduces a viable strategy to expand the light-response range while preserving the plasmonic effect in the IR region of plasmonic semiconductors. The resulting enhancement in photocatalytic reactions enables effective solar harvesting and utilization. Our findings contribute to the advancement of CO₂ reduction technologies and offer new avenues for sustainable energy production.

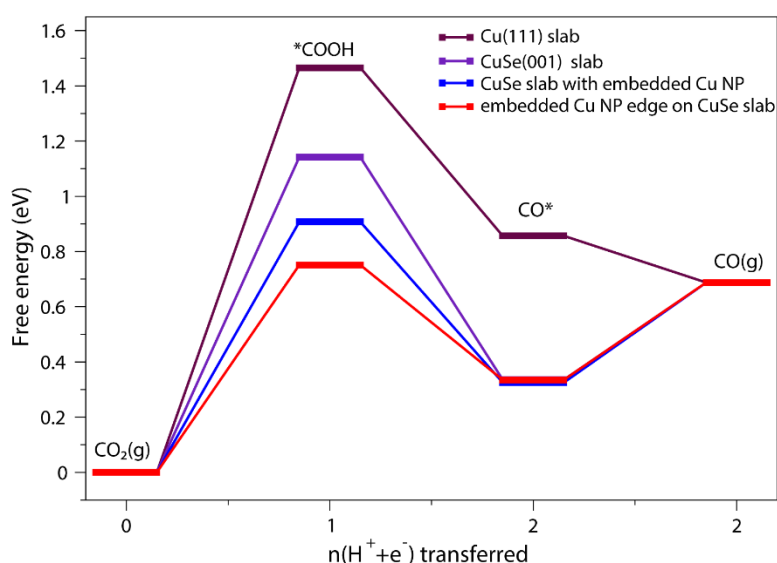


Figure 1: Free energy diagram of the overall CO₂RR pathway for Cu(111) surface, CuSe(001), CuSe slab with embedded Cu NP and embedded Cu NP edge on CuSe slab.

Investigating the Formation and Characteristics of Strong Metal-Support Interaction with Size-Selected Pt Clusters (< 1nm) on r-TiO₂(110)

Tobias Hinke¹, Sebastian Kaiser,¹ Philip Petzoldt¹, Martin Tschurl¹, Friedrich Esch¹, Ueli Heiz¹, Paolo Lacovig², Alessandro Baraldi³

¹ School of Natural Sciences, Technical University of Munich, Germany

² Sincrotrone Trieste, Italy

³ Physics Department and CENMAT, University of Trieste, Italy

Metal oxidic support materials exhibit a great influence on the mechanical and chemical stability of small transition metal particles and consequently lead to the alteration of their reactivity and selectivity.

One example of this impact is the strong metal-support interaction (SMSI), that is known to induce significant changes in the activity of Pt catalyst particles on reducible oxide supports at elevated temperatures [1]. This effect is hard to differentiate from sintering effects employing only activity measurements or spectroscopic methods.

For small particles with < 1nm the formation, structure and impact on the overall reaction is still heavily disputed. Whereas a simple overlayer structure theory is observed for bigger particles [2], small (< 1nm), highly reactive noble metal clusters may conceivably form an SMSI state that differs from the one observed for larger particles. In this case, a changed electronic structure without a significant change of the interface structure is expected to reason for changes of the catalyst's properties.

In order to understand this difference between larger and smaller particles a profound understanding of SMSI-state formation, stability and the characteristic properties on an atomistic level is necessary.

The investigation of metal oxide single crystals decorated with sub-nanometer transition metal particles are used as model systems in order to comprehending the observed, particle-size dependent deviations.

Here, we deposited 1 %ML Pt-clusters (< 1nm) on a mildly reduced rutile TiO₂(110) single crystal for investigating the change of activity upon heating to temperatures between 350K – 700K. The type of SMSI state present was deduced using a combination of XPS, s-XPS and STM measurements. Correlations between SMSI structure and both changes of thermal and photochemistry were investigated with TPD and photocatalytic measurements, respectively. The formation of the SMSI state was found to be heavily influenced by the amount of surface defect sites. Furthermore, combined studies of CO adsorption and resonant PES experiments were conducted, resulting in a possible differentiation between sintering effects and SMSI state formation as a function of treatment temperature.

These results provide important insights into the nature of the SMSI state and highlight the importance of particle size.

[1] S. Bonanni et.al., J. Am. Chem. Soc. **134** (2012), 7, 3445–3450.

[2] P. Petzoldt et.al., J. Phys. Chem. C **126** (2022), 38, 16127–16139.

Sub-nano platinum clusters supported on conductive metal oxides vs. graphite: size- and support-dependent electrocatalysis

Tsugunosuke Masubuchi¹, Zihan Wang¹, Michael P. Obrien¹, Scott L. Anderson¹,
Simran Kumari², Zisheng Zhang³, Philippe Sautet², Anastassia Alexandrova³

¹ Department of Chemistry, University of Utah, Salt Lake City, UT, USA

² Department of Chemical and Biomolecular Engineering, UCLA, Los Angeles, CA, USA

³ Department of Chemistry and Biochemistry, UCLA, Los Angeles, CA, USA

We present an experimental and theoretical study of the electrocatalytic activity of supported sub-nano platinum clusters (Pt_n). Pt_n on indium tin oxide (ITO) and fluorine-doped tin oxide (FTO) exhibit size-dependent activity for the hydrogen evolution reaction (HER) [1, 2]. HER activity is negligible for isolated Pt atoms (Pt_1), increasing rapidly with cluster size such that Pt_7 and Pt_8 catalysts have roughly double the activity *per* Pt atom compared to the top surface layer atoms of polycrystalline Pt. These active Pt_n /ITO [1] and Pt_n /FTO [2] are associated with highly fluxional Pt hydride states that are generated with applied potentials, which provide multiple sites with optimal binding energy for H and hence high HER activity and high H under-potential deposition currents. We also report electrocatalysis by Pt_n clusters deposited on highly oriented pyrolytic graphite (HOPG), chosen as a model support representing sp^2 -hybridized carbon electrodes. The HER activity of $Pt_{4,7}$ /HOPG is found to be even higher than that for $Pt_{4,7}$ /FTO at the same Pt loading (Figure 1), but activity and stability are strongly affected by deposition conditions (i.e., soft landing vs. hard landing vs. subplantation). We will discuss the nature of the deposited Pt_n /HOPG interactions effected by deposition energy by probing associated cluster processes such as sintering, subplantation, and defect creation. We will also show some applications of these cluster catalysts to other useful electrochemical reactions such as the oxygen reduction reaction (ORR) [3] and alcohol electro-oxidation [4].

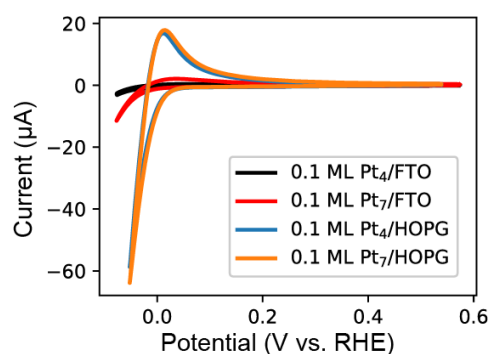


Figure 1: Cyclic voltammograms obtained for Pt_n /FTO and Pt_n /HOPG ($n = 4, 7$) in 0.1 M $HClO_4$.

- [1] S. Kumari, T. Masubuchi, H.S. White, A. Alexandrova, S.L. Anderson, P. Sautet, J. Am. Chem. Soc. **145** (2023) 5834–5845.
- [2] Z. Zhang, T. Masubuchi, P. Sautet, S.L. Anderson, A.N. Alexandrova, Angew. Chem. Int. Ed. **62** (2023) e202218210 (9 pages).
- [3] A. von Weber, E.T. Baxter, H.S. White, S.L. Anderson, J. Phys. Chem. C **119** (2015) 11160–11170.
- [4] A. von Weber, E.T. Baxter, S. Proch, M.D. Kane, M. Rosenfelder, H.S. White, S.L. Anderson, Phys. Chem. Chem. Phys. **17** (2015) 17601–17610.

Dynamic Interaction of CO₂ with a Ru/ γ -Al₂O₃ Catalyst – A Temporal Analysis of Products (TAP) Study

Corinna Fauth¹, Anja Lenzer¹, Ali M. Abdel-Mageed^{1,2}, R. Jürgen Behm^{1,3}

¹ Institute of Surface Chemistry and Catalysis, Ulm University, D-89069 Ulm, Germany

² Leibniz Institute for Catalysis (LIKAT Rostock), D-18059 Rostock, Germany

³ Institute of Theoretical Chemistry, Ulm University, D-89069 Ulm, Germany

Ruthenium nanoparticles (NPs) supported on inorganic oxides act as highly active catalysts for several reactions, including the CO_x methanation [1], CO oxidation [2], Fischer-Tropsch reaction [3], or reverse water-gas shift (RWGS) reaction [4]. Thereby, the interaction of CO₂ with the catalyst plays an important role. The reaction may occur in an associative or dissociative way possibly involving changes in the Ru oxidation state. Aiming at a detailed picture of the interaction of CO₂ with supported Ru catalysts we investigated the dynamic reduction and oxidation of Ru/Al₂O₃, exploring the reversible replenishment of active oxygen (O_{act}) by interaction with CO₂ by temporal analysis of products (TAP) reactor measurements under well-defined reaction conditions. In these multi-pulse experiments, we compared the oxidation strength of O₂ and CO₂ pulses and further investigated the interaction of isotope marked C¹⁸O₂ with the catalyst and adsorbed species present on the catalyst.

We used a commercial 5.0 wt.% Ru/ γ -Al₂O₃ catalyst (100 m² g_{cat}⁻¹, mean Ru particle diameter 1.6 nm) supplied by Johnson Matthey. After pretreatment of the catalyst in 10% O₂/N₂ at 150 °C for 30 min (O150) we performed multi-pulse experiments in a home-built TAP reactor described in ref. [5]. Piezo-electrically driven pulse valves generated gas pulses (1.5-3.2×10¹⁶ molecules per pulse) with high reproducibility. The effluent gas from the catalyst bed, which was fixed in a quartz glass microreactor, was detected by a quadrupole mass spectrometer (QMG 700, Pfeiffer) located in a UHV chamber (background pressure 8×10⁻⁹ mbar).

First, the reversible removal and replenishment of O_{act} on Ru/Al₂O₃ was monitored during alternating sequences of CO/Ar and O₂/Ar pulses at 190 °C, 250 °C, 300 °C. We determined the amount of O_{act} removal from the CO consumption in the CO pulse titration. At all temperatures, the CO pulses completely reduced the RuO₂ particles formed during O150, resulting in CO₂ leaving the catalyst bed and carbonate species building up. In the following sequence of O₂ pulses approx. 60% of the initial O_{act} content was replenished at 190 °C, and this fraction increased with higher temperature. Similar experiments using CO₂ demonstrated that also CO₂ is able to deposit oxygen on the pre-reduced Ru surface, however, with a significantly lower deposition rate compared to O₂. In the presence of H₂, the amount of O_{act} deposition by CO₂ was significantly increased to a level comparable to that of O₂, which we attribute to the formation of highly reactive water (RWGS reaction). Finally, in multi-pulse experiments with isotope marked C¹⁸O₂ on the pre-reduced catalyst, we followed the simultaneous i) O_{act} deposition, ii) oxygen exchange between CO₂ and adsorbed species, and iii) decomposition of surface carbonate. In conclusion, the interaction of CO₂ with Ru/Al₂O₃ includes both changes in the Ru oxidation state and in the adsorbate layer. Therefore, these TAP measurements are highly relevant for the mechanistic understanding of various catalytic reactions on supported Ru involving CO₂.

[1] Eckle et al., J. Phys. Chem. C **115** (2011) 1361

[2] Over, M. Muhler, Prog. Surf. Sci. **72** (2003) 3.

[3] Claeys et al., Top. Catal. **26** (2003) 139.

[4] Aitbekova et al., J. Am. Chem. Soc. **140** (2018) 1373

[5] Leppelt et al., Rev. Sci. Instrum. **78** (2007) 104103.

Vibrational Spectroscopy and Reactivity of Ultra-Small Silica and Silicate Fragments in the Gas-Phase: Potential Implications for Interstellar Dust Growth and Astrochemistry

Sandra M. Lang,¹ Bianca-Andreea Ghejan,¹ Thorsten M. Bernhardt,¹ Joost M. Bakker,² Joan Mariñoso Guiu,³ Andreu Avel·li de Donato Perez,³ Stefan T. Bromley³

¹ *Institute of Surface Chemistry and Catalysis, Ulm University, Germany*

² *Radboud University, Institute for Molecules and Materials, FELIX Laboratory, The Netherlands*

³ *Departament de Ciència de Materials i Química Física & Institut de Química Teòrica i Computacional (IQTCUB), Universitat de Barcelona, Spain*

Silicates are ubiquitously found as small dust grains throughout the universe. These particles are frequently subject to high-energy processes and subsequent condensation in the interstellar medium (ISM), where they are broken up into many ultra-small silicate fragments. Such fragments can be astrochemically relevant for the formation and dissociation of small molecules, such as H₂, H₂O, O₂, or CO₂. In our work, we use methods that are well established in the field of cluster chemistry and physics and are now transferred to addressing astrochemically relevant materials: infrared multiple-photon dissociation (IR-MPD) spectroscopy combined with ion trap and flow tubes reaction studies. With this approach, we aim to gain insight into the geometric structure of ultra-small silica and silicate fragments, their growth process, as well as their reactive and catalytic properties.

In particular, we will present first results on the infrared spectrum of the cationic pyroxene monomer MgSiO₃⁺, its surprisingly strong interaction with molecular oxygen, and potential initial steps of particle nucleation via adsorption of Mg.¹ Furthermore, we have investigated the interaction of ultra-small silica clusters with water, which might present an alternative process for dust particle growth. The IR-MPD spectra of silica-water complexes not only reveal the hydroxylation of the clusters but also indicates an increased stability compared to bare silica clusters. Besides the strong interaction towards water, we also observed small silica clusters to be highly reactive towards CO₂, with some cluster sizes even mediating the dissociation of CO₂ to CO. Such reactive properties might have important implications for the role of silicate dust particles in the formation of complex organic molecules in the ISM.

1. Mariñoso Guiu, J.; Ghejan, B.-A.; Bernhardt, T. M.; Bakker, J. M.; Lang, S. M.; Bromley, S. T., *ACS Earth and Space Chem.* **2022**, 6, 2465

Capacity and mechanism of water storage in gas-phase silicon oxide clusters studied by thermal desorption spectrometry

Toshiaki Nagata, Ken Miyajima, Fumitaka Mafuné

Department of Basic Science, School of Arts and Sciences, The University of Tokyo, Japan

Silicon oxide (silica) plays an important role in the chemical evolution of the universe. Particularly, the formation and storage of water in silica are important for the chemistry of early-stage planets. In this context, the reactivity of gas-phase silica clusters ($\text{Si}_n\text{O}_m^\pm$) with H_2O molecules has been studied [1]. In this study, we investigated the stable compositions of $\text{Si}_n\text{O}_m\text{H}_k^+$ ($n = 3-8$) clusters, formed by reactions of silica clusters with H_2O , and H_2O release processes from these clusters using gas-phase thermal desorption spectrometry.

Silicon oxide clusters were generated by laser ablation of a Si rod in the presence of O_2 mixed with He carrier gas. The generated clusters were reacted with H_2O vapor to form $\text{Si}_n\text{O}_m\text{H}_k^+$ clusters at room temperature. The clusters were then heated in a temperature-controlled tube (300–1000 K) and analyzed by a time-of-flight mass spectrometer. Density functional theory (DFT; M06-L/aug-cc-pVTZ) calculations were performed to investigate the stable geometry and energetics of a part of the observed species.

Among the observed species, clusters with $\text{Si}_n\text{O}_{2n+i}\text{H}_{2i+1}^+ (= (\text{SiO}_2)_n(\text{H}_2\text{O})_i\text{H}^+)$ compositions were prominent. These clusters satisfy the stoichiometry based on Si^{4+} , O^{2-} , and H^+ , where the closed-shell electronic structures are achieved, and this is thought to be the reason why these clusters are stable. The clusters sequentially released H_2O molecules upon heating (Fig. 1a). After heating to 1000 K, clusters with $i = 1-3$ were abundant for $n = 3-8$ although these clusters seem to be able to release more H_2O molecules considering their chemical formulae. For instance, H_2O was not released from $\text{Si}_3\text{O}_7\text{H}_3^+$ ($n = 3, i = 1$) even at 1000 K. The H_2O desorption energies (ΔE) were obtained from the experimental temperature dependence and the DFT calculations (Fig. 1b). Based on the calculated structures, H_2O desorption can be classified to (i) the release of H_2O molecules weakly bound by hydrogen bonds ($\Delta E < 1$ eV; e.g., from $\text{Si}_3\text{O}_{11}\text{H}_{11}^+$) and (ii) the H_2O release from clusters with no H_2O units but OH groups ($\Delta E \approx 2$ eV; e.g., from $\text{Si}_3\text{O}_9\text{H}_7^+$). The H_2O release from $\text{Si}_3\text{O}_7\text{H}_3^+$, not observed in the experiments, was calculated to require quite high ΔE (ca. 5 eV). These results suggest that the H_2O binding abilities of $\text{Si}_n\text{O}_{2n+i}\text{H}_{2i+1}^+$ clusters are mainly determined by their geometric structures.

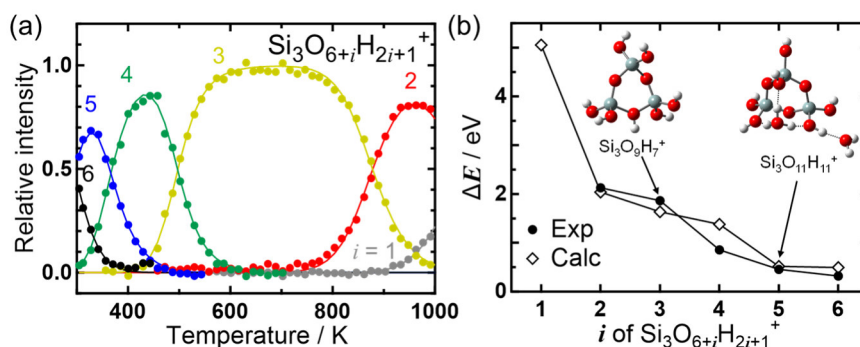


Figure 1: (a) Relative intensities of $\text{Si}_n\text{O}_{2n+i}\text{H}_{2i+1}^+$ at 300–1000 K and (b) ΔE for H_2O desorption ($n = 3$).

[1] M. Arakawa, T. Omoda, A. Terasaki, J. Phys. Chem. C **121** (2017) 10790.

Small Silicon Oxide Clusters – Optical Photodissociation and Photochemical Properties

Taarna Studemund¹, Kai Pollow¹, Marko Förstel¹ and Otto Dopfer¹

¹ *Institut für Optik und Atomare Physik, Technische Universität Berlin, Germany*

An essential constituent in the evolution of solar systems, planets – like the Earth – and other celestial bodies is interstellar dust, whose key components are μm -sized silica and metal silicates [1]. Currently, among the possible precursors for macroscopic dust grains, only molecular SiO has been identified in interstellar regions and circumstellar disks [2]. Experimental measurements on polyatomic Si_nO_m^+ cations, in combination with quantum chemical calculations, are expected to answer open questions on further intermediates of the dust grain formation. Consequently, we present the first optical spectra for Si_nO_m^+ cations larger than SiO^+ and Si_2^+ [2,3]. Photodissociation spectroscopy of mass-selected ions in a tandem mass spectrometer coupled to a laser vaporization source (Figure 1) is used to determine electronic and optical properties of the clusters under investigation [4]. Electronic photodissociation data generated by action spectroscopy are compared and interpreted with TD-DFT calculations (Figure 2).

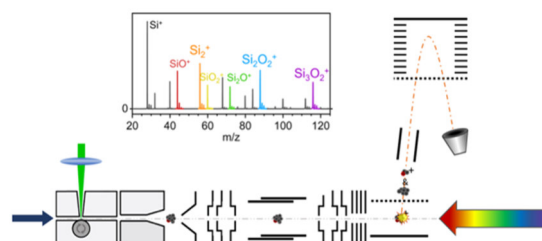


Figure 1: Summed mass spectra of general small Si_nO_m^+ clusters and schematic of the used laser vaporization setup.

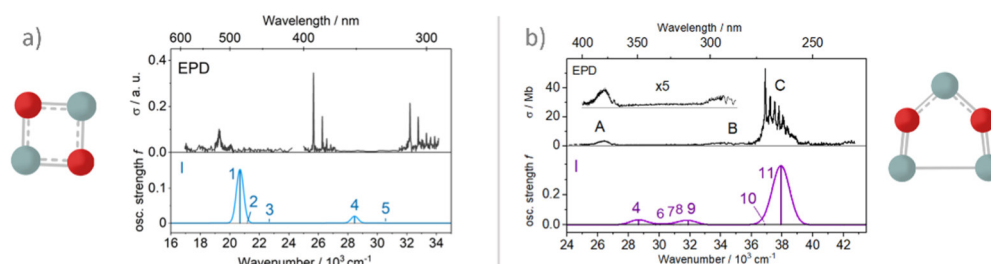


Figure 2: Calculated ground state structures of the lowest lying isomers for measured EPD spectra and comparison to vertical TD-DFT spectra of a) Si_2O_2^+ (UB3LYP/6-311++(2d,2f)/cc-pVTZ) and b) Si_3O_2^+ (UCAM-B3LYP-D3/cc-pVTZ)

- [1] K. Nagashima, A. N. Krot, and H. Yurimoto, *Nature* **428**, 6986 (2004).
- [2] R. W. Wilson, A. A. Penzias, K. B. Jefferts, M. Kutner, and P. Thaddeus, *ApJ* **167** (1971).
- [3] T. Studemund, K. Pollow, S. Verhoeven, E. Mickein, O. Dopfer, and M. Förstel, *J. Phys. Chem. Lett.* **13**, 33 (2022).
- [4] M. Förstel, B. K. A. Jaeger, W. Schewe, P. H. A. Sporkhorst, and O. Dopfer, *Rev. Sci. Instrum.* **88**, 12 (2017).
- [5] T. Studemund, K. Pollow, M. Förstel, and O. Dopfer, submitted (2023).

Optical Spectra of the Smallest Silicon Carbide Cations

Kai Pollow¹, Taarna Studemund¹, Pierluigi Moretti¹, Alexander Breier¹, Otto Dopfer¹

¹ Institut für Optik und Atomare Physik, TU Berlin, Germany

Silicon carbide (SiC) compounds play a pivotal role in both astrophysics and semiconductor development. Silicon carbide grains have been detected in the vicinity of carbon-rich stars, where their properties greatly impact our understanding of dust evolution [1]. Moreover, in the field of materials science, SiC is widely recognized for its potential as a semiconductor material. In this contribution, we investigate the optical spectra of the smallest mixed silicon carbide cations, Si_nC_m^+ ($n+m=2-4$), to gain valuable insights into their geometric and electronic structure.

Using advanced spectroscopic techniques (electronic photodissociation of mass-selected ions in a quadrupole/time-of-flight tandem mass spectrometer coupled to a cryogenic laser vaporization source [2]), we experimentally determine the optical spectra of these fundamental Si_nC_m^+ cations [3,4]. Additionally, we compare our experimental findings with quantum chemical calculations.

By elucidating the optical spectra and electronic structure of these SiC cations, we provide crucial insights into their relevance in astrophysics, aiding in the understanding of dust evolution in the vicinity of C-rich stars. Furthermore, our findings contribute to the development of novel semiconductor materials, exploiting the bottom-up approach for enhanced material design and engineering.

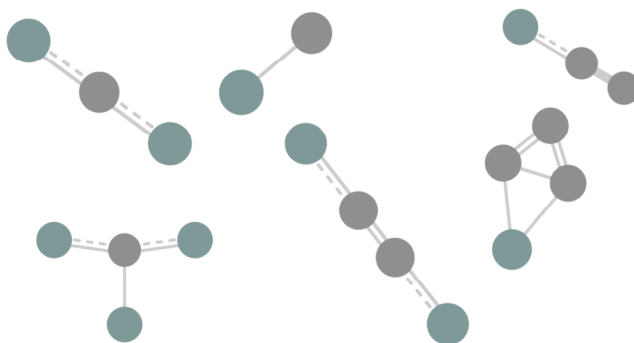


Figure 1: Ground state geometries for the smallest Si_nC_m^+ cations discussed in our contribution.

[1] Tao Chen et al., MNRAS **509**, 2022, 5231.

[2] M. Förstel, B.K.A. Jaeger, W. Schewe, P.H.A. Sporkhorst, O. Dopfer, Rev. Sci. Instrum. **88** (2017) 123110.

[3] T. Studemund, K. Pollow, S. Verhoeven, E. Mickein, O. Dopfer, M. Förstel, J. Phys. Chem. Lett. **13**, 7624 (2022).

[4] M. Förstel, R.G. Radloff, K.M. Pollow, T. Studemund, O. Dopfer, J. Mol. Spectr. **377**, 111427 (2021).

Collisional excitation and dissociation of dust molecules and nanoparticles by ion impacts in space and laboratories

Masato Nakamura¹, Itsuki Sakon,²

¹ College of Science and Technology, Nihon University, Japan

² Department of Astronomy, Graduate School of Science, University of Tokyo, Japan

Small particles called "interstellar dust" are responsible for dimming of celestial bodies from afar. Most of interstellar molecules are supposed to be produced on these dust surfaces. However, dust molecules are constantly being exposed to cosmic radiation. To investigate weathering of dust molecules in space, Sakon et al.'s [1] have performed a space exposure experiment. Laboratory-synthesized nanomaterials such as quenched carbonaceous materials (QCM), PAHs (Polycyclic aromatic hydrocarbons), fullerenes, and other nanoparticles were exposed in vacuum for one year on the International Space Station's Experiment Module "Kibo". Samples were collected and analyzed with IR microscopes. Furthermore, a series of comparative laboratory experiments have been performed to examine the metamorphism of samples. Both experiments suggested dehydrogenation takes place due to impacts by charged particles.

To investigate the mechanism of metamorphism, collisions of dust molecules with charged particles are simulated within the framework of classical dynamics. Among dust molecules, the CO is one of the most abundant molecules in interstellar space and the proton is a major component of the stellar (solar) winds. Collisional excitation and collision-induced dissociation (CID) by proton impact play important roles in the chemical evolution of interstellar molecules. The classical trajectory (CT) calculation and the sudden-limit model [2] are applied to simulate collision processes with charged particles. The excitation spectrum and threshold energy for dissociation are calculated. The calculation has been carried out also for other carbon-contained molecules such as CH and CN. To avoid large computational efforts, larger molecules and clusters are treated as assemblies of small fragment molecules. The dehydrogenation observed in the experiments are well reproduced.

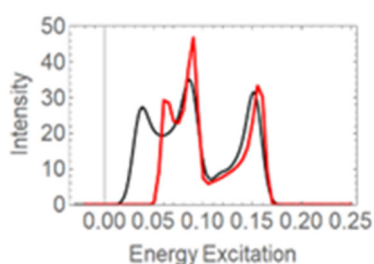


Figure 1: Calculated energy-transfer spectrum of CO fragment molecule by proton impacts at the incident energy of 27 eV. Red and black curves represent the results of the classical trajectory calculation and the sudden-limit model, respectively. Spectrum peaks correspond to elastic scatterings and binary collisions.

[1] I. Sakon et al., Journal of Japan Society for Aeronautical and Space Science, **66**, (2018) 381

[2] A. Ichimura and M. Nakamura, Phys. Rev. A **69**, (2004)022716

He-Tagged Action Spectroscopy of PAHs

Reider A. M.¹, Kappe M.¹, Schmidt M.¹, Reichegger J.¹, Scheier P.¹

¹ *Institute for ion physics and applied physics, University of Innsbruck, Technikerstraße 25, 6020 Innsbruck, Austria*

Measuring absorption spectra of cold molecules in the gas phase holds significant importance, particularly in identifying absorption characteristics in stellar spectra originating from molecular species in interstellar space. However, only a limited number of molecules have been exclusively associated with such absorption features thus far. Among the promising candidates are polycyclic aromatic hydrocarbons (PAHs). PAHs are a class of large, carbon-based molecules composed of fused aromatic rings, which exhibit enhanced stability compared to other molecular species of similar size and have been found abundantly in the interstellar medium [1].

With IR spectroscopy as a tool for finding the molecular fingerprints of molecules in the gas phase, we can gain valuable insight into the composition and specific identification of different PAH molecules as carriers of absorption features in the interstellar medium.

To do so, we utilise superfluid helium nanodroplets as an ultra-cold and inert reaction matrix for the formation of charged PAH clusters, where additional He attachment serves as a non-perturbing messenger for high-resolution IR absorption spectra [2].

This work is supported by the Austrian Science Fund, FWF via projects number P34563 and W1259.

[1] R. Gredel et al., A&A 530, A26, 2011

[2] P. Martini, et al. PRL 127, 26, 2021

A modified particle in a box model

Nima-Noah Nahvi¹, Parker Crandall¹, Otto Dopfer¹

¹ *Institut für Optik und Atomare Physik, TU Berlin, Germany*

Adamantane and diamantane are molecules with a cuboid carbon structure and are discussed to be possible carriers for diffuse interstellar bands. In recent work, the optical spectra of the adamantane and diamantane radical cations (Ada⁺, Dia⁺) were measured for the first time [1, 2]. Ada⁺ and Dia⁺ both have similar electronic $D_2(^2E_{(u)}) \leftarrow D_0(^2A_{1(g)})$ transitions at 1.853 and 1.710 eV, respectively. In this work, we try to explain the energetic red shift between both transitions with a sophisticated particle-in-a-box model.

It turns out that one does not get reliable results using the classical particle-in-a-box model. Therein, we modify this simple model by adding an interior infinite potential into a small region in the box. The stationary Schrödinger equation for the modified model is solved analytically with the help of the Python library SymPy [3]. With the modified model, we are able to calculate the red shift of the electronic transitions from Ada⁺ to Dia⁺. Furthermore, it is possible to estimate the carbon valence electron radius. We discuss the effect of electron-donating and electron-withdrawing substituents. Lastly, we apply the model to similar cuboid molecules like cubane.

[1] P. Crandall et al., The Astrophysical Journal Letters **900** (2020) L20.

[2] P. Crandall et al., The Astrophysical Journal **940** (2022) 104.

[3] A. Meurer et al., PeerJ Computer Science **3:e103** (2017).

Blackbody infrared radiative dissociation and master equation modelling of hydrated peroxycarbonate radical anions

Magdalena Salzburger¹, Michael Hütter, Milan Ončák¹, Christian van der Linde¹, Martin K. Beyer¹

¹*Institut für Ionenphysik und Angewandte Physik, Universität Innsbruck, Austria*

If molecular clusters are stored for several seconds under ultra-high vacuum conditions, dissociation due to ambient blackbody radiation can be observed. Thereby, absorption of blackbody infrared photons leads to vibrational excitation and eventually to dissociation of the cluster (see Figure 1). This process, known as blackbody infrared radiative dissociation (BIRD), can be simulated with master equation modelling, predicting temperature dependent dissociation rates for given dissociation energies. By comparing rates from master equation modelling with experimental rates, dissociation energies of the molecular clusters can be determined. For reliable energetics, however, the temperature dependence of the dissociation rates must be modelled correctly, which also requires BIRD experiments over a wide temperature range.

Master equation modelling is particularly difficult for water clusters, as the water molecule is mobile, and often several low-lying isomers are populated. Recently, we developed a new multiple well approach for master equation modelling, where multiple isomers are taken into account. We showed for hydrated carbonate clusters [1], that this multiple well approach can improve the accuracy of the energetics. Now, the new approach is tested on hydrated $\text{CO}_4^{\bullet-}$. Experimentally, we observe for $\text{CO}_4^{\bullet-}(\text{H}_2\text{O})$ loss of water and for $\text{CO}_4^{\bullet-}(\text{H}_2\text{O})_2$ loss of water as well as loss of CO_2 . This additional channel and the growing number of local minima increase the complexity of the master equation model. Different further improvements for the master equation model are tested, including the description of a roaming water molecule as a particle in a box and the consideration of tight transition states that connect selected isomers.

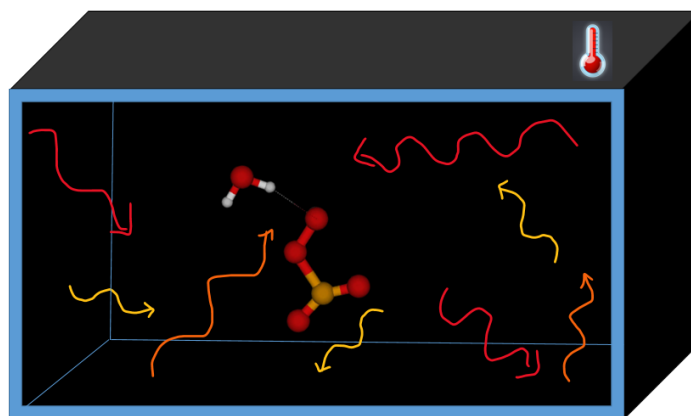


Figure 1: Blackbody infrared radiative dissociation of hydrated peroxycarbonate radical anions

[1] M. Salzburger, M. Ončák, C. van der Linde, M.K. Beyer, J. Am. Chem. Soc. **144**, **47** (2022) 21485–21493

Photochemistry of Pyruvate Embedded in Sea Salt Clusters

Sarah Madener¹, Ethan M. Cunningham¹, Jessica C. Hartmann¹, Barbara Obwallner¹, Christian van der Linde¹, Milan Ončák¹ and Martin K. Beyer¹

¹ *Institut für Ionenphysik und Angewandte Physik, Universität Innsbruck, Austria*

Marine aerosol is one of the most important naturally occurring aerosol systems, due to the large coverage of Earth's surface by the ocean. Aerosols in general have a great influence on Earth's climate through their direct and indirect interaction with solar radiation. Besides inorganic salts such as sodium chloride, also organic material such as acids, terpenes, lipids and saccharides are incorporated in marine aerosols. Through the exposure to sunlight, these organic materials can undergo photochemical processing and, as a consequence, they can produce highly reactive species, for example OH· radicals. Pyruvic acid is one of the most abundant α -carboxylic acids in the atmosphere. In this work, the photochemistry of pyruvate in a salt environment has been investigated. Previous work on the photochemistry of glyoxylate has shown that the acid undergoes photolysis leading to non - stoichiometric fragments that incorporate a $\text{CO}_2^{\cdot-}$ radical anion [1]. In this work, we investigate whether other acids also undergo a photolysis process, when embedded in a salt environment, or if glyoxylate is a special case.

All spectra for this work were recorded using a 9.4T FTICR mass spectrometer and a UV/VIS OPO laser system. The measured wavelength range lies between 210 and 400 nm, including the environmentally relevant actinic region from 290 - 400 nm. In total, two systems were measured, one being pure sodium pyruvate clusters $\text{Na}_n(\text{CH}_3\text{COCOO})_{n-1}^+$, $n = 4, 5$ and the other one being sodium chloride clusters where one chloride ion is substituted by pyruvate $\text{Na}_n\text{Cl}_{n-2}(\text{CH}_3\text{COCOO})^+$, $n = 4 - 8$. For two cluster sizes in the sodium chloride system and for both pure sodium pyruvate clusters, non - stoichiometric fragments were observed. However, despite the fact that photolysis is the main degradation pathway in the atmosphere for pyruvic acid [2], only traces of this phenomenon could be found in the experiments conducted here. This suggests that the salt environment suppresses the photolysis.

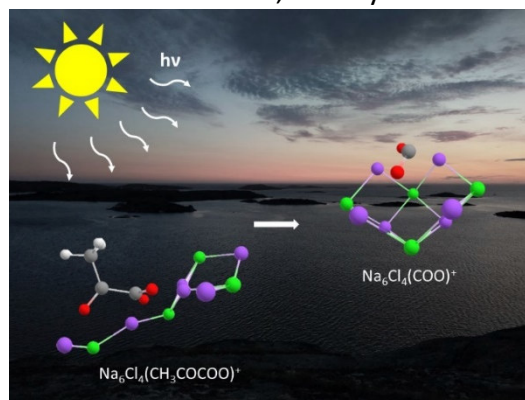


Figure 5: Artistic representation of the pyruvate photolysis

- [1] N.K. Bersenkovitsch, M. Ončák, C. van der Linde, A. Herburger and M. K. Beyer, *Phys Chem Chem Phys* **20** (2018) 8143.
- [2] A.E. Reed Harris, M. Cazaunau, A. Gratien, E. Pangui, J. -F. Doussin and V. Vaida, *J Phys Chem A* **121** (2017) 8348.

Searching for the Origin of Magic Numbers Amongst Sodium Chloride Clusters

J. C. Hartmann, C. van der Linde, M. Ončák, M. K. Beyer

*Institut für Ionenphysik und Angewandte Physik, Universität Innsbruck,
Technikerstr. 25, 6020 Innsbruck, Österreich*

As one of the main components of sea salt aerosols, sodium chloride is involved in numerous atmospheric processes such as cloud formation and photochemical as well as chemical reactions, significantly affecting the climate on Earth. [1] Gas phase clusters are ideal models to study fundamental physical and chemical properties of sodium chloride. According to previous studies [2], these properties are significantly affected by the cluster size. Of particular interest are magic cluster sizes, which exhibit high intensities in mass spectra.

In order to understand this size dependency, we performed a combined experimental-theoretical study, focusing on the relative stability as well as their dissociation behavior. In contrast to earlier studies [3], our calculations show that the binding energy of a single NaCl unit or the respective ion (Na^+ or Cl^-) to the smallest anionic $(\text{NaCl})_x\text{Cl}^-$ and cationic $(\text{NaCl})_x\text{Na}^+$ magic cluster with $x = 4$ is lower than that of the neighboring cluster sizes and thus cannot be the reason for the special stability.

Sustained off-resonance irradiation collision-induced dissociation (SORI CID) experiments performed in a Fourier transform ion cyclotron resonance mass spectrometer (FT-ICR MS) reveal, that the loss of neutral clusters $(\text{NaCl})_x$ with even x (especially $x = 2$ and $x = 4$) is in most cases more favorable than the loss of single NaCl units, as assumed so far [2]. This can be explained by the calculated high stability of neutral clusters $(\text{NaCl})_x$ with even x , whose minimum energy structures are cubic, resembling the sodium chloride crystal lattice.

Analysis of the density of states as well as the Rice-Ramsperger-Kassel-Marcus (RRKM) rates for the anionic and cationic magic cluster with $x = 4$ and the neighboring cluster sizes with $x = 3$ and $x = 5$ yields an explanation for the high stability of the smallest magic clusters. Our findings emphasize the importance of considering the kinetics of the cluster dissociation, not only the respective energetics.

[1] N. K. Bersenkovitsch, M. Ončák, C. van der Linde, A. Herburger, M. K. Beyer, Phys. Chem. Chem. Phys. **20** (2018) 8143-8151

[2] T. D. Schachel, H. Metwally, V. Popa, L. Konermann, J. Am. Soc. Mass Spectrom. **27** (2016) 1846-1854

[3] M. Lintuluoto, J. Mol. Struct. - THEOCHEM **540** (2001) 177-192

2D Study of Nitrogen Cluster Growth by Rayleigh Scattering

Wolfgang Christen,

Eduardo Garcia Alonso, Bora Bulut, Young Chae Chung, Maria Fernanda Valle Sejo

Department of Chemistry, Humboldt University, Germany

Nucleation, condensation and the formation of nanoparticles in a gaseous environment are fundamental issues. A better understanding of these processes is useful e.g. for an improved comprehension of atmospheric processes such as cloud formation.

Our experimental capabilities allow the routine generation of nanoparticles consisting of atmospherically relevant molecules, such as $(\text{CH}_4)_n$, $(\text{C}_3\text{H}_8)_n$, $(\text{CO})_n$, $(\text{CO}_2)_n$, $(\text{H}_2\text{O})_n$, $(\text{N}_2)_n$, $(\text{O}_2)_n$, etc. An important characteristic is the size, n , of the particles, which we can tune continuously from the individual molecule up to particles with a radius of about 10 nm, using a pulsed supersonic jet obtained by the adiabatic expansion of a gas under very high pressure into vacuum. Until recently, we had to estimate the mean size of the generated particles using empirical scaling laws [1]. These may not be accurate, valid at high source densities, or available at all for the system of interest. Hence, we have complemented our experiment by an advanced optical setup for laser-induced Rayleigh scattering [2].

In this contribution we present a comprehensive experimental investigation of the generation of nitrogen nanoparticles by a pulsed high-pressure supersonic jet expansion of the pure gas through a parabolic nozzle into vacuum. In this study source pressure is varied between 2 MPa and 11 MPa and source temperature between 230 K and 310 K. The mean particle size is characterized by time and space resolved Rayleigh scattering measurements, in combination with time resolved residual gas pressure readings. One of the goals of this investigation is to estimate the distance where particle growth ceases. Because of the small scattering cross section Rayleigh signals typically are weak and thus in almost all previous studies (for N_2 : [3,4]) the supersonic jet is probed at very short distances where particles still might grow. Hence, in this study Rayleigh data are obtained for different nozzle-laser distances. In addition, the dependence of the mean particle size on stagnation pressure and stagnation temperature is discussed with respect to the prediction of Hagena [1].

[1] O. F. Hagena, Rev. Sci. Instrum. **63** (1992) 2374

[2] W. Christen, M. M. Kermani, C. Monte, in preparation

[3] K. C. Gupta, N. Jha, P. Deb, D. R. Mishra, J. K. Fuloria, J. Appl. Phys. **118** (2015) 114308

[4] A. Murakami, J. Miyazawa, H. Tsuchiya, T. Morisaki, N. Tsutagawa, Y. Narushima, R. Sakamoto, H. Yamada, Plasma Fusion Res. **5** (2010) S1032

Kinetic Energy Released in the Vibrational Autodetachment of Sulfur Hexafluoride Anion

Bruno Concina, Guillaume Montagne, Serge Martin, Christian Bordas

*Institut Lumière Matière, Université de Lyon, Université Claude Bernard Lyon 1, CNRS,
F-69622 Villeurbanne, France
bruno.concina@univ-lyon1.fr*

This work is part of a long term study on the delayed electron emission of negatively charged molecules and small clusters, interpreted as thermionic emission [1]. Our approach is based on the measurement in a velocity map imaging (VMI) spectrometer of the delayed electron kinetic energy release distribution (KERD) and on the development of statistical modeling relying on the detailed balance principle.

Sulfur hexafluoride SF_6 is of particular interest for industry: it is widely used as a gaseous dielectric and in plasma etching. This molecule is also known to be a greenhouse gas with an extremely long lifetime in the Earth's atmosphere, which reinforces the interest of studying the formation and the decay of the SF_6^- anion.

The KERD in the vibrational autodetachment (VAD) from SF_6^- has been measured in a velocity map imaging spectrometer for delays in the range of few tens of microseconds [2]. The experimental KERD is analyzed within the framework of the detailed balance: first using the standard Langevin model and subsequently using a more refined and realistic model based on the experimental attachment cross section. A discussion on the processes involved in the attachment and the VAD is presented based on an empirical fit of the attachment cross section. The lifetime derived from the model is in good agreement with the experimental time window, strengthening the theoretical approach for this model system.

[1] B. Concina and C. Bordas, J. Phys. Chem. A **126** (2022) 7442

[2] B. Concina, G. Montagne, S. Martin, and C. Bordas, J. Chem. Phys. **154** (2021) 234306

Ionization and Dissociation Energies of Dysprosium Monoxide, DyO

Sascha Schaller, Johannes Seifert, Giacomo Valtolina, Boris G. Sartakov, André Fielicke, Gerard Meijer

Fritz-Haber-Institut der Max-Planck-Gesellschaft, Berlin, Germany

Understanding of lanthanide oxides (LnO) is challenging due to their complex electronic structure, which results from the open 4f (except Lu) and 5d valence shells of the Ln atoms. A motivation for the study of such molecules is the chemi-ionization reaction: $\text{Ln} + \text{O} \rightarrow \text{LnO}^+ + \text{e}^-$ [1]. This associative ionization reaction requires that the ionization energy (IE) of the molecule is lower than its Ln-O binding energy (D_0) and thus exothermic ($\Delta H_0 = \text{IE} - D_0 < 0$). Notably, such formation reaction can proceed also in extremely dilute environments, like the interstellar medium, as stabilization of the dimer is reached without the need of third body collisions or radiative cooling. This is comparably unusual for small diatomic molecules. So far, associative ionization has already been observed in the oxidation of a number of transition and lanthanide metals, including praseodymium, neodymium, samarium, and gadolinium.

Previous reports for the oxidation of dysprosium atoms are contradictory. Thermochemical studies and electron impact ionization led to estimates for IE and D_0 of DyO, but the values are associated with large uncertainties. Furthermore, a recent measurement of $D_0(\text{DyO}^+)$ implies $\Delta H_0 = +0.33(2)$ eV, however, this conflicts with the earlier reported values for IE and D_0 [2].

Here we report on the characterization DyO and DyO^+ in a supersonic molecular beam by applying a variety of spectroscopic approaches using different REMPI and PFI schemes, MATI, and (V)UV single-photon ionization. Isotope specific excitation schemes allow to obtain rotationally resolved spectra, and several Rydberg-series converging to the ionization limits of different rotational states of DyO^+ . The Rydberg series can be clearly assigned starting with the lowest $J=7.5$ state. Beside these long-living Rydberg molecules, a number of short-lived molecular states are found. From the spectroscopic data obtained for the fermionic ^{161}DyO and the bosonic ^{162}DyO , the values of IE and D_0 are determined with a high precision. This leads to the conclusion that the reaction $\text{Dy} + \text{O} \rightarrow \text{DyO}^+ + \text{e}^-$ clearly proceeds exothermic.

[1] N. S. Shuman et al., Chem. Rev. **115** (2015) 4542

[2] M. Ghiassee et al., J. Phys. Chem. A **127** (2023), 169

Size dependent structures of platinum oxide cluster cations and anions studied by ion mobility-mass spectrometry

Yuto Nakajima, Toshiaki Nagata, Keijiro Ohshimo, Fuminori Misaizu

Department of Chemistry, Graduate School of Science, Tohoku University, Japan

Platinum clusters are potential candidates for new redox catalysts because bulk-phase platinum is widely used as such catalysts. For instance, Pt_{19}^- is a promising candidate as a catalyst to promote O_2 reduction reactions forming H_2O in fuel cells because of the higher reactivity of Pt_{19}^- than that of bulk-phase or nanosized Pt [1]. Atomic-level structures of clusters are essential factors for size-dependent catalytic activities. Thus, it is vital to elucidate how cluster structures change with size for utilizing clusters as novel redox catalysts. Structures of gas-phase metal oxide clusters provide a model for understanding the detailed mechanism of redox reactions catalyzed by the clusters, such as the dynamics of O atoms through reactions. In this study, we revealed the structures of platinum oxide cluster cations and anions ($\text{Pt}_n\text{O}_n^{+/-}$) depending on their sizes ($n = 4-7$) by using ion mobility-mass spectrometry combined with quantum chemical calculations [2]. $\text{Pt}_n\text{O}_m^{+/-}$ cluster ions were generated by laser vaporization of Pt in the presence of O_2 mixed in the carrier gas. The generated cluster ions were injected into an ion-drift cell, where collision cross sections (CCSs) of the clusters with He atoms were measured. The ions which exited from the ion-drift cell were analyzed by mass spectrometry. Candidate structures and energies of the $\text{Pt}_n\text{O}_n^{+/-}$ cluster ions were obtained by DFT calculations (B3LYP/Pt: SDD, O: 6-311+G(2d)). Geometrical structures of the ions were assigned by comparison of the experimental CCSs with the theoretical values. The observed cluster ions had predominant compositions of $n:m = 1:1$ both for cations and anions. The CCSs of $\text{Pt}_n\text{O}_n^{+/-}$ increased monotonically with the cluster size for $n = 4-7$, as shown in **Fig. 1**. For the cluster cations, Pt_4O_4^+ was assigned to a planar structure from its CCS. For $n = 5$ and larger Pt_nO_n^+ , the experimental CCSs agreed better with three-dimensional structures than with planar isomers. Thus, the structures of cationic Pt_nO_n^+ change from planar to three-dimensional structures at $n = 5$. On the other hand, theoretical CCSs of planar structures in anionic Pt_nO_n^- consistently agreed with the experimental results for $n = 4-7$. These results suggest that Pt_nO_n^- anions prefer bulky planar structures compared to Pt_nO_n^+ cations.

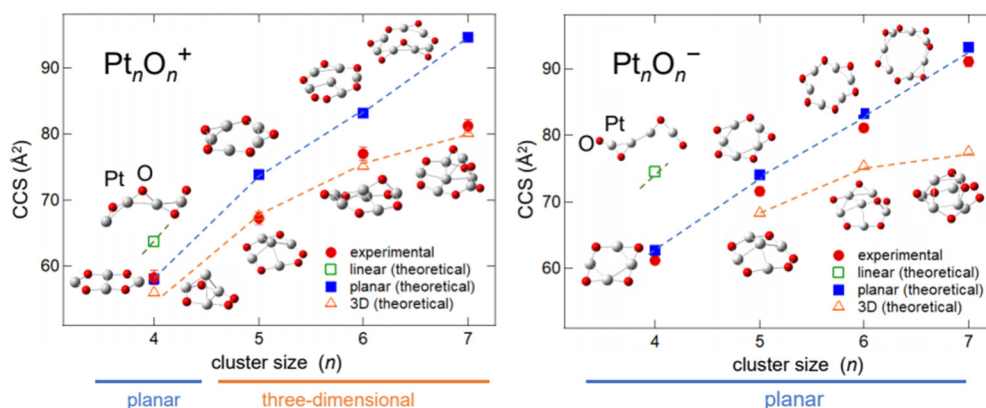


Figure 1: Experimental and theoretical collision cross sections (CCSs) of $\text{Pt}_n\text{O}_n^{+/-}$.

- [1] T. Imaoka, H. Kitazawa, W.-J. Chun, K. Yamamoto, *Angew. Chem. Int. Ed.* **54** (2015) 9810.
- [2] Y. Nakajima, M. A. Latif, T. Nagata, K. Ohshimo, F. Misaizu, *J. Phys. Chem. A* **127** (2023) 3570.

IR spectra and structures of saturated ruthenium cluster carbonyl cations $\text{Ru}_n(\text{CO})_m^+$ ($n=1-6$)

David Yubero Valdivielso, Christian Kerpel, Wieland Schöllkopf, Gerard Meijer and
André Fielicke

Fritz-Haber-Institut der Max-Planck-Gesellschaft, Berlin, Germany

Metal cluster carbonyls have been an important class of substances for developing a profound understanding of the binding in polynuclear coordination compounds.[1] Ionic carbonyls in the gas phase have the advantage that their composition can be precisely determined by means of mass spectrometry. By applying infrared multiple photon dissociation (IR-MPD) spectroscopy, a size-selective structural characterization of such metal cluster complexes becomes possible.[2]

Gas-phase synthesis of cationic Ru carbonyls has been reported before for the tetra to hexanuclear carbonyls of Ru and their structures as derived via application of the Wade-Mingos rules have been compared to those predicted by means of density functional theory calculations.[3] Here, we substantiate these structural assignments by comparing gas-phase IR-MPD spectra observed for the full series of saturated cationic Ru carbonyls $\text{Ru}(\text{CO})_5^+$, $\text{Ru}_2(\text{CO})_9^+$, $\text{Ru}_3(\text{CO})_{12}^+$, $\text{Ru}_4(\text{CO})_{14}^+$, $\text{Ru}_5(\text{CO})_{16}^+$ and $\text{Ru}_6(\text{CO})_{18}$ with IR spectra calculated using DFT for the putative ground-state isomers of these carbonyls. A multitude of differently activated CO ligands is identified in these cationic cluster carbonyls, reaching from terminal, over non-symmetrically bridging (semi-bridging) ligands with varying degrees of interaction to additional Ru atoms towards symmetrically bridging CO ligands.

- [1] D. M. P. Mingos and D. J. Wales, *Introduction to Cluster Chemistry*, Prentice-Hall, London, 1990.
- [2] A. Fielicke, *Chem. Soc. Rev.* **2023**, 52, 3778-3841.
- [3] S. M. Lang, S. U. Fortig, T. M. Bernhardt, M. Krstic and V. Bonacic-Koutecky, *J. Phys. Chem. A*, 2014, **118**, 8356-8359.

2D Raft Structures of Au Nanoclusters ($N < 100$) Grown from Atoms on Amorphous Carbon: Experiment and Theory

Sean Lethbridge¹, James E. McCormack¹, Thomas JA Slater², Theodoros Pavloudis¹, Richard E Palmer¹

¹ *Nanomaterials Lab, Swansea University, United Kingdom*

² *Cardiff Catalysis Institute, Cardiff University, United Kingdom*

The question of metastability always underpins nanostructure fabrication. It is highly pertinent to the functional performance of nanomaterials, e.g., the evolution of nanocatalyst particles is a central issue in their activity/selectivity/durability. Here we explore the atomic structure of Au clusters (1-100 atoms) assembled from gold atoms sputtered onto amorphous carbon TEM supports, for comparison with clusters deposited from the beam. We find persistent evidence of 2D monolayer rafts competing with 3D cluster structures to at least size $N=60$ atoms and this is consistent with new DFT theory calculations.

The nuclearity and atomic structure were determined by aberration-corrected scanning transmission electron microscopy (STEM) in the high-angle annular dark field (HAADF) mode [1]. The cluster size measurements employed a two-step image analysis process, whereby the intensity of single atoms was determined to calibrate the intensity of the clusters themselves. The relationships between cluster size and cluster structure were obtained.

The main result from the analysis of the grown Au nanoparticles with size < 100 atoms is the common formation of 2D rafts (typically one atom high). DFT calculations suggest the 2D structures are energetically stabilized by the graphene surface in the size regime up to at least 60 atoms, so that they compete well with 3D structures, which are also observed on the surface. These 2D cluster structures are expected to behave quite differently from a catalytic point of view than the competing 3D forms.

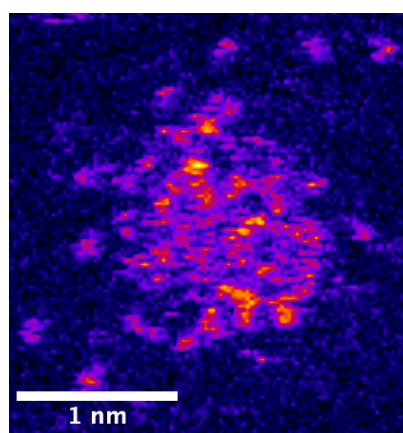


Figure 1: ac-STEM image of a Au_{54} raft structure at 8Mx magnification assembled from Au atoms on amorphous carbon.

[1] D. Foster, R. Ferrando, R. E. Palmer, *Nature Comms.* 9 1 (2018). doi: 10.1038/s41467-018-03794-9

Graph Neural Network Accelerate Cluster Structure Searching

Linwei Sai¹, Li Fu,² Jijun Zhao²

¹ Department of Science, Hohai University, China

² Department of Physics, Dalian University of Technology, China

Determining cluster structure requires finding the lowest energy structure from a large number of isomers. First-principles calculations are time-consuming to optimize isomers and calculate energy, which is the bottleneck of cluster structure search. Clusters or molecular structures are naturally suitable for description by graph networks. The authors developed a graph neural network [1] and introduced an attention mechanism to sum the effects of neighboring atoms on the central atom, thereby learning the local structure of clusters. The network can accurately predict the binding energy and force of the cluster. Combined with the BFGS local optimization algorithm, the efficient local optimization of cluster structure is realized, which is at least 1 order of magnitude faster than first-principles calculation. Using Ag₁₆, Ag₂₀, and Ag₂₄ as training sets, the authors successfully searched and discovered some new Ag₁₄₋₂₆ minimum energy structures [2]. The network can also predict the HOMO and HOMO-LUMO energy gap properties of clusters.

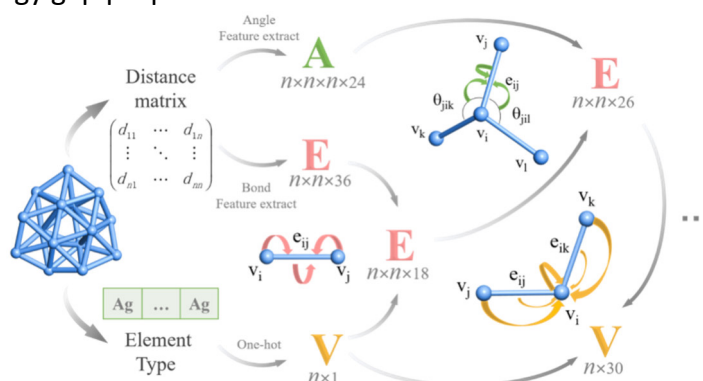


Figure 1: Feature extraction and graph convolution operations.

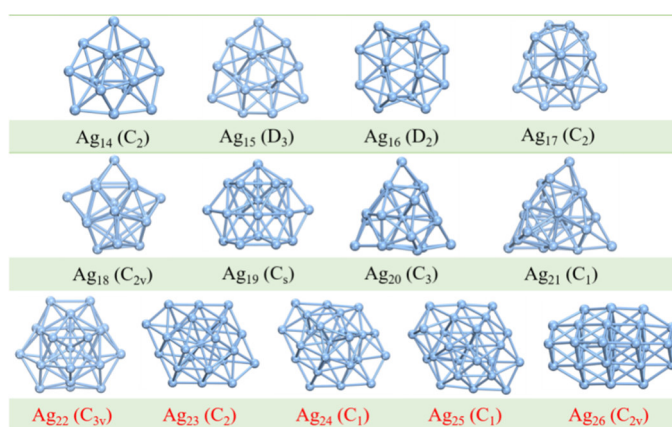


Figure 2. Lowest-energy structures of Ag_n clusters (14 ≤ n ≤ 26). The point group symmetry is given in parenthesis. Red color highlights the newly found lowest-energy structures.

[1] L. W. Sai, L. Fu, Q. Y. Du, J. J. Zhao, Front. Phys. **1** (2023) 13306.

Imaging the Various Shapes of Large Rare Gas Clusters

Mario Sauppe¹, Andre Al Haddad², Alessandro Colombo¹, Linos Hecht¹, Gregor Knopp², Katharina Kolatzki¹, Bruno Langbehn³, Caner Polat¹, Kirsten Schnorr², Zhibin Sun², Paul Tümmeler⁴, Carl Frederic Ussling¹, Simon Wächter¹, Alex Weitnauer¹, Julian Zimmermann¹, Maha Zuod¹, Thomas Möller³, Christoph Bostedt², and Daniela Rupp¹

¹ *Laboratory for Solid State Physics, ETH Zurich, Switzerland*

² *Paul Scherrer Institute, Switzerland*

³ *Institute of Optics and Atomic Physics, Technical University of Berlin, Germany*

⁴ *Institut für Physik, Universität Rostock, Germany*

Rare-gas clusters often serve as model systems in studies of the interaction of high-intensity lasers with matter. They are comparatively easy to produce, their average size can be tuned, and their electronic structure is quite simple due to van der Waals-bonded atoms, making them readily accessible to theoretical and experimental approaches. The intense pulses of X-ray free-electron lasers (FELs) can be used to determine the shape of nanoscale particles by coherent diffractive imaging (CDI). Previous CDI experiments on large rare gas clusters (100 nm) produced in a supersonic gas expansion showed rather complex shapes such as agglomerates of two or more spherical subclusters [1, 2], i.e., strongly deviating from ideal icosahedra known for smaller clusters [3]. To study the shapes of large rare gas clusters with high spatial resolution and to better understand their growth processes, we performed a CDI experiment with argon clusters at the new Maloja endstation at SwissFEL [4]. The clusters were created in a supersonic gas expansion with a 100 μm nozzle and imaged at photon energies of up to 1 keV (1.24 nm). The majority of the clusters are spherical, but we also find other shapes indicative of agglomeration. Of particular interest are specimens containing small clusters connected to a large cluster only by a thin bridge. An example of this previously unknown phenomenon is shown in Fig. 1.

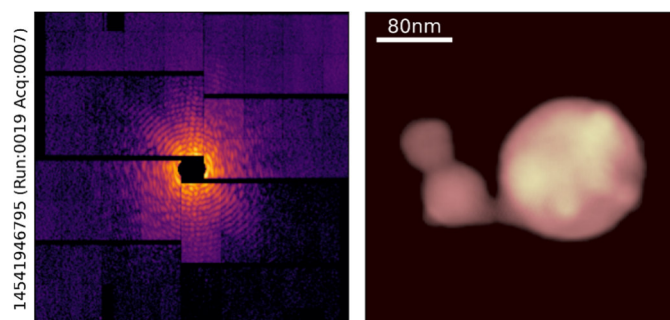


Figure 1: Left CDI pattern and right corresponding real-space reconstruction of an argon cluster agglomerate, produced at 40 bar and 160 K.

- [1] D. Rupp et al., *New Journal of Physics* **14** (2012) 055016
- [2] D. Rupp et al., *The Journal of Chemical Physics* **141** (2014) 044306
- [3] H. Haberland, "Rare Gas Clusters" in *Clusters of Atoms and Molecules* (1994), Springer Series in Chemical Physics 52, Springer Berlin, Heidelberg
- [4] Z. Sun et al., *Chimia* **76** (2022) 529

Pivotal role of the B₁₂-core in the structural evolution of B₅₂–B₆₄ clusters

Xue Wu¹, Linwei Sai,² Jijun Zhao³

¹ State Key Laboratory of Metastable Materials Science & Technology and Key Laboratory for Microstructural Material Physics of Hebei Province, School of Science, Yanshan University, Qinhuangdao 066004, China

² School of Science, Hohai University, Changzhou 213022, China

³ Key Laboratory of Materials Modification by Laser, Ion and Electron Beams (Dalian University of Technology), Ministry of Education, Dalian 116024, China

An icosahedral B₁₂ cage is a basic building block of various boron allotropes, and it also plays a vital role in augmenting the stability of fullerene-like boron nanoclusters. However, the evolution of compact core-shell structures is still a puzzle. Using a genetic algorithm combined with density functional theory calculations, we have performed a global search for the lowest-energy structures of B_n clusters with $n = 52$ – 64 , which reveals that bilayer and core-shell motifs frequently alternate as the ground state. Their structural stability is assessed, and the competition mechanism between various patterns is also elucidated. More interestingly, an unprecedented icosahedral B₁₂-core half-covered structure is identified at B₅₈, which bridges the gap between the smallest core-shell B₄@B₄₂ and the complete core-shell B₁₂@B₈₄ cluster. Our findings provide valuable insights into the bonding pattern and growth behavior of medium-sized boron clusters, which facilitate the experimental synthesis of boron nanostructures.

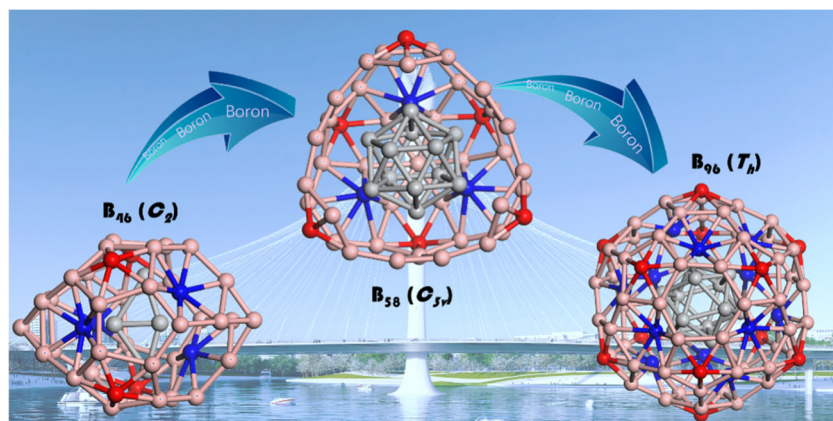


Figure 1: An unprecedented icosahedral B₁₂-core half-covered structure is identified at B₅₈, which bridges the gap between the smallest core-shell B₄@B₄₂ and the complete core-shell B₁₂@B₈₄ cluster.

[1] X Wu, R Liao, X Liang, L Sai, Y Liu, G Yang and J Zhao, 2023, DOI: 10.1039/d3nr01310c

π - π Interactions in Host-Guest Complexes Revealed by Cryogenic Ion Mobility-Mass Spectrometry

Ryosuke Ito, Kejiro Ohshimo, Fuminori Misaizu

Department of Chemistry, Graduate School of Science, Tohoku University, Japan

Crown ethers play an important role in the field of host-guest chemistry owing to their ability to encapsulate the guest ions efficiently and selectively. We previously studied the conformations of dibenzo-24-crown-8 (DB24C8) (Fig. 1a) complexes with alkali metal ions using ion mobility-mass spectrometry (IM-MS) and confirmed the coexistence of two conformers, closed and open [1]. In $\text{Na}^+(\text{DB24C8})$, the abundance ratio of the conformers was closed:open = 0.25:1 at 86 K [1]. In dinaphtho-24-crown-8 (DN24C8) (Fig. 1b), it is expected that the closed conformer should be more strongly stabilized due to the stronger π - π interactions between aromatic rings. In this study, conformers of DN24C8 complexes with Na^+ and K^+ ions were separated by cryogenic IM-MS, and their structures were identified to investigate the effect of π - π interactions on guest ion recognition by crown ethers.

Gas-phase metal ion-crown ether complexes were sampled by electrospray ionization (ESI) method using methanol solutions of DB24C8 or DN24C8 and inorganic salt (NaCl, KCl). Ions were then delivered to a cryogenic ion drift tube for conformer separation and mass-analyzed by a reflectron-type time-of-flight mass spectrometer. We performed all IM-MS experiments under the presence of He buffer gas in the ion drift tube. By evaluating the drift velocity in the drift tube, we determined the experimental collision cross section (CCS) for each complex. Using quantum chemical calculations, both theoretical CCSs and relative energies were obtained for candidate structures. Conformations of the complexes were assigned by comparing the experimental and theoretical CCSs, in addition to the consideration of the stabilities of the candidate structures.

As a result, two types of conformers, closed and open, were separately observed at 86 K (Fig. 1c,d). These two conformers have different distances between the two naphthalene rings of the DN24C8. The abundance ratio of the conformers was closed:open = 1:0.15 at 86 K for $\text{Na}^+(\text{DN24C8})$. Namely, the relative abundance ratio of the closed conformer was larger than that for $\text{Na}^+(\text{DB24C8})$. In the quantum chemical calculations visualizing the extent of the π - π interactions, DN24C8 complexes were found to have wider regions of π - π interactions than the DB24C8 complexes. Therefore, the closed conformations were concluded to be predominant for the DN24C8 complexes due to the stronger π - π interactions.

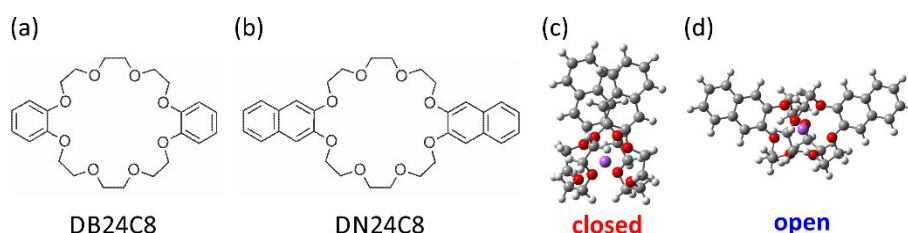


Figure 1: Formulas of (a) DB24C8 and (b) DN24C8, and stable structures of (c) closed and (d) open conformers of $\text{Na}^+(\text{DN24C8})$ calculated at the M05-2X/6-311++G(d,p) level of theory.

[1] K. Ohshimo, X. He, R. Ito, K. Tsunoda, S. Tainaka, F. Misaizu, EPJ Tech. Instrum. **10** (2023) 11.

How Photoelectron Spectroscopy on Ag Nanoparticles Resolved Old Controversy of Materials Science

M.Tchaplyguine¹, G. Öhrwall¹, M.Danilson^{1,2}, S.Appelfeller¹, O.Björneholm³

¹MAX-IV, Lund University, Lund, Sweden

²Tallinn University of Technology, Tallinn, Estonia

³Department of Physics, Uppsala University, Uppsala, Sweden

The change of the electronic structure in metal atoms upon oxidation manifests itself not only in the valence, but also in a characteristic binding energy shift of the *core* electron levels – the so-called oxide shift. The positive charge on the metal atom in the oxide makes it more difficult to remove a core electron from it than from the corresponding metallic substance. In other words, the binding energy of a core electron becomes higher in oxides, and thus the oxide shift is typically positive. This was experimentally confirmed by x-ray photoelectron spectroscopy (XPS) for nearly all metals, but not for silver. Since the pioneering work of G.Schön in 1973 [1], the oxide shift for the Ag 3d core-level was again and again reported to be negative [2,3]. Moreover, the Ag 3d levels of the Ag(I)- and Ag(III)-oxides were not only detected lower in binding energy than for the metal but also close to each other– separated by less than 0.5 eV –against the expectations for these significantly differing substances.

The current work addressed the old controversy of the oxide shifts for silver in an XPS study on free and deposited metallic-silver and silver-oxide nanoparticles (NPs). A magnetron-sputtering-based vapour-aggregation source was used to fabricate the particles as free in a beam [4]. First, these particles were probed by XPS “on-the-fly”, in the beam, and then they were deposited and again characterized by XPS- directly after the deposition.

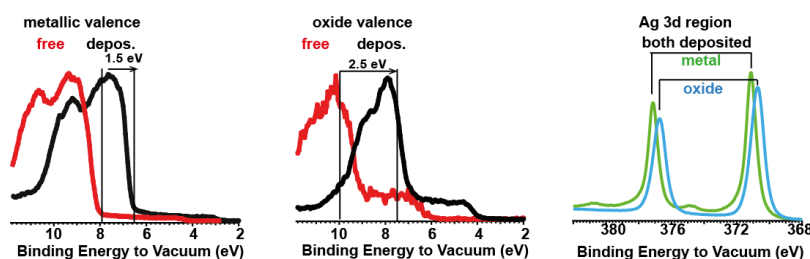


Figure 1. left-valence spectra for metallic-Ag NPs, free and deposited; centre -valence spectra for Ag-oxide NPs, free and deposited; right – Ag 3d spectra for deposited metallic-Ag and Ag-oxide NPs as recorded.

The ability to record both the free-particle spectra calibrated to the vacuum level and the deposited-particle spectra referenced to the Fermi level of a silicon substrate allowed establishing the difference in the apparent binding energy for the two types of calibration. Due to the Fermi level alignment upon deposition, the valence levels of the metallic Ag and Ag oxide particles moved down in binding energy by ~1.5 eV and ~2.5 eV, respectively (Fig.1). Correspondingly, all the core-levels, including Ag 3d, were pulled down differently for the metal and for the oxide. In its turn, it led to the Ag 3d level appearing at an apparently lower binding energy than its counterpart in metal particles. On the vacuum-referenced *absolute* binding energy, accessible for free particles, the oxide Ag 3d level *is* higher, as expected, as it is for other metals, and as observed in our work [5].

[1] G.Schön, Acta Chem. Scand. 27 (1973) 2623.

[2] G.B.Hoflund, Z.F.Hazos, G.N.Salaita, Phys.Rev.B 62 (2000) 11126.

[3] D.Lützenkirchen-Hecht, Surf.Scie.Spect.18 (2011) 96; D.Lützenkirchen-Hecht, Surf.Scie.Spect.18 (2011) 102.

[4] M.Tchaplyguine, M.-H.Mikkilä, O.Björneholm. In 21st Century Nanoscience–A Handbook, K.Sattler (2020).

[5] E. Tzomos, M.-H. Mikkilä, G. Öhrwall, O. Björneholm, M. Tchaplyguine, Surf.Scie. 733 (2023) 122307.

Effect of nanoparticle size on Boron-Doped Transition Metals

Jie Zhao¹, Fernando Buendia-Zamudio,¹ Sergey M. Kozlov¹

¹ Department of Chemical and Biomolecular Engineering, National University of Singapore, Singapore

Through the reduction of metal salts with borohydride, boron can be incorporated into transition metals. The profound influence of boron on the catalytic properties of surfaces, such as Pd and Pt, has been well-established. However, the geometric, electronic, and energetic properties of boron-doped systems have not been studied systematically. In this study, we delve in the thermodynamics and kinetics involved in the incorporation of boron into both 1.5 nm nanoparticles (NPs) and extended (111) surfaces of various metals including Ir, Rh, Ni, Pd, Pt, Cu, Ag, Au, and Al by using Density Functional Theory (DFT) calculations. The results revealed stability of boron atoms within interstitial subsurface positions in Rh, Pt, and Pd (111) surfaces. The presence of low coordination sites within NPs enhances the diffusion towards subsurface sites, leading to the emergence of in-surface sites that are not typically observed on (111) surfaces. Notably, these specific locations were observed to exhibit exceptional thermodynamic stability, particularly in Rh, Ir, and Ni NPs. In contrast to the extended surfaces, the barriers for boron migration from adsorption sites to in-surface and subsurface positions were calculated to decreased to < 1 eV on terrace sites and < 0.4 eV on edge sites on all NPs except Ir, as shown in Figure 1. The incorporation of boron led to a notable shift in the d-band center of neighboring metal atoms towards Fermi level, amounting to approximately ~ 0.5 eV. The significant alteration in electronic properties provides a compelling explanation for the substantial impact of boron on the catalytic activity of transition metal catalysts.

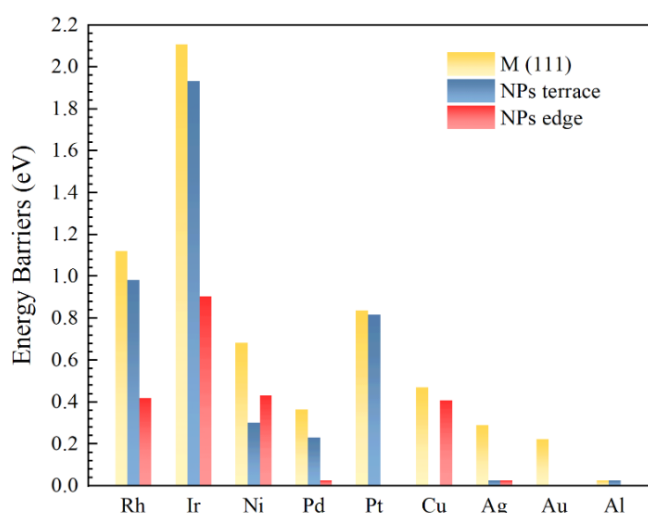


Figure 1: Gibb free energy barriers for the migration process of one boron atom on metal {111} surface and M₁₄₀ nanoparticle at 298 K

X-ray induced explosion dynamics of methane clusters

Frederic Ussling¹, co-authors of Community Beamtime Proposal No. 2176²

¹ *Laboratory for Solid State Physics, ETH Zurich, Switzerland*

² *European XFEL Hamburg, Germany*

Short wavelength free-electron lasers (FELs) enable the investigation of individual nanometre-sized particles, such as viruses or large biomolecules, via single-shot coherent diffractive imaging [1]. However, the intense X-ray pulses needed for single-molecule imaging also lead to ultrafast radiation damages, thus limiting the achievable resolution [2]. Several studies have been carried out to investigate possible energy dissipation pathways which preserve the scattering-relevant structure upon excitation [3-5]. In this context, hydride compound systems, i.e. methane or ammonium clusters serve as model systems for bio-molecules. Under certain conditions these systems eject fast protons, thus taking away excess charge and energy. This "proton boost" has been predicted to preserve the system's backbone [5]. In our experimental study, we investigate the dissociation dynamics of methane clusters upon irradiation with intense FEL pulses. Using ion spectroscopy methods, we investigate the conditions for fast protons in the range of photon energy and FEL intensity relevant for single particle imaging. Our analysis shows that protons indeed massively dominate the spectra in a certain intensity regime. However, the protons' mean kinetic energy is highest in another intensity range, where the yields of hydrogen and heavier ions are close to their stoichiometric distributions in the cluster. Our results can be explained in the picture of the transition from Coulomb explosion to hydrodynamic expansion. We find that the Coulomb explosion of a heterogeneous system leads to massive segregation and the disproportionate acceleration of the light ions, while the hydrodynamic expansion developing at the edge of the cluster does not favour strongly one of the species. In particular, towards the highest focal intensities, as needed for single particle imaging, our observations show that the proton boost does not play a relevant role in the ion dynamics.

[1] H.N. Chapman et al., *Nature* **470** (2011) 73-77

[2] R. Neutze et al., *Nature* **406** (2000) 752-757

[3] S.P. Hau-Riege et al., *PRL* **98** (2007) 198302

[4] B. Ziaja et al., *Phys Rev. A* **84** (2011) 033201

[5] P. DiCintio et al., *PRL* **111** (2013) 123401

Observation of Penning Electron Detachment by Electronically-Excited Potassium Atoms in High Rydberg States

Tatsuya Chiba¹, Moritz Blankenhorn¹, Shiyang Wang¹, Kathryn Foreman¹, Kit H. Bowen¹

¹ Department of Chemistry, Johns Hopkins University, USA

Penning ionization is a well-studied process where neutral atoms or molecules are ionized by collisions with partners in electronic excited states ($A + N^* \rightarrow A^+ + N + e^-$). In analogy with this, Penning detachment is a process where electronically excited energy donors collide with anions to free the excess electron ($A^- + N^* \rightarrow A + N + e^-$). The cross sections of Penning detachment have been investigated both theoretically [1-3] and experimentally [4-6] to achieve better understanding of the kinetic processes in the stellar atmosphere and D-region of ionosphere. While the Penning detachment cross section is predicted to be heavily dependent on the excited states of the neutral collision partners, their relation is not fully investigated experimentally.

In this study, Penning detachment of SF_5^- by excited potassium was observed, and its dependence on the excitation energy of potassium was investigated. SF_5^- anion was generated by introducing sulfur hexafluoride into the laser photoemission ion source. SF_5^- ion beam was crossed with potassium atoms in Rydberg excited states. Figure 1 shows the mass spectra of SF_5^- with the presence of potassium in ground state (Fig1 (a)) and 24d Rydberg excited state (Fig1 (b)), which show significant depletion of SF_5^- ion signal by excited potassium. By scanning the Rydberg states of potassium from 9d to 30d, the dependence of depletion efficiency on the excitation energy was observed.

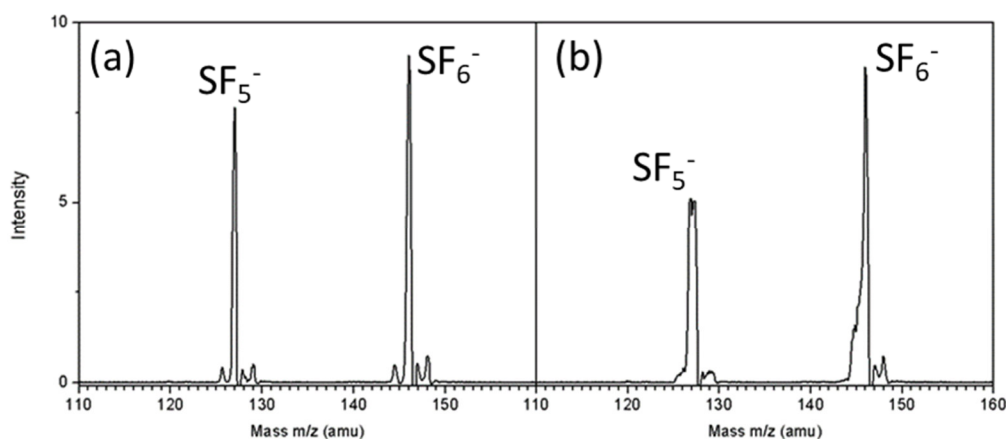


Figure 1: Mass spectra of SF_5^- (a) crossed with ground state potassium (b) crossed with excited potassium in 24d Rydberg state.

- [1] B. Blaney, R.S. Berry, Phys. Rev. A **3** (1971) 1349.
- [2] F. Martín, R.S. Berry, Phys. Rev. A **55** (1997) 1099.
- [3] F. Martín, R.S. Berry, Phys. Rev. A **55** (1997) 4209.
- [4] F.C. Fehsenfeld, D.L. Albritton, J.A. Burt, H.I. Schiff, Can. J. Chem. **47** (1969) 1797.
- [5] D. Doweck, J.C. Houver, C. Richter, N. Anderson, Z. Phys. D **18** (1991) 231.
- [6] A. Midey, I. Dotan, J.V. Seeley, A.A. Viggiano, Int. J. Mass Spectrom. **280** (2009) 6.

DFT+U Provides a Low-Cost Method to Calculate Precise Optical Spectra of Silver Clusters

Mohit Chaudhary^{1,2}, Hans-Christian Weissker^{1,2}

¹ *Centre interdisciplinaire de Nanoscience à Marseille (CINaM), Marseille, CNRS and Aix-Marseille University*

² *European Theoretical Spectroscopy Facility, www.etsf.eu*

The surface-plasmon resonance (SPR) in noble-metal clusters finds applications in diverse fields like bio-imaging, solar energy conversion, and sensing. Time-Dependent Density-Functional Theory (TD-DFT) is the most widely used method to study the cluster's optical response. In the case of Ag clusters, the optical properties are primarily produced by the delocalized s electrons but is also strongly influenced by inter-band transitions from the occupied d orbitals. Simple functionals such as LDA or GGA fail to accurately describe the d-electrons, generally placing them too close to the Fermi energy (E_F). Consequently, the inter-band transitions start at lower energies than expected, leading to too low SPR energies and over-broadening of the SPR peak. One approach to address this issue is to use hybrid or range-separated hybrid functionals [1], which significantly improve the description of localized states, but are numerically very expensive, barring their application to bigger clusters. In our present work, we use the DFT+U method as implemented in the Octopus Package [3], to improve the description of the d-states in Ag clusters. Using a unique value of U for all sizes, we obtain excellent agreement with experimental absorption spectra for Ag clusters ranging from a few to several hundreds of atoms, at a cost much lower than when using hybrids. Tests for larger gold clusters are ongoing and promising. This opens the possibility to carry out calculations for complex systems like biomolecules coupled to large silver clusters with precise, realistic SPR resonances.

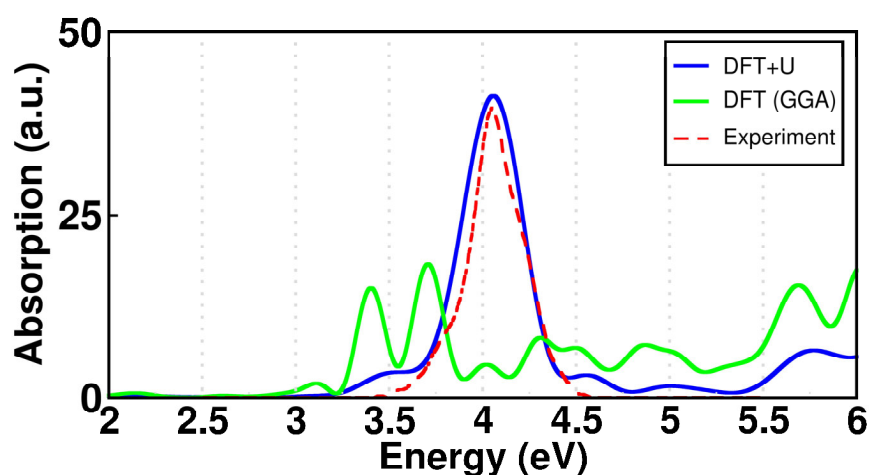


Figure: Comparison of the absorption spectra for Ag_{55} calculated using DFT (GGA) and DFT+U methods, alongside the experimental result¹.

- [1] B. Anak, M. Bencharifa, F. Rabilloud, Royal Society of Chemistry Advances 4 (2014), 13001-13011
- [2] N. Tancogne-Dejean, *et al.*, The Journal of Chemical Physics 152 (2020), 124119

High-Resolution Electronic Spectra of Gold Cluster Cations

Kai Pollow,¹ Taarna Studemund,¹ Nima-Noah Nahvi,¹ Marko Förstel,¹ Roland Mitric,² Stuart Mackenzie,³ Andre Fielicke,⁴ Otto Dopfer¹

¹ *Institut für Optik und Atomare Physik, TU Berlin, Germany*

² *Institut für Theoretische Chemie, Universität Würzburg, Germany*

³ *Physical and Theoretical Chemistry Laboratory, University of Oxford, United Kingdom*

⁴ *Fritz-Haber-Institut der Max-Planck-Gesellschaft, Berlin, Germany*

Gold is a versatile material with unique properties that account for its importance in chemistry, catalysis, medicine, nanomaterials, electronics, and fundamental research. For example, small gold cluster cations were shown to activate C=C, O-O, C-H and C-O bonds. A theoretical description of even small gold clusters is still challenging due to relativistic effects, multireference character of electronic states, and strong spin-orbit coupling. In this presentation, we will present optical photodissociation spectra of small gold cluster cations (Au_{2-4}^+) ranging from the near IR to the UV and their complexes with ligands (Ar, N_2 , N_2O), which provide detailed information about the potential energy surfaces of the ground and excited electronic states of these seemingly simple systems [1-6]. By improving the sensitivity and selectivity of the mass-selective photodissociation approach coupled to a laser desorption source by two orders of magnitude [2], unprecedented spectral details are resolved. The often highly irregular vibronic spectra provide precise experimental benchmarks for theoretical quantum chemical approaches, which are quite challenging for this type of clusters.

[1] B.K.A. Jaeger, M. Savoca, O. Dopfer, N.X. Truong, *Int. J. Mass Spectrom.* **402** (2016) 49-56

[2] M. Förstel, B.K.A. Jaeger, W. Schewe, P.H.A. Sporkhorst, O. Dopfer, *Rev. Sci. Instrum.* **88** (2017) 123110

[3] M. Förstel, W. Schewe, O. Dopfer, *Angew. Chem. Int. Ed.* **58** (2019) 3356-3360

[4] M. Förstel, K.M. Pollow, K. Saroukh, E.A. Najib, R. Mitric, O. Dopfer, *Angew. Chem. Int. Ed.* **59** (2020)

[5] M. Förstel, K. Pollow, T. Studemund, O. Dopfer, *Chem. Eur. J.* **27** (2021)

[6] M. Förstel, N.-N. Nahvi, K. Pollow, T. Studemund, A.E. Green, A. Fielicke, S.R. Mackenzie, O. Dopfer, *Nat. Sciences* **3** (2023) e20220023

Characterization of Pyrrole Dimer Cations and Their Solvated Clusters by IR Spectroscopy

Dashjargal Arildii¹, Yoshiteru Matsumoto,² Otto Dopfer¹

¹ *Institut für Optik und Atomare Physik, Technische Universität Berlin, Germany*

² *Department of Chemistry, Shizuoka University, Japan*

Aside from π H-bonding, cation/anion- π , and π - π stacking interactions, the charge resonance (CR) is a fundamental and very strong force in charged arene dimers [1]. In aromatic dimer cations, the positive charge is shared between the molecules depending on their ionization energy (IE) differences. Because of the charge resonance interaction between the monomers, a splitting between the two electronic states results in the charge resonance band due to the coupling of those electronic states. Even though the charge resonance interactions have been studied extensively over the years, only a rough estimation of the asymmetry in the charge distribution in the dimer is possible because of the broadness of the CR transition.

To this end, we previously demonstrated a new high-resolution experimental approach (infrared photodissociation spectroscopy (IRPD)) to precisely probe the charge distribution and the CR interaction in aromatic dimer cations for the prototypical case of the pyrrole dimer cation (Py_2^+). Py ($\text{C}_4\text{H}_5\text{N}$) is a five-membered heterocyclic ring which has a single isolated and uncoupled NH stretch oscillator whose frequency is strongly dependent on its charge state [1-3]. However, due to the finite width of the free NH stretching peak in the IRPD spectrum of Py_2^+ , the structural isomers of Py_2^+ are not easily and directly distinguishable (Figure 1). Therefore, herein we characterize Py_2^+ by IRPD and dispersion-corrected density functional theory calculations (B3LYP-D3/aug-cc-pVTZ) depending on the formation methods and internal temperature of the dimer cation. Analysis of IRPD spectra of mass-selected Py_2^+ and its cold $\text{Py}_2^+\text{-Ar}$ and $\text{Py}_2^+\text{-N}_2$ clusters combined with geometric parameters of intermolecular structures and binding energies provides a clear picture of the pyrrole dimer structures.

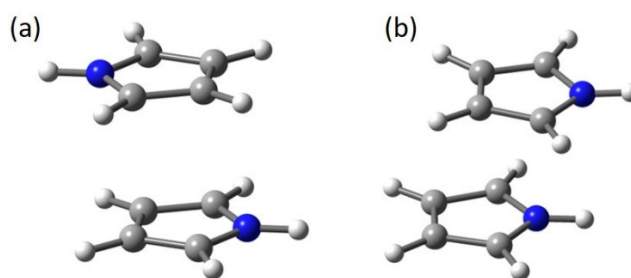


Figure 1: Optimized isomers of Py_2^+ at the B3LYP-D3/aug-cc-pVTZ level (a) antiparallel and (b) parallel

- [1] K. Chatterjee, Y. Matsumoto, O. Dopfer, *Angew. Chem. Int. Ed.* **58** (2019) 3351
- [2] M. Schütz, Y. Matsumoto, A. Bouchet, M. Öztürk, O. Dopfer, *Phys. Chem. Chem. Phys.* **19** (2017) 3970
- [3] D. Arildii, Y. Matsumoto, O. Dopfer, *J. Phys. Chem. A* **127** (2023) 2523

Electronic state of a bis(μ -oxo) di-manganese oxide cluster revealed by XAS and XMCD

O.S. Ablyasova ^{a,b,*}, M. Ugandi ^c, E.B. Boydas ^c, M. Timm ^a, M. Flach ^{a,b}, M. da Silva Santos ^{a,b},
B. von Issendorff ^b, V. Zamudio-Bayer ^a, K.Hirsch ^a, M. Römelt ^c, J.T. Lau ^{a,b}

*a) Abteilung für Hochempfindliche Röntgenspektroskopie, Helmholtz-Zentrum Berlin für
Materialien und Energie, Albert-Einstein-Straße 15, 12489 Berlin, Germany;*

*b) Physikalisches Institut, Universität Freiburg, Hermann-Herder-Straße 3, 79104 Freiburg,
Germany;*

*c) Institut für Chemie, Humboldt-Universität zu Berlin, Brook-Taylor-Straße 2, 12489 Berlin,
Germany,*

** olesya.ablyasova@helmholtz-berlin.de*

The oxidation and spin states of the CaMn_4O_5 cluster of oxygen-evolving complex are crucial for understanding dioxygen formation in the Kok cycle. In particular, the S_4 state is notoriously difficult to model or to observe because of the millisecond time scale of the S_3 - S_0 transition [1]. Two competing models for the S_4 state, responsible for O_2 formation, exist [2] that feature distinctively different oxidation states of +4 and +5 of the manganese atom at the reaction site. Despite the fact that the spin states of the manganese atoms in state S_4 are still under debate, the reactivity of the CaMn_4O_5 cluster is believed to be spin-dependent [3].

In this work, we report on the characterization of gas-phase manganese oxide complexes via X-ray absorption spectroscopy (XAS) and X-ray magnetic circular dichroism (XMCD), measured in ion yield mode at the manganese $L_{2,3}$ -edge on a series of cryogenically cooled, mass-selected manganese oxide ions [4]. We identify oxidation and spin states by comparison with XAS and XMCD spectra of reference manganese compounds with known oxidation states, in combination with multireference calculations.

Our most important result is the identification of a bis(μ -oxo) bridged dimanganese oxide species with manganese(V) in a high-spin state. This is the first observation of the elusive manganese(V) high-spin state in a polymanganese oxido complex [5,6, 7]. The observed result might have implications for the oxidation and spin states of the CaMn_4O_5 complex in the S_4 state.

[1] N. Cox et al., Annu.Rev.Biochem., 2020, 89, 795.

[2] J. Barber., Nature Plants, 2017, 3(4), 17041.

[3] V. Krewald et al., Inorganic Chemistry, 2016, 55(2):488–501.

[4] M. G. Delcey, et al. Phys. Chem. Chem. Phys. 2022, 24:3598–3610.

[5] R. Gupta, et al Proceedings of the National Academy of Sciences, 2015, 112, 5319–5324

[6] H. M. Neu, et al, Accounts of Chemical Research, 2015, 48, 2754–2764.

[7] T. Taguchi, et al, Journal of the American Chemical Society 2012 134 (4), 1996-1999.

Ta atoms & clusters on Pt (111) – a combined XPS, STM, DFT and TPD study

Kevin Bertrang¹, Tobias Hinke¹, Julius Boie¹, Matthias Knechtges¹, Sebastian Kaiser¹,

Federico Loi², Alessandro Baraldi³, Sergio Tosoni², Ueli Heiz¹

¹ School of Natural Sciences, Technical University of Munich, Germany

² ELETTRA Sincrotrone Trieste

³ Physics Department and CENMAT, University of Trieste, Italy

Understanding the behaviour of metal oxide interfaces is crucial for advancing our knowledge of interfacial phenomena and their impact on material properties. In this study, we aimed to gain a deeper understanding of Ta/Ta_xO_y films and their interfaces with Pt. Understanding the oxidation state and changes within the film, as well as the oxygen stoichiometry at the interface, is an important first step for developing novel applications.

In this study, we investigated the interfacial behavior between Pt and Ta by depositing submonolayer quantities of Ta atoms and clusters onto a Pt (111) surface. The system was probed using high resolution X-ray photoelectron spectroscopy (HRXPS) with synchrotron radiation to gain profound insights into the stability and mobility of Ta species in relation to temperature, coverage, and oxidation degree. At liquid He temperatures highly mobile Ta atoms are immobilized enabling unambiguous probing of Ta/Pt interactions. Upon increasing temperature or oxidative pressure dynamic processes become dominant, that lead to the formation of agglomerates stable up to high temperatures (700 K). We took STM images showing the morphology of the Ta_xO_y agglomerates and their monodisperse distribution. Smoluchowski ripening of these agglomerates can be observed upon dosing H₂ pressures up to 5×10^{-7} mbar. At temperatures above 700 K a retrievable subsurface alloy is formed. This alloy was further investigated in reactivity studies using temperature programmed desorption (TPD) experiments.

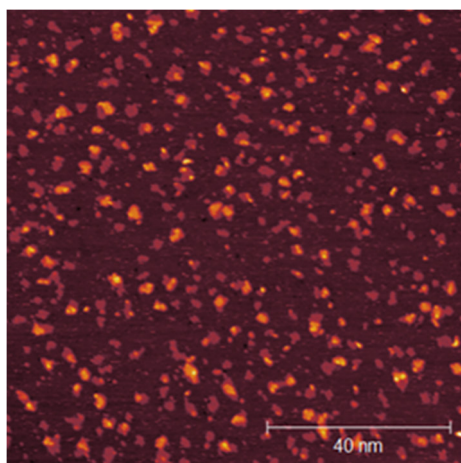


Figure 1: STM image showing flat Ta oxide agglomerates on a Pt surface.

To complement the experimental findings, density functional theory (DFT) calculations were performed to gain a deeper understanding of the cluster structures.

Iron complexes with complete and incomplete first solvation shell investigated by x-ray absorption spectroscopy

Max Flach^{1,2}, Konstantin Hirsch¹, Martin Timm¹, Mayara da Silva Santos^{1,2}, Olesya Ablyasova^{1,2}, Aryna Hreben¹, Bernd von Issendorff², J. Tobias Lau^{1,2}, Vicente Zamudio-Bayer¹

¹ Helmholtz-Zentrum Berlin für Material und Energie, Germany

² Physikalisches Institut, Albert-Ludwigs-Universität Freiburg, Germany

Water plays an essential role as a solvent in chemical processes in biological, catalytic and atmospheric chemistry. In these fields a good understanding of interaction between transition metal complexes and water molecules is of major interest^[1-4]. The interaction between water molecules and transition metal complexes has been subject of various studies on liquid and gas phase samples focused on the changes in electronic^[5,6], geometrical structures^[7,8] and bond properties^[9]. However the interaction of water molecules and transition metal complexes is still not fully understood especially the changes in the electronic structure with respect to the number of water molecules bonding to a transition metal complex. Oxygen 1s x-ray absorption spectra pre-edge features are known to originate from water-metal d interaction^[5], but how the electronic structure and furthermore how these spectral features depend on the number of water molecules bonding to a transition metal complex is not yet understood. In this study we contribute to this question by providing x-ray absorption spectra (XAS) of the iron L- and oxygen K-edge of iron complexes $[\text{Fe}(\text{H}_2\text{O})_6]^{2+}$ and $[\text{FeOH}(\text{H}_2\text{O})_n]^+$ ($n=0-3$) in the gas phase. The measured spectra are compared to simulated ones from time-dependent density functional theory (TD-DFT). As we can well resolve the oxygen K-edge we are able to observe excitation energy shifts of the pre-edge features with respect to the contribution of the number of water molecules to the LUMO orbital in the iron hydroxide series. The amount of these excitation energy shifts correlates with how strongly the water molecules participate in the LUMO Fe-OH hybrid orbital. A comparison between the oxygen K-edge of $[\text{Fe}(\text{H}_2\text{O})_6]^{2+}$ and $[\text{FeOH}(\text{H}_2\text{O})_n]^+$ shows low energy features are present in $[\text{FeOH}]^+$ as well as in $[\text{Fe}(\text{H}_2\text{O})_6]^{2+}$ at similar energies but are narrower in the $[\text{Fe}(\text{H}_2\text{O})_6]^{2+}$ spectrum. Compared to literature these oxygen K-edge low energy features are also at similar energies but less distinct for the literature liquid phase spectra. The iron L-edge spectra show less changes as in all our samples iron is in the oxidation state 2+ as expected. However a comparison of the iron L₃-edge of gas phase $[\text{Fe}(\text{H}_2\text{O})_6]^{2+}$ with liquid phase XAS of 1M FeCl_2 in H_2O reveals a broadening from the gas phase to the liquid phase. These preliminary results are part of an on going study on the way to provide deeper insight in the interaction of water molecules with transition metal complex.

- [1] H. Pye et al., Atmospheric Chemistry and Physics **20** (2020) 4809-4888
- [2] H. Yuansheng et al., Water Research **179** (2020) 115914
- [3] H. Trzesniowski et al., J. Phys. Chem. Lett. **14** (2023) 545-551
- [4] T. Pasinszki et al., Nanomaterials **10** (2020) 917
- [5] L. Näslund et al., J. Phys. Chem. A **107** (2003) 6869-6876
- [6] K. Atak et al., J. Phys. Chem. B, **117** (2013) 12613–12618
- [7] B. Marsh et al., Phys. Chem. Chem. Phys. **17** (2015) 23195-23206
- [8] O. Boukar et al., New J. Chem. **45** (2021) 10693-10710
- [9] O. Sander et al., J. Phys. Chem. A **123** (2019) 1675-1688

Surface to volume transition in cluster Coulomb explosions

K. Raspe¹, D. Komar¹, L. Kazak^{1, 2}, N. Iwe¹, B. Krebs¹, F. Martinez¹,
K.-H. Meiwes-Broer^{1, 3}, and J. Tiggesbäumker^{1, 3}

¹ Institute of Physics, University of Rostock, 18059 Rostock, Germany

² present address: Institute for Quantum Optics, Ulm University, 89081 Ulm, Germany

³ Department of Life, Light and Matter, University of Rostock, 18059 Rostock, Germany

In the interaction of atomic clusters with strong laser fields, an expanding nanoplasma is formed, whereas the resulting ion charge-state and energy distributions give insight into the expansion dynamics. When conducting strong-field experiments on clusters in a molecular beam, the particle size and laser intensity distributions, as well as saturation effects contribute to the ion signals and can mask details of the nanoplasma evolution [1]. In this contribution, the intensity-difference spectrum technique [2] is applied to record charge-state resolved ion energy spectra [3] from the Coulomb explosion of clusters. With increasing laser intensity, a change in the expansion pattern is observed in Ar_N . At low laser intensities low-energy cuts show up in the ion yields, which are not obtained at higher fluence. This indicates a surface-driven expansion, which transforms into a volume-driven Coulomb explosion. A detailed analysis reveals information on the charging process, i.e., the complex interplay of outer ionization, recombination, Debye screening and the phenomenon of ionization saturation. Our recent nanoplasma studies on single-sized silver clusters (see Fig. 1) using digital ion traps [4] provide a novel view on the Coulomb explosion dynamics, i.e., the impact of a well-defined particle size.

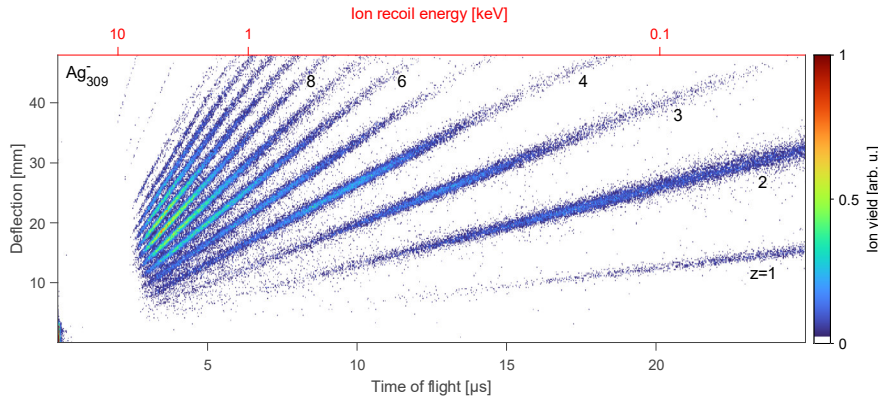


Figure 1: Time-of-flight-deflection histogram of the Coulomb explosion of size-selected silver clusters (Ag_{309}^-) after exposure to strong femtosecond laser fields ($I_L = 2.53 \cdot 10^{15} \text{ W/cm}^2$). The different atomic charge states and their corresponding recoil energy distribution are indicated by diagonal lines in the histogram. Representative ion recoil energies are shown.

- [1] M. R. Islam, U. Saalman, and J. M. Rost, Phys. Rev. A **73** (2006) 041201
- [2] P. Wang, A. Sayler, K. Carnes, B. Esry, and I. Ben-Itzhak, Opt. Lett. **30** (2005) 664
- [3] D. Komar, K.-H. Meiwes-Broer, and J. Tiggesbäumker, Rev. Sci. Instrum. **87** (2016) 103110
- [4] K. Raspe, M. Müller, N. Iwe, R. N. Wolf, P. Oelßner, F. Martinez, L. Schweikhard, K.-H. Meiwes-Broer, and J. Tiggesbäumker, Rev. Sci. Instrum. **93** (2022) 043301

FEL studies of complex metal nanoparticles and their structural dynamics

Sharath Sasikumar¹, Dr. Simon Dold¹, Dr. Yevheniy Ovcharenko¹, Dr. Michele Devetta³,
Prof.Dr. Paolo Piseri,² Dr. Tommaso Mazza¹

¹ *European X-Ray Free Electron Laser GmbH, Germany*

² *Università degli Studi di Milano "La Statale", Italy*

³ *CNR - Consiglio Nazionale delle Ricerche, Italy*

The study of isolated nanoparticles produced in the gas phase is of fundamental importance for understanding how properties of matter evolve from atomic and molecular features to those typical of bulk materials. Our work uses a Pulsed Microplasma Cluster Source (PMCS) for controlled gas phase synthesis of transition metal nanoparticle aggregates. With it we experimentally address in the time domain the coalescence process in complex aggregates, which is relevant for the understanding and control of gas-phase synthesis methods when size, stoichiometry, structure and morphology are of concern. Stoichiometric control is achieved by doping of carrier gas [1]. We have assessed the capability to control the mass and structure of the clusters using mass spectrometry with momentum imaging of cluster ions excited by UV [2]. This is used in an IR pump UV probe scheme to study coalescence dynamics in the few picosecond range. Femtosecond processes like the quenching of non-equilibrium nanoparticles can be studied via Pump-probe experiments at FELs allowing us to compare their observed structural relaxation to existing models for coalescence dynamics.

[1] D'Elia et al., Phys. Chem. Chem. Phys., 22, 6282-6290 (2020)

[2] T. Mazza et al., New Journal of physics **13**, 023009 (2011)

Interlayer Excitons in MoS₂/WS₂ Heterostructures

Annika Bergmann¹, Johannes Reinhold,¹ Mustafa Hemaïd¹, Rico Schwartz¹, Ziyang Gan², Antony George², Andrey Turchanin², and Tobias Korn¹

¹ *Institute of Physics, University of Rostock, Germany*

² *Institute of Physical Chemistry, Friedrich Schiller University Jena, Germany*

Since the exfoliation of graphene in 2004 [1], there has been a continuously growing pool of two-dimensional materials, which for example includes semiconducting transition metal dichalcogenide (TMDC) monolayers. In contrast to conventional bulk semiconductors, the single-layer thickness of TMDCs provides a large surface area that can be used to efficiently study interfacial effects between the TMDC monolayer and other materials deposited on it. Interesting examples are interlayer charge transfer and interlayer excitons that occur in TMDC heterostructures [2].

We stack TMDC monolayers of MoS₂ and WS₂ that were obtained either by exfoliation from a bulk crystal or chemical vapor deposition growth [3] to form bilayer heterostructures.

The resulting samples are characterized using photoluminescence (PL) and Raman spectroscopy. PL quenching and the existence of the Raman interlayer shear mode provide information about the quality of the interlayer contact. For well-coupled heterostructures we observe interlayer excitons and investigate their dependence on temperature as well as on the twist angle between the constituent monolayers.

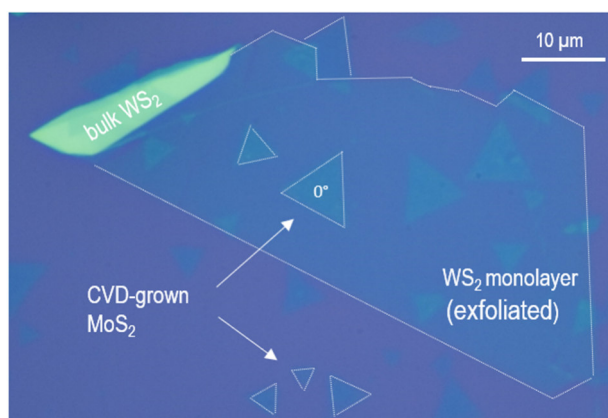


Figure 1: Optical microscope image of MoS₂/WS₂ heterostructures formed by combining chemical vapor deposition-grown MoS₂ monolayers and an exfoliated WS₂ monolayer.

- [1] K.S. Novoselov, A.K. Geim, *Science* **306** (2004) 666
- [2] Fang et al., *Proc. Natl. Acad. Sci. USA* **111** (2014) 6198
- [3] A. George et al., *J. Phys. Mater.* **2** (2019) 016001

P-type Doping of MoS₂ through Cluster Injection

Xueyu Liu^{1,2}, Fengqi Song,^{1,2}

¹ National Laboratory of Solid State Microstructures, Collaborative Innovation Center of Advanced Microstructures, and School of Physics, Nanjing University, Nanjing 210093, China

² Atom Manufacturing Institute (AMI), Nanjing 211805, China

Transition Metal Disulfide (TMD) materials have emerged as the preferred choice for sub-nanometer transistors as chip processes continue to shrink down to 3nm, in order to sustain Moore's law. However, it has been observed that doping two-dimensional semiconductor materials, such as TMDs, is relatively challenging. For instance, while methods like oxygen plasma have been utilized for N-type doping of TMDs^[1], there is still a lack of effective solutions for P-type doping of TMD materials^[2].

In our study, we have successfully achieved P-type doping of bilayer MoS₂ by injecting Nb-n clusters, employing a cluster injection technique with quality selection. Through comparative experiments, we have determined that Nb-10 clusters are an appropriate size for injection. To estimate the approximate parameters required for injecting Nb-10 clusters into bilayer MoS₂, we have employed the Monte Carlo tracking algorithm. Our results suggest that an accelerating voltage of approximately 600eV is optimal. Additionally, we have compared the annealing conditions required for the injected samples and found that annealing at 700K for 10 minutes effectively repairs most defects while preserving electrical activity.

By fine-tuning the parameters, we have achieved a Nb-10 cluster beam with a current of 10nA, which easily meets the AEIC standard doping concentration of $8.7 \times 10^{17}/\text{cm}^3$. Due to this high beam signal, the injection process for a one-inch-sized bilayer MoS₂ sample can be completed within just 30 minutes. Transport measurements of the implanted MoS₂ demonstrate a transition from N-type to P-type behavior, accompanied by a significant reduction in the Schottky barrier at the metal electrode interface.

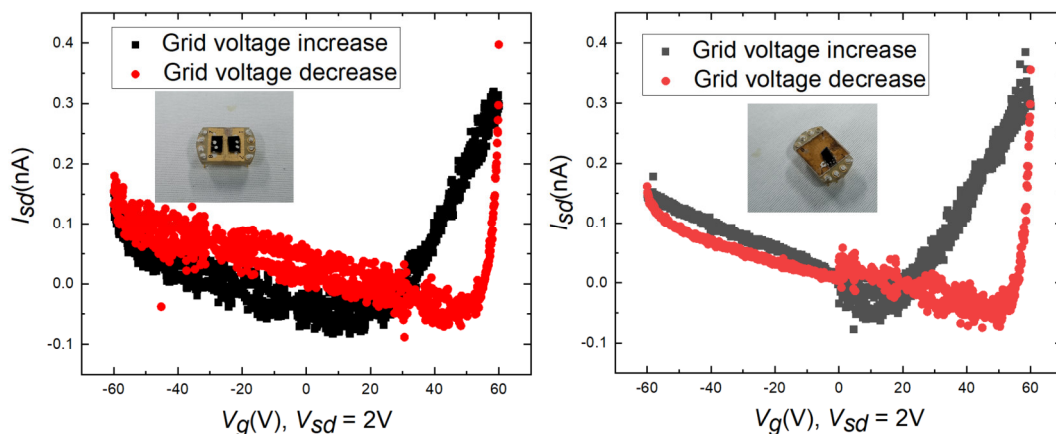


Figure 1: The gate voltage scanning field image of MoS₂ after Nb₁₀ cluster injection

[1] Wang S, Zeng X, Zhou Y, et al. High-Performance MoS₂ Complementary Inverter Prepared by Oxygen Plasma Doping[J]. ACS Applied Electronic Materials, 2022, 4(3): 955-963.

[2] Laskar M R, Nath D N, Ma L, et al. p-type doping of MoS₂ thin films using Nb[J]. Applied Physics Letters, 2014, 104(9): 092104.

Luminescence Threshold Size of Size-Separated CdTe Nanoparticles

Ryo Takahata^{1,2}, Masaki Saruyama^{1,2}, Toshiharu Teranishi^{1,2}

¹ *Institute for Chemical Research, Kyoto University, Japan*

² *Department of Chemistry, Kyoto University, Japan*

Semiconductor nanoparticles (NPs) can be applied for various fields such as solar energy conversion, photo- and electro-luminescence, sensing, detector, and so on.^{1,2} Among the semiconductor NPs, cadmium chalcogenide (CdE) NPs possess the advantages of facilely-tunable exciton peaks. The CdE NPs exhibit the quantum size effect; CdS NPs and CdSe NPs show blue shifts of exciton peaks in the visible to the ultraviolet range with decreasing the size^{3,4} while the blue shift can be observed from near IR to the visible range for CdTe NPs.⁵ Another factor in controlling the physicochemical properties is the chemical composition of these CdE NPs. For example, the core/shell structures lead to a red-shift of exciton peaks from the only cores and enhancement of photoluminescence efficiency.⁶ Solid solution NPs of CdTe and CdS exhibit the middle energy of bandgaps between the bandgaps of CdTe and CdS.⁷ As for minor composition changes, defects can dominate the physicochemical properties of CdE NPs. In particular, as reported previously, the S defects suppress photoluminescence from excitons and cause broad peaks at longer wavelengths than exciton peaks.⁸ The physicochemical properties of CdE NPs vary by the quantum size effect and the chemical compositions. Therefore, developing the methods to obtain well-size/composition-controlled NPs is complicated but significant for elucidating their structure-specific properties and applications.

In this study, we separated two kinds of CdTe NPs by polyacrylamide gel electrophoresis (PAGE). In both NPs, the size of separated CdTe NPs decreased with increasing running distance of PAGE. We discovered that the smaller CdTe NPs showed not only the blue shift of exciton peaks in absorption and luminescence spectra but also the sudden drop of luminescence intensity at around 1.5 nm. The detailed X-ray absorption fine structures (XAFS) analysis revealed that the coordination number (CN) of Cd–Te bonds around Cd in luminescent CdTe NPs is larger than that of non-luminescent CdTe NPs. This suggests that the introductions of the Te²⁻ vacancies cause the deviation from the perfect tetrahedral coordination (CN= ~4) of CdTe(S) crystals. These results insist that Te²⁻ ions eluted at a specific size (~1.5 nm), and the Te²⁻ vacancies strongly suppress the photoluminescence of CdTe NPs. Size separation is a useful technique to reveal the size-dependent physicochemical properties of nanomaterials independent of synthesis conditions.

- [1] X. Zou, Y. Zhang, *Chem. Soc. Rev.* **44** (2015) 5148–5180.
- [2] K. Y. Zhang, Q. Yu, Q. Wei, S. Liu, Q. Zhao, W. Huang, *Chem. Rev.* **118** (2018) 1770–1839.
- [3] Y. Wang, N. Herron, *Phys. Rev. B* **42** (1990) 7253–7255.
- [4] M. Nirmal, C. B. Murray, M. G. Bawendi, *Phys. Rev. B* **50** (1994) 2293–2300.
- [5] J. Jasieniak, M. Califano, S. E. Watkins, *ACS Nano* **5** (2011) 5888–5902.
- [6] W. W. Yu, Y. A. Wang, X. Peng, *Chem. Mater.* **15** (2003) 4300–4308.
- [7] S. K. Poznyak, N. P. Osipovich, A. Shavel, D. V. Talapin, M. Gao, A. Eychmüller, N. Gaponik, *J. Phys. Chem. B* **109** (2005) 1094–1100.
- [8] H. Bao, Y. Gong, Z. Li, M. Gao, *Chem. Mater.* **16** (2004) 3853–3859.

Experimental investigation of Nonlinear Optical properties of Colloidal Gr@Co Core/Shell Nanoparticles

Adeleh Granmayehrad¹, Elham Darabi,² Alaa Kadhim Manea²

¹ Department of Basic Science, Roudehen Branch, Islamic Azad University, Roudehen, Iran

² Plasma Physics Research center, Science and Research Branch, Islamic Azad University, Tehran, Iran

Recent studies have focused on Graphene, a single atomic layer of graphite, due to its novel electronic and structural properties. Due to the strong optical properties of Graphene, core shell nanoparticles with metal shells covering a Graphene core cause an extremely nonlinear response [1]. These nanoparticles have shown specific advantages by virtue of unique combination of strong field enhancement and wide ranging [2]. In this paper, the linear optical behavior of the synthesized core-shell structured Gr@Co nanoparticles was studied by UV-vis spectral analysis. The crystallinity and chemical composition of the products are analyzed by powder XRD pattern and EDX. The particle size, morphology and the formation of uniform Co shell over the Gr core are visualized by the SEM analysis. Moreover, the optical nonlinearity of the Gr@Co core-shell nanoparticles is examined by z-scan technique using continuous wave 532nm laser which showed interesting optical nonlinearity and exhibited switching behavior from reverse saturated absorption to saturated absorption, which could be useful for numerous photonic applications like, Q-switching and optical limiting.

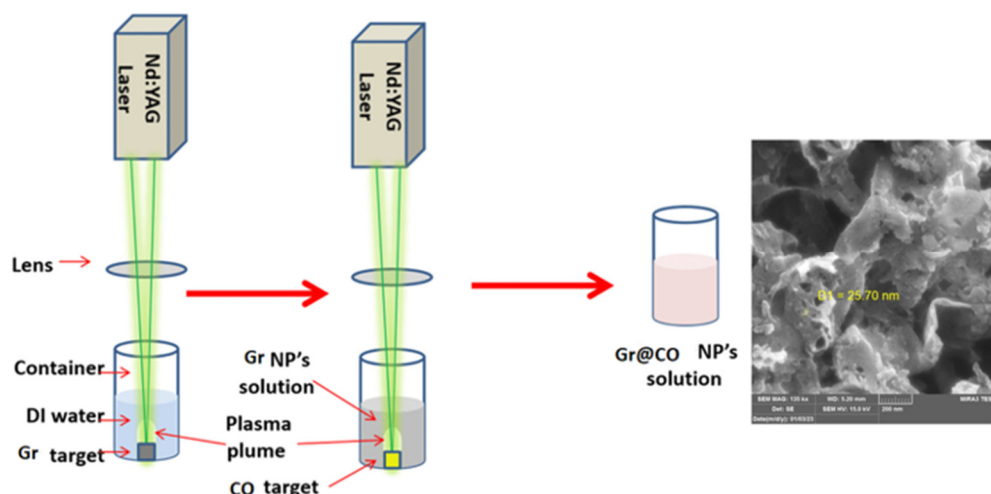


Figure 1: Schematic illustration of laser ablation of Gr@Co core-shell NPs experimental setup

[1] Tayebah Naseri and Mohsen Balaei, J. Opt. Soc. Am. B, **35**(2018) 2278-2285.

[2] Singh A, Shishodia MS., Physica E Low Dimens Syst Nanostruct, **124** (2020) 114288.

Tunable SPR bands of asymmetric plasmonic gold nanostructures; nanorods and nanostars

Hanieh Yazdanfar¹, Seyedeh Mehri Hamidi¹

¹ *Laser and Plasma Research Institute, Shahid Beheshti University, Iran*

Plasmonic metal nanoparticles are very interesting both from a fundamental science point of view, and also for their many possible applications. Noble metals nanoparticles represent extraordinary label-free biosensors due to their surface plasmon resonance (SPR) [1]. The excitation of SPR leads to light absorption stronger than other materials [2]. The unique morphology and modern shape controlled synthesis of anisotropic gold nanostructures has offered novel characteristics and new prospects for biomedical and biosensing applications, as well as they exhibit excellent tunability, photostability and biocompatibility. The SPR wavelength of asymmetric gold nanoparticles can be tuned from infrared region to the visible where biosensors with specific wavelengths are needed. The resonance frequencies, width, number and intensity of the absorption bands highly depend on the size, shape, structure, and orientation of particles [2, 3]. Symmetric Au nanospheres have only one plasmon band in visible range limited to be tuned to the NIR region by increasing the size [4]. In this work, we have reduced the Au nanosphere symmetry and synthesized gold nanorods and nanostars based on reduction of Tetrachloroauric acid in stable basic environment and they have been characterized as novel plasmonic structures. When a nanosphere is elongated along one axis, the free electrons have two available directions to oscillate [4] and the SPR band splits into two modes: a strong band in NIR wavelengths and a weak band in the visible wavelengths similar to that of gold nanospheres corresponding to electron oscillations parallel and perpendicular to the long axis of nanorods and nanostars' tips, attributed to longitudinal and transverse plasmon bands, respectively [1, 2]. The longitudinal plasmonic band is characteristic of anisotropic nanostructures. Its wavelength is sensitive to the synthesis conditions and the aspect ratio of the gold nanorods and nanostars' tip. It is tunable and can be red-shifted from the visible to near-infrared with increasing aspect ratio [3]. The SPR bands of our 25nm Au nanorods occur at 540nm and 750nm for transverse and longitudinal modes, respectively. Absorption spectra of nanostars show absorption band at 580nm with a shoulder at 560nm which belong to the hybrid absorption of the core and the transverse mode of the tips. Another band at 670nm attributed to the longitudinal resonance of the tips. In this study, we have investigated the synthesis parameters and the results show the amount of NaOH plays a crucial role on controlling the size, aspect ratio and morphology of these nanostructures as well as the reaction yield and the intensity, wavelength and signal to noise ratio of the bands. In addition, SPR band width and intensity, tunability and the strength of the nanoparticles interaction in nanostars and nanorods have been compared with each other.

[1] J. Cao, T. Sun, and K.T.V. Grattan, *Sensors and actuators B: Chemical* **195** (2014) 332-351.

[2] T.A. El-Brolosy, T. Abdallah, M.B. Mohamed, S. Abdallah, K. Easawi, S. Negm, H. Talaat, *The European Physical Journal Special Topics* **153** (2008) 361-364.

[3] X. Huang, M.A. El-Sayed, *Journal of advanced research* **1.1** (2010): 13-28.

[4] Y. Hu, X. Liu, Z. Cai, H. Zhang, H. Gao, W. He, P. Wu, C. Cai, J.J. Zhu, Z. Yan, *Chemistry of Materials* **31.2** (2018) 471-482.

Atomistic self-assembly of nanostructure in liquid metals

Nicola Gaston

The MacDiarmid Institute for Advanced Materials and Nanotechnology, Department of Physics, The University of Auckland, New Zealand

The manipulation of interatomic interactions for structural self-assembly is a seductive promise of nanotechnology, most tantalisingly made evident by biological examples in nature. Much of the promise of sustainability in materials science comes from the idea of such structural control being able to be achieved at low energetic cost.

At the risk of anthropomorphising atoms, this talk will present some examples of how, by developing an understanding of how particular atoms want to behave, we can manipulate structure by proxy. Not through forcible manipulation of atoms, but through understanding their environmental preferences, and how these change through many-body interactions as they assemble.

The use of low-temperature liquid metals, such as gallium, as media for the dilution of other metals has led to an increasing variety of examples of how temperature- and concentration-dependent interactions can be used to direct the self-assembly of nanostructure, with astonishing precision, resulting in novel pattern formation [1]. This talk will introduce the use of ab initio molecular dynamics for the elucidation of the mechanisms of structural formation, whether via the differential mobility of dopant metal atoms [2], or due to the formation of structure at the surface of the liquid metal [3]. The concentration-dependence of the alloy behaviour will also be discussed [4].

Finally, the mechanism of nanocrystal formation within liquid metals will be discussed, based on ab initio calculations [5], giving insight into the atomistic self-assembly process.

[1] Tang, J., Lambie, S., Meftahi, N., Christofferson, A., Yang, J., Ghasemian, M., Han, J., Allieux, F., Rahim, A., Mayyas, M., Daeneke, T., McConville, C., Steenbergen, K., Kaner, R., Russo, S., Gaston, N., Kalantar-Zadeh, K., Unique surface patterns emerging during solidification of liquid metal alloys. *Nat. Nanotech.* 16, 431–439, (2021).

[2] S. Lambie, K. G. Steenbergen & N. Gaston, A mechanistic understanding of surface Bi enrichment in dilute GaBi systems. *Phys. Chem. Chem. Phys.* 23, 14383–14390, (2021).

[3] J. Tang, S. Lambie, N. Meftahi, A. J. Christofferson, J. Yang, J. Han, Md. A. Rahim, M. Mayyas, M. B. Ghasemian, F.-M. Allieux, Z. Cao, T. Daeneke, C. F. McConville, K. G. Steenbergen, R. B. Kaner, S. P. Russo, N. Gaston, and K. Kalantar-Zadeh, Oscillatory bifurcation patterns initiated by seeded surface solidification of liquid metals. *Nature Synthesis*, 1, 158–169. (2022).

[4] S. Lambie, K. G. Steenbergen, & N. Gaston, Concentration dependent alloying behaviour of liquid GaAu. *Chem. Comm.*, 58, 13771–13774, (2022).

[5] S. A. Idrus-Saidi, J. Tang, S. Lambie, J. Han, M. Mayyas, M. B. Ghasemian, F.-M. Allieux, S. Cai, P. Koshy, P. Mostaghimi, K. G. Steenbergen, A. S. Barnard, T. Daeneke, N. Gaston, K. Kalantar-Zadeh, Liquid metal synthesis solvents for metallic crystals, *Science*, 378, 1118–1124, (2022).

Study of oxidation property and structural transition of size-selected tantalum nanoclusters with atomic precision

Shengyong Hu^{1,2}, Fengqi Song^{1,2}

¹National Laboratory of Solid State Microstructures, Collaborative Innovation Center of Advanced Microstructures, School of Physics, Nanjing University, Nanjing 210093, China

²Atom Manufacturing Institute (AMI), Nanjing 211805, China

With the continuous advancement of experimental technology, it has become feasible to utilize clusters as fundamental building blocks to assemble infinite new materials with specific functions in a “bottom-up” manner. Tantalum and its oxides possess exceptional properties, making them highly promising for a diverse range of applications such as anti-corrosive coatings, electrolytic capacitors, surgical tool coatings, among others. Furthermore, Ta can be utilized to produce various refractory superalloys employed in jet engines, chemical laboratory equipment, nuclear reactors, and vehicles. However, there have been few experimental reports on size-selected Ta clusters so far [1].

Here we produced a series of size-selected Ta_N (N=147, 309, 561, 923, 1415, 2057, 6525, 10000, 20000) clusters using a gas-phase condensation cluster beam source. The thermal stability of these clusters was confirmed by AC-STEM imaging. XPS and EDS investigation reveal that Ta_N clusters are prone to oxidization and swell larger diameters than pure Ta_N clusters. Moreover, oxidized Ta clusters were found to have amorphous structures while pure ones have ordered structure. Furthermore, the oxidized Ta clusters can be partly de-oxidized by prolonged electron beam irradiation, and eventually dense and ordered structure is formed. During in situ heating, high temperature induced crystallization is observed. When the temperature exceeds 1000°C, part of clusters with fewer than 309 atoms exhibit decahedral and icosahedral structures, but the quintic symmetry structure disappears in larger clusters which resemble crystalline tantalum pentoxide films [2]. The temperature at which this process takes place is much lower than the melting point of tantalum and its oxides, and the ordered structure that results from annealing continues to remain unchanged after six months of being exposed to air at ambient temperature. This study may provide a novel perspective on the fabrication of single crystal nanostructures through heating or electron beam irradiation by utilizing clusters with precisely controllable numbers of atoms (N) as fundamental building blocks.

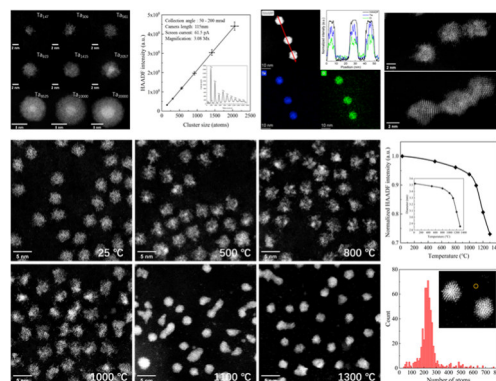


Figure 1: Production and characterization of size-selected Ta_N cluster with atomic-level precision.

[1] Singh V, Grammatikopoulos P, Cassidy C, *Journal of nanoparticle research* 16 (2014): 1-10.

[2] Perez I, Carrejo JLE, Sosa V, *Journal of Alloys and Compounds* 712 (2017): 303-310.

In silico modelling of coated CdTe/CdS/ZnS quantum dots for nanosafety

Konstantinos Kotsis¹

¹ *School of Physics, University College Dublin, Ireland*

Quantum dots (QD) are nanocrystalline structures with unique, often size dependent, optical properties. QDs have been widely used as semiconductor materials in electronic devices or as photostable fluorescent labels for biomedical applications. However, before using QDs in patients for diagnostic imaging, a detailed study of the interactions in the human body, specifically as to whether they accumulate, if they are biodegradable, how they are eliminated as well as whether they induce long-term cytotoxicity, is necessary. QDs with a cadmium-containing core, a metallic shell and organic ligands for steric stabilisation were synthesized at BOKU/Austria [1, 2]. Measurements of the physicochemical properties and possible cytotoxic effects show that PEG-QDs indicate higher colloidal stability in the cell media after 24h than NAC-QDs. The cell viability was lower for PEG-QDs than for NAC-QDs. ROS production was significantly higher for PEG-QDs than for NAC-QDs and all QDs were internalized into the cells, at which CLSM images indicated the formation of QD aggregates.

To facilitate the interpretation regarding aggregation, corona formation, dissolution rates, and cytotoxicity of the coated QDs in silico modelling of the molecular dynamics is utilised. The structures of PEG-CdTe/CdS/ZnS, NAC-CdTe/CdS/ZnS and DHLA-PEGO750Me-CdTe/CdS/ZnS were modelled using a python tool. Electronic structure properties were calculated with quantum chemical methods and molecular properties with molecular dynamics methods. The descriptors served in the prediction of the reactivity and biological activity as well as stability and solubility of the coated QDs in cell media. Moreover, to identify the types of aggregation and to obtain dissolution rates of the coated QDs in water computations of molecular dynamics of large scale were needed and the data only partially support the experimental findings. Corona formation studies and predictions of cytotoxicity are in progress. This work was funded through EU Horizon 2020 Programme, grant n^o 731032 (NanoCommons), and SFI grant n^o 16/IA/4506.

[1] F. Part, C. Zaba, O. Bixner, T. A. Grunewald, H. Michor, S. Küpcü, M. Debreczeny, E. De Vito Francesco, A. Lassenberger, S. Schrittwieser, S. Hann, H. Lichtenegger, E.-K. Ehmöser, Doping Method Determines Para- or Superparamagnetic Properties of Photostable and Surface-Modifiable Quantum Dots for Multimodal Bioimaging, *Chemistry of Materials* **30** (2018) 4233-4241.

[2] C. Zaba, O. Bixner, F. Part, C. Zafiu, C. W. Tan, E. K. Sinner, Preparation of water-soluble, PEGylated, mixed-dispersant quantum dots, with a preserved photoluminescence quantum yield. *RSC Advances* **6** (2016) 27068-27076.

Temperature Determination of a Single Nanoparticle in the Gas Phase using Fluorescence Thermometry

Sophia Leippe¹, Björn Bastian¹, Benjamin Hoffmann¹, Knut R. Asmis^{1*}, Florian Johst², Sonja Krohn³, Alf Mews^{2*}

¹ *Wilhelm-Ostwald-Institute for Physical and Theoretical Chemistry, University of Leipzig, Germany*

² *Institute for Physical Chemistry, University of Hamburg, Germany*

³ *Fraunhofer IAP-CAN, Germany*

Nanoparticles (NPs) possess distinct size-dependent properties and find application in a variety of fields such as medicine, heterogeneous catalysis, fluorescent imaging or optoelectronics [1]. To better understand NP behavior access to their intrinsic properties is required. We therefore characterize individual NPs isolated in the gas phase to avoid heterogeneity of a NP ensemble and perturbing interactions with the environment. This deeper understanding is anticipated to contribute to the improvement of NP performance, particularly in areas such as catalytic selectivity and sensitivity in sensing applications. We employ a methodology for characterizing individual NPs that is based on non-destructive mass determination in a cryogenic ion trap. This setup enables us to perform action spectroscopy within the visible and infrared regime by detecting adsorption and desorption of messenger molecules [2,3].

In order to gain a better understanding of processes taking place on the NP, we are modeling the energy balance. Here, the NP temperature is a crucial parameter (see Fig. 1), which we aim to determine by fluorescence thermometry using CdSe/CdS quantum dots. Other open question we are addressing concern modeling sorption kinetics and manipulating the charge of trapped NPs.

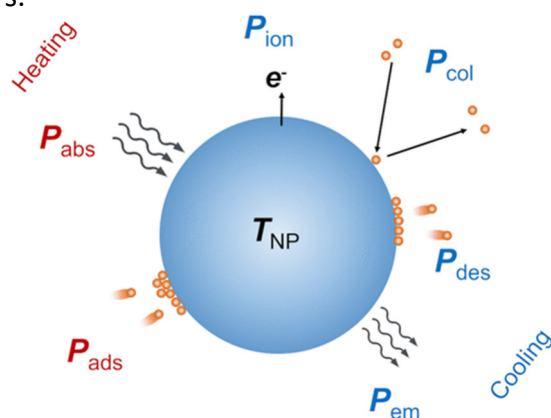


Figure 1: The energy balance of a NP depends on various heating (red) and cooling channels (blue) that influence the NP temperature: absorption and emission of electromagnetic radiation, ad- and desorption of and collision with gas molecules and emission of electrons [2].

- [1] M.A. Boles, M. Engel, D.V. Talapin, *Chemical Reviews* **116** (2016) 11220
- [2] B. Hoffmann, T. Esser, B. Abel, K.R. Asmis, *Journal of Physical Chemical Letters* **15** (2020) 6051
- [3] B. Hoffmann, S. Leippe, K.R. Asmis, *Molecular Physics* (2023) e2210454

Brain-like resistive switching phenomena in gas-phase deposited nanoparticle arrangements

N. Carstens¹, B. Adejube¹, R. Gupta¹, T. Strunskus^{1,2}, A. Hassanien³, S. Brown⁴, F. Faupel^{1,2}, A. Vahl^{1,2}

¹ *Institute for Materials Science – Chair for Multicomponent Materials, Faculty of Engineering, Kiel University, Kaiserstraße 2, D-24143 Kiel, Germany*

² *Kiel Nano Surface and Interface Science KiNSIS, Kiel University, Christian-Albrechts-Platz 4, D-24118 Kiel, Germany*

³ *Department of Condensed Matter Physics, J. Stefan Institute, Jamova 39, Ljubljana 1000, Slovenia*

⁴ *The MacDiarmid Institute for Advanced Materials and Nanotechnology, School of Physical and Chemical Sciences, Te Kura Matu, University of Canterbury, Private Bag 4800, Christchurch 8140, New Zealand*

The rise of Big Data and artificial intelligence imposes a significant growth in the demand on information processing capabilities. The field of neuromorphic engineering draws inspiration from information processing in highly interconnected neuron assemblies and offers great potential to create novel, more efficient electronics. Memristive devices with reconfigurable resistance states are highly promising for bio-inspired electronics. Filamentary resistive switching devices in cross-bar arrangement have already attracted vast research interest, e.g., for in-memory computing or as a facilitator for highly parallel vector-matrix multiplication. However, biological information processing in neural networks does not only differ from conventional integrated circuits in the type of fundamental building units, but also in the principle of their arrangement and organization: While integrated circuits rely on top-down fabrication approaches and rigid structural connectivity, neural networks feature a dynamic self-organization of neurons and synapses. To fully capture the robustness and efficiency of biological information processing, there is a high demand to understand the arrangement principles and to find a technological basis for transferring bottom-up approaches to functional electronics.

Metal and metal alloy nanoparticles from gas phase synthesis are a promising material platform to study bottom-up fabrication of nanocomposites and nanogranular devices with resistive switching properties. In this contribution, Ag, AgAu and AgPt nanoparticles (NPs) are fabricated in a magnetron-based gas aggregation source and arranged in nanogranular devices. The arrangement of NPs in dielectric matrices can be either sparse (i.e. in nanocomposites featuring NPs embedded in dielectric matrices) or highly interconnected (i.e. in particle networks at the percolation threshold). In either case, the NPs act as a reservoir for mobile Ag cations, enabling resistive switching based on formation and dissolution of conducting filaments. NP-based devices have the potential to cover a range of bio-inspired features, which will be discussed in this contribution at the example of highly volatile memristive switching with spike-like response in sparse AgPtNP/SiO_xN_y nanocomposites [1] as well as avalanche behavior and distributed switching in AgNP networks at the percolation threshold [2].

Acknowledgements: Funded by the Deutsche Forschungsgemeinschaft (DFG, German Research Foundation) – Project-ID 434434223 – SFB 1461.

[1] N. Carstens, T. Strunskus, F. Faupel, A. Hassanien, A. Vahl, Particle and Particle Systems Characterization (2023) 2200131

[2] N. Carstens, B. Adejube, T. Strunskus, F. Faupel, S. Brown, A. Vahl, Nanoscale Advances (2022) 10.1039/d2na00121g

Mass-selected morphology-controlled Hafnium clusters and their oxidation behavior

Zixiang Zhao^{1,2}, Kuo-Juei Hu^{1,2}, Fengqi Song^{1,2}

¹ National Laboratory of Solid State Microstructures, Collaborative Innovation Center of Advanced Microstructures, and School of Physics, Nanjing University, Nanjing 210093, China

² Atom Manufacturing Institute (AMI), Nanjing 211805, China

The characteristics of nanoclusters depend on their morphology and size, and more excellent characteristics can be obtained by artificially manipulating their morphologies and sizes, expanding the range of applications. For example, the electrical, optical and catalytic properties of nanoclusters, such as resistance, surface plasmon resonance bands and area-to-volume ratio, can be adjusted by modulating their morphologies [1]. In addition, there has been considerable researches on the mechanism of nanoclusters formation of various morphologies [2].

Here, we report a study on hafnium nanoclusters of a series of specific size were generated by a magnetron sputtering gas phase condensation cluster beam source, which is equipped with a time-of-flight mass filter offering a mass resolution of $M/\Delta M \approx 50$. By modulating the sputtering power, the helium and argon gas flow rates, their morphologies can be modified from sphere to multi-branch, including spherical, bipedal, tripod, and even quadruped shapes. The formation mechanism of multi branched nanoclusters is attributed to the mutual attachment of smaller primary nucleated nanoclusters [3]. According to the statistical results of the STEM and TEM images, it is found the higher the sputtering power and the lower the gas rate, the closer the morphology is to the sphere. The EDS and XPS measurements show that only large spherical clusters ($N > 7000$) violate complete oxidation, which is consistent with previous statistics. The present work provides a modulation method for cluster morphology, expanding the application range of cluster in various fields

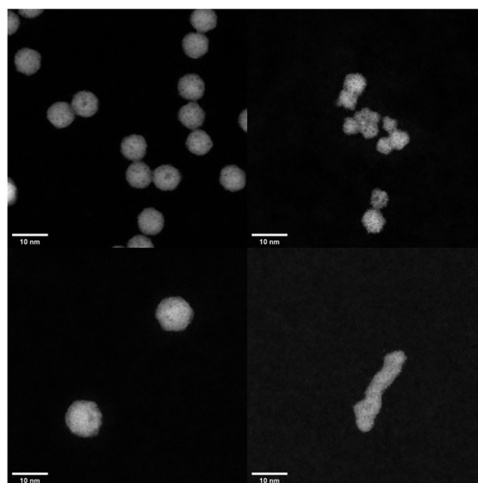


Figure 1: The STEM images of mass-selected Hf_{5083} and Hf_{12431} clusters

[1] Jiang Y, Du Z, Liu F, et al. Gas phase fabrication of morphology-controlled ITO nanoparticles and their assembled conductive films[J]. *Nanoscale*, 2023, 15(8): 3907-3918.

[2] Chepkasov I V, Gafner Y Y, Gafner S L. Changing of the shape and structure of Cu nanoclusters generated from a gas phase: MD simulations[J]. *Journal of Aerosol Science*, 2016, 91: 33-42.

[3] Meyer R, Gafner J J, Gafner S L, et al. Computer simulations of the condensation of nanoparticles from the gas phase[J]. *Phase Transitions*, 2005, 78(1-3): 35-46

Highly Sensitive and Stretchable Strain Sensor Based on Conductive Network Consisting of Pd Nanoparticles

Zhengyang Du^{1,2}, Jian Chen^{1,2}, Yilun Jiang^{1,2}, Fei Liu^{1,2}, Pen Mao^{1,2}, Min Han^{1,2}

¹National Laboratory of Solid State Microstructures and Collaborative Innovation Centre of Advanced Microstructures, Nanjing University, Nanjing 210093, China

² College of Engineering and Applied Sciences and Jiangsu Key Laboratory of Artificial Functional Materials, Nanjing University, Nanjing 210023, China

Flexible strain sensors with mechanically compliant, human-friendly and high-performance features have attached huge attention because of their potential applications in many fields[1,2]. Multiple conductive nanomaterials have been used to construct flexible strain sensor, however there is still remained challenge in the development of strain sensors with both high sensitivity and wide sensing range. Here we report a strain sensor based on the tunnel effect in the percolation networks consisting of Pd nanoparticles arrays. Because the conductivity of percolation networks is highly dependent on the mean distance between nanoparticles, sensors exhibit a high sensitivity (GF of 382), and benefited from the quantum transport characteristic in tunnel effect, the thermal noise of the sensor decreases significantly, permitting our device show a remarkable resolution as fine as strain of 3×10^{-5} . By choosing proper polymeric elastomers as scaffold, the stretchability and dynamic response ability of sensor could be dramatically improved, providing the opportunity for our devices to serve as high-performance strain sensors with a wide sensing range of 45%. As a result, sensors exhibit both high sensitivity and wide sensing range, which make it promising candidate for application in e-skins and wearable electronics [3,4].

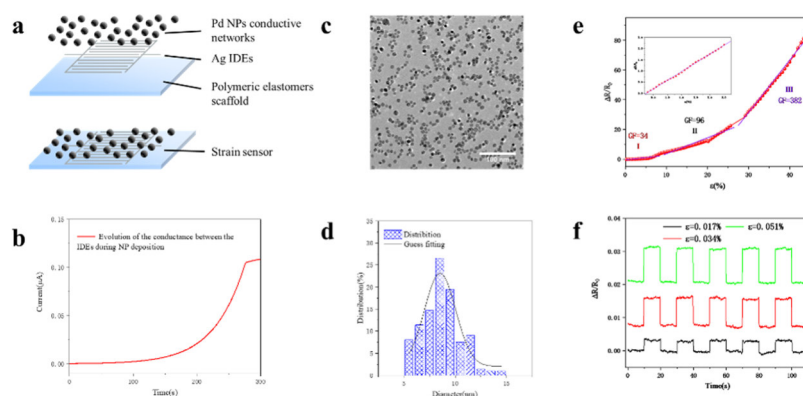


Figure 1. Construction and characterization of strain sensor based on Pd NPs. **a** A schematic diagram of strain sensor. **b** Evolution of the conductance between the IDEs during NP deposition. **c** TEM image of conductive networks of Pd NPs. **d** size distribution of NPs measured from **b**. **e** Resistive response of a strain sensors based on nanoparticles arrays under a monotonic increased tensile strain from 0% to 45%. **f** Resistive response of loading and unloading cycles for different strain.

- [1] Chen. M, Luo. W, Xu. Z, Nature communications. **10**(2019), 4024.
- [2] Du. Z, Chen. J, Liu. C, Materials. **13**(2020), 4838.
- [3] Wang. S, Xu. J, Wang. W, Nature. **555**(2018), 83-88
- [4] Dong. H, Sun. J, Liu. X, ACS Appl. Mater. Interfaces. **14**(2022), 15504–15516.

A

Abbas, I.	64, 71, 84, 115, 123, 126
Abdel-Mageed, A.	118, 130
Ablyasova, O. S.	58, 88, 158, 160
Adejube, B.	172
Aizpurua, J.	99
Akazawa, S. K.	122
Al Haddad, A.	19, 94, 148
Alexandrova, A.	6, 129
Alonso, E. G.	141
Alonso, J. A.	7
Altantzis, T.	71, 123, 126
Álvarez-García, A.	109
Anderson, S. L.	6, 129
Andersson, G. G.	33
Andreazza, P.	111
Antonsson, E.	93
Appelfeller, S.	151
Arakawa, M.	24, 43
Ard, S.	63
Arildii, D.	157
Armentrout, P. B.	39
Armillotta, F.	66
Arndt, M.	81
Aschi, M.	72
Asiri, M.	33
Asmis, K. R.	28, 37, 38, 61, 95, 108, 171
Ayala, C.	45

B

Bahodurov, J.	127
Bakker, J. M.	23, 39, 56, 60, 131
Bakkers, E. P. A. M.	12
Balalta, D.	71, 123, 126
Balbás, L. C.	65
Baletto, F.	35
Bals, S.	71, 123, 126
Bansmann, J.	118
Baraldi, A.	128, 159
Barke, I.	54
Barnes, J. V.	102
Baronio, S.	66
Bartolomei, M.	47
Bastian, B.	171
Baumann, T. M.	90
Behm, R. J.	118, 130
Behrens, S.	125
Bensiradj, N. E. H.	106
Berden, G.	23
Berger, E.	45
Berger, F.	61
Bergmann, A.	163
Bergmeister, S.	20
Bernhardt, T. M.	59, 67, 96, 124, 131
Bertrang, K.	159
Beyer, M. K.	138, 139, 140
Bidoggia, D.	66
Bielecki, J.	19, 94

Bieske, E.	22
Bischoff, F. A.	38
Bischoff, T.	74
Björneholm, O.	151
Blanchard, N.	111
Blankenhorn, M.	46, 154
Boie, J.	159
Boisron, O.	97, 111
Boll, R.	90
Bonacchi, S.	75
Borah, R.	115
Bordas, C.	142
Borgeaud dit Avocat, D. P.	102
Bostedt, C.	19, 93, 94, 148
Bowen, K.	46, 154
Boydas, E. B.	158
Breier, A.	134
Brewer, E. I.	57, 70
Bromley, S. T.	21, 131
Brown, S. A.	10, 172
Bruder, L.	18
Bruno E. Ramírez-Galindo	81
Bucher, M.	93
Buendia-Zamudio, F.	152
Bulut, B.	141
Buschmann, D. A.	77

C

Callegari, C.	91
Calvo, F.	110
Campos-Martínez, J.	47
Camus, E.	111
Carlin, R.	107
Carstens, N.	172
Casapu, M.	125
Chakraborty, A.	37, 61
Chatterley, A. S.	90
Chaudhary, M.	155
Chen, J.	98, 174
Chen, S.	118
Chen, Z.	126
Cheng, D.	119
Cheshnovsky, O.	12, 85
Chiba, T.	46, 154
Chinnabathini, V. C.	115
Chiu, T.-H.	117
Chorkendorff, I.	122
Christen, W.	141
Chung, Y. C.	141
Clark, A. H.	83
Coffee, R. N.	93
Colding-Fagerholt, S.	122
Colombo, A.	19, 91, 94, 148
Concina, B.	142
Copéret, C.	64, 84
Coreno, M.	86, 89
Coroa, J.	64, 80, 84
Coslovich, G.	93
Cottancin, E.	42, 97, 111
Crandall, P.	137

Crudden, C. M.	77
Cunningham, E. M.	139
Czechowsky, J.	125

D

D'Acapito, F.	115
D'Antoni, P.	75
Da Roit, N.	125
da Silva Santos, M.	58, 88, 108, 158, 160
Damsgaard, C. D.	121, 122
Danilson, M.	151
Darabi, E.	166
De Fanis, A.	90
De Knijf, K.	104
de Sousa, T.	81
De, S.	89
Debnath, S.	37, 38
Dehnen, S.	41
Devetta, M.	86, 162
di Fraia, M.	91
Diercks, J. S.	83
Dingenen, F.	115
Dold, S.	19, 94, 162
Doll, M.	57
Dopfer, O.	133, 134, 137, 156, 157
Drewes, J.	82
Du, Z.	174
Duda, O.	57

E

Echt, O.	20
Erk, B.	90
Erukala, S.	90
Esch, F.	128

F

Fagiani, M. R.	38
Faupel, F.	82, 172
Fauth, F.	130
Feinberg, A. J.	90
Fennel, T.	90, 91, 92, 93
Ferguson, K.	93
Fernández, E. M.	65
Ferrari, P.	8, 23, 104
Fielicke, A.	8, 143, 145, 156
Fischer, P.	52, 87
Flach, M.	58, 88, 158, 160
Floyd, A. M.	45
Foreman, K.	154
Förstel, M.	133, 156
Fortunelli, A.	27, 72, 75
Fries, D. V.	50
Front, A.	32
Fu, L.	147

G

Gallei, M.	93
Gan, Z.	163
Gao, M.	127
Gao, Y.	69
Garzón, I. L.	15, 109
Gaston, N.	168
Gatchell, M.	47
George, A.	163

Gerke, F.	93
Gerlich, S.	81
Germán, E.	7
Gewinner, S.	38
Geyer, P.	81
Ghejan, B.-A.	131
Giesel, P. F.	87
González-Lezana, T.	47
Gopal, R.	89
Gorkhover, T.	93
Goy, F.	19, 94
Graf, C.	19, 93, 94
Grandjean, D.	64, 71, 84, 115, 123, 126
Granmayehrad, A.	166
Gratious, S.	79
Green, A. E.	57
Grellmann, M.	28, 95
Gruber, E.	20
Grunwald-Delitz, M.	52
Grychtol, P.	90
Gupta, R.	172

H

Häkkinen, H.	72
Halfpap, I.	93
Hamidi, S. M.	167
Han, M.	13, 98, 174
Hansen, K.	52
Hartmann, J. C.	139, 140
Hartmann, R.	90
Hassanien, A.	172
Haverkort, J.	12
Hecht, L.	19, 91, 94, 148
Heilrath, A.	90
Heiz, U.	128, 159
Helveg, S.	122
Hemaid, M.	163
Herranz, J.	83
Hervieux, P.-A.	53
Hillenkamp, M.	42, 97, 100, 111
Hinke, T.	128, 159
Hirai, H.	73
Hirsch, K.	58, 88, 108, 158, 160
Ho, G. W.	127
Hoffmann, A.	90
Hoffmann, B.	171
Höltzl, T.	56, 60, 62
Horio, T.	43
Horn, F.	108
Hreben, A.	88, 160
Hu, E.	126
Hu, K.-J.	101, 173
Hu, S.	169
Hütter, M.	138

I

Ilchen, M.	90
Inoue, T.	113
Ito, R.	150
Ito, S.	76
Iwasa, T.	73
Iwe, N.	100, 161
Izquierdo, M.	90

J

Jakobs, G.	19, 94
Jankowski, A.	52
Janssens, E.	8, 64, 71, 80, 84, 104, 115, 123, 126
Jia, M.	8
Jiang, Y.	174
Jin, J.	28, 95
Johst, F.	171
Jorewitz, M.	28, 37
Joschko, M.	19, 94
Juurlink, L.	60

K

Kai, A.	33
Kaiser, S.	128, 159
Kappe, M.	68
Kappes, M.	125
Kavka, N.	95
Kazak, L.	161
Kébaïli, N.	26
Kerpál, C.	145
Kersten, H.	82
Kibsgaard, J.	121, 122
Kling, M. F.	93
Knecht, A.	74
Knechtges, M.	159
Knopp, G.	19, 94, 148
Kolatzki, K.	19, 90, 91, 94, 148
Kollotzek, S.	47
Komar, D.	161
Kono, S.	24
Korn, T.	163
Kotsis, K.	170
Koyasu, K.	76
Kozlov, S. M.	120, 127, 152
Krabbe, A.	122
Krebs, B.	90, 161
Krishnan, S. R.	89
Krohn, S.	171
Kruse, B.	90, 91, 92
Kruse, S.	58
Kryger-Baggesen, J.	121
Kumari, S.	6, 129
Kushavah, D.	12
Kuster, M.	90
Kv, A.	79

L

Lacovig, P.	128
Lang, S. M.	59, 67, 131
Langbehn, B.	90, 91, 148
Langer, B.	93
Lau, J. T.	58, 88, 108, 158, 160
Leach, S.	37, 61, 108
Lehr, A.	103
Leidinger, P.	83
Leippe, S.	171
Lenzer, A.	130
Lermé, J.	97, 100, 111
Lethbridge, S.	146
li de Donato Perez, A. A.	131
Li, Y.	37, 61
Lian, D.	53
Lievens, P.	71, 104, 115, 123
Lisjak, D.	105

Liu, C.	13, 22
Liu, C.-W.	117
Liu, F.	174
Liu, G.	46
Liu, Q.	93
Liu, X.	164
Liu, Y.	78, 116
Loi, F.	159
López, M. J.	7
Ltaief, L. B.	89
Lu, S.	101
Luczak, M.	50
Luque-Ceballos, J. C.	109
Lushchikova, O. V.	47, 60, 68
Lyon, J. T.	107

M

Mackenzie, S. R.	9, 57, 70, 156
Madener, S.	139
Mafuné, F.	132
Maier, S. A.	13
Maliakkal, C.	125
Malola, S.	72
Mandal, S.	79
Manea, A. K.	166
Manfredi, G.	53
Mao, P.	13, 98, 174
Maran, F.	75
Mariñoso Guiu, J.	131
Marlton, S.	22
Martin, S.	142
Martinez, F.	100, 161
Masenelli-Varlot, K.	42
Mason, J.	70
Masubuchi, T.	6, 129
Matsumoto, Y.	157
Matus, M. F.	72
Mazza, T.	86, 90, 162
McCormack, J. E.	146
Medel, R.	58
Meijer, G.	143, 145
Meiwes-Broer, K.-H.	54, 100, 161
Meizyte, G.	57
Meng, F. L.	127
Merli, A.	74
Metha, G. F.	33
Mews, A.	171
Meyer, J.	60
Meyer, M.	90
Mikolaj, P.	59
Misaizu, F.	144, 150
Mitrić, R.	95, 156
Miyajima, K.	132
Möller, S.	93
Möller, T.	74, 90, 91, 148
Mondal, S.	89
Montagne, G.	142
Montano, J.	90
Monti, M.	72
Moreira, M.	42, 97, 111
Moretti, P.	134
Moseler, M.	19, 94
Mottet, C.	32
Mudrich, M.	89
Müller, F.	38, 61

N

Nagata, T.	132, 144
Nahvi, N.-N.	137, 156
Nakajima, A.	113
Nakajima, Y.	144
Nakamura, M.	135
Nakashima, T.	73
Nambo, M.	77
Nassar, M.	106
Needham, J. L.	121
Neumaier, M.	125
Nguyen, M.	8
Nguyen, T. H. T.	115
Niedner-Schatteburg, G.	50
Nilsen, A. J.	121
Niu, Y.	13
Noffz, G.	90
Nyulászi, L.	56, 62

O

O'Brien, M.	6, 129
O'Connell-Lopez, S. M. O.	90
Obwaller, B.	139
Ogando, E.	99
Öhrwall, G.	151
Ohshimo, K.	144, 150
Oldenburg, K.	54
Ončák, M.	20, 138, 139, 140
Osipov, T.	93
Ouchane, S.	26
Ovcharenko, Y.	90, 162

P

Paiss, P.	12
Palmer, R. E.	13, 30, 122, 146
Pant, D.	71, 126
Papamichail, D.	71, 123
Pavloudis, T.	146
Paz-Borbón, L. O.	109
Pearcy, P. A. J.	57, 70
Pedalino, S.	81
Pellarin, M.	42, 97, 111
Peltz, C.	19, 91, 92, 93, 94
Penna, T.	108
Peressi, M.	66
Petzoldt, P.	128
Phadke, S.	64, 83, 84
Pinna, N.	78, 116
Pirani, F.	47
Piseri, P.	86, 91, 162
Plekan, O.	91
Polat, C.	148
Pollow, K.	133, 134, 156
Polonskyi, O.	82
Popolan-Vaida, D. M.	45
Powell, J. A.	93
Pradeep, D.	56
Prince, K.	91

Q

Quilliam, J.	107
-------------------	-----

R

Rafie-Zinedine, S.	19, 94
Raspe, K.	100, 161
Ray, D.	93
Redlich, B.	23
Rehders, S.	82
Reichegger, J.	47
Reichenbach, T.	19, 94
Reider, A. M.	68
Reinhold, J.	163
Ren, Y.	12
Riboldi, S.	86
Richardson, C. N.	107
Richter, R.	89
Riedel, S.	58
Rivacoba, A.	99
Rivas, D. E.	90
Rivic, F.	103
Rodrigues, V.	42, 97
Roiban, L.	42, 111
Roldan Cuenya, B.	31
Rolles, D.	93
Romeggio, R.	122
Rörmelt, M.	158
Roy, R.	12, 85
Rudenko, A.	93
Rühl, E.	93
Rupp, D.	19, 90, 91, 94, 148
Rupp, P.	93
Rüttimann, P.	83

S

Safonova, O.	64, 83, 84
Sai, L.	147, 149
Sakon, I.	135
Sala, A.	66
Salzburger, M.	138
Sandoval-Menjivar, J.	7
Sanzone, G.	80
Sartakov, B. G.	143
Saruyama, M.	165
Sasikumar, S.	86, 162
Sato, Y.	77
Sauer, J.	37, 38, 61, 108
Sauppe, M.	19, 91, 94, 148
Sautet, P.	6, 129
Scardamaglia, M.	66
Schäfer, R.	103
Schaller, S.	143
Scheier, P.	20, 47, 68
Schenk, F.	19, 94
Schlosser, D.	90
Schmidt, M.	68
Schmidt, T. J.	83
Schnorr, K.	19, 94, 148
Schöllkopf, W.	38, 145
Schöpfer, G.	20
Schubert, M.L.	91
Schwartz, R.	163
Schwedland, W.	61
Schweikhard, L.	52, 87, 100
Secher, N. M.	122
Sedano Varo, E.	121
Seel, F.	90
Seifert, J.	143
Seiffert, L.	90

Sekine, Y.	24
Sementa, L.	75
Senfftleben, B.	90, 91
Sharma, V.	89
Shuman, N.	63
Signorell, R.	44, 102
Silalahi, R. P. B.	117
Simmen, E.	102
Singh, G.	85
Sinha-Roy, R.	53
Slater, T. J. A.	146
Sloth, O. F.	122
Song, F.	101, 112, 164, 169, 173
Song, J.	71, 126
Song, X.	38
Stapelfeldt, H.	90
Stener, M.	27, 72, 75
Stromberg, I.	20
Strüder, L.	90
Strunskus, T.	82, 172
Studemund, T.	133, 134, 156
Stüker, T.	58
Subramanian, A.	120
Summers, A.	93
Sun, H.	80
Sun, Z.	19, 94, 148
Szalay, M.	56, 60

T

Tahmasbi, H.	60
Takahata, R.	165
Takano, S.	73, 77
Taketsugu, T.	73
Tambosi, R.	26
Tankard, R. E.	121, 122
Tanyag, R. M. P.	90
Tchaplyguine, M.	151
Teranishi, T.	40, 165
Terasaki, A.	24, 43
Tiggesbäumker, J.	90, 100, 161
Timm, M.	58, 88, 108, 158, 160
Tosoni, S.	159
Trallero-Herrero, C.	93
Tschurl, M.	128
Tsukuda, T.	14, 73, 76, 77
Tuemmler, P.	92
Tufani, A.	105
Tümmeler, P.	19, 91, 94, 148
Turchanin, A.	163

U

Ugandi, M.	158
Ugarte, D.	42
Ulmer, A.	90
Urbietta, M.	99
Ussling, F.	19, 74, 94, 148, 153

V

Vaes, J.	126
Vahl, A.	82, 172
Vaida, M. E.	51, 96, 124
Valdivielso, D. Y.	145
Valle Sejo, M. F.	141
Valtolina, G.	143
van der Linde, C.	138, 139, 140

van der Tol, J.	104, 115
Vanbuel, J.	8
Verbruggen, S. W.	115
Vesselli, E.	66
Viggiano, A.	63
Vilesov, A. F.	17, 90
von Issendorff, B.	19, 49, 58, 88, 94, 158, 160

W

Wächter, S.	148
Wang, D.	125
Wang, G.	13
Wang, L.-S.	11
Wang, S.	154
Wang, Y.	78, 116
Wang, Z.	6, 129
Waters, L. B. F. M.	23
Watson, P. D.	57, 70
Wei, J. S.	127
Weigelt, C.	124
Weissker, H.-C.	110, 155
Weitnauer, A.	148
Wensink, F. J.	39
Wiehn, C.	50
Windeck, H.	61
Winkeler, M.	107
Winzely, A.	83
Wu, X.	149

Y

Yang, H.	102
Yang, Y.	53
Yano, J.	25
Yarema, M.	19, 94
Yazdanfar, H.	167
Yazdani, N.	19, 94
Yin, J.	64, 80, 84
Yoder, B. L.	102
Yousef, H.	90

Z

Zabala, N.	99
Zabel, M.	90
Zamora, B.	56, 62
Zamudio-Bayer, V.	58, 88, 108, 158, 160
Zappa, F.	47
Zarkua, Z.	115
Zhang, H.	19, 94
Zhang, S.	13
Zhang, T. X.	127
Zhang, X.	46
Zhang, Y.	112
Zhang, Z.	6, 129
Zhao, J.	147, 149, 152
Zhao, Z.	173
Zherebtsov, S.	93
Zhu, B.	69
Zhu, S.	66
Zhu, Y.	36
Zijlstra, R.	56
Zimmermann, J.	148
Ziołkowski, P.	90
Zouaghi, N.	106
Zunger, A.	12
Zuod, M.	148

